

REPORT NO.
EERC 75-15
JUNE 1975

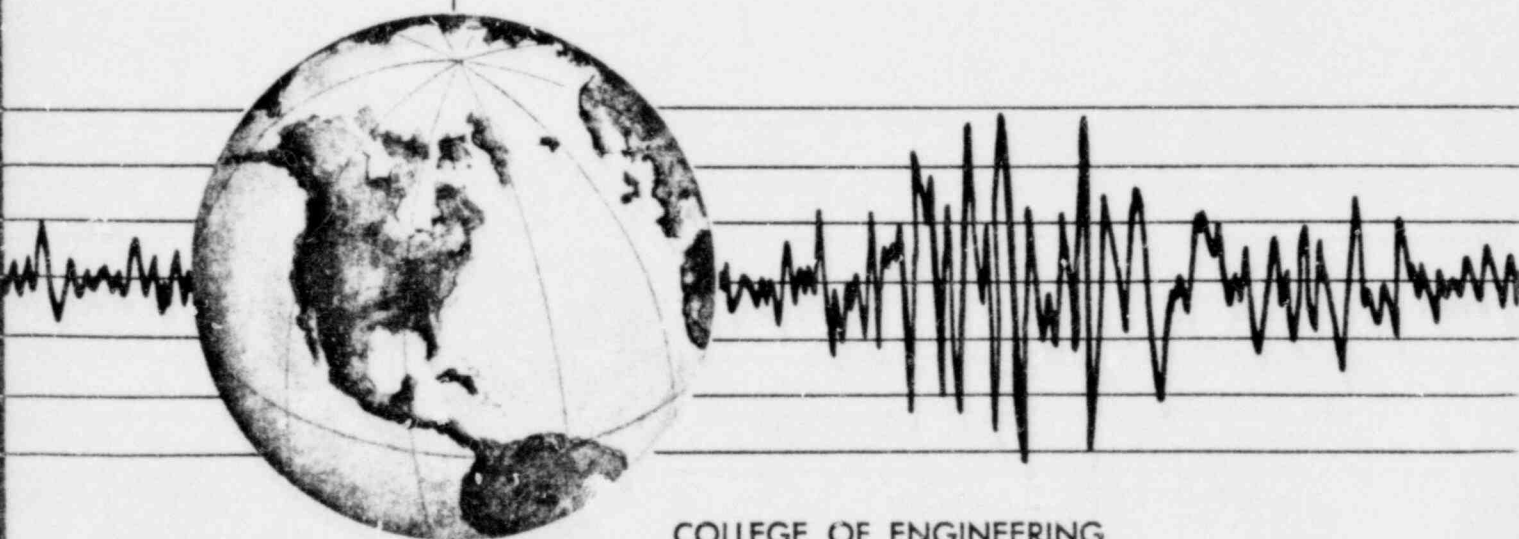
EARTHQUAKE ENGINEERING RESEARCH CENTER

A LITERATURE SURVEY— COMPRESSIVE, TENSILE, BOND AND SHEAR STRENGTH OF MASONRY

by

RONALD L. MAYES
RAY W. CLOUGH

Report to the National Science Foundation



COLLEGE OF ENGINEERING

UNIVERSITY OF CALIFORNIA · Berkeley, California

8107270198 810717
PDR ADOCK 05000266
G PDR

A LITERATURE SURVEY - COMPRESSIVE, TENSILE, BOND
AND SHEAR STRENGTH OF MASONRY

By

Ronald L. Mayes

and

Ray W. Clough

Prepared under the sponsorship of
National Science Foundation
Grant NSF AEN73-07732 A02

Report No. EERC 75-15
Earthquake Engineering Research Center
College of Engineering
University of California
Berkeley, California

June 1975

ABSTRACT

The literature survey presented collates most of the available relevant information on the compressive, tensile, bond and shear strength of masonry. The report is divided into two chapters. The first, on the compressive, tensile and bond tests of small test specimens, summarizes information on the basic tests that determine different properties of non-homogeneous, masonry assemblages. These basic tests are important in that they provide practical methods for the site control of masonry quality by measuring the integrated effect of any variations in component materials and workmanship.

The second chapter summarizes most investigations performed on the shear strength of different assemblages and includes sections on test techniques, monotonic tests, model tests and cyclic tests.

Further discussion and analysis of the results from the experiments described here will be presented in a following Earthquake Engineering Research Center report EERC 75-21.

ACKNOWLEDGEMENT

This investigation was sponsored by the National Science Foundation under Grant No. NSF AEN73-07732 AO2. The authors acknowledge the research performed by all investigators that made a survey such as this possible.

TABLE OF CONTENTS

	<u>Page</u>
ABSTRACT	iii
ACKNOWLEDGEMENT	v
TABLE OF CONTENTS	vii
LIST OF TABLES	ix
LIST OF FIGURES	xi
1. COMPRESSIVE, TENSILE AND BOND ELEMENT TESTS	1
1.1 Introduction	1
1.2 Prism Compression Tests	1
1.2a Mechanism of Failure	3
1.2b Variables Influencing Prism Compressive Strength	24
(i) Platen Restraint	24
(ii) Effects of Prism Shape	25
(iii) The Effect of Capping	26
(iv) The Effect of Bond Type	26
(v) Masonry Unit Strength	27
(vi) Mortar	29
(vii) Joint Thickness	33
(viii) Workmanship	35
1.3 Tensile and Bond Strength Tests	37
1.3a Tensile Strength of Individual Units	37
1.3b Bond Strength Tests	41
1.3c Tensile Strength of Masonry Assemblages	58
2. SHEAR STRENGTH OF MASONRY ASSEMBLAGES	67
2.1 Introduction	67
2.2 Test Techniques	69

TABLE OF CONTENTS (Contd.)

	<u>Page</u>
2.3 Monotonic Shear Load Tests	75
2.4 Shear Strength of Model Structures	118
2.5 Cyclic Shear Behaviour of Masonry Assemblages	144
REFERENCES	185

LIST OF TABLES

<u>Table</u>	<u>Page</u>
1-1 Strength of Gypsum Cube Prisms with Different Joint Materials	4
1-2 Strength of Concrete Block Prisms With Different Joint Materials	6
1-3 Percentage Sand Gradation for Optimum Packing	29
1-4 ASTM C-144 Requirements for Masonry Mortar Aggregate	30
1-5 Recommended Water Cement Ratios	30
1-6 ASTM C-270 Minimum Strength Requirements of Standard Mortars	31
1-7 Experimental Strengths of Standard Mortars	31
1-8 Effect of Sand Gradation on Mortar Strength	31
1-9 Effect of Mortar Compressive Strength on Ultimate Compressive Strength of 4-in. Brick Prisms	32
1-10 Effect of Mortar Joint Thickness on Prism Strength	33
1-11 Physical Properties of Mortar	44
1-12 Couplet Bond Tension Strengths	46
1-13 Average Results of Combined Stress Couplet Tests Brick: Stiff Mud, Side Cut, Clay, Vacuum Treated	48
1-14 Couplet Bond Tension Strength	52
1-15 Couplet Bond Shear Strength	53
1-16 Experimental Data on the Compressive, Tensile and Bond Strength of Standard Mortars	58
2-1 Recommended Relationship Between the Height to Width Ratio of a Pier and the Ultimate Shear Strength	81
2-2 Recommended Relationship Between the Height to Width Ratio of a Pier with Reinforcement and the Ultimate Shear Strength	82
2-3 Behaviour of Walls Under Test	84
2-4 Behaviour of Walls Under Test	86
2-5 Behaviour of Walls Under Test	88

LIST OF TABLES (contd.)

<u>Table</u>	<u>Page</u>
2-6 Racking Strengths	97
2-7 Dimensionless Data for Edge Load With Racking	100
2-8 Mean Compressive Stress, Mean Shear Stress and Principal Tensile Stress for Six Walls	107
2-9 Summary of Results of Walls Tested With Monotonic Load	119
2-10 Experimental Parameters of Hysteretic Loops	148
2-11 Static Test Wall Details	150
2-12 Static Test Results	151
2-13 Material and Pier Properties	157
2-14 Ultimate Strengths and Ductility Indicators	161
2-15 Wall Panel Dimensions and Properties	166
2-16 Failure Loads for Walls Without Confining Plates	167

LIST OF FIGURES

<u>Figure</u>	<u>Page</u>
1-1 Prism Tests	2
1-2 Modes of Failure of Gypsum Cement Cubes	5
1-3 Idealised Stress Distribution in A Masonry Unit	8
1-4 Failure Criteria of Brick Masonry	10
1-5 Comparison of Measured and Computed Values of Masonry Strength	14
1-6 Brick and Mortar Stresses Due to an Applied Compressive Load	16
1-7 Theoretical Envelope Relating the Tensile and Compressive Stresses in Brick at Failure	18
1-8 Variation of ρ With Joint Thickness - Theoretical and Exp imental Results Compared	20
1-9 Variation of the Prism Strength With the Relative Thickness of the Mortar Joint and Masonry Unit	23
1-10 Pier Compressive Strength vs. Mortar Compressive Strength . .	34
1-11 Tensile Strength Test	40
1-12 Brick Couplet Test	42
1-13 Arrangements for Combined Stress Tests	45
1-14 Combined Stress Couplet Strength Curves	49
1-15 Bond Tension Test Arrangement	51
1-16 Shear Box Test Arrangement	51
1-17 Shear Strength of Brick Couplets Subjected to Vertical Compression	56
1-18 Shear Strength of Brick Couplets Subjected to Vertical Compression	57
1-19 Variation of Stress Component Normal to Bed at Masonry Disc Center	59
1-20 Effect of Direction of Bed Joint Angle on Masonry Disc Tensile Strength	61
1-21 N vs E_B/E_M Curves	63
1-22 Diagonal Tensile Strength vs. Mortar Tensile Strength	64

LIST OF FIGURES (Contd.)

<u>Figure</u>	<u>Page</u>
2-1 Typical Shear Walls	68
2-2 External Hold Down	70
2-3 Internal Hold Down	70
2-4 Racking Panel	70
2-5 Stress Pattern in a Laterally Loaded Wall Panel Model With Window Openings. Note the Diagonal Tension Stresses in the Center Pier	72
2-6 Stress Pattern in a Diagonal Tension Test	73
2-7 Edge Load with Racking	74
2-8 Diagonal Load Frame	74
2-9 Cantilever Load Test	74
2-10 Double Pier Test Set-Up	76
2-11 Typical Panel Dimensions	78
2-12 Typical Panel Dimensions	80
2-13 Haller's Test Specimen	90
2-14 Empirical Shear Strength vs. Applied Compressive Stress . .	92
2-15 Typical Test Specimen	93
2-16 Stress Distribution for Edge Load with Racking	99
2-17 Graph of Data for Edge Load vs. Racking Load	102
2-18 Edge vs. Racking Load for Low Strength Mortar	104
2-19 Stresses at the Center of the Element	105
2-20 Ultimate Strengths of Brickwork Walls Subjected to Horizontal and Vertical Loads	108
2-21 Dependence of τ_{xy0} Upon the Quality of Mortar	109
2-22 Test Set-Up	110
2-23 Effect of Compressive Stress	112
2-24 Effect of the Length of the Wall. Compressive Stress = 85 PSI	112

LIST OF FIGURES (Contd.)

<u>Figure</u>	<u>Page</u>
2-25 Effect of the Thickness of the Wall	113
2-26 Effect of Mortar Composition. Compressive Stress = 85 PSI	113
2-27 Effect of Brickwork Age	114
2-28 Effect of Wetting Bricks During Construction	114
2-29 Meli's Test Set-Up	116
2-30 Typical Failure Envelopes for Various Failure Mechanisms . .	116
2-31 Proposed Load-Distortion Curve	116
2-32 Shear Wall Test Structure	121
2-33 Load-Deflection Curves for Shear Wall Structures	122
2-34 Variation of Shearing Modulus of Brickwork	123
2-35 Relationship Between Ultimate Shear Stress and Precompression	126
2-36 One-Sixth Scale Model Test Structure	128
2-37 Load Deflection - Case 1	129
2-38 Load Deflection - Case 2	129
2-39 Load Deflection - Case 3	130
2-40 Load Deflection - Case 6	130
2-41 Cross-Wall Test Structure	133
2-42 Deflection of Model Structure	134
2-43 Deflection of Model of Full-Scale Structure	134
2-44 Comparison of the Analytical and Experimental Deflections . .	135
2-45 Comparison of the Analytical, Experimental Full-Scale and Adjusted Model Deflections	135
2-46 Deflections of the Structures at Various Floor Levels	137
2-47 Model Test Structure	138
2-48 Variation of Shear Modulus with Precompression	139

LIST OF FIGURES (Contd.)

<u>Figure</u>	<u>Page</u>
2-49 Comparison of Deflections Obtained From Experimental and Analytical Results	139
2-50 Vertical Stress at Section $X_1 - X_1$	141
2-51 Structures Analysed to Investigate Influence of Flange and Slab Width	142
2-52 Variation of Deflection/Rigidity With Flange and Slab Width .	143
2-53 Typical Load-Distortion Curves Under Alternating Loads . . .	146
2-54 Idealized Hysteretic Behaviour	146
2-55 Load-Deflection Curve for Yield Failure	152
2-56 Load-Deflection Curve for Shear Failure	152
2-57 Typical Double Pier Test Specimen	155
2-58 Definition of Ultimate Loads	158
2-59 Definition of Ductility Indicators	159
2-60 Average Stiffness vs. Average Lateral Displacement	162
2-61 Average Stiffness vs. Average Gross Shear Stress	162
2-62 Average Stiffness vs. Average Lateral Displacement	162
2-63 Average Stiffness vs. Average Gross Shear Stress	162
2-64 Diagrammatic Representation of Energy Dissipation	163
2-65 Strain Hardening Enhancement of Ultimate Load	169
2-66 Typical Shear Failure Under Monotonic Loading	170
2-67 Relative Effectiveness of Vertical and Horizontal Shear Steel	172
2-68 Shear Transfer by Dowel Action	172
2-69 Walls Without Confining Plates. Cyclic Load Degradation . .	176
2-70 (a) Unconfined Compression Zone Failure	177
(b) Buckling of Previously Yielded Reinforcing	177
2-71 Dimensions of Confining Plates	178

LIST OF FIGURES (Contd.)

<u>Figure</u>		<u>Page</u>
2-72	(a) Confining Plate in RBM Construction	179
	(b) Confining Plate in Hollow Cell Construction	179
2-73	(a) F13 - Confined Crushing Zone After Cycling at ±1 in. (D. F. = 6.3)	181
	(b) CBU-3 Confined Crushing Zone After Cycling at ±1 in. (D. F. = 5.0)	181
2-74	(a) F13 After Cycling at ±1 in.	182
	(b) CBU-3 After Cycling at ±1 in.	182

1. COMPRESSIVE, TENSILE AND BOND ELEMENT TESTS

1.1 Introduction

The compressive, tensile and bond tests on small test specimens constitute the basic tests for determining different properties of non-homogeneous masonry assemblages. A thorough knowledge of these tests and the behaviour of the component materials during the tests will aid the reader in understanding the behaviour of larger masonry assemblages subjected to more complex test procedures. The basic tests are also important in that they provide practical methods for the site control of masonry quality by measuring the integrated effect of any variations in component materials and workmanship.

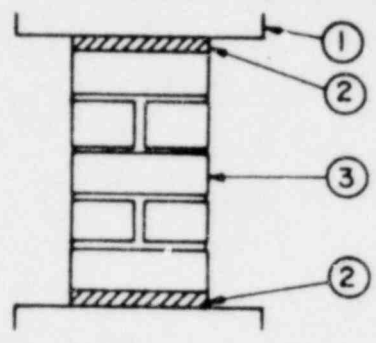
The behaviour of the small assemblages in the basic tests is the result of the heterogeneous action of the mortar, masonry unit and grout (if it is present), and the purpose of this chapter is to provide a brief but comprehensive summary of the knowledge available.

Two extremely good surveys on different aspects of the prism compressive test have already been presented. The first by Monk⁽¹⁾ in 1967 was a historical survey and analysis of the compressive strength of brick masonry. The second by Foster⁽²⁾ was a literature survey and report of experimental work emphasising the importance of the geometric shape and boundary conditions of prisms in obtaining realistic results for use in design. The pertinent aspects of the two reports are included here but the emphasis of the following summary of prism compressive tests is on work published more recently.

1.2 Prism Compression Tests

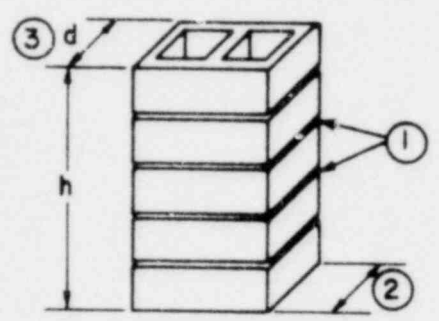
Prisms are small specimens of brickwork. Typical examples are given in Figure 1-1 which also provides definitions of terms by

A COMPRESSION TEST OF PRISMS



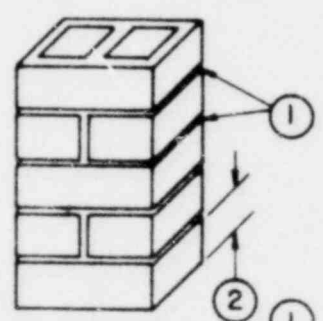
- ① TESTING MACHINE
- ② CAPPING
- ③ MASONRY PRISM

B TYPICAL PRISMS



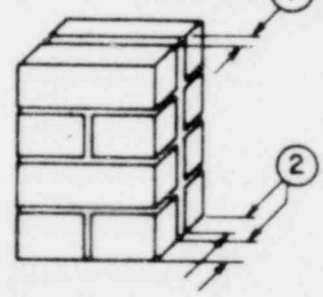
SINGLE WYTHE STACK-BONDED UNFILLED PRISM. 5 COURSES.

- ① MORTAR BEDS
- ② 1 BRICK WIDTH = 1 WYTHE
- ③ HEIGHT TO DEPTH RATIO = h/d



SINGLE WYTHE GROUTED COMMON-BONDED PRISM. 5 COURSES.

- ① MORTAR PERPEND
- ② ONE COURSE



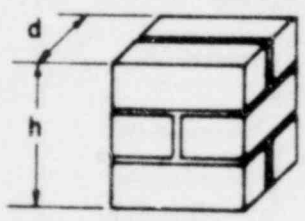
DOUBLE WYTHE GROUTED COMMON-BONDED PRISM. 4 COURSES.

- ① GROUT CORE
- ② BRICK WIDTHS = 2 WYTHES

REINFORCING BRICKS

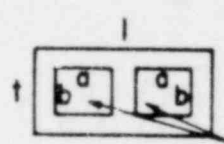
SOLID BRICKS 25% HOLES

C THE U.K. 9" BRICKWORK CUBE



NOTE: $h/d = 1$

D NETT AREA



GROSS AREA = $1 \times t$
NETT AREA = $t(1 - 2ab)$

- ① GROUT SPACES

FIGURE 1-1 PRISM TESTS

illustration. For the determination of compressive strength, some capping material (e.g. plaster, softboard, plywood) is usually placed on the top and bottom of the prisms, which are then loaded axially in compression to failure. The failure load divided by the net area provides an estimate of the masonry compressive strength.

1.2a Mechanism of Failure

The tensile splitting of masonry assemblages in compression is a rather old empirical observation. The mode of failure, unless Euler buckling or eccentric bending dominates, is a tensile rupture at right angles to the direction of compressive strain. The resulting compressive strength of an assemblage is usually between the compressive strengths of the mortar and the masonry unit. In order to examine in more detail the mode of compressive failure, it is useful to study the results of tests on hypothetical synthetic material systems with exaggerated joint-unit strain relationships. It has been recognized for some time that the vertical splitting of the masonry unit is related to the lateral strain of the mortar joint. In most masonry assemblages the elasticity of the mortar (one or two million psi) is lower than that of the brick (about four to six million psi) or concrete block (about two to four million psi). Therefore, its free lateral deformation is substantially greater than that of the brick or concrete block assuming that the Poisson ratios are similar. Because the masonry unit at the mortar interface must undergo the same lateral expansion as the mortar, due to friction, bond, etc., the lateral expansion of the mortar is restrained, producing tensile strains in the masonry unit. This phenomenon was qualitatively shown in two series of tests. The

first, a series of gypsum-cement cubes, was tested in the SCPRF⁽¹⁾ laboratories with aluminium joints and polyethylene joints. The moduli of elasticity of the materials were as follows

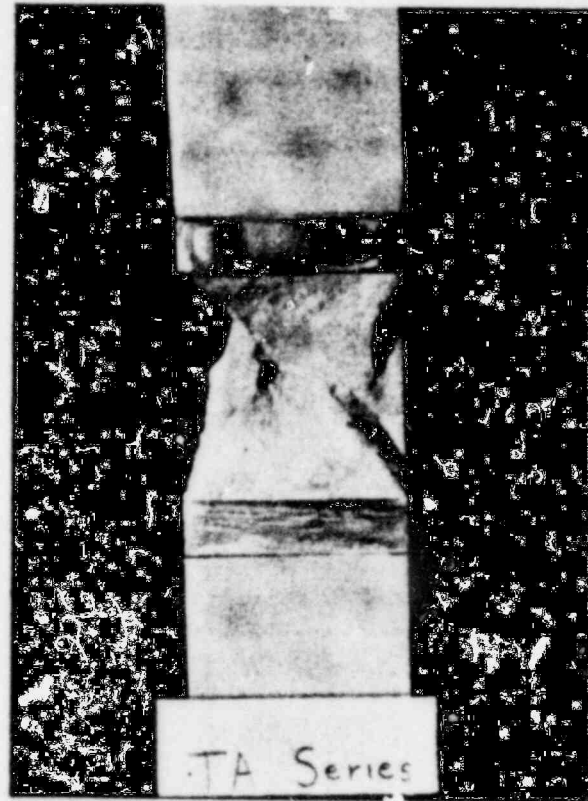
Gypsum Cement	0.9×10^6 psi
Aluminium	10.6×10^6 psi
Polyethylene	0.05×10^6 psi

When the gypsum-aluminium system was tested a characteristic tensile split was produced (Figure 1-2). Since the aluminium is about ten times stiffer than the gypsum, the lateral strains of the cubes are tending to be compressive. Thus, the joint material restrains the cube against tensile splitting, permitting a shear failure at an apparently higher compressive strength. With the polyethylene being about one eighteenth as stiff as the gypsum, the lateral strains in the cubes become tensile, resulting in a characteristic vertical splitting, yielding an apparently lower compressive strength. The results of tests on five gypsum cubes tested in the SCPRF laboratories with each of the two materials are as follows

TABLE 1-1

Gypsum Cubes with aluminium joints	Gypsum Cubes with polyethylene joints
3100 psi	1218 psi
3750	1300
4125	1337
4250	1412
<u>4475</u>	<u>1425</u>
3938 psi Average	1338 psi Average

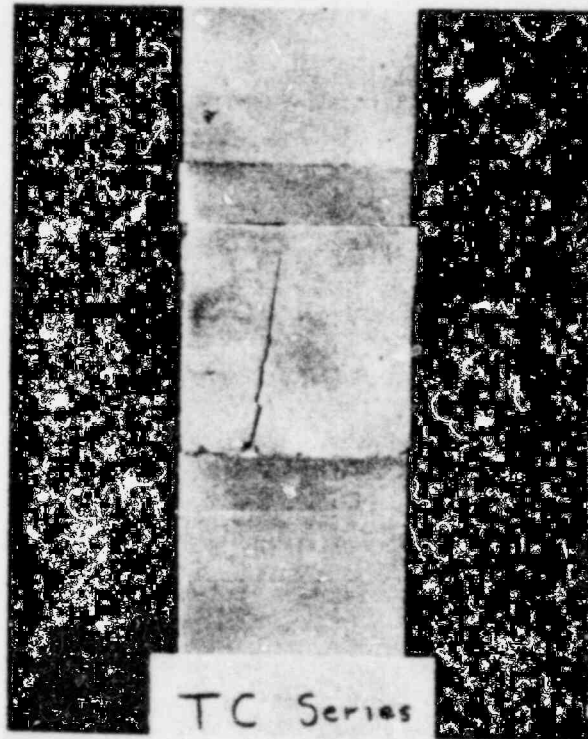
From Reference 1



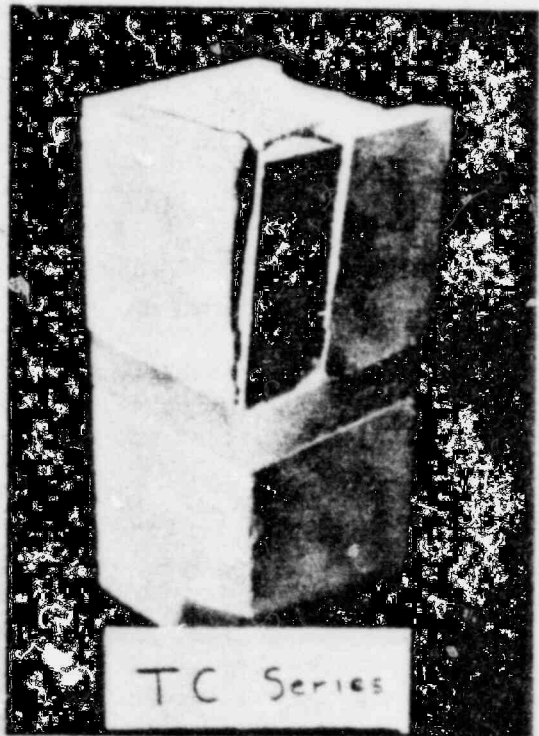
(a) SHEAR FAILURE WITH ALUMINUM JOINTS



(b) DETAILED VIEW OF SHEAR FAILURE



(c) TENSILE-SPLITTING FAILURE WITH POLYETHYLENE JOINT



(d) DETAILED VIEW OF TENSILE-SPLITTING FAILURE

FIGURE 1-2 MODES OF FAILURE OF GYPSUM CEMENT CUBES

From Reference 1

Williams⁽³⁾ performed a similar series of tests with three-block high, concrete prisms. The concrete blocks were 11 5/8" x 3 3/4" x 3 5/8" with an endwise crushing strength of 5000 psi. He used steel, rubber and three types of mortar as the jointing materials. The steel and rubber jointing materials were banded to the concrete blocks with epoxy resin. The results of the tests are presented in Table 1-2.

TABLE 1-2

Jointing Material	Compressive Strength (psi)	
	Mortar	Prism
Steel 1/16" and 1/8"		4750
Rubber 1/8", 1/4" and 1/2"		2200
Mortar	950	4030
Mortar	2040	4420
Mortar	2600	4570

From Reference 3

The failure mechanism of the metal-jointed prisms was by crushing, initiated at any part of the prism and often in several places simultaneously. The rubber-jointed specimens exhibited a splitting failure with a sudden formation of one or two vertical cracks in the inner block initiated from the joint. The prisms with the highest strength mortar tended toward the behaviour of the metal-jointed prisms whereas the low strength mortar prisms failed more like the rubber-jointed prisms.

Assuming that the prime mode of compressive failure in masonry assemblages is tensile splitting, it is now in order to summarise

the variables affecting this phenomenon. Broadly, the physical properties of the mortar, grout and masonry unit, together with their geometric relationships control the compressive strength. Past investigators have tried to relate the compressive strength, the modulus of rupture, the tensile strength and the shearing strength of the masonry unit to the compressive strength of the assemblage. Physical properties determined for mortar materials have been usually confined to compressive and tensile strengths. Previous data concerning the geometric relationships have included slenderness ratio of the assemblage, joint thickness, net area, and coring patterns. In addition to these variables there is the influence of workmanship to be considered. Thus, when broken into its constituents, the compressive strength of a masonry assemblage is a complex matter. In a later section of this chapter the influence of these parameters is reviewed.

Because a multitude of parameters govern the compressive strength of masonry assemblages, a reasonably accurate quantitative estimate of the compressive strength is possible only if these parameters are considered simultaneously. Two attempts have been made to quantitatively determine the compressive strength of masonry prisms and both will be outlined.

Hilsdorf⁽⁴⁾ in 1967 presented an analytical procedure to predict the compressive strength of masonry based on a stress analysis consideration. The analytical result he obtained is compared with experimental results determined in the study. A summary of Hilsdorf's procedure follows. Figure 1-3 shows the development of stresses as they may occur in a single brick within

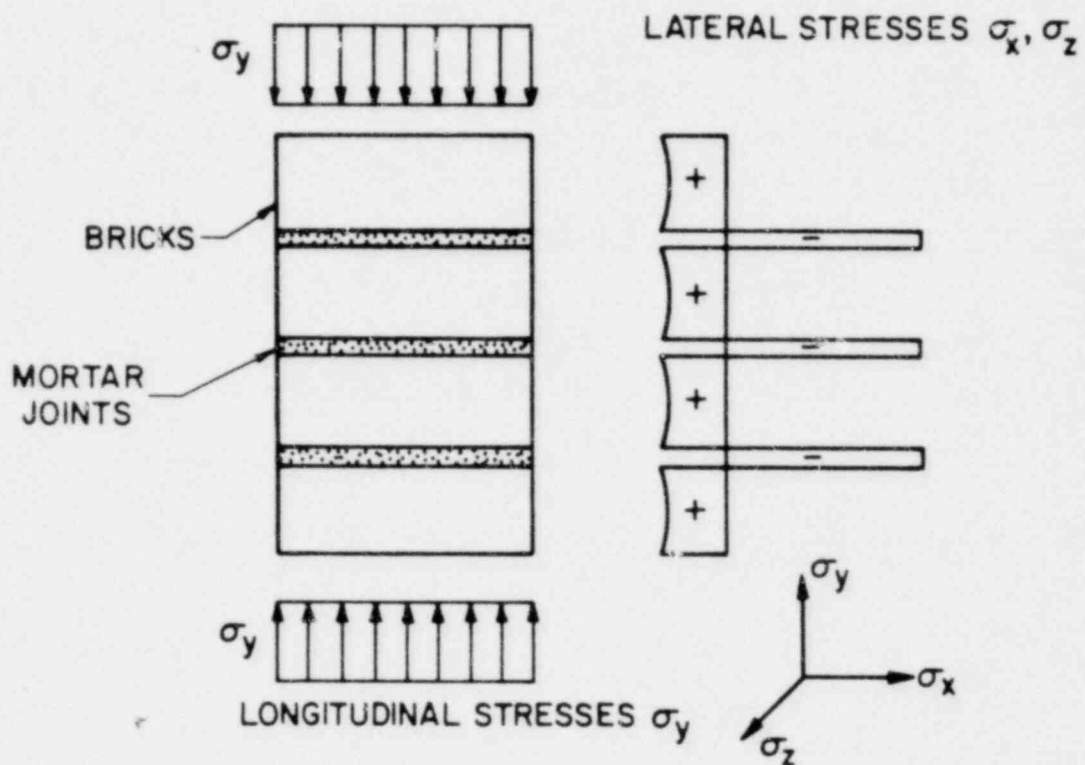


FIGURE 1-3 IDEALIZED STRESS DISTRIBUTION IN A MASONRY UNIT

a masonry unit subjected to axial compression. It is assumed that the lateral tensile stresses in the x and z directions, σ_x and σ_z , are equal. In Figure 1-4 these stresses are given as a function of the local maximum stresses, σ_y , which act in the direction of the external load. Line A in Figure 1-4 represents the failure criterion for the triaxial strength of the bricks and indicates the combinations of compressive stresses σ_y and lateral stresses σ_x and σ_z which will cause local failure or cracking of the brick. The exact shape of this failure criterion curve is presently unknown. If bricks follow Mohr's theory of failure assuming a straight line envelope, then this failure criterion would correspond to a straight line as shown in Figure 1-4. If, as often is the case, the compressive stress being applied to the mortar is greater than the uniaxial compressive strength of the mortar, the mortar has to be laterally confined. Therefore, a certain minimum lateral compressive stress has to act upon the mortar. This stress is counterbalanced by tensile stresses in the uncracked sections of the bricks. These minimum tensile stresses are represented by Line C in Figure 1-4. With increasing external load or increasing local stress, the minimum lateral tensile stress increases. Under the best conditions, failure of the masonry occurs when the lateral tensile strength of the brick is smaller than the stress which is necessary to sufficiently confine the mortar. Therefore, the intersection of the failure criterion Line A and the minimum lateral stress Line C corresponds to the ultimate load of the masonry unit.

Hilsdorf presented the following equation in an attempt to express the failure criterion described above in an analytical form.

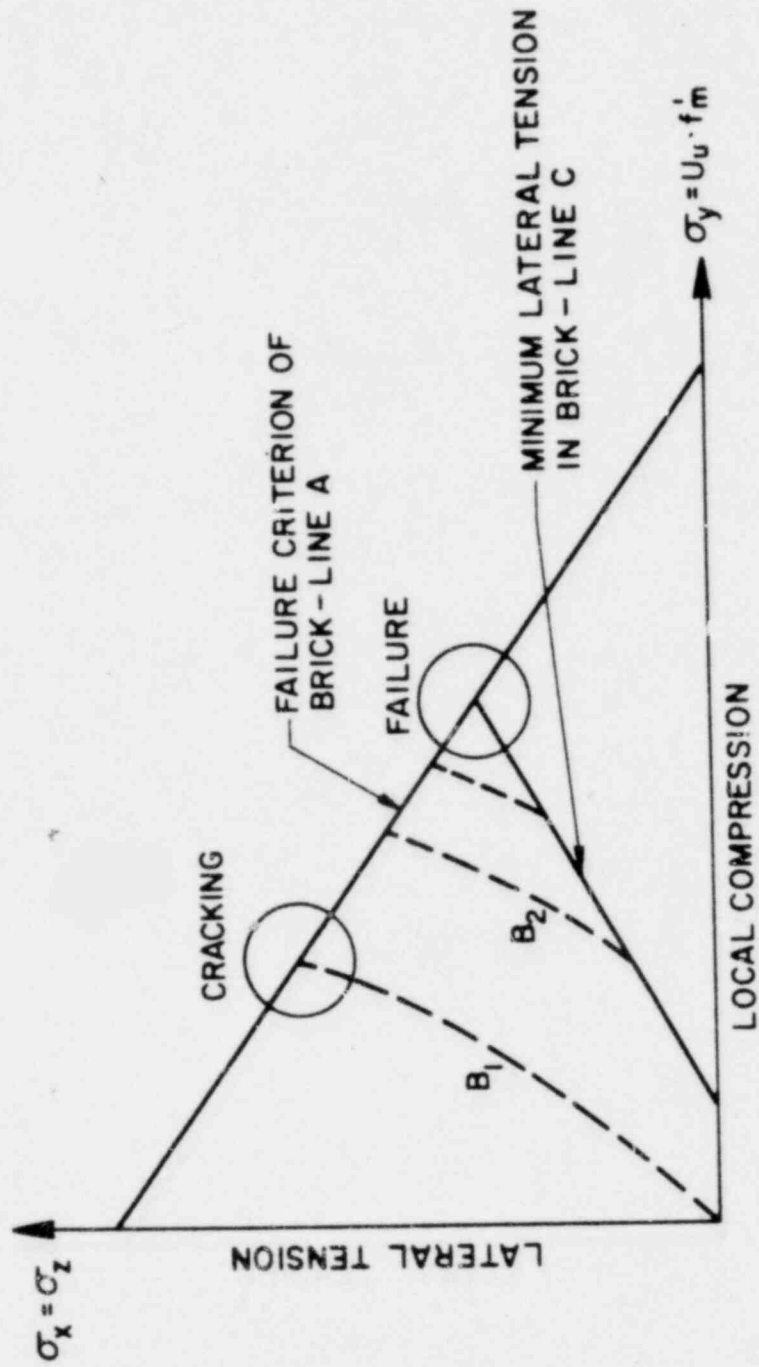


FIGURE 1-4 FAILURE CRITERIA OF BRICK MASONRY

No information on the behaviour of bricks under triaxial stresses was available. Therefore, it was assumed that the failure criterion Line A corresponds to a straight line, which can be represented by

$$\sigma_x = \sigma_z = \sigma_{tb} \left[1 - \frac{\sigma_y}{\sigma_{cb}} \right] \quad (1-1)$$

where σ_{cb} equals the compressive strength of brick and σ_{tb} equals the strength of brick under biaxial tension. Line C corresponds to the minimum lateral tensile stress which has to act in the brick to sufficiently confine the mortar. It depends on the behaviour of the mortar under triaxial compression. As no tests were carried out, it was assumed that the strength of the mortar under triaxial compression is similar to the strength of concrete under triaxial compression. Richart, Brandtzaeg and Brown⁽⁵⁾ in their investigation of the triaxial strength of concrete found that it could be approximated by

$$f'_1 = f'_c + 4.1 \sigma_z \quad (1-2)$$

where f'_1 is the compressive strength of a laterally confined concrete cylinder, f'_c is the uniaxial compressive strength of a concrete cylinder and σ_z is the lateral confinement of the cylinder. If this equation is valid for mortars, then the minimum lateral confinement of the mortar joint is

$$\sigma_{xm} = \frac{1}{4.1} (\sigma_y - \sigma_{cm}) \quad (1-3)$$

where σ_{xm} is the lateral compressive stress in the mortar joint, σ_y is the local stress in the y-direction and σ_{cm} is the uniaxial

compressive strength of mortar. For simplicity let us assume that the lateral stresses σ_x in bricks and mortar joints are uniformly distributed over the height of the bricks and mortar. Then from equilibrium

$$\sigma_{xb} t_b = \sigma_{xm} t_m \quad (1-4)$$

where σ_{xb} is the lateral tensile stress in the bricks, t_b is the height of the brick and t_m is the height of the joint. Substituting this in Equation (1-3) we get an expression for Line C in Figure 1-4.

$$\sigma_{xb} = \frac{t_m}{4.1 t_b} (\sigma_y - \sigma_{cm}) \quad (1-5)$$

From Equations (1-1) and (1-2) the magnitude of the maximum local stress at failure σ_y can be determined by the intersections of Lines A and C.

$$\sigma_y = \sigma_{cb} \frac{4.1 \sigma_{tb} + \alpha \sigma_{cm}}{4.1 \sigma_{tb} + \alpha \sigma_{cb}} \quad (1-6)$$

where

$$\alpha = \frac{t_m}{t_b}$$

Using the non-uniformity coefficient at failure U_u , the average masonry stress at failure can be expressed as

$$\sigma_{ym} = f'_m = \frac{\sigma_y}{U_u} = \frac{\sigma_{cb}}{U_u} \frac{4.1 \sigma_{tb} + \alpha \sigma_{cm}}{4.1 \sigma_{tb} + \alpha \sigma_{cb}} \quad (1-7)$$

$$f'_m = \frac{\sigma_{cb}}{U_u} \frac{4.1 + \alpha \frac{\sigma_{cm}}{\sigma_{tb}}}{4.1 + \alpha \phi}$$

where
$$\phi = \frac{\sigma_{cb}}{\sigma_{tb}} .$$

Therefore
$$\rho = \frac{f'_m}{\sigma_{cb}}$$

$$= \frac{1}{U_u} \frac{4.1 + \alpha \frac{\sigma_{cm}}{\sigma_{tb}}}{4.1 + \alpha \phi}$$

i.e. masonry compressive strength increases with increasing compressive strength of bricks and mortar, with increasing tensile strength of bricks and with decreasing ratio of joint thickness to height of brick. It should be realised that U_u is not a constant but depends on a number of parameters including the joint thickness and the mortar strength.

A comparison of the analytical and experimental strength results are presented in Figure 1-5. The compressive strength of the test specimens could be predicted to within $\pm 20\%$ of the actual values. Hilsdorf concluded by stating that before a general applicability of Equation (1-7) could be recommended, various characteristic properties of masonry have to be established. These are

(1) The coefficient of non-uniformity U_u as a function of
 (a) quality of workmanship; (b) type and compressive strength of mortar; (c) type of bricks; (d) pattern of masonry unit and coring of bricks; (e) thickness of joints.

(2) The behaviour of bricks and mortars subjected to defined triaxial stress states.

(3) A relationship between the strength of bricks under biaxial tension, uniaxial tension and flexure.

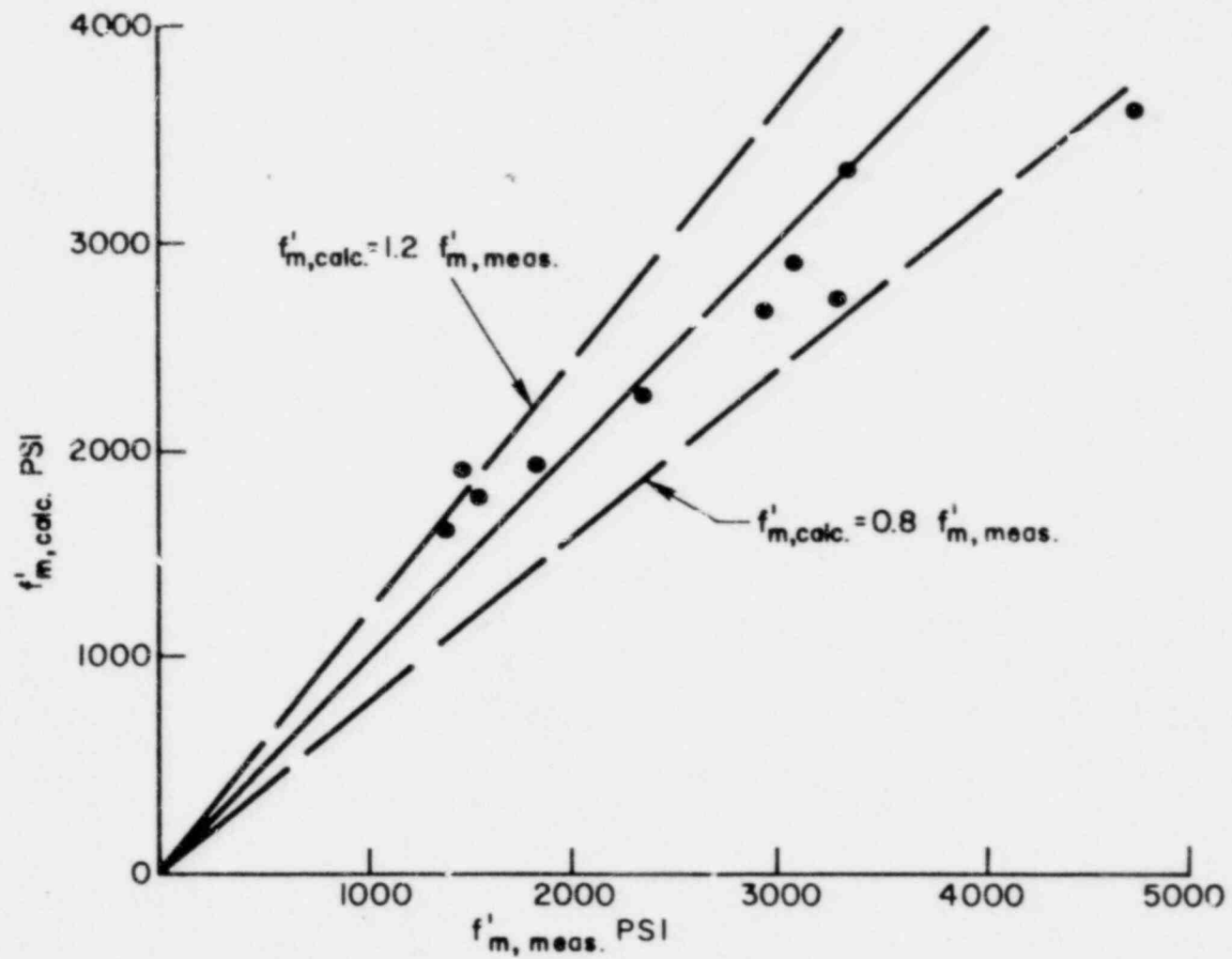


FIGURE 1-5 COMPARISON OF MEASURED AND COMPUTED VALUES OF MASONRY STRENGTH

From Reference 5

A second attempt to quantitatively predict the compressive strength of masonry prisms was presented by Francis, Horman and Jerrems⁽⁶⁾ in 1970. Their analytical procedure was based on a strain consideration and a summary of their derivation follows. The prism shown in Figure 1-6(a) is subjected to an axial compressive stress σ_y . The lateral stresses induced in a central brick and in the mortar joint above or below it are shown in Figure 1-6(b). The extensional strains in the x and z directions in the brick are therefore as follows

$$\begin{aligned} e_{xb} &= \frac{1}{E_b} [\sigma_{xb} + \nu_b (\sigma_y - \sigma_{zb})] \\ e_{zb} &= \frac{1}{E_b} [\sigma_{zb} + \nu_b (\sigma_y - \sigma_{xb})] \end{aligned} \quad (1-8)$$

Similarly, in the mortar joint the extensional strains are

$$\begin{aligned} e_{xm} &= \frac{1}{E_m} [-\sigma_{xm} + \nu_m (\sigma_y + \sigma_{zm})] \\ e_{zm} &= \frac{1}{E_m} [-\sigma_{zm} + \nu_m (\sigma_y + \sigma_{xm})] \end{aligned} \quad (1-9)$$

where E_b is the modulus of elasticity of the brick; E_m is the modulus of elasticity of the mortar; ν_b is the Poisson ratio for the brick and ν_m is the Poisson ratio for the mortar. The lateral expansion is assumed to be the same in brick and mortar. Thus

$$\begin{aligned} e_{xb} &= e_{xm} \\ e_{zb} &= e_{zm} \end{aligned} \quad (1-10)$$

Also, for equilibrium, the total lateral tensile force on the brick

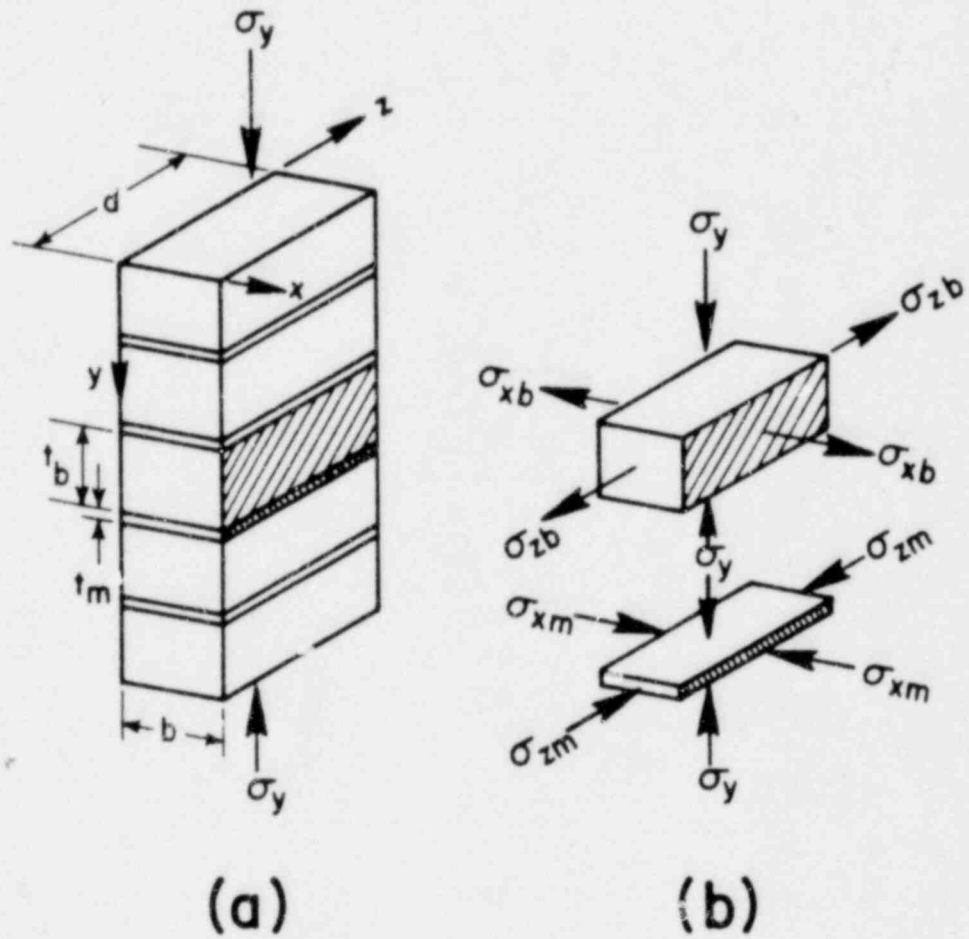


FIGURE 1-6 BRICK AND MORTAR STRESSES DUE TO AN APPLIED COMPRESSIVE LOAD

must be balanced by the total lateral compressive force on the mortar joint, in both the x and z directions. In the x direction therefore

$$\sigma_{xb} d t_b = \sigma_{xm} d t_m \quad (1-11)$$

or

$$\sigma_{xm} = \frac{t_b}{t_m} \sigma_{xb} = \alpha \sigma_{xb} \quad \text{and similarly} \quad (1-12)$$

$$\sigma_{zm} = \alpha \sigma_{zb}$$

where $\alpha = \frac{t_b}{t_m}$ and t_b is the thickness of the brick and t_m is the thickness of the mortar joint. By equating e_{xb} and e_{xm} , and e_{zb} and e_{zm} and substituting for σ_{xm} and σ_{zm} we obtain

$$\sigma_{xb} = \sigma_{zb} = \frac{\sigma_y (\beta v_m - v_b)}{1 + \alpha\beta - v_b - \alpha\beta v_m} \quad (1-13)$$

where $\beta = \frac{E_b}{E_m}$.

The lateral tensile stress σ_{xb} induced in the brick is bound to reduce f'_m , the value of σ_y at which compressive failure occurs; in the limit if σ_{xb} and σ_{zb} were equal to the lateral tensile strength σ_{tb} of the brick, a lateral tensile failure would occur even if the compressive stress σ_y were zero (Point A in Figure 1-7). At the other extreme, the limit would be the compressive stress $f'_m = \sigma_{cb}$, the value necessary to cause failure in the absence of lateral tensile stresses (Point B in Figure 1-7).

The way in which the value of f'_m varies with σ_{xb} and σ_{zb} between these extreme limits is not known for brick but, as

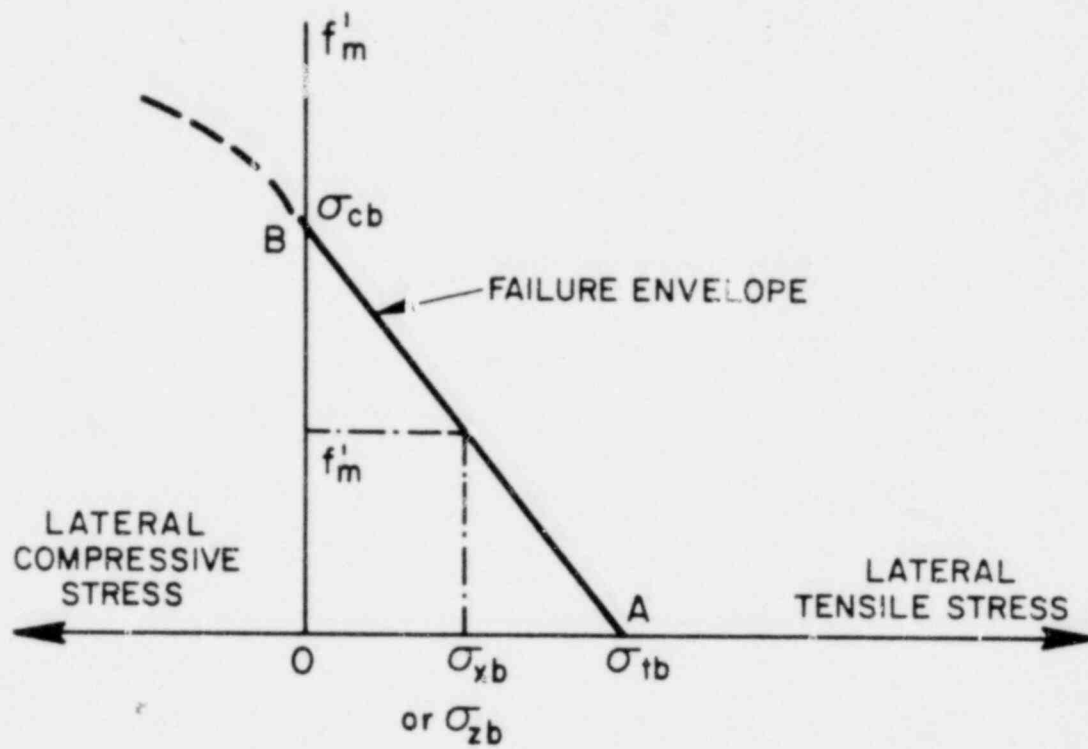


FIGURE 1-7 THEORETICAL ENVELOPE RELATING THE TENSILE AND COMPRESSIVE STRESSES IN BRICK AT FAILURE

Hilsdorf suggested, the Mohr's Theory of failure was assumed. The relationship can be expressed by the equation

$$\sigma_{xb} = \frac{1}{\phi} (\sigma_{cb} - f'_m) \quad (1-14)$$

where

$$\phi = \frac{\sigma_{cb}}{\sigma_{tb}}$$

Substituting this expression for σ_{xb} in the previous equation the following relationship between f'_m and σ_{cb} is obtained.

$$\rho = \frac{f'_m}{\sigma_{cb}} = \frac{1}{1 + \frac{\phi(\beta v_m - v_b)}{(1 - v_b) + \alpha\beta(1 - v_m)}} \quad (1-15)$$

The term $(1 - v_b)$ in the denominator is normally very much smaller than $\alpha\beta(1 - v_m)$ and ρ can be represented with sufficient accuracy, by

$$\rho = \frac{1}{1 + \frac{\phi(\beta v_m - v_b)}{\alpha\beta(1 - v_m)}} \quad (1-16)$$

The authors⁽⁶⁾ conducted an experimental program on the compressive strength of four block high prisms, where the thickness of the mortar joints was the major parameter. Two different types of clay bricks were used in their experimental program, one a solid brick and the other a perforated brick. The theoretical and experimental results are presented in Figure 1-8. The theory indicates a less pronounced difference between the performance of the two types of brick than was found experimentally. The reason for this discrepancy the authors stated probably lies in the method of

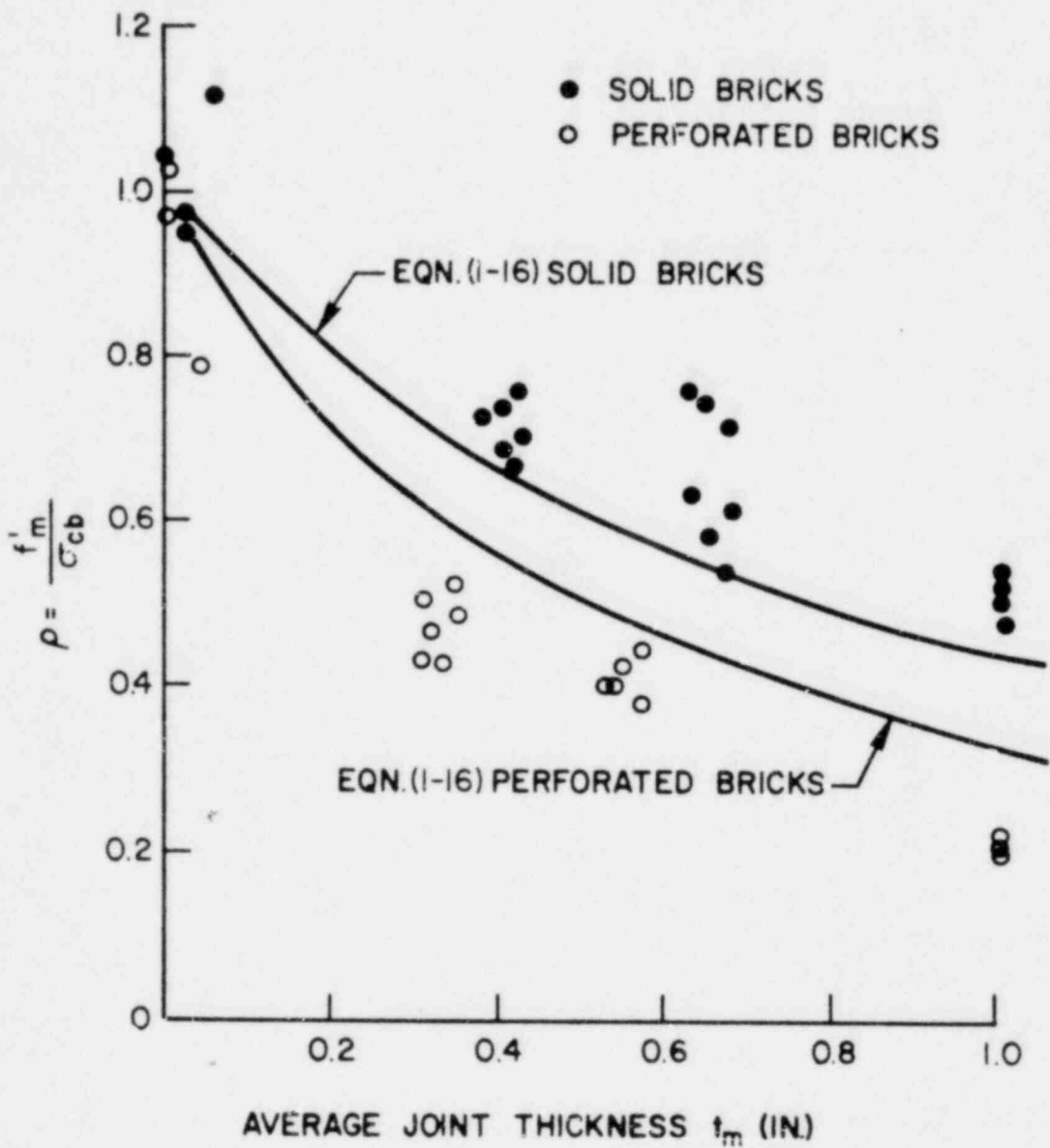


FIGURE 1-8 VARIATION OF ρ WITH JOINT THICKNESS - THEORETICAL AND EXPERIMENTAL RESULTS COMPARED

From Reference 6

estimating the lateral tensile strength, as to date only crude methods are available.

In addition to predicting the effect of joint thickness, the authors stated that their failure mechanism indicates several well-known phenomena associated with the compressive strength of brickwork:

(1) The strength of brickwork should increase with an increase in the compressive strength of bricks and modulus of elasticity of mortar.

(2) A large ϕ , representing bricks having low lateral tensile strengths compared to their compressive strengths, has a deleterious effect on the strength on the prism. This has been verified by an extensive test program recently completed by the British Ceramic Research Association ⁽⁷⁾.

(3) The presence of vertical joints, which have a much lower lateral tensile strength than that of the bricks, may be expected to reduce further the compressive strength under axial load, although this can be improved if good bond strength is achieved.

The authors concluded by saying that although their proposed mechanism of failure does not take into account all the relevant factors, it is a start in the right direction, as it appears to be capable of explaining a number of well-known but apparently unconnected phenomena associated with the behaviour of brickwork in compression.

As both of the methods just presented are approximate it is appropriate to examine the limitations and assumptions of each. Both formulations assume

(a) $\sigma_x = \sigma_z$

(b) There is perfect bond between the brick and mortar interfaces

(c) There is a uniform lateral and vertical stress distribution

(d) Mohr's Theory of Failure applies for brick.

In addition, the formulation of Francis et al⁽⁶⁾ assumes that both brick and mortar have Hookean behaviour up to failure. In the assumed stress distributions of both methods, Figures 1-3 and 1-6, the shear stress at the brick mortar interface is ignored, consequently the failure criteria presented are only valid for an element at the centroidal axis. In addition both methods assume that failure occurs in the brick and propagates through the mortar joint. Both methods ignore the possibility of a failure initiating either in the mortar joint or by bond failure at the mortar, brick interface.

A comparison of the results of the two methods is shown in Figure 1-9 where the ratio $\frac{f'_m}{\sigma_{cb}}$ is plotted against $\frac{t_m}{t_b}$ for the case where $\sigma_{cb} = 4000$ psi, $\sigma_{tb} = 400$ psi, $\sigma_{cm} = 2000$ psi, $\nu = \nu_b = \nu_m = 0.15$, $\beta = \frac{E_b}{E_m} = 2$ and $U_n = 1$.

To improve on the quantitative relationships presented, information on the complex strain distribution over the height of the masonry unit and the mortar joint needs to be determined before better models of the failure mechanism can be developed. In order to include an important section of masonry units - (i.e. reinforced hollow clay and concrete blocks), the effect of the grouted core should also be included in the previous derivations. Generally the

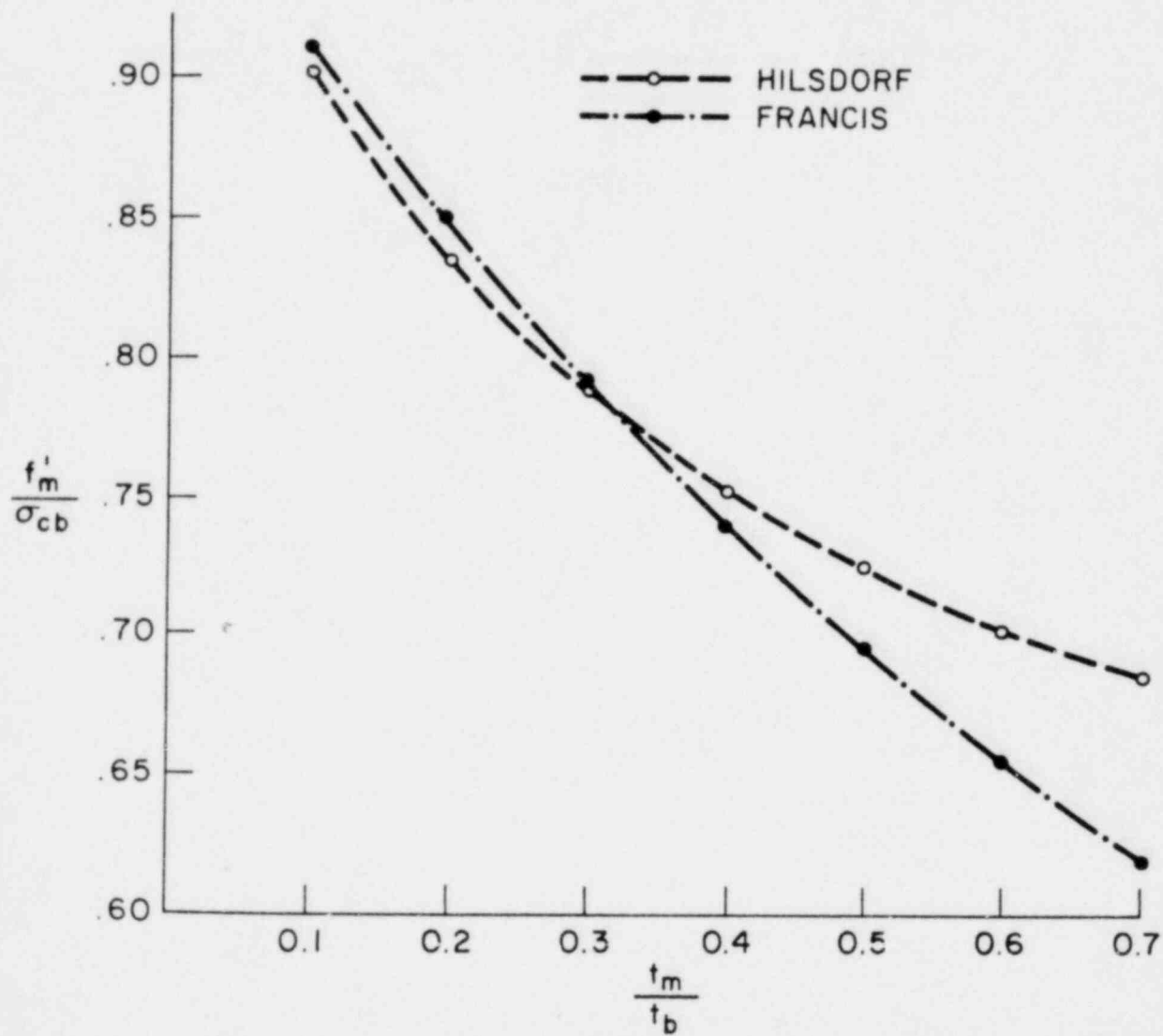


FIGURE 1-9 VARIATION OF THE PRISM STRENGTH WITH THE RELATIVE THICKNESS OF THE MORTAR JOINT AND MASONRY UNIT

weaker, and more flexible grout material will increase the biaxial tension in the masonry units. In addition to the effect of the grout the influence of the vertical mortar joint should be included to simulate the running or common bond construction.

1.2b Variables Influencing Prism Compressive Strength

There are two broad groups of variables that affect the prism compressive strength. The first of these are the factors which interact to modify the stress patterns in prisms under test and lead to apparent masonry strengths which differ from the results obtained on full size samples. These factors comprise prism shape or geometry, prism capping, and type of masonry bond, and are discussed at length in Foster's ⁽²⁾ literature survey. The second group are the factors which interact to determine the actual mechanism of failure of the prism. These include the masonry material, the mortar, the joint thickness and the workmanship, and are discussed at length in Monk's ⁽¹⁾ survey.

(i) Platen Restraint

If a homogeneous isotropic material is tested in compression between platens or capping material of higher elastic modulus than the test specimen, no tensile stresses are induced in the test piece. The higher the modulus of the capping and the higher the friction between the test piece and the platens, the greater the modification to the stress system in a direction requiring increased load to failure. This is the effect of "platen restraint." When platens or capping of lower modulus or stiffness than the test material are used, the test piece is subjected

to tensile stresses arising from the greater lateral strains of the platens or capping. For rigid masonry materials which are substantially weaker in tension than in compression, this tensile splitting effect can lead to a considerable reduction in the load necessary for failure.

(ii) Effects of Prism Shape

The effect of platen restraint is to give an erroneously high estimate of masonry compressive strength. The use of such results in design is potentially dangerous and must be avoided. It would be expected that, in the event of platen restraint the greater the height or number of courses, the more the masonry in the center of the specimen would be free from artificial stresses. An initial decrease in apparent strength as the number of courses increased, tending toward a constant strength limit would be expected. This behaviour pattern is amply demonstrated by the literature with regard to both the failure mode and apparent strength. Nominal 9 in cubes have demonstrated initial splitting followed by shear^(8,9) clearly indicating mixed stress patterns. Sinha and Hendry's⁽¹⁰⁾ results indicate that the shear strength of the brick markedly influence the behaviour of 9 in x 9 in prisms as the number of courses decrease.

A number of investigations have shown that increasing the height of the specimen or number of courses leads to lower failure loads^(2,10-13). The achievement of constant strength above about 4 courses for single wythe prisms of brick⁽¹²⁾ and of concrete block⁽²⁾, and above an h/d ratio of about 5 for 2 and 3 wythe prisms⁽¹³⁾, was also demonstrated. A minimum number of

four courses has been recommended for both brick and concrete masonry prisms in Belgium⁽¹⁴⁾.

(iii) The Effect of Capping

A variety of materials have been used between the steel platen of the testing machine and the masonry specimen to achieve uniform distribution of applied load. There is substantial evidence that considerable modification of the stress pattern occurs with prisms of low h/d ratios or few courses. West et al^(15,16) tested 9 in cubes using various combinations of mortar and plaster capping, and plywood and strawboard packing. Platen restraint led to apparent strengths 50% higher than those obtained with mortar capping on both ends. Len zner⁽¹⁷⁾ measured lateral strains in the bricks in 9 in cubes, while under compression. Capping with mortar was shown to increase the lateral strain by 75% over the value obtained using plywood only. Yokel et al⁽¹⁸⁾ obtained strengths 44% lower when plaster was substituted by fibreboard as capping on 3-course concrete masonry prisms.

It is clear that on prisms of low h/d ratios, the end preparation of the samples can introduce considerable uncertainties in the test results; these end effects can be avoided by the use of prisms of high h/d.

(iv) The Effect of Bond Type

Brickwork in vertical compression fails by vertical splitting induced by tensile forces in the biaxial state of stress. It would therefore be expected that prisms with vertical mortar

joints simulating common bond, would better represent full size brickwork and give lower strengths than stack bonded prisms. While it has been shown in some specific cases that stack bonded prisms are no stronger than common bonded prisms^(19,20) it would appear unwise to accept this as generally true⁽¹²⁾. Stafford-Smith and Carter⁽²¹⁾ demonstrated that peak values of horizontal tensile stress in compression loaded walls are associated with the vertical joints. The higher Young's Modulus obtained for stack-bonded prisms is an indication of different performance, and lower strengths for double wythe prisms compared with single wythe indicate the potential significance of vertical mortar joints⁽²²⁻²⁵⁾. It is concluded that the bond type in the prism should simulate the bonding in the structure as closely as possible.

(v) Masonry Unit Strength

Many investigators have tried to relate masonry unit strength to wall or prism strength for a given mortar. The so-called "efficiency" of the wall or prism has been expressed as the ratio of wall or prism strength to the masonry unit strength. The influence of the method of testing on the mode of failure of a single unit (shear failure) as compared to that of the unit in a wall or prism (tensile splitting) has not been fully recognized in this effort. The most comprehensive compilation of brick masonry compressive data was prepared by the Building Code Committee of the U. S. Department of Commerce in 1926⁽²⁶⁾, covering the results of 708 individual tests. From this work no notable consistency between brick strength and masonry strength was observed.

Besides brick compressive strength the correlation of other brick strength properties with wall strength has been investigated. The 1928 NBS program⁽²⁷⁾ was probably the most extensive attempt in this matter. Ratios of the following brick properties relative to wall strength were computed;

Compressive strength of half brick flatwise
 Compressive strength of half brick edgewise
 Modulus of rupture of brick flatwise
 Tensile strength of brick
 Shearing strength of brick.

In the conclusions to the NBS work it is stated, "The strengths of the solid walls were more clearly related to the shearing strengths of the bricks than to any other strength property measured. The compressive strength of the half bricks flatwise appeared to be the next best measure and was better than the compressive strength on edge, modulus of rupture and the tensile strength of the bricks." Bragg⁽²⁸⁾ obtained good correlation with wall strength using either the compressive strength or the transverse strength of the units. On the other hand, data from the SCPRF National Testing Program⁽²⁴⁾ showed some correlation between brick compressive strength and prism strength and very little between brick modulus of rupture and prism strength.

To summarise, the present knowledge neither proves nor disproves the fact that the compressive strength flatwise of a half unit is a reasonable measure of wall or prism strength. Masonry compressive strength will be determined by some combination of unit properties together with mortar properties.

Given a wide enough range of products, unit properties will tend to correlate with one another. Thus a statistical correlation will be expected between any one unit property (e.g. compressive or tensile strength) and compressive strength of masonry made from the same units. Such correlations have indeed been obtained⁽²⁹⁾. It is emphasized that such relations are statistical and not functional. Therefore they may not be a sound basis of prediction in specific cases.

(vi) Mortar

Mortar proportions have been traditionally expressed as paste-sand ratios that vary from 1:2 1/4 to 1:3 by volume. This is based, in part, on the amount of paste that is necessary to approximately fill the voids. Given a series of uniform spheres, the theoretical per cent of voids can vary from 26 to 48 percent, depending on the scheme of packing. Experiments carried out on actual uniform sphere systems give characteristically a void ratio of 38 percent. Actual sands have void ratios that will vary from 25 to 40 percent. This suggests that some optimum packing is possible through sand gradation. Experimentally, the lowest void volume achieved is about 16.8 percent, using a mixture of particles as follows:

TABLE 1-3

	Percent of Total Volume	Relative Diameter
Coarse	70	50.5
Medium	20	8.0
Fine	10	1.0

Requirements for aggregate to be used in masonry mortar include the following proportions and relative diameters, based on ASTM C-144:

TABLE 1-4

	Percent of Total Volume	Relative Diameter
4 - 8	5% max	25 - 12.5
8 - 100	70% - 100%	12.5 - 2.0
100 - 200	15% - 25%	2.0 - 1.0
greater 200	10% max	< 1.0
Fineness Modulus = 1.6 to 2.5		

Thus it is observed that natural sands used for masonry mortars may have particle size distributions which are different from that needed for optimum packing. Hence, the relatively high percent of voids in sands requires the amount of paste mentioned above, together with the water, to produce a workable mix. For some standard types of mortar the following water cement ratios have been found necessary to produce workability for an average masons hand⁽³⁰⁾.

TABLE 1-5

ASTM Mortar Type	W/C Ratio	Average Flow
M(1C:1/4 L : 3S)	0.74	124.3
S(1C:1/2 L : 4 1/2 S)	1.13	130.2
N(1C:1 L : 6S)	1.64	122.7

The minimum required strengths of standard mortars, moist cured as prescribed in ASTM C-270 are

TABLE 1-6

ASTM Mortar Type	28-day Strength
M(1C:1/4 L : 3S)	2500 psi
S(1C:1/2 L : 4 1/2 S)	1800 psi
N(1C:1 L : 6S)	750 psi
O(1C:2 L : 9S)	350 psi
K(1C:4 L : 15S)	75 psi

An actual series of tests produced the following values ⁽²⁴⁾.
The sand was varied from 2 1/4 to 3 parts by volume.

TABLE 1-7

ASTM Mortar	28-day	Compressive Strength
Type	1:2 1/4	1:3
M	7392 psi	5358 psi
N	3663 psi	2479 psi
K	643 psi	363 psi

It is seen that a considerable difference in mortar strength can result by varying the amount of sand. The influence of sand gradation is seen in the following data ⁽²⁵⁾ obtained on a type N mortar with a 1:3 paste-sand ratio.

TABLE 1-8

Sand Gradation	28-day Strength	
	Compression	Tension
Fine	1869 psi	262 psi
Medium	2445 psi	380 psi
Coarse	2713 psi	333 psi
Coarse to Fine blend	2382 psi	287 psi
Fine to Coarse blend	2290 psi	327 psi

The effect of sand gradation is nowhere near as marked as that of paste-sand volume ratios.

The influence of the mortar formulation on the prism strength is very marked. Table 1-9 shows typical influences of mortar composition on prism strengths⁽²⁰⁾.

TABLE 1-9

Effect of Mortar Compressive Strength on Ultimate Compressive Strength of 4-in Brick Prisms*

Mortar			Prisms		
Type	Proportions by Volume	Compressive Strength** psi	n	Mean Compressive Strength, f'_m psi	Strength Ratio
M	1C:1/4 L : 3S	2503	5	5805	1.06
S	1C:1/2 L : 4 1/2S	1292	5	5497	1.00
N	1C:1 L : 6S	579	5	3900	0.71
O	1C:2 L : 9S	262	5	2905	0.53

*4 by 8 by 16-in prisms built with one type of brick (11,771 psi) and 3/8-in joints

**28-day air-cured cube strength

From Reference 20

Roughly, the prism strength is reduced by more than half as one goes from type M to type O ASTM mortar. Because the type M mortar is about 12 times as strong as the type O mortar, it is obvious that prism strength is not directly controlled by the mortar strength.

Greenley⁽³¹⁾ and Watstein and Allen⁽³²⁾ considered the effect of additives on the prism and mortar strengths. Greenley

added a chemical additive which substantially increased the strength of the mortar and consequently the prism strength. The results are presented in Figure 1-10. The increased mortar strength had a greater effect on the high-strength bricks. Watstein and Allen considered the effect of high bond organically modified mortars and concluded that the average compressive strength of standard prisms built with high bond mortar was 37 percent greater than those built with conventional mortar; the secant moduli of elasticity were 25 percent greater.

(vii) Joint Thickness

The influence of joint thickness relative to the height of the masonry unit has been recognised as a significant parameter of the prism strength and was included in both attempts to quantify the compressive strength of prisms. Figure 1-8 from reference 6 and Table 1-10 from reference 20 indicate the magnitude of the effect for various masonry units.

TABLE 1-10

Mortar Joint Thickness in ²	Prisms ¹ Compressive Strength ³	Strength Ratio
1/4	6550 psi	1.00
3/8	5850 psi	0.89
1/2	4900 psi	0.75
5/8	4050 psi	0.62
3/4	3150 psi	0.48

¹ Prisms 4 in thick, 8 in long and 16 in high

² Type S mortar used in all specimens

³ Values taken from a faired curve derived from two separate plots.

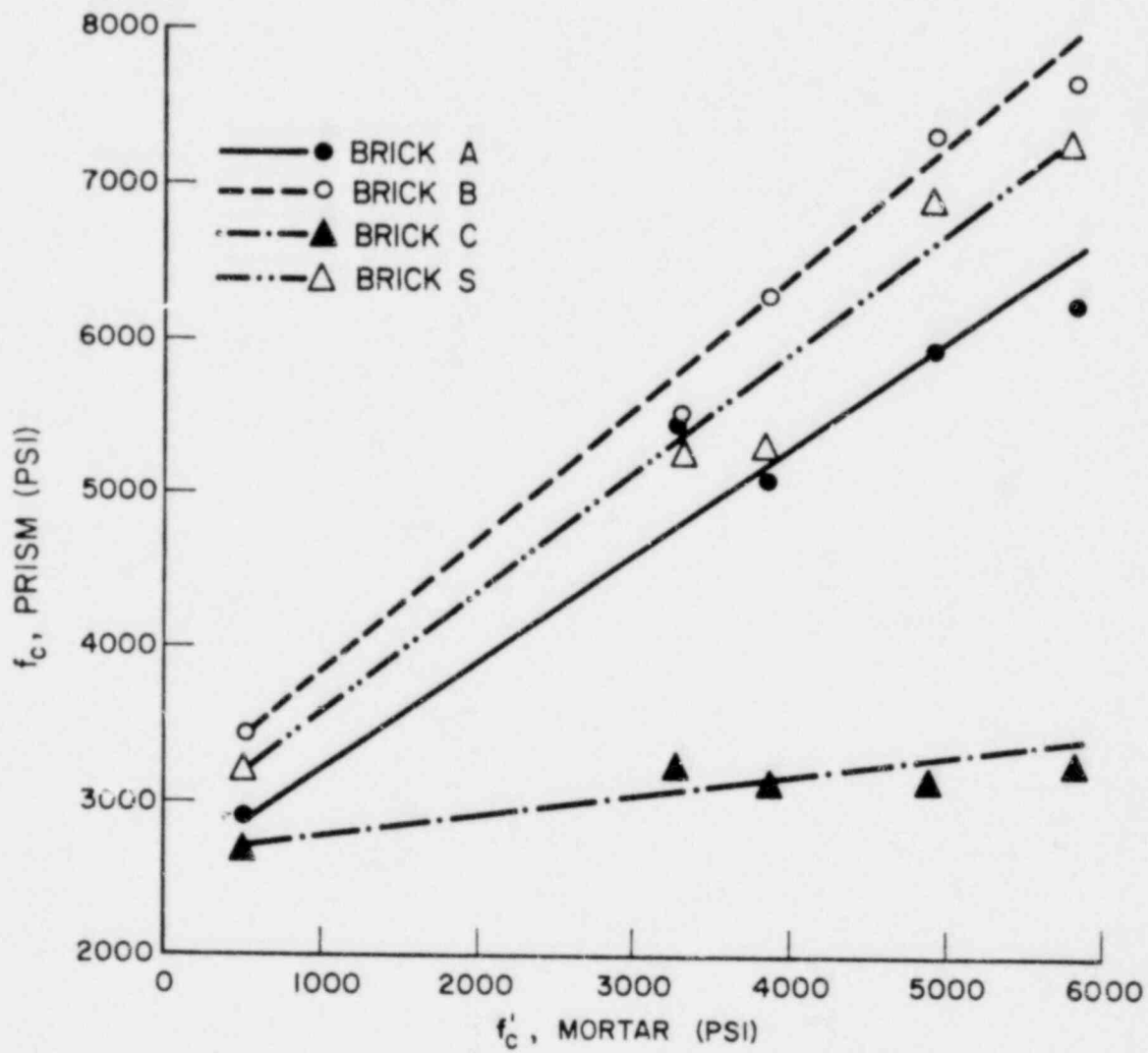


FIGURE 1-10 PIER COMPRESSIVE STRENGTH VS. MORTAR COMPRESSIVE STRENGTH

From Reference 31

(viii) Workmanship

In common with other building materials, the strength of clay masonry is affected by workmanship. The deep furrowing of bed joints and the partial filling of vertical head and collar joints are practices that reduce strength to some degree. Thick joints as discussed in the previous section will lower strength. Addition of line above specification limits to improve workability will also result in strengths that may be below design expectations.

Code recognition of the influence of workmanship is shown in the 1964 Edition of the Uniform Building Code which reduces allowable stresses in many categories by a factor of two for uninspected work as compared to inspected work. From time to time, investigators have tried to compare the effects of various kinds of workmanship on masonry strength. Most of this work has been sporadic and inconclusive. However, a serious attempt in this area of investigation was made as part of the 1928 wall testing program at the National Bureau of Standards⁽²⁷⁾. Two "grades" of workmanship were used. "Commercial" or "ordinary" workmanship was characterized by complete absence of vertical joint filling, deep grooving of horizontal joints and comparatively high speed laying. In the "supervised" or "superior" workmanship these characteristics were avoided.

For wall specimens built with brick with strengths from 3000 to 4000 psi, superior workmanship resulted in masonry strengths approximately 60 to 80 percent greater than for specimens built with ordinary workmanship. For specimens built

with an 8700 psi brick the increase was only about 30 percent. A rather limited investigation in the SCPRF laboratories⁽³³⁾ considered the effect of workmanship on the strength of 8 in. brick prisms built with an 11,866 psi brick and ASTM type S mortar. In this case, superior workmanship resulted in an increase in prism strength of about 14 percent.

The filling of head and collar joints, the avoidance of deeply furrowed bed joints and the use of as thin a joint as permitted by the dimensional variations of the units are all workmanship factors that will improve the strength of the masonry. Safety factors should reflect the use of good supervised workmanship that is characteristic of the well-designed and engineered use of any structural material. Where uninspected, workmanship is to be permitted, appropriate design reduction factors should be employed. While the available data do indicate that this factor decreases with increasing brick strength, the data are too few to derive definite functional relations by statistical methods.

1.3 Tensile and Bond Strength Tests

The tensile and bond strength tests, although not as extensively studied as the prism compressive test, are equally as important. One of the major difficulties faced by investigators in this area is the development of test techniques that determine properties appropriate for the analysis of larger elements. Because of this difficulty many different testing techniques have been proposed and used in various programs with a consequent lack of correlation among them. There are basically three broad areas of interest: first, the tensile strength of the individual masonry unit; second, the bond strength between the mortar joint and the masonry unit; and third, the tensile strength of a small test specimen, such as a circular disc, indicating the combined behaviour of the components.

1.3a Tensile Strength of Individual Units

Many investigators have included the results of the standard ASTM C-67 modulus of rupture test in their reports but few have compared it with other methods of obtaining the tensile strength of an individual unit. Thomas and O'Leary⁽³⁴⁾ conducted an extensive investigation in which five methods of obtaining the tensile strength of clay bricks were compared. The three major types of tests considered in the study were the flexure or modulus of rupture test, the direct tensile test and an indirect tensile test. In addition two different types of tests were performed on core samples taken from the full brick.

The standard ASTM C-67 flexure or modulus of rupture test consists of supporting the unit on two roller supports 7 inches

apart and loaded at mid-span. The modulus of rupture is calculated from the formula

$$\frac{3wl}{2bd^2}$$

where w is the maximum load, l the distance between supports, b the width of the specimen and d the depth. The direct tensile test consisted of gluing plates onto the ends of the unit and applying a direct axial load. The indirect tensile test was based on a study by Kosenhaupt, Van Riel and Wyler⁽³⁵⁾. They studied the plane strain problem involved when compressive forces are applied along opposite faces of a concrete cube. Using mathematical and photoelastic techniques they showed that the tensile stress was fairly uniform along the plane of the load application and given by

$$\frac{0.648P}{dl}$$

where P is the compressive force, d the equivalent diameter and l the length of the specimen. Thomas and O'Leary used this method to obtain the indirect tensile strength of the brick units. Indirect and expanding plug tests were performed on core samples taken from the center and end of the brick units. The authors used two basic brick units for their program, a solid clay brick and a perforated clay brick with three 1-inch diameter holes. The indirect tensile strength calculated on the width of the bricks produced a higher stress than on the length. For the solid units the ratio of the tensile splitting strength to compressive strength expressed as a percentage varied from 8.9 to 10.9, whereas for the perforated unit

the range was 7.9 to 10.3. Cores cut from the ends of the extruded bricks produced lower strengths than cores cut from the center of the bricks. The authors postulated that the reason for the lower strength is almost certainly due to the poorer packing of the unfired clay at the ends of the brick during the extrusion process. The mean tensile strength of the center cores compares reasonably well with the strength obtained by splitting the unit across the width.

The direct tensile strength of bricks measured when the units are pulled apart by an axially applied load is thought to be of little value because a) it is an extremely slow test requiring 24 hours to cure before testing can take place, b) accidental eccentricity of loading is extremely difficult to avoid, and c) for extruded bricks, if tested on the full length, failure will almost certainly occur adjacent to the end plates, or if the length of the unit is reduced by cutting each end prior to fabricating the test piece the least tensile strength of the remainder of the unit will be measured rather than the tensile strength at a randomly selected position.

Because of the difficulty involved in determining the tensile strength of the large class of hollow clay and concrete units the California Concrete Masonry Technical Committee adopted the direct tensile strength test as part of their standards for the California Quality Control Specifications. Although the same problems as outlined by Thomas and O'Leary exist, it is believed that this is the best method available at present for determining the tensile

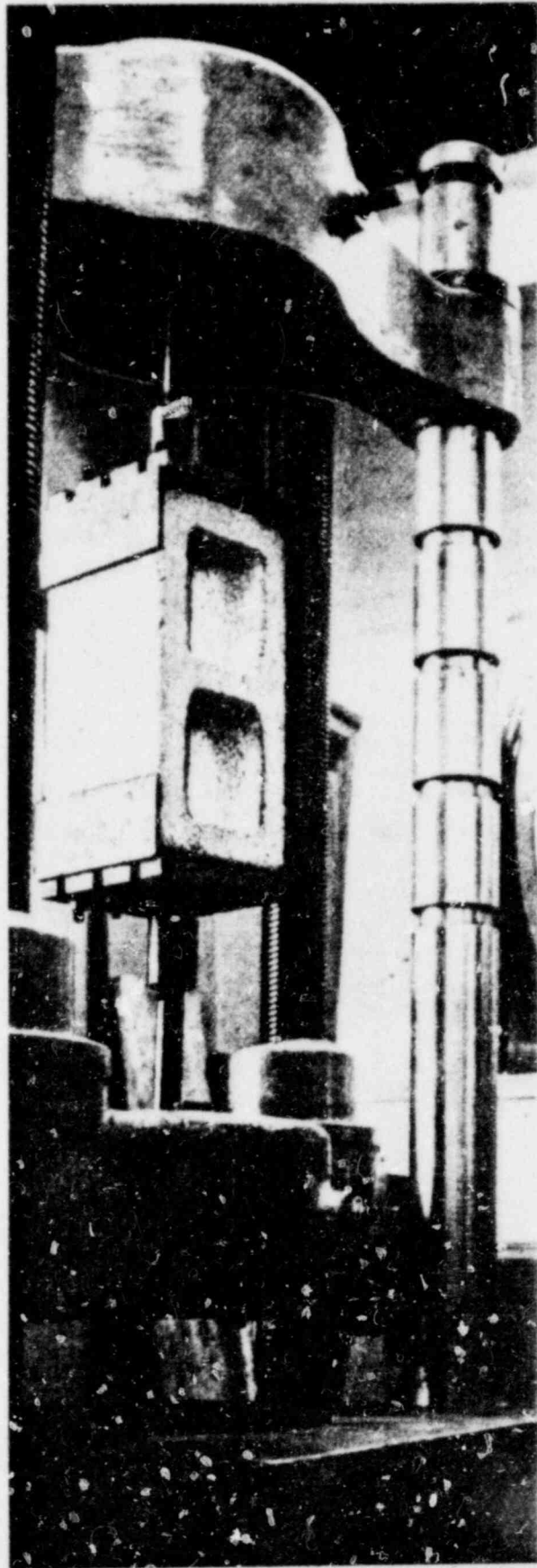


FIGURE 1-11 TENSILE STRENGTH TEST

strength of hollow units. A photograph of the test setup is shown in Figure 1-11.

In conclusion, it is clear that more comparative experimental studies are required to determine reliable, accurate and relevant information on the tensile strength of both solid and hollow masonry units.

1.3b Bond Strength Tests

The bond strength between the mortar and masonry unit consists of two major components. The first, the tensile bond strength, is the strength developed when a tensile load normal to the bonded faces is applied. The second, the shear bond strength, is the strength developed when a mortar masonry joint is subjected to a shear load. Several experimental programs have investigated various facets of the bond strength between the mortar joint and the masonry unit. Most of the studies have used solid clay units as the masonry material although Sahlin⁽⁴⁴⁾ has reported on some concrete masonry tests. Three of the most extensive studies^(39,41,42) were performed in association with shear tests on piers in order to establish failure criteria for the pier under combined stress conditions.

In adopting cross brick couplets (Fig. 1-12) for bond tension tests, Polyakov⁽³⁶⁾ found difficulty in fixing the application of load in the center of the couplet, and also in laying the bricks. He made the assembly in the form of a cube, shown in Figure 1-12, made of two halves mortared together and pulled apart by special clamps. Other research workers, Pearson⁽³⁷⁾ and Kampf⁽³⁸⁾ found

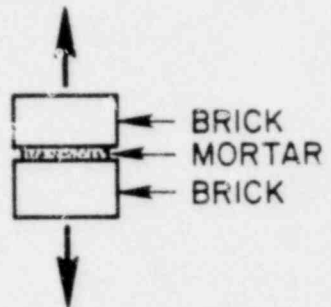


FIGURE 1-12 BRICK COUPLET TEST

the test quite satisfactory and it is now generally accepted that cross brick couplets give satisfactory results for bond in tension. Pearson used selected bricks for the top and, for economy, a common unselected brick for the bottom. Before placing the mortar for assembly he treated the lower brick with high early strength cement grout to ensure failure on top of the joint. This of course is contrary to the practice at site. It would appear that Pearson's results for bond tension were higher than normal because the mortar was prevented from losing any moisture to the bottom brick.

Davison⁽⁴⁵⁾ found that the bond strength between the mortar joint and the upper brick was less than that between the mortar joint and the lower brick. He attributed this to the fact that before laying, the upper brick moisture from the mortar will be absorbed into the lower brick. Therefore the consistency of the mortar is less when the upper brick is hard due to this loss of moisture.

Benjamin and Williams⁽⁴¹⁾ reported on a comprehensive set of couplet tests. The various test arrangements for the different stress combinations are shown in Figure 1-13 and Table 1-11 provides a summary of the compressive and tensile strengths of the different mortars. Table 1-12 provides results for couplet bond tension tests ($\theta = 0$ in Figure 1-13) for the same mortars considered in Table 1-11. It is significant to note that when the mortar bond to the brick was placed in direct tension, failure occurred at about 20 percent or less of the mortar tensile strength or at not more than 2 percent of the ultimate compressive strength.

The results of the authors' couplet tests presented in Table 1-13 and Figure 1-14 show that the shear strength of the mortar

TABLE 1-11
PHYSICAL PROPERTIES OF MORTAR

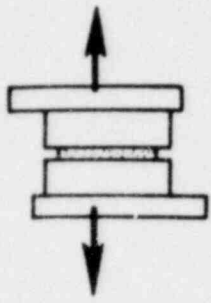
Mortar Proportions ^a	28-day Compress. Strength (psi)	28-day Tensile Strength (psi)	Mortar Flow (%)	Mortar Retentivity (%)	Reference
1C:0.25FC:3S	3260 ^c	402	95-100	77	Stanford Shear Wall Project
1C:0.25L:3S	3050	300	95-100	--	"
1C:0.50L:4.5S	1200	145	b	63	V.P.I Tests
1C:1L:6S	500	55	b	73	"
1C:0.25L:3S	2500	225	b	55	"

From Reference 41

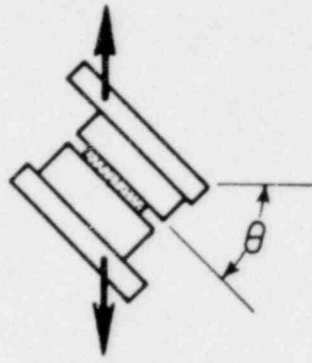
- a. Proportions by dry loose volume.
- b. Depends on water percentage.
- c. Wall specimens were actually tested at an age of 14 days when the mortar strength was approximately 2500 psi.

TI

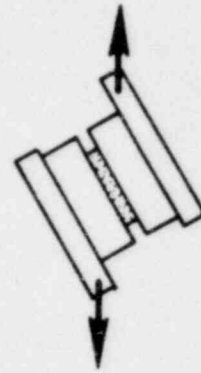
COI
SH



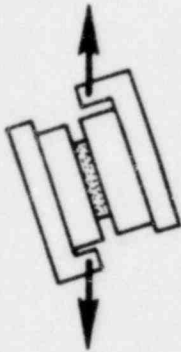
TENSION
 $\theta = 0^\circ$



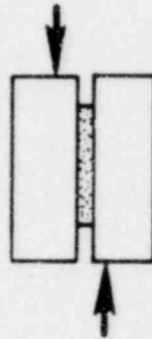
TENSION AND SHEAR
 $\theta = 45^\circ$



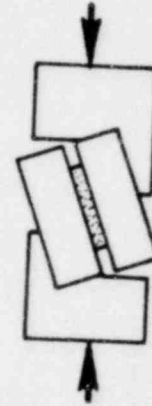
TENSION AND SHEAR
 $\theta = 60^\circ$



TENSION AND SHEAR
 $\theta = 75^\circ$



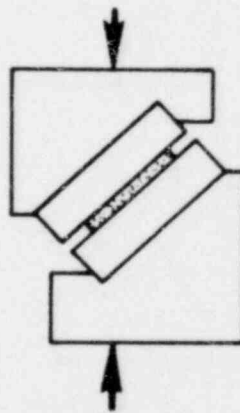
SHEAR
 $\theta = 90^\circ$



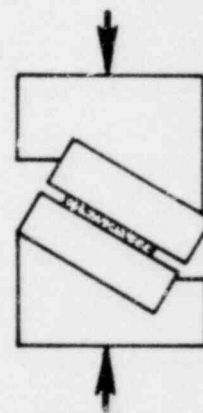
COMPRESSION AND SHEAR
 $\theta = 105^\circ$



COMPRESSION AND SHEAR
 $\theta = 120^\circ$



COMPRESSION AND SHEAR
 $\theta = 135^\circ$



COMPRESSION AND SHEAR
 $\theta = 150^\circ$

FIGURE 1-13 ARRANGEMENTS FOR COMBINED STRESS TESTS

From Reference 41

TABLE 1-12
COUPLET BOND TENSION STRENGTHS

TEST CONDITIONS							BOND STRENGTH PSI
Mortar Proportions	Mortar Flow	Mortar Retentivity	Brick Type	Brick Suction 8bm.	Reference	Number of Specimens	
1C:0.25F.C.:3S	95-100	77	1	corrected to zero by 1/2 hr. soaking	Stanford Project	10	high 42.5 low 24.7 avg. 37.1
1C:0.25L:3S	95-100	not measured	1	corrected to zero by 1/2 hr. soaking	"	9	high 36.2 low 14.3 avg. 25.1
1C:0.25L:3S	95-100	77	1	corrected to zero by 24 hrs. soaking	"	10	high 51.3 low 33.0 avg. 43.5
1C:0.25L:3S	100-110	56	2	10 - 20	V.P.I. Tests	8	high 36.0 low 1.0 avg. 18.7
1C:0.50L:4.5S	100-110	63	2	10 - 20	"	8	high 52.0 low 23.0 avg. 40.3
1C:1L:6S	100-110	73	2	10 - 20	"	8	high 54.0 low 22.0 avg. 35.2
1C:0.50L:4.5S	95-105	66	3	10 - 20	"	12	high 59.0 low 26.0 avg. 40.8
1C:0.15L:3S	-	--	4	brick set wet	Canadian Tests	5	high 88.0 low 43.0 avg. 65.0

From Reference 41.

joints is greatly affected by the normal stress acting on the joint. An average coulomb relationship for the strength of the mortar joint is given by the authors as follows

$$\sigma_{xy} = \sigma_{xy0} + 1.1 \sigma_y \quad (1-17)$$

where σ_{xy} is the shearing resistance of the mortar joint, σ_{xy0} the shearing resistance of the mortar joint for zero normal stress and σ_y the normal stress acting on the mortar joint, (compression positive). An average value of σ_{xy0} of about 230 psi is indicated from Figure 1-14. In this equation σ_{xy} is the maximum shearing stress developed on the section and should be multiplied by 2/3 to obtain the average stress on the joint. Because the failure envelope plotted in Figure 1-14 is non-linear Equation (1-12), is only applicable when the normal stress is compressive and greater than 60 psi. For compressive stresses below 60 psi and all tensile stresses the data in Figure 1-14 indicate that the following relationship is more applicable.

$$\sigma_{xy} \text{ (max)} = 150 + 3 \sigma_y \quad (1-18)$$

$$\sigma_{xy} \text{ (average)} = 100 + 2 \sigma_y \quad (1-19)$$

The authors made two observations concerning Equation (19). First, when $\sigma_{xy} = 0$, σ_y becomes -50 psi. This would indicate a tensile bond failure of the joint at a value which is in approximate agreement with the values reported in Tables 1-12 and 1-13. Second, for the normal stress σ_y on the joint equal to zero, the equation

TABLE 1-13

AVERAGE RESULTS OF COMBINED STRESS COUPLET TESTS
BRICK: STIFF MUD, SIDE CUT, CLAY, VACUUM TREATED

Mortar	Test Angle degrees	Ultimate Shear Stress	Ultimate Normal Stress	Number of Specimens
		$\frac{3}{2} \frac{P}{A} \sin \theta$ psi	$\frac{P}{A} \cos \theta$ psi	
A-1(14) high quality	0°	0	38.8	5
	45°	39.5	26.3	5
	60°	57.7	22.3	5
	75°	82.5	15.8	5
	90°	148	0	5
	105°	307	64.2 c*	6
	120°	451	174 c	5
	135°	927	618 c	4
A-2(14) medium quality	0°	0	32.0	5
	45°	34.5	23.0	5
	60°	47.2	18.2	5
	75°	72.7	12.9	5
	90°	109	0	5
	105°	279	49.9 c	5
	120°	364	145 c	6
	135°	801	534 c	5
B(14) low quality	0°	0	30.7	5
	45°	35.5	23.7	5
	60°	63.7	24.5	5
	75°	74.2	13.3	5
	90°	118	0	5
	105°	319	56.8 c	5
	120°	393	151 c	5
	135°	904	602 c	5

*The letter "c" emphasizes that normal stress is compressive.

From Reference 41.

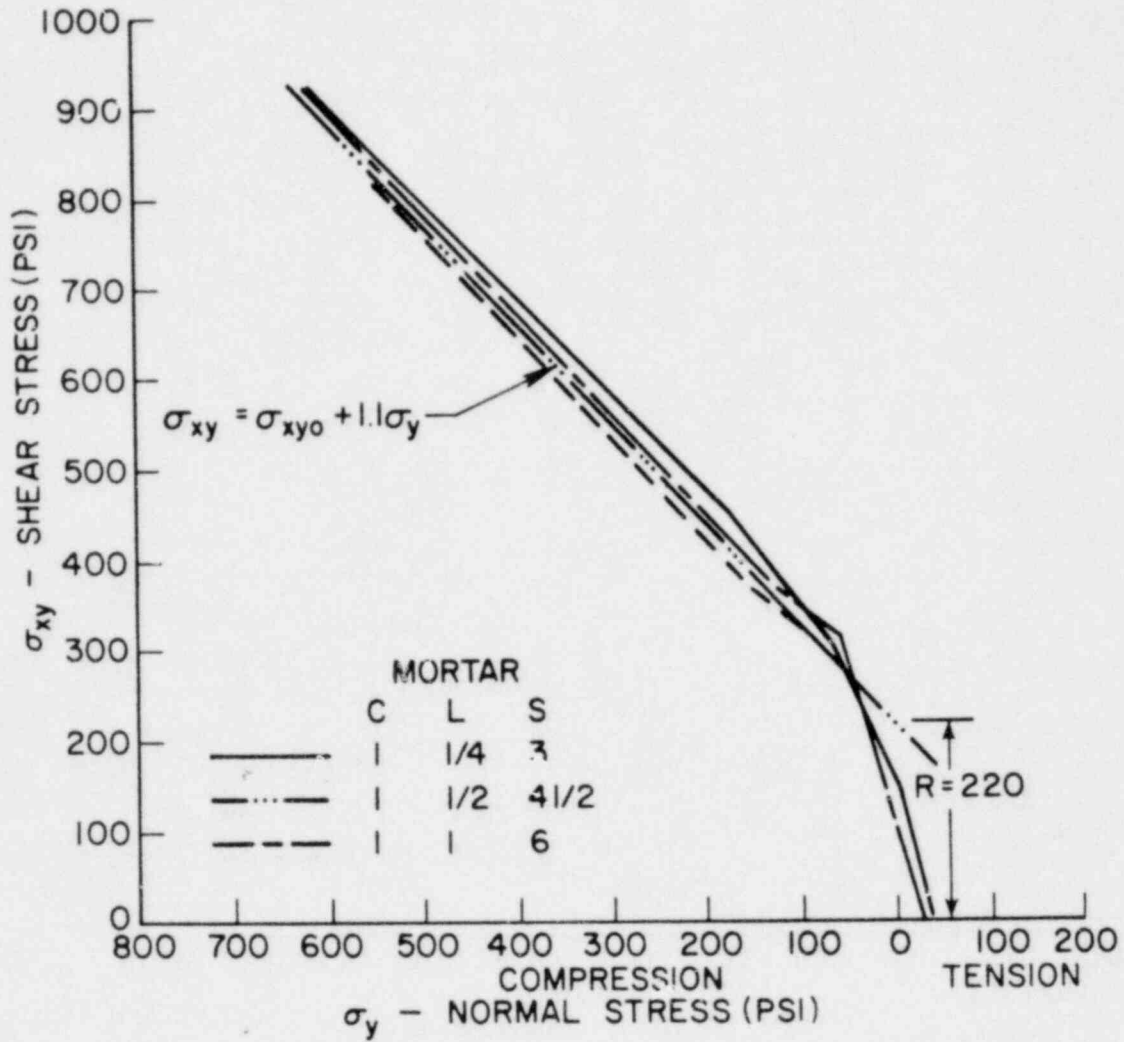


FIGURE 1-14 COMBINED STRESS COUPLET STRENGTH CURVES

indicates that the average shear strength of the joint is about 100 psi. Since this is a case of pure shear it would be logical to expect the failure to be in tension, and a value closer to the tensile strength of the mortar might have been anticipated. The explanation put forward by the authors depends on the fact that the failure is initiated at the joint surface. The phenomenon of the shear bond strength in cases of pure shear being lower than the true tensile strength of the mortar, is similar to the tensile bond strength being lower than the true tensile strength of mortar.

Hendry^(39,43) et al performed bond and shear strength tests using the test setup shown in Figures 1-15 and 1-16. The test material in both sets of tests consisted of one-sixth scale model bricks with an average crushing strength of 4350 psi. The test samples had a bonded area of one square inch.

For a given type of brick and mortar the bond strength is affected by the moisture content of the bricks at the time of laying. To investigate this phenomenon Sinha and Hendry⁽⁴³⁾ dipped their bricks in water for periods of time varying from 5 seconds to 2 hours before the couplets for the tension and shear tests were made. The moisture content of each sample was determined and the results of the bond tension tests are shown in Table 1-14, while those of the bond shear tests with no compressive load are in Table 1-15. From these results, it is clear that the moisture content of the bricks at the time of laying influences the bond strength of the brickwork, although Thomas and Simms⁽⁴⁰⁾ concluded from a small number of full size tests that it was not a very important factor. Sinha and Hendry's results agree with those of

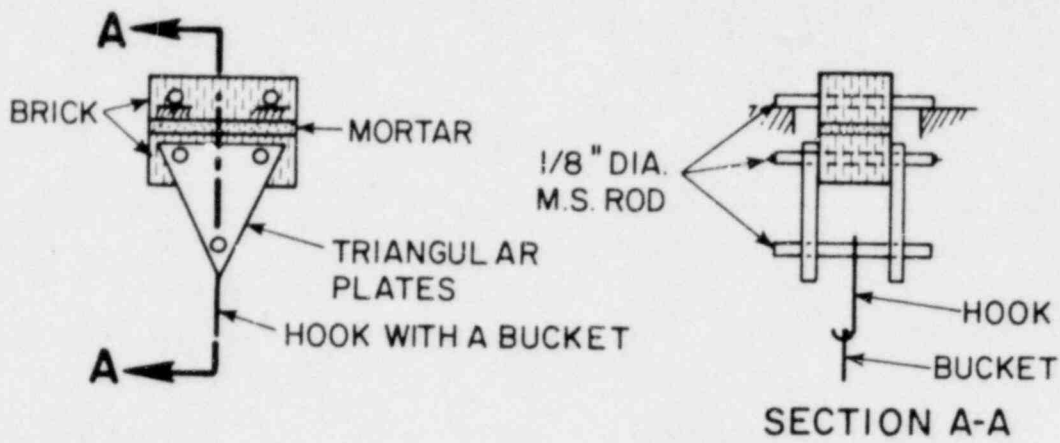


FIGURE 1-15 BOND TENSION TEST ARRANGEMENT

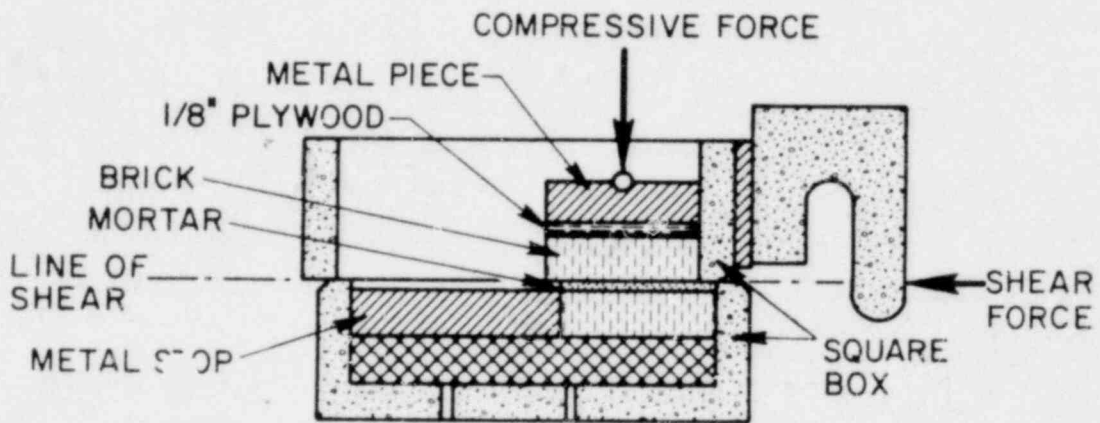


FIGURE 1-16 SHEAR BOX TEST ARRANGEMENT

TABLE 1-14
 COUPLET BOND TENSION STRENGTH
 Area of couplets = 1.0 in²

	Treatment of brick before use					
	Dry	Dipped in water for 5 s	Dipped in water for 2 min	Dipped in water for 5 min	Dipped in water for 10 min	Dipped in water for 2 h
Mortar strength- 1-in. cube psi	1900					1120
Moisture content (%)	0.66	3.38	9.91	11.66	11.81	12.17
Bond tension strength psi	20.38	57.25	84.88	39.75	7.50	2.50
	16.50	10.25	45.75	28.63	81.00	6.90
	11.75	60.00	15.75	7.50	63.00	6.25
	70.08	24.75	34.00	69.00	40.00	2.25
	72.00	17.00	47.00	60.00	7.00	6.00
	29.00	13.00	59.00	70.00	64.00	10.75
	18.00	100.00	66.00	45.00	43.00	6.00
	33.00	66.00	73.00	35.00	8.00	2.25
	27.00	48.00	64.00			5.50
		66.00			2.25	
Avg	33.07	44.00	55.54	44.40	39.20	5.06

From Reference 43.

TABLE 1-15
 COUPLIET BOND SHEAR STRENGTH
 Area of couplets = 1 in²

	Treatment of brick before use					
	Dry	Dipped in water for 5 s	Dipped in water for 2 min	Dipped in water for 5 min	Dipped in water for 10 min	Dipped in water for 2 h
Mortar strength- 1-in cubes psi	1900					1120
Moisture content (%)	0.66	3.38	9.91	11.66	11.81	12.37
Bond tension strength psi	32.40 39.60 59.40 68.40 83.60 75.60 75.60	50.40 46.80 57.60 46.08 97.20 86.40 64.80 86.40	64.80 46.80 46.80 50.40 94.40 86.40 109.60 84.80 46.80 84.80	45.72 39.60 39.60 43.20 88.20 75.60 61.20 97.20 79.20	56.88 46.80 46.80 49.32 21.60 108.00 86.40 52.40 75.60 75.60	28.70 20.00 12.95 21.30 28.80 18.00 9.00 30.06
Avg	62.10	67.12	71.60	63.30	61.94	21.10

From Reference 43.

Semenstov described in Polyakov's⁽³⁶⁾ work. Semenstov concluded that the wetting of bricks before laying with cement mortar substantially increases the bond, but that saturated bricks lead to a large reduction in bond strength.

From the tensile and shear bond results⁽⁴³⁾, the authors proposed the following general relationship between bond tension σ_{tb} and shear bond σ_{xyo} with no compressive stress for solid bricks and a 1:3 cement mortar.

$$\sigma_{xyo} = 8.8\sqrt{\sigma_{tb}} \quad (1-20)$$

Murthy and Hendry⁽³⁹⁾ found that their bond shear was 2.3 times the bond tension. Polyakov⁽³⁶⁾ found that the ratio of bond shear to bond tension depends on the value of bond tension and is given by the following relationship

$$\frac{\sigma_{xyo}}{\sigma_{tb}} = 2.25 - 0.5 \sigma_{tb} \quad (1-21)$$

The Russian standards and code have limited the permissible bond tension to 1.8 kg/cm² (25.6 psi) and Semenstov suggested the following relationship

$$\sigma_{xyo} = 1.7 \sigma_{tb} \quad (1-22)$$

To determine the effect of precompression on the shear strength of the couplets Hendry et al^(39,43) performed a series of tests with the equipment shown in Fig. 1-16, using a varying compressive load. In both series of tests the authors assumed the total shear strength of the couplets to consist of bond shear and frictional

resistance and to be represented by

$$\sigma_{xy} = \sigma_{xyo} + f \sigma_y \quad (1-23)$$

where f is the coefficient of friction. In both investigations an initial series of tests were conducted to establish the coefficient of friction. The couplets were made by placing tissue paper between the top brick and the mortar joint to eliminate the bond shear. Sinha and Hendry found that the relationship between compressive stress and frictional shear stress is linear up to a shear stress of 154 psi, the compressive stress being 200 psi at this limit. The corresponding values in Murthy and Hendry's tests were 105 and 145 psi, respectively. The coefficient of friction determined from the two studies was 0.74 and 0.725, respectively. The shear strength of the couplets in the linear shear stress range where bond shear was eliminated could be given by $\sigma_f = f \sigma_y$ where σ_f is the shear stress of the couplet due to friction alone on the brick mortar boundary - Figures 1-17 and 1-18.

To predict the shear strength when bond shear was not eliminated the authors used the relationship given by Equation (1-23), where σ_{xyo} was determined experimentally. The theoretical results presented in Figures 1-17 and 1-18 were calculated from Equation (1-23). The relationship between the compressive stress and the shear stress was found to be linear up to a shear stress of 181 psi in Sinha and Hendry's test and 105 psi in Murthy and Hendry's test. In Sinha and Hendry's test the shear strength did not increase again until the compressive strength exceeded 245 psi. There was an apparent increase in shear resistance when the compressive stress

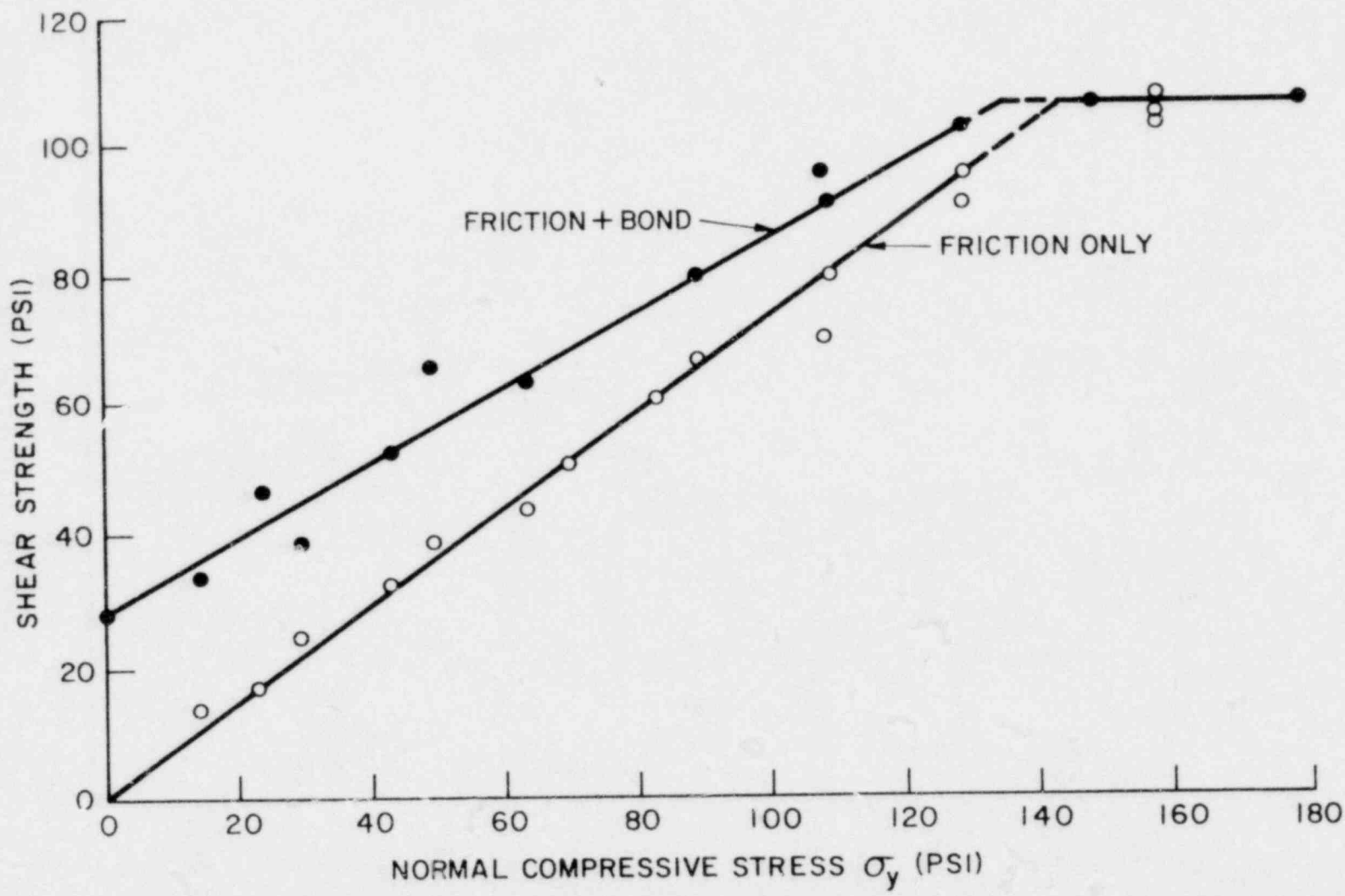


FIGURE 1-17 SHEAR STRENGTH OF BRICK COUPLETS SUBJECTED TO VERTICAL COMPRESSION

From Reference 39

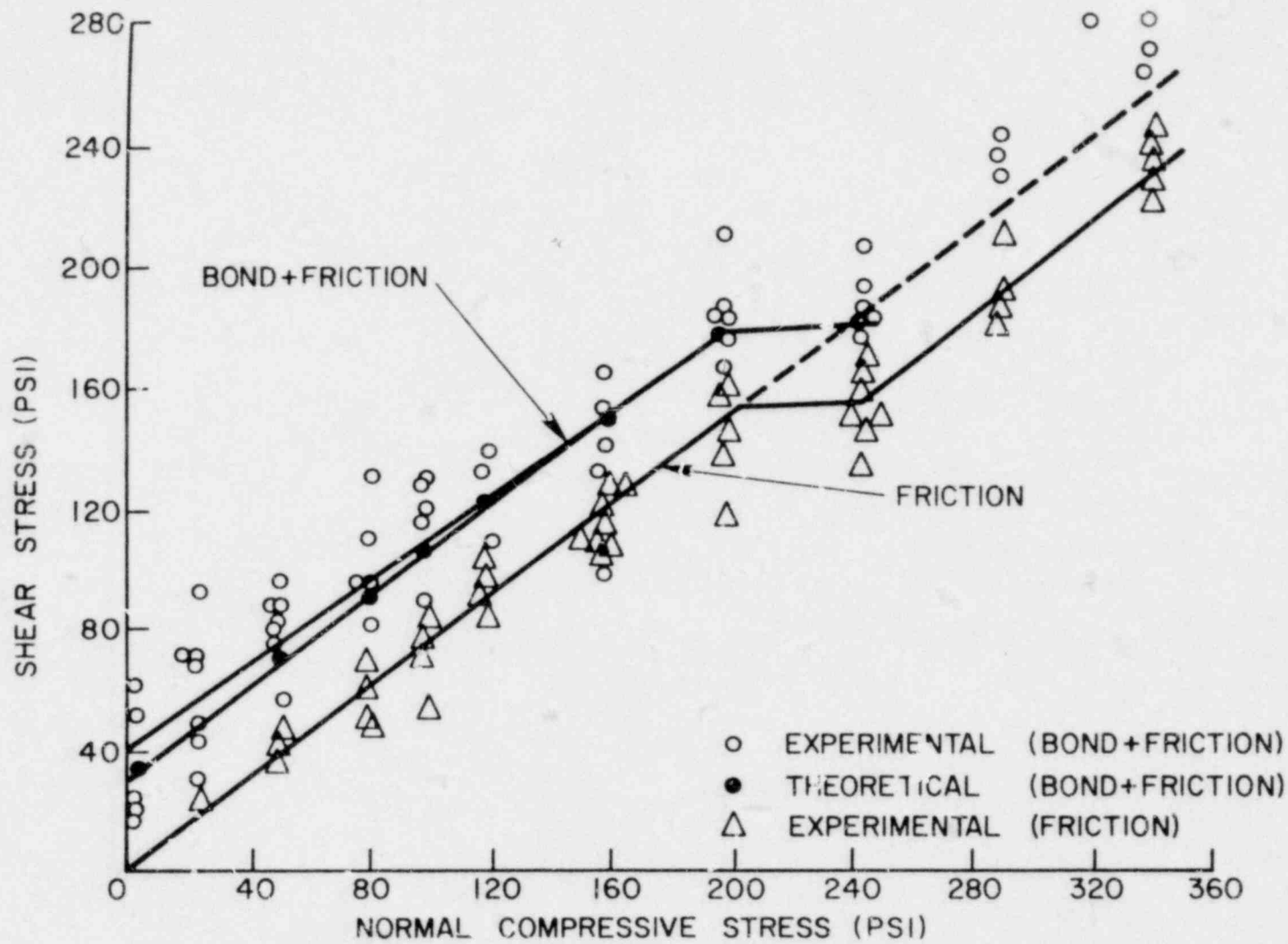


FIGURE 1-18 SHEAR STRENGTH OF BRICK COUPLETS SUBJECTED TO VERTICAL COMPRESSION

From Reference 43

exceeded 245 psi, which the authors assumed to be due to frictional resistance alone.

Although there is little information available for concrete masonry, the information reported by Sahlin⁽⁴⁴⁾ agrees with the tests reported by Benjamin and Williams⁽⁴¹⁾ for brick mortar joints. The data given by Sahlin in Table 1-16 indicate that the tensile strength of mortar is about 10 percent of its ultimate compressive strength and that the bond strength in tension is about 20 percent of the tensile strength or 2 percent of the compressive strength.

TABLE 1-16

Mix Cement:Lime:Sand	Type of Mortar	Compressive Strength psi	Tensile Strength psi	Bond Strength psi
1:1 1/4 : 4 3/4	M	2000-2500	250-275	58
1:2 : 7	S	1240-1290	155-180	26

8 x 8 x 16 inch concrete units with 57.1 percent net area and absorption 15.3 to 17.1 were used.

From Reference 44

1.3c Tensile Strength of Masonry Assemblages

In order to evaluate the tensile strength of a composite masonry unit, Johnson and Thompson⁽⁴⁶⁾ developed a diametral test procedure similar to the indirect Brazilian test for concrete. The test consisted of applying a compressive point load along the diameter of a circular masonry disc as shown in Figure 1-19. If the masonry disc is considered to be a homogeneous material the variation of the stress component normal to the mortar bed at the disc center is given in Figure 1-19. To evaluate the applicability of the test the authors tested a large number of 15 inch diameter

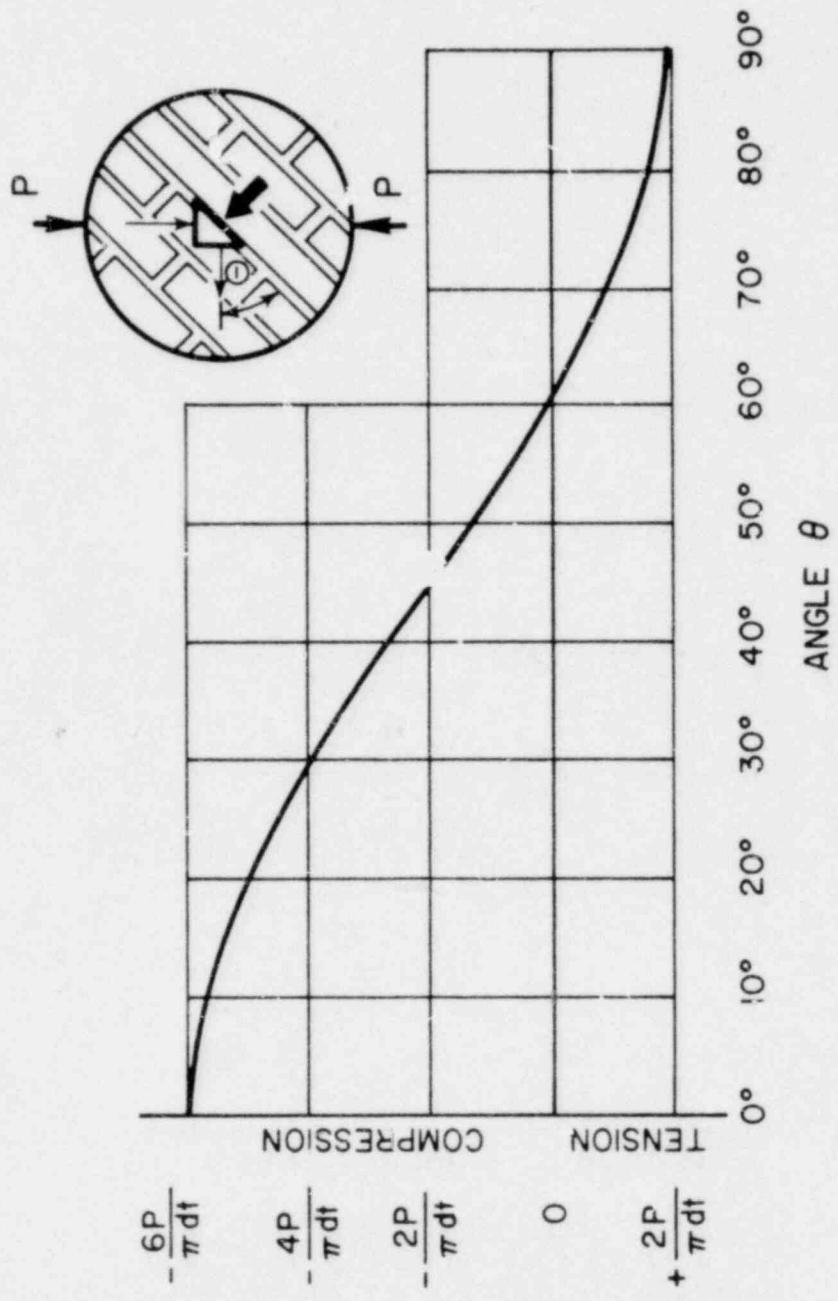


FIGURE 1-19 VARIATION OF STRESS COMPONENT NORMAL TO BED AT MASONRY DISC CENTER

discs. The two major variables of the investigation were the angle of the mortar bed to the line of application of the compressive load and the strength of the mortar. The results of the investigation are presented in Figure 1-20.

The authors concluded by stating that some of the general findings of the investigation may have more significance than some of the specific numerical results. They outlined the general findings as follows: The diametral testing of masonry discs proved to be a simple, feasible procedure for the measurement of the respective tensile properties. The coefficient of variation within the test series was unusually low for this type of material and indicates the reliability of results that may be obtained with the composite unit. A further advantage of masonry disc diametral testing is the variety of information that can be obtained by the rotation of the bed joint with respect to the direction of the principal tensile stress. When the angle between the direction of the principal tensile stress and the bed joint is 90° , the results of the diametral testing of the masonry discs give a measure of bond strength between the mortar and the brick. When the angle between the direction of the principal tensile stress and the bed joint is 45° , the results of the diametral testing of the masonry disc becomes a measure of the shear strength of a masonry assemblage which is applicable to masonry beams and shear walls.

The diametral testing of masonry discs was utilized in the Structural Clay Products Small Specimen Testing Program⁽²⁴⁾, and later was the object of a theoretical analysis by Stafford-Smith et al⁽⁴⁷⁾. Included in the theoretical analysis was a comparison

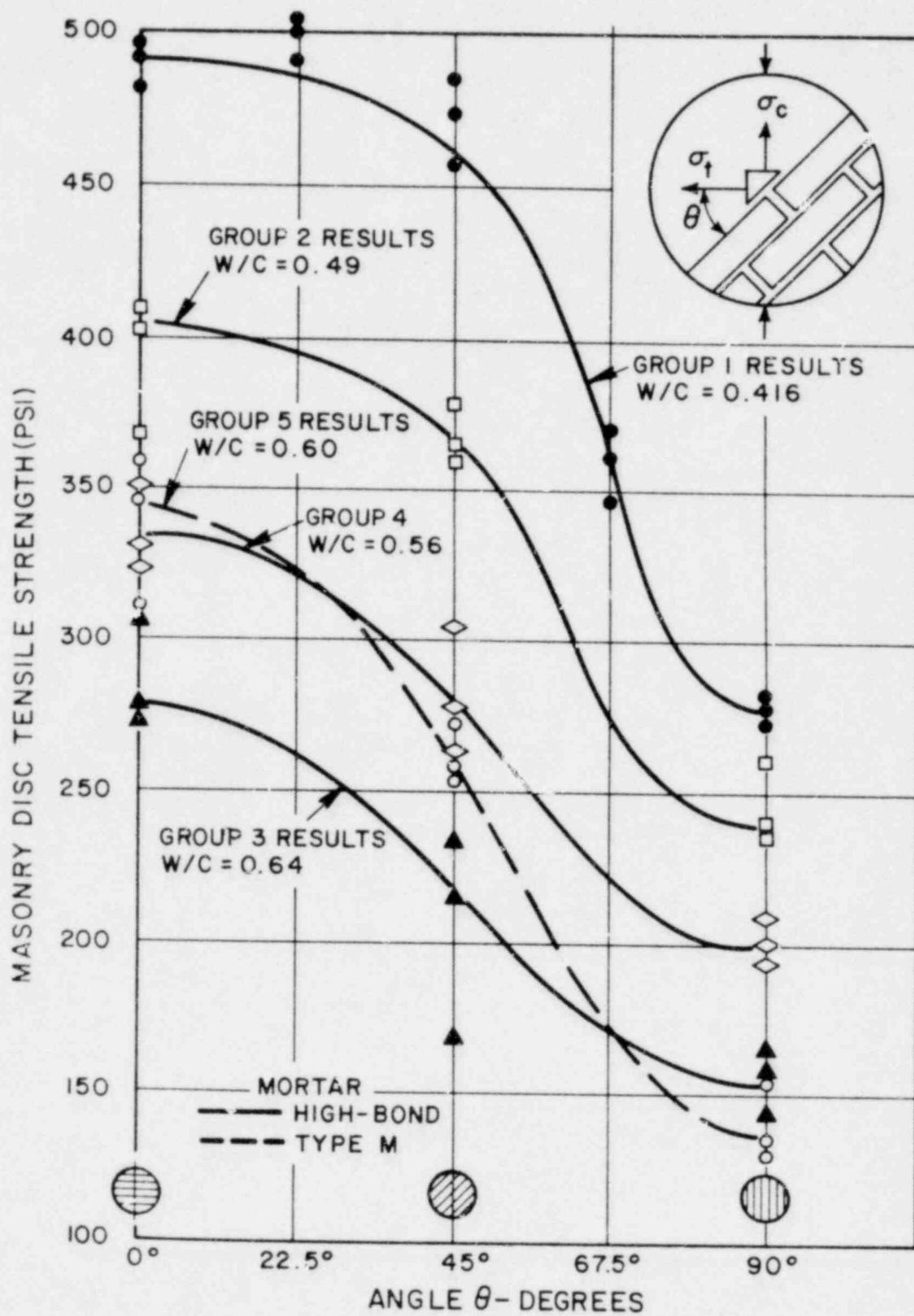


FIGURE 1-20 EFFECT OF DIRECTION OF BED JOINT ANGLE ON MASONRY DISC TENSILE STRENGTH

From Reference 46

of some of the theoretical results with the experimental results obtained in the Structural Clay Products Small Specimen Test Program. Stafford-Smith et al performed a linear finite element analysis on the circular masonry disc used in the diametral test procedure, for the case of the bed joint at 45 degrees to the line of the load application. In the analysis the authors varied the brick to mortar modular ratio and calculated the maximum principal tensile stress from the formula

$$\frac{NP}{\pi Dt}$$

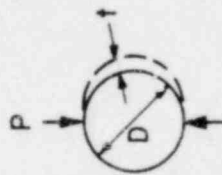
and plotted N against $\frac{E_B}{E_m}$. The plot is shown in Figure 1-21. In Johnson and Thompson's⁽⁴⁶⁾ paper and the SCP⁽²⁴⁾ report the maximum principal stress was assumed to be

$$\frac{2P}{\pi Dt}$$

i.e. that of a homogeneous disc. Stafford-Smith et al recalculated the diagonal tensile strength of the SCP tests and plotted them against the mortar tensile strength - Figure 1-22. It is clear that for the plot presented, the tensile strength of the discs calculated by the authors approximates the tensile strength of the mortar.

The authors concluded that the diagonal tensile strength of the brickwork is approximately equal to either the tensile strength of the mortar or the tensile strength of the brick whichever is less. They further concluded that in the particular problem of diagonally loaded brickwork discs, concentration of high principal

FOR ANY VALUE OF THE BRICK:MORTAR
 MODULAR RATIO E_B/E_M THE CURVE
 GIVES THE VALUE OF "N" WHICH
 SHOULD BE USED TO DETERMINE f_{dt}
 THE MAXIMUM PRINCIPAL TENSILE STRESS
 IN THE MORTAR.



$$f_{dt} = NP / \pi Dt$$

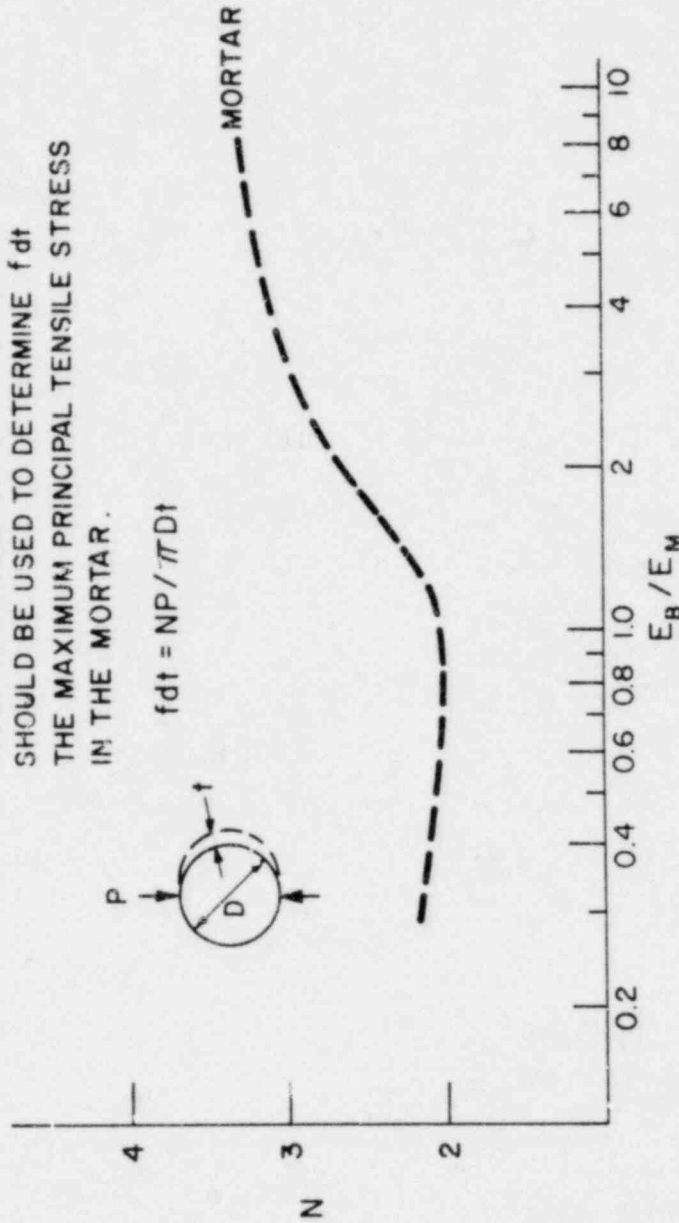


FIGURE 1-21 N VS. E_B/E_M CURVES

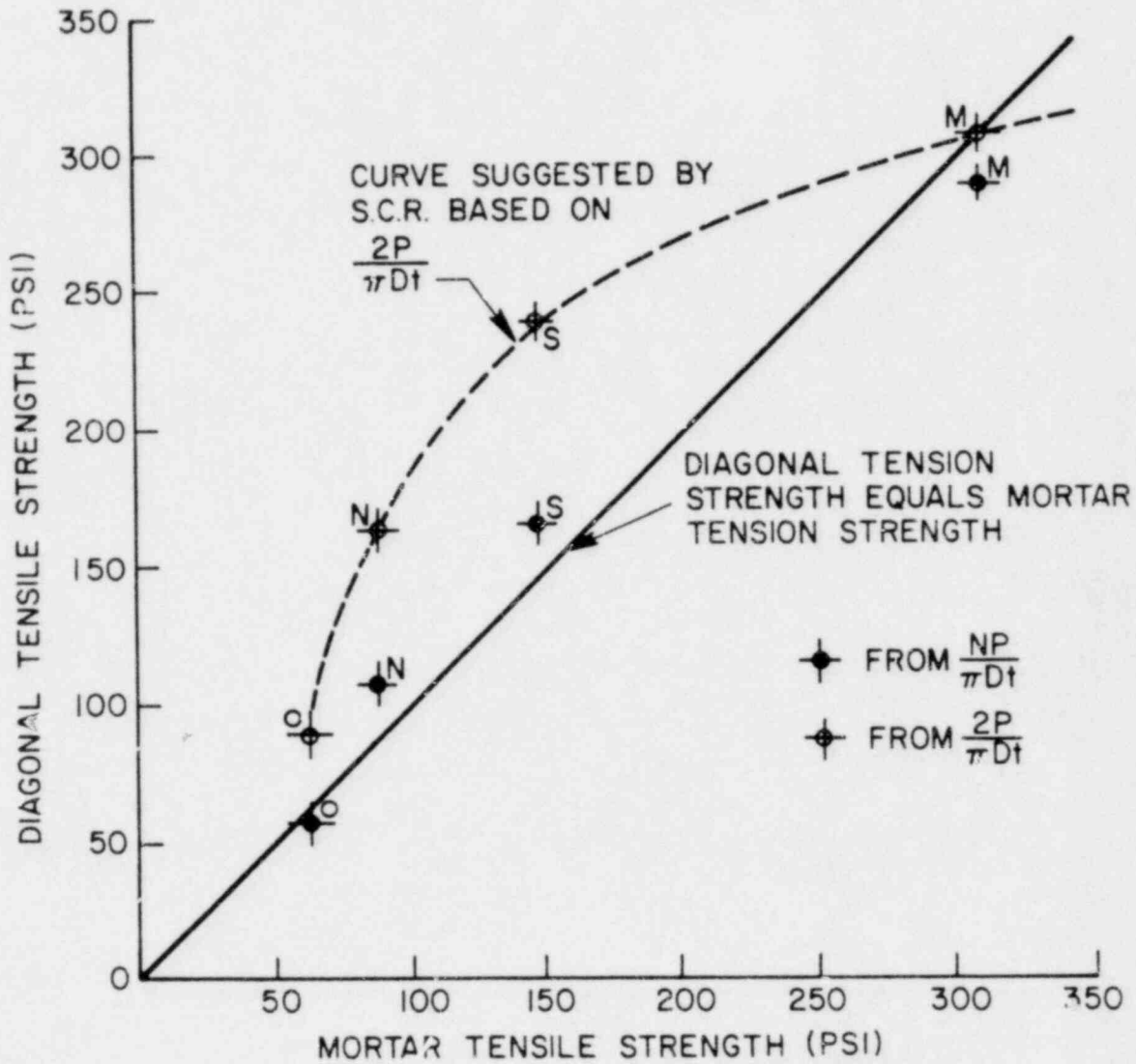


FIGURE 1-22 DIAGONAL TENSILE STRENGTH VS. MORTAR TENSILE STRENGTH

tensile stresses was found to be induced in the elements of lesser stiffness, the greater the modular ratio of the materials the larger the peak tensile stresses. In addition they stated that in the stress analysis of non-homogeneous materials such as brickwork an analysis based on the assumption of a homogeneous material may lead to substantial underestimates of the maximum stresses.

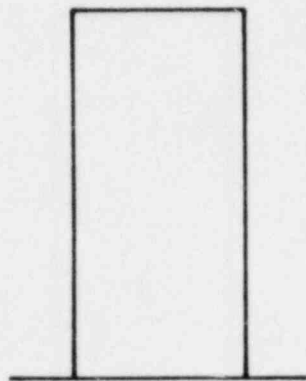
2. SHEAR STRENGTH OF MASONRY ASSEMBLAGES

2.1 Introduction

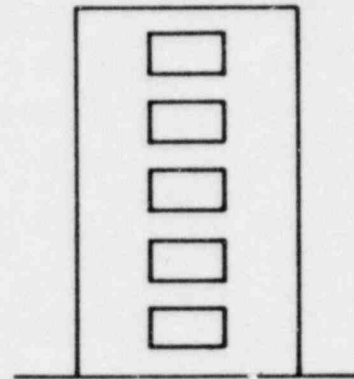
An important consideration in the analysis of a masonry building is the ability of the structure to withstand lateral loads. In seismic areas of the world large lateral loads are induced by earthquakes and in both seismic and non-seismic regions lateral loads arise from wind loadings. Most masonry buildings consist of various assemblages of different types of shear walls, (Figure 2-1) and the resistance to the lateral loads is predominantly by their in-plane shear resistance. Consequently the experimental and theoretical behaviour of individual, or components of individual, shear walls are of interest in understanding the behaviour of masonry buildings subjected to lateral loads.

The object of many early experimental research programs in this area was to determine the resistance of masonry assemblages to monotonic shear loads. As research progressed, investigators tried to determine failure criteria for different assemblages subjected to various combinations of shear and compressive loads. More recently investigators have also considered the behaviour of various assemblages under cyclic loading. The properties of interest in these programs have been the ultimate strength and/or yield strength, the mode of failure, the stiffness degradation and hysteretic behaviour and the effect of different parameters on these properties.

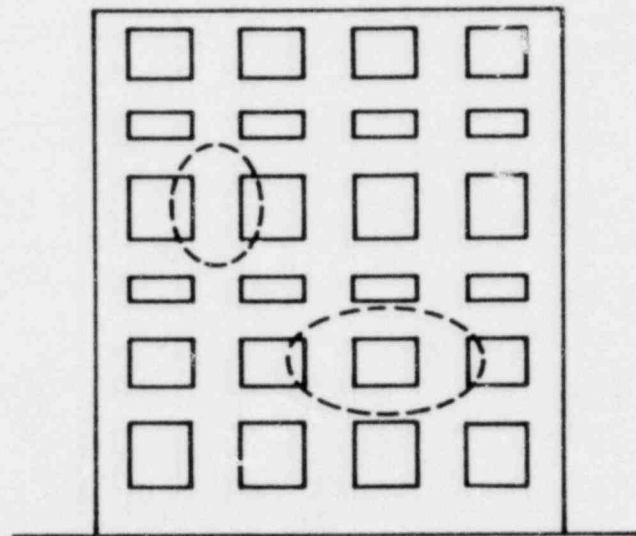
Only a limited number of major investigations has been performed on the shear strength of masonry assemblages. Each program will be briefly summarized and the pertinent results and conclusions presented. The second section of the chapter outlines the various test techniques



VERTICAL
CANTILEVER



COUPLED
SHEAR WALL



PERFORATED SHEAR WALL

FIGURE 2-1 TYPICAL SHEAR WALLS

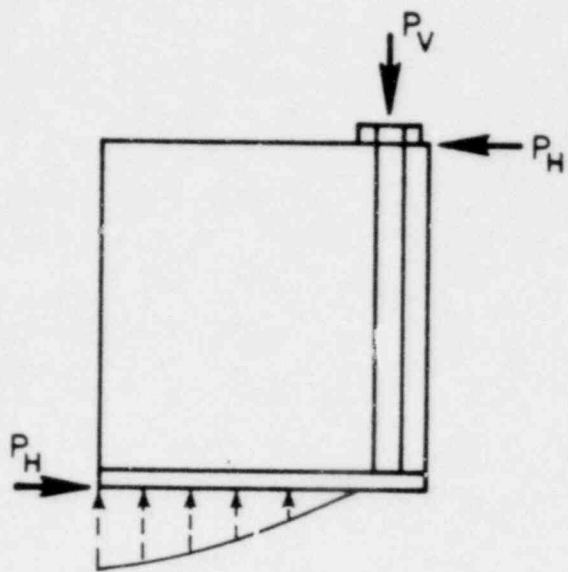
used in the different investigations, the third section briefly summarizes investigations that utilized the monotonic type of load. The fourth section summarizes investigations performed on models of masonry buildings while the fifth section summarizes investigations on the cyclic behaviour of masonry assemblages.

2.2 Test Techniques

Development of sophisticated mechanical and electrical equipment over recent years has led to an increase in the sophistication of apparatus able to be used in experimental investigations. Consequently, the scope and aims of many programs have broadened, yielding more detailed and relevant information.

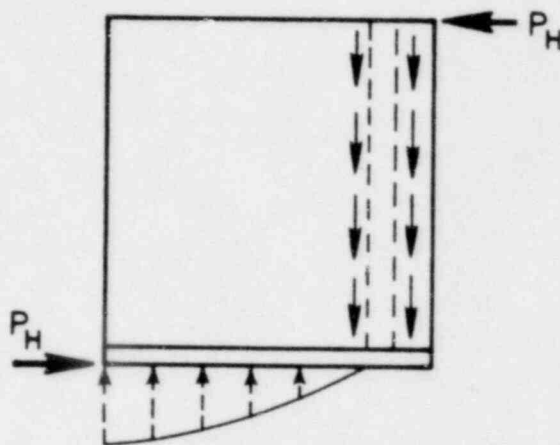
Investigators over the last two decades have used many different test techniques in their experimental programs on the shear strength of masonry assemblages. The diversity of methods has arisen because of the difficulty in simulating the actual load conditions of a masonry component in an experimental program. In this section, most of the basic experimental techniques that have been used will be outlined.

One of the first methods used in the determination of the shear strength of masonry walls was that shown in Fig. 2-2. The external hold-down force R was applied to resist the overturning moment of the panel. This method was used by Schneider⁽⁴⁸⁾, Scrivener et al^(49,50) and the Structural Clay Products Research Foundation^(51,52) in their test programs. The method also formed the basis of the standard procedure of racking tests described in ASTM E 72-68. This method of test provides only a relative measure of the shearing or diagonal tension resistance of a panel and is useful only for comparison with construction tested in the same manner. To what extent the state of stress is influenced by the boundary conditions and the tie-downs is a matter of speculation.



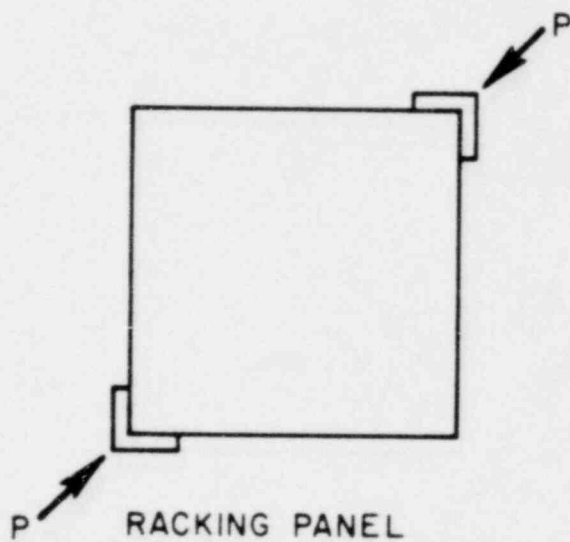
EXTERNAL HOLD DOWN

FIGURE 2-2



INTERNAL HOLD DOWN

FIGURE 2-3



RACKING PANEL

FIGURE 2-4

The above method was modified by Schneider⁽⁵³⁾ in a second series of tests he performed in 1959 and was also utilized by Scrivener⁽⁵⁴⁾ in one of his series of three tests. Instead of using the external force to resist the overturning moment, an internal hold-down anchor depicted in Figure 2-3 was used. Here the objection of a large external compressive stress at the edge of the panel is eliminated. However, since overturning resistance depends upon the development of bond between the jamb steel and the grout, a certain flexibility in types and arrangement of jamb steel is lost.

Probably one of the most frequent techniques used to determine the relative shear strengths of walls is that shown in Figure 2-4. This method was used in the extensive test program performed by Blume and Associates⁽⁵⁵⁾ for the Western States Clay Products Association. In that study a qualitative photoelastic model of a wall with two openings under a story shear F was performed. The results presented in Figure 2-5 indicate the diagonal tension stresses in the center pier between window openings. Figure 2-6 indicates a square photoelastic specimen loaded on a diagonal in the same manner in which the actual diagonal test was constructed. The report⁽⁵⁵⁾ stated that the similarities between the two figures is evident and Figure 2-6 shows that failure should occur as a result of extensive tensile stresses across the vertical diagonal. Borchelt⁽⁵⁶⁾ used the diagonal test method but added a compressive load as shown in Figure 2-7.

Schneider⁽⁵⁷⁾, in 1967, performed a series of tests on concrete masonry piers with the test set-up shown in Figure 2-8. The geometry of the system was maintained by the struts at the end of the openings and the axial and shear loads were applied by a system of jacks and tie

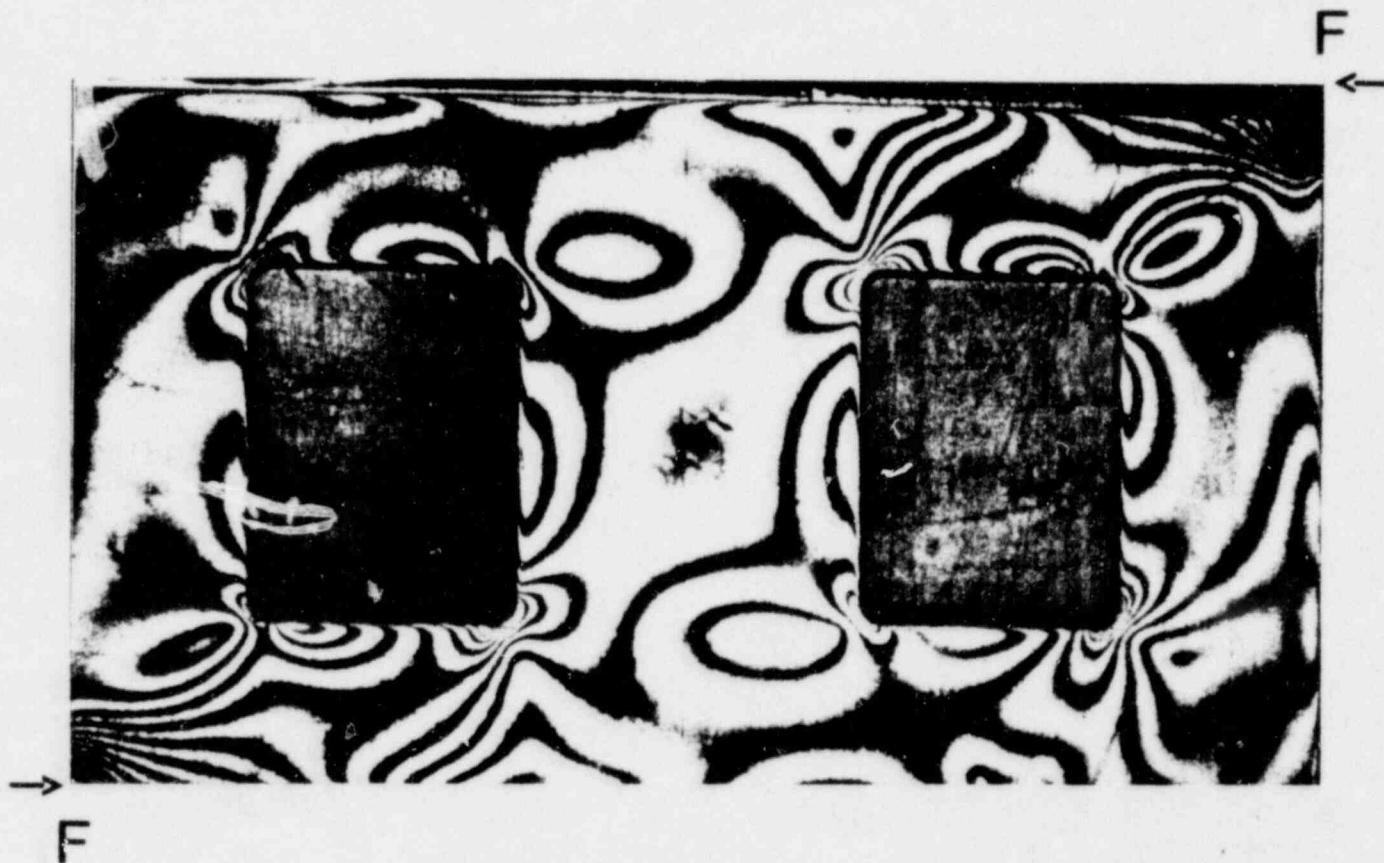


FIGURE 2-5 STRESS PATTERN IN A LATERALLY LOADED WALL PANEL MODEL WITH WINDOW OPENINGS. NOTE THE DIAGONAL TENSION STRESSES IN THE CENTER PIEK.

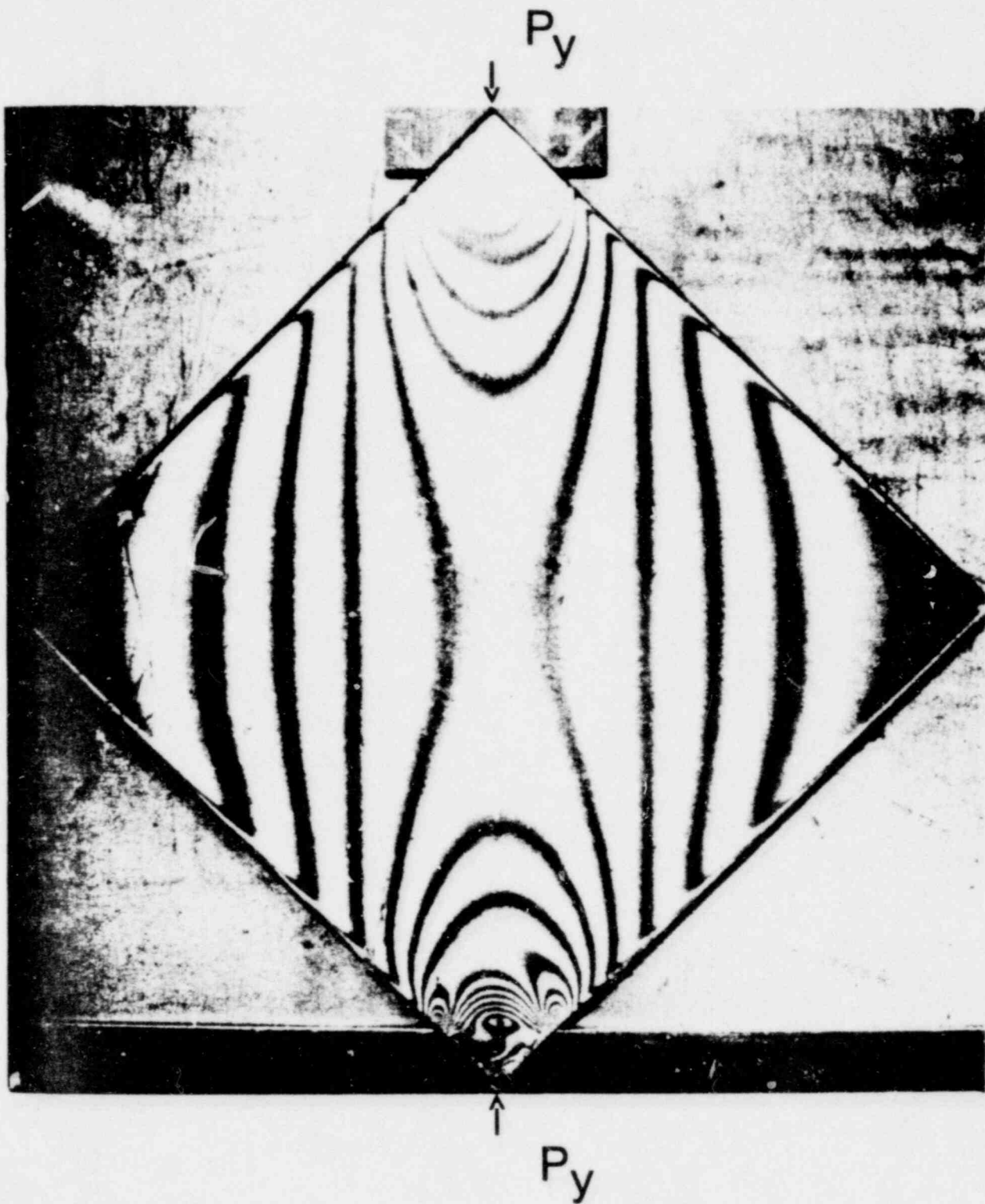
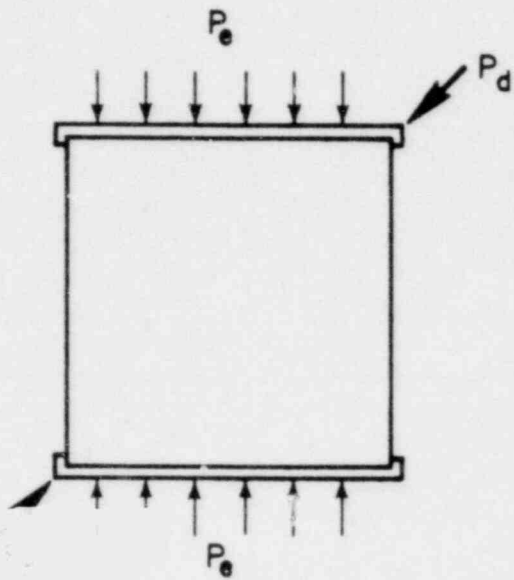
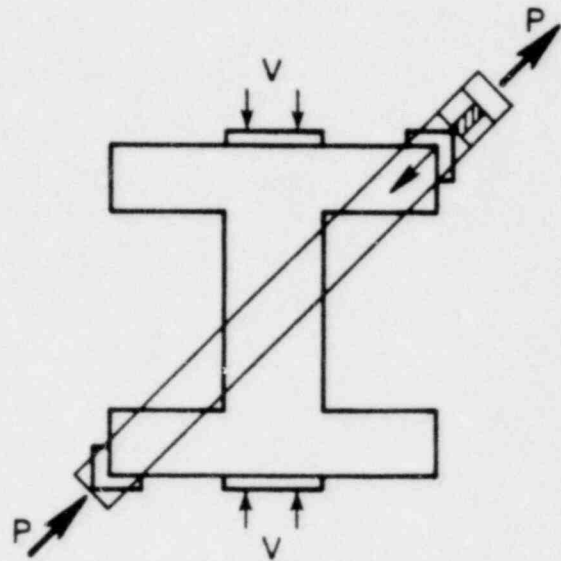


FIGURE 2-6 STRESS PATTERN IN A DIAGONAL TENSION TEST.



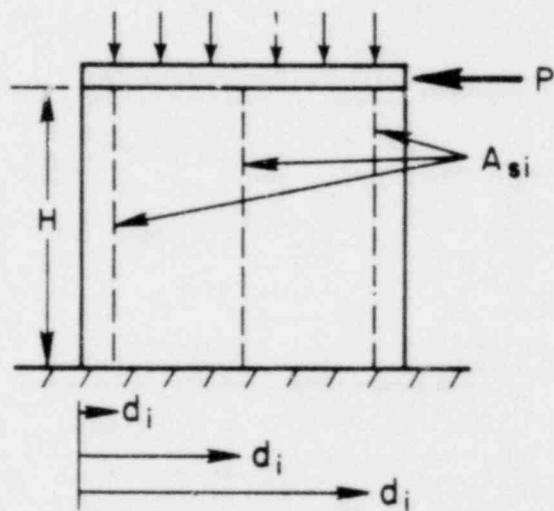
EDGE LOAD WITH RACKING

FIGURE 2-7



DIAGONAL LOAD FRAME

FIGURE 2-8



CANTILEVER LOAD TEST

FIGURE 2-9

rods. Schneider believed that this procedure came closest to simulating the manner in which lateral forces are imposed on a pier within a building wall.

The limited number of cyclic loading tests performed by Williams⁽³⁾, Meli⁽⁵⁸⁾ and the New Zealand Pottery and Ceramics Research Association⁽⁵⁹⁾ (PACRA) utilized the cantilever specimen shown in Figure 2-9. The resistance to the overturning moment was provided by whatever internal reinforcement was in the piers. This is a variation of the internal hold-down method used by Scrivener and Schneider. In the case of Williams and PACRA's tests, the vertical load was applied by a system of springs and rollers.

An extensive program being performed by Mayes and Clough⁽⁶⁰⁾ attempts to approximate the boundary conditions of the piers in a structure, as closely as possible, in the experimental test set-up. (Figure 2-10). The major advantage of this test technique is the ability of the panels to simulate the variation in the overturning moment on a pier. In addition, the test panel closely approximates the boundary conditions that the piers experience in an actual structure.

2.3 Monotonic Shear Load Tests

The equipment required for cyclic load tests is generally more costly and sophisticated than that required for monotonic load tests, and consequently much of the early research was performed using monotonic loads. This section summarizes the results and conclusions of the investigations on the shear strength of masonry assemblages subjected to monotonic loadings. The first group of investigations summarized, are those that utilized the test techniques shown in Figures 2-2, 2-3, and 2-8. The second group consists of those investigations that utilized test techniques similar to those shown in Figures 2-4 and 2-7.

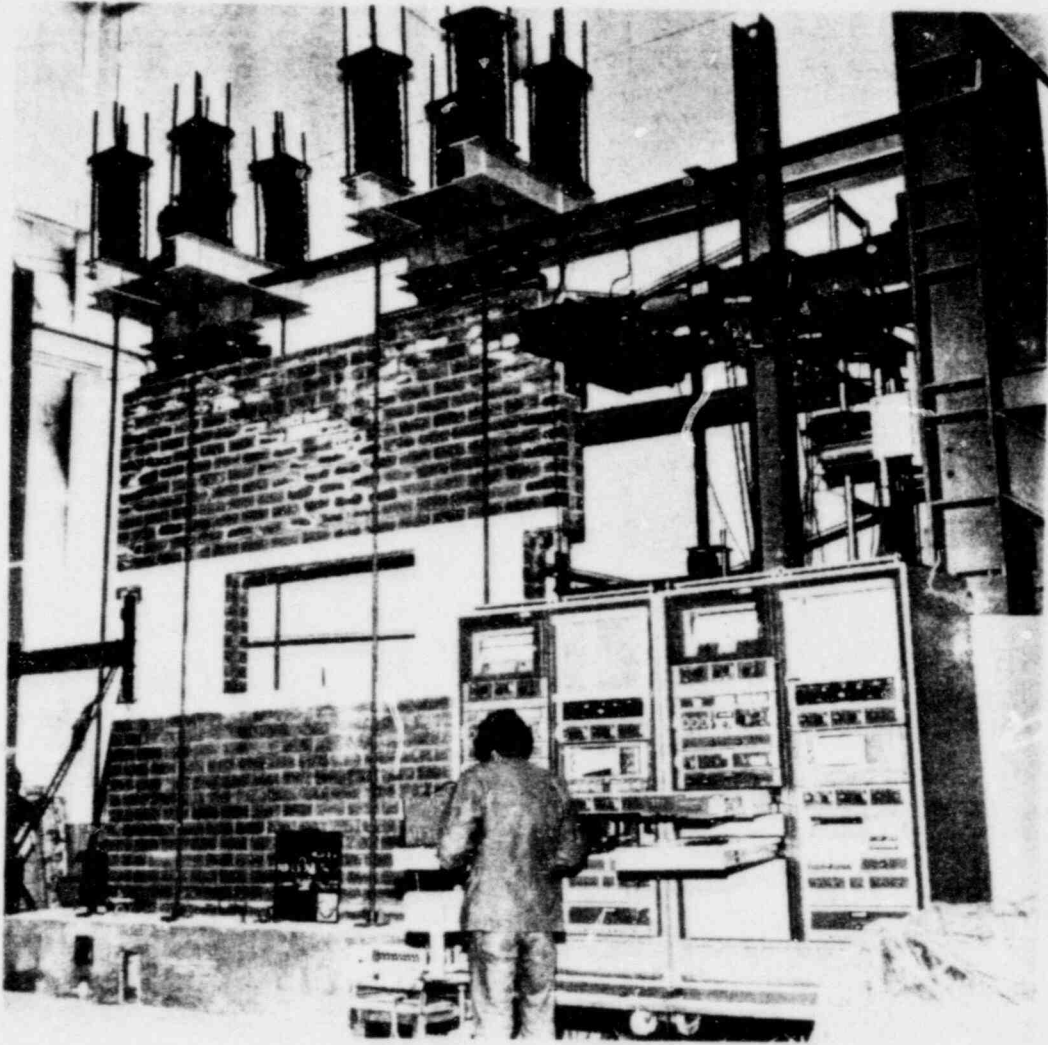


FIGURE 2-10 DOUBLE PIER TEST SET-UP

Schneider⁽⁵³⁾ performed 36 full-scale tests on three basic types of masonry (clay brick, concrete block and Shel-Brik), using the test technique shown in Figure 2-3. Typical dimensions of the elements he tested are shown in Figure 2-11. The brick walls tested consisted of the double wythe grouted construction made from 3 1/4" x 3 1/4" x 10" clay units. The concrete block walls consisted of 8" x 8" x 16" hollow concrete blocks. The Shel-Brik walls comprised two basic sizes, namely 6" x 6" x 16" and 8" x 6" x 16" units. The conclusions drawn by the author from the results presented are as follows:

- (1) With a height to width ratio of approximately 1, the walls tested registered an ultimate shear strength of 145 psi on the gross area, regardless of the variation in the specific parameter of a particular test.
- (2) The type of mortar mix as it was varied in the tests, apparently had little effect upon the overall shear resistance of the brick walls. Although the straight lime mortar mix possessed practically no shear resistance, its bonding ability was at least sufficient to help tie the wall together so that it functioned as a thoroughly integrated unit.
- (3) The existence of an opening discontinuity and its shape within the wall exerted a strong influence upon the behaviour of the brick walls. The shear resistance was definitely not reduced in direct proportion to the reduction in net panel width across the openings. As the relative opening size increased, the rate of decrease in shear resistance of the wall became smaller.
- (4) No basic difference between the shear resistance of stack and running bond concrete block masonry seemed to exist, other factors such as workmanship and amount of reinforcing remaining the same.

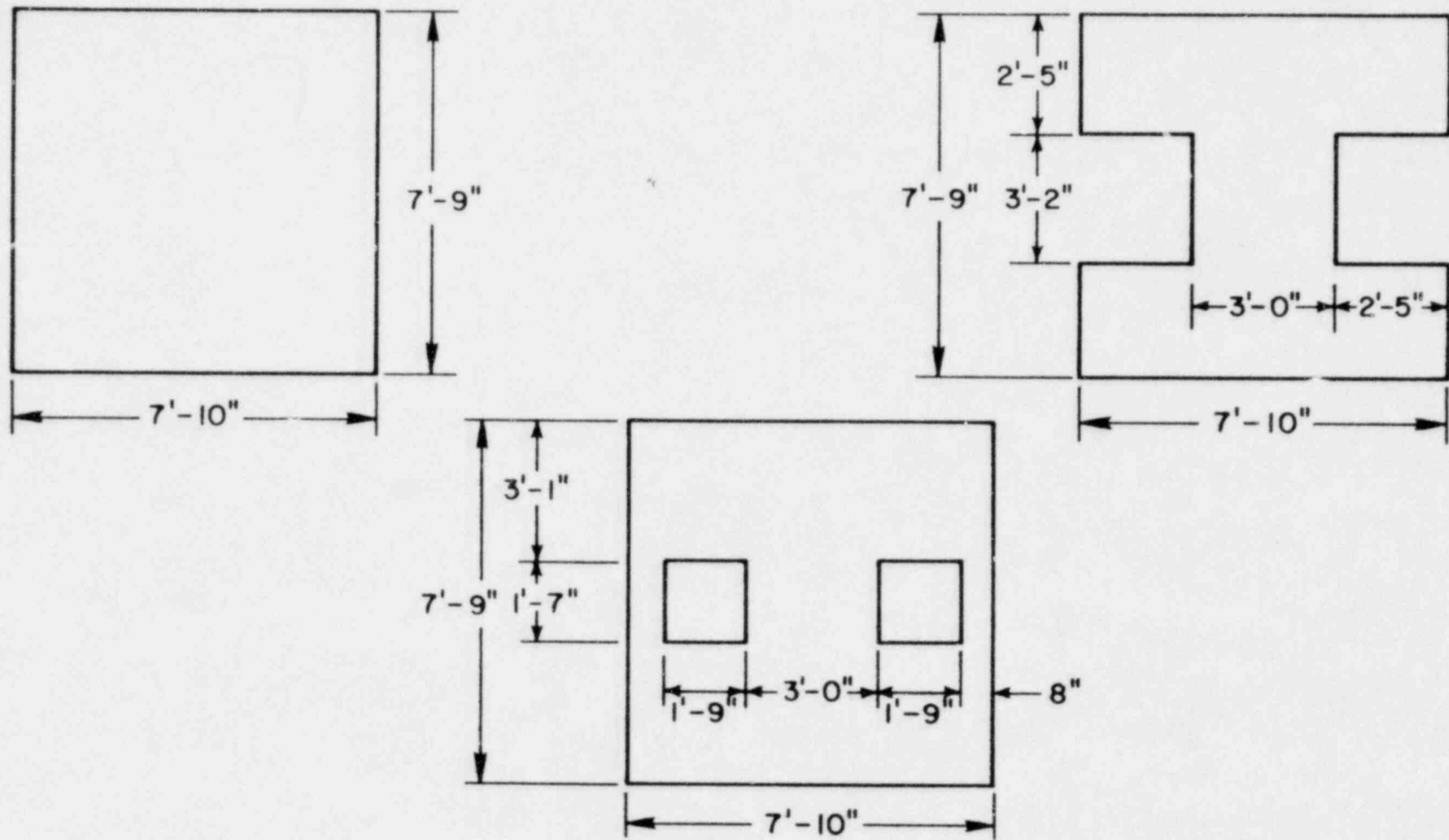


FIGURE 2-11 TYPICAL PANEL DIMENSIONS

From Reference 53

(5) Insofar as reinforced grouted masonry is concerned, the basic failure mechanism is one of diagonal tension and any structural unit composed of this material must, of necessity, be reinforced properly to resist this stress condition. In the case of concrete block, little difference existed between the ultimate loads sustained by similarly constructed walls reinforced on the basis of either $0.003 bd$ or $0.002 bd$ where b is the width and d the thickness of the wall, indicating that reinforcement equal to $0.002 bd$ was sufficient to develop the ultimate shear resistance of the grouted masonry. The load at which the first crack was formed was noticeably lowered by a reduction in the amount of wall steel.

(6) The intermittently-filled cell walls, which resisted a total load of about 67% of that sustained by the solid grouted walls, evidenced a considerable lack of rigidity even in the lower load range. In the region between first crack and ultimate load, the increase in deflection was quite rapid with failure occurring rather suddenly.

It should be noted that several of the conclusions presented above by Schneider⁽⁵⁷⁾ are in direct contradiction with conclusions presented by other authors.

Schneider conducted another series of 50 full-scale tests on panels consisting of single concrete-block masonry piers. The test technique employed was that shown in Figure 2-8, and typical panel dimensions are shown in Figure 2-12. Each panel was constructed from standard 8" x 8" x 16" concrete block units. The conclusions drawn by the author from the results presented are as follows:

(1) Shear strength definitely increases with a decrease in the height to width ratio (H/W) of the pier, and the rate of increase jumps sharply below a H/W ratio of 1:1.

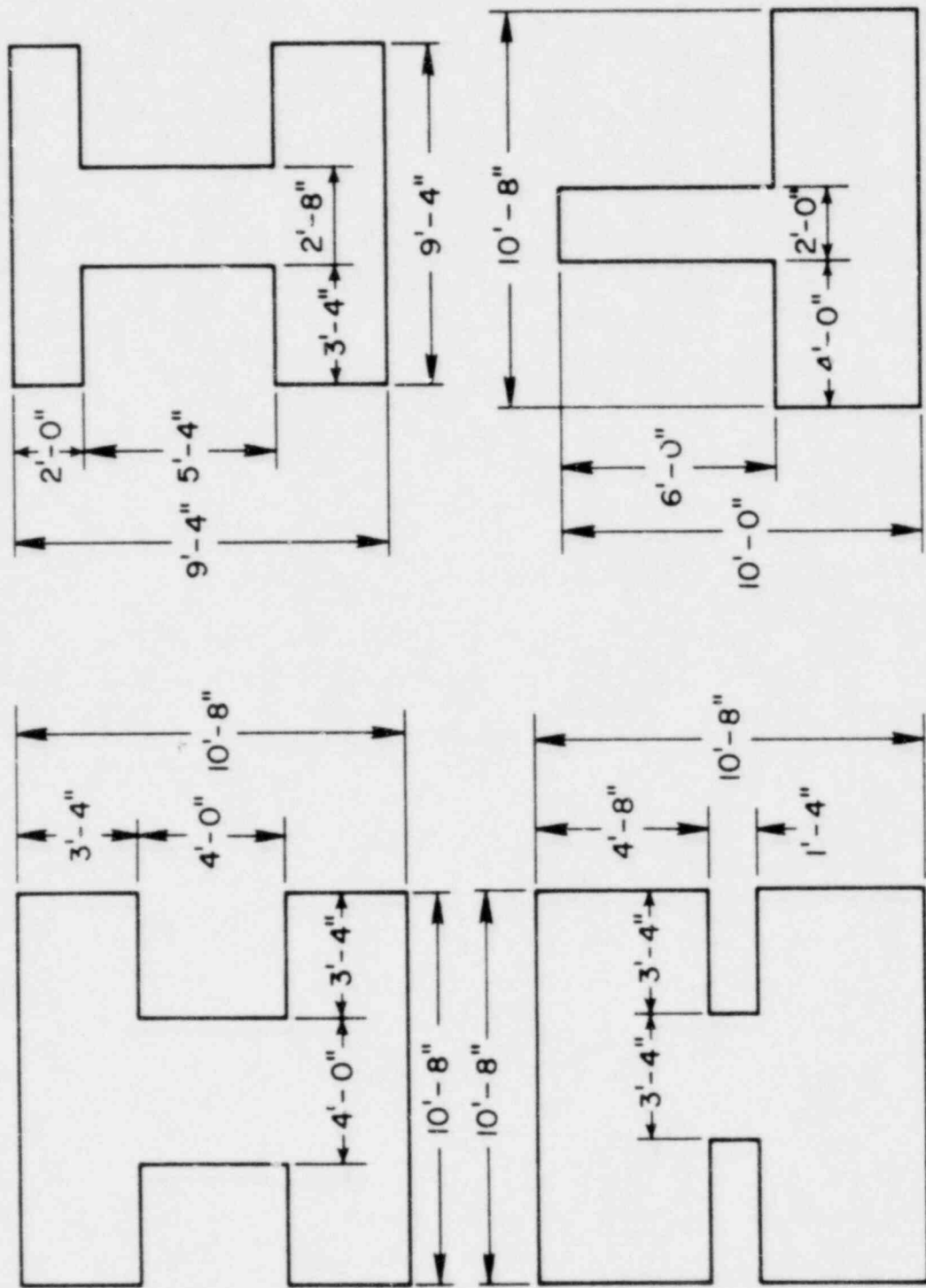


FIGURE 2-12 TYPICAL PANEL DIMENSIONS

From Reference 57

(2) The very consistency of the test results throughout the range of H/W ratios selected for analysis suggests the following relationship for average ultimate shear stress of a pier contained within a shear wall where horizontal reinforcement is not provided. In the following tables V represents the shear force and b the thickness of pier.

TABLE 2-1

Fixed Pier Elements		Cantilever Pier Elements	
H/W	Ultimate Shear Stress-psi	H/W	Ultimate Shear Stress-psi
0.2:1 < H/W < 1:1	$\frac{V}{bW} = 310 - 1.5H/W$	1:1 < H/W < 3:1	$\frac{V}{bW} = 95 - 15H/W$
1:1 < H/W < 3:1	$\frac{V}{bW} = 152.5 - 17.5H/W$	3:1 < H/W	$\frac{V}{bW} = 50$
3:1 < H/W	$\frac{V}{bW} = 100$		

From Reference 57

(3) The presence of adequate horizontal reinforcement materially increases the shear resistance of the pier. The consistent nature of the test results suggests certain relationships between the H/W ratios and ultimate shear stress where adequate horizontal web reinforcement occurs. These are expressed in Table 2-2. Although the term "adequate horizontal reinforcement" was not specifically defined in the report, the results of Table 2-2 are based on experiments where the horizontal reinforcement consisted of No. 5 bars 8 in. on centers.

TABLE 2-2

Fixed Pier Elements

H/W	Ultimate Shear Stress-psi.
$0.2:1 \leq H/W \leq 1:1$	$V/bW = 347.5 - 112.5 H/W$
$1:1 \leq H/W \leq 3:1$	$V/bW = 290 - 55 H/W$
$3:1 \leq H/W \leq 4:1$	$V/bW = 200 - 25 H/W$
$4:1 \leq H/W$	$V/bW = 100.$

From Reference 57

(4) Concrete masonry, if properly reinforced, exhibits a tendency towards a ductile-like behaviour throughout the loading sequence. On the basis of defining ductility as the ratio of the total deflection experienced to the deflection at the first shear crack, the ductility exceeds two.

(5) Although the amount and orientation of the shear reinforcing influenced the shear capacity, the bar spacing did not prove to be a significant factor within the range of reinforcing spacings utilised in these tests, i.e. up to four feet on centers.

The results presented in Table 2-1 for $H/W \geq 3:1$ and Table 2-2 for $H/W \geq 4:1$ infer that all piers satisfying these ratios have the same ultimate load. This inference neglects the possibility of predicting the ultimate load of a pier failing in flexure as outlined in the following investigation.

Scrivener et al ^(49,50,54) performed a series of tests on reinforced concrete hollow masonry walls 8'-8" high and 8' long constructed from 6" thick standard units. Each set of tests had a different objective, and hence each will be outlined separately. In the first set of six tests, Scrivener ⁽⁵⁴⁾ wanted to determine the factors influencing the flexural

type of failure. To achieve this he used a test setup similar to that shown in Figure 2-3, with the reinforcing distributed throughout the wall. The results of the tests are presented in Table 2-3.

The conclusions drawn by the author from the results presented are as follows:

(1) The amount and distribution of vertical reinforcement are the critical factors in determining the stiffness and failure load. Both the stiffness and failure load increase with an increase in the amount of vertical steel. The most effective position for the reinforcement is in the periphery of the wall.

(2) The inclusion of horizontal bond beams does not significantly alter the stiffness or failure load.

(3) The failure load is predictable and the calculations for obtaining this failure load are simple. In these tests, failure loads were usually predictable to within $\pm 5\%$. The most inaccurate prediction underestimated the failure load by 12%. The failure load may be calculated by assuming that all vertical steel has yielded and that the center of compression is at the toe of the wall. The resisting moment of the wall is then the sum of the moment of the yield force in each bar times the lever arm distance from the toe of the wall to the center line of the bar. From Figure 2-9,

$$P_u = \frac{\sum A_{si} d_i \sigma_y}{H} \quad (2-1)$$

where P_u is the ultimate load, A_{si} the area of the i th bar, d_i its distance from the toe of the wall, σ_y the yield stress of the steel and H the effective height of the pier.

TABLE 2-3

BEHAVIOUR OF WALLS UNDER TEST

64

Wall		Wall "elastic" stiffness* (lb/in)	Theoretical prediction of failure load (lb)
A1	6 in blocks, unreinforced	1,500 lb, opening of horizontal crack above first course	Lifting off first course as a whole 1,550
A2	6 in blocks, vertical 5/8 in rods at each end of wall.	Horizontal cracking at base, horizontal cracking above first course at 4,000 lb, vertical cracks appeared at 8,000 lb.	2.5 x 10 ⁵ 15,000 lb, wall lifted off base. above first course, third course, and fifth course 14,600
A3	6 in blocks, vertical 5/8 in rods at each end of wall three 1/2 in rods within.	Horizontal cracking at base at 8,000 lb. horizontal cracking above first, second, and fourth courses at 14,000 lb, vertical cracks appeared at 16,000 lb.	1.0 x 10 ⁵ 26,000 lb, a 1/16 in crack above first course 25,400
A4	6 in blocks, reinforced as wall A3 and in addition bond beams with two 1/2 in bars in fourth and ninth courses.	Horizontal cracking at base and above first course and third course at 10,000 lb, vertical cracks appeared at 22,000 lb.	5.7 x 10 ⁵ 24,000 lb, a 1/8 in crack above first course and major horizontal cracks above and below lower bond beam. 25,600
A5	Two leaves, 4 in blocks, inner leaf vertically reinforced with 1/2 in rods at each end of wall and three 3/8 in rods within, outer leaf unreinforced, leaves tied with 8 s.w.g. crimped ties.	Horizontal cracking, outer leaf, at base and above first, sixth, and seventh courses at 4,000 lb, horizontal cracking, inner leaf at base and above first, second and sixth courses at 8,000 lb, vertical cracking, inner leaf, at 10,000 lb, horizontal crack above first course, outer leaf opened to 1/10 in at 12,000 lb.	1.6 x 10 ⁶ 15,000 lb, a 1/4 in crack above first course of outer leaf some crushing at toe of inner leaf. 15,700
A6	Two leaves, 4 in blocks, inner leaf reinforced as inner leaf of wall A5, outer leaf with four 3/8 in vertical rods not welded to base rods, leaves tied with 1 in x 1/8 in gauge shaped ties.	Horizontal cracking, outer leaf at base.	1.3 x 10 ⁶ 18,000 lb, at 4/10 in lifting off base of outer leaf. 15,800
* Wall "elastic" stiffness is calculated on the longitudinal deflection at the tenth course			

In the second series of twelve full-scale tests Scrivener⁽⁴⁹⁾ was interested in determining the effect of different distributions of reinforcing steel on the shear mode of failure of the walls. To prevent the yield failure occurring he used the test setup shown in Figure 2-2 where R was increased in proportion to P to prevent an overturning moment on the wall. The results of the tests are summarized in Table 2-4.

The conclusions drawn by the author from the results presented are

(1) Vertical and horizontal reinforcing steel are equally effective in providing satisfactory crack behaviour and failure loads.

(2) Walls with evenly distributed reinforcing have a later onset of severe cracking than walls where the reinforcement is concentrated in the wall periphery.

(3) With a low percentage of reinforcing, failure occurs soon after the onset of severe cracking. With higher percentages of reinforcing, the failure load is much greater than the load causing severe cracking.

(4) As the load-deflection curves showed no linear portion and the curve shapes showed no pattern from wall to wall, the stiffness (or load-deflection ratio at a point on the curve) did not seem to bear any direct relationship with the percentage of reinforcement. However, for steel percentages from zero to 0.4% (gross area), at first crack (width approximately 0.001") the stiffness varied from 1.9×10^3 kip/in to 5.5×10^3 kip/in. At severe cracking (some widths exceeding 0.01") the stiffness varied from 1.1×10^3 kip/in to 4.4×10^3 kip/in.

(5) Higher failure loads were obtained with walls with higher percentages of reinforcing up to 0.3% of the gross cross-sectional area

TABLE 2-4
BEHAVIOUR OF WALLS UNDER TEST

Wall	Reinforcing			Percentage (b) (%)	First Crack(d)		Severe Cracking(e)		Failure Load(f) (kip)
	Vertical Bars Peripheral	Vertical Bars Within	Horizontal Bars (a)		Load Causing (kip)	"Stiffness" $\times 10^{-3}$ (c) (kip/in.)	Load Causing (kip)	"Stiffness" $\times 10^{-3}$ (c) (kip/in.)	
C1	—	—	—	0	16	5.3	28	1.1	28
D2	2-5/8"	—	—	.104	32	4.9	48	4.4	68
C10	—	—	2-5/8"	.173	24	3.0	28	2.3	48
			⊕ 2-1/2"						
C7	2-5/8"	—	2-1/2"	.173	40	2.7	48	2.7	60
C8	2-5/8"	1-1/2"	1-1/2"	.173	44	2.1	48	.9	56
C9	2-5/8"	2-1/2"	—	.173	52	2.0	56	.6	60
D11	2-5/8"	—	—	.173	36	1.9	40	1.6	65
			⊕ 2-1/2"						
C3	2-5/8"	3-1/2"	—	.205	48	3.0	56	2.5	70
D12	2-5/8"	3-1/2"	2-1/2"	.272	60	2.8	72	1.8	104
D4	2-5/8"	3-1/2"	4-1/2"	.340	64	4.9	92	3.2	In excess of 112
D13	2-5/8"	3-5/8"	3-5/8"	.420	44	5.5	76	2.0	96
D14	2-5/8"	3-5/8"	4-5/8"	.470	48	2.4	80	2.0	112

Notes:

- The horizontal reinforcing in the top bond beam, which for each wall consisted of 2-1/2" bars (except for walls D13 and D14 where 2-5/8" bars were used), is not included in the table or in the percentage of reinforcing.
- The percentage of reinforcing is calculated on the percentage area of steel divided by the gross cross-sectional area of the wall i.e., in this case $8' - 8" \times 5 - 5/8"$.
- The "stiffness" is calculated on the requisite load divided by the deflection at the load end, 10th course.
- First crack is the first crack visible to the naked eye -- some .001" wide.
- Severe cracking is the stage where some part of the crack pattern has cracks of width .01"
- Failure load is that maximum load which could just be sustained by the wall.

of the wall, which corresponds to 100 kip failure load. Above this percentage, additional reinforcing had little effect on the failure load. From the walls with optimum (0.3%) or higher percentage of reinforcing, the ultimate horizontal shear stress (ultimate load divided by the gross cross-sectional area) was found to be 170 psi.

The objectives of the third series of six full scale tests performed by Scrivener⁽⁵⁰⁾ was to determine the effect of full and partly-filled cavities and to compare the performance of these walls with an "equivalent" reinforced concrete wall. The results of the tests are summarized in Table 2-5. Scrivener summarized his conclusions as follows:

(1) A masonry wall with all cavities filled with grout can withstand a higher load before first crack, severe cracking and failure and is stiffer than the equivalent wall with only reinforced cavities filled. The strength increase is from 20% to 50%.

(2) Although the stiffness of a fully-filled masonry wall and the "equivalent" reinforced concrete wall are very similar, the masonry wall is only some 60% as strong as the reinforced concrete wall.

The Structural Clay Products Research Foundation conducted two series of tests on walls 8' high by 8' long. The objective of the first series of tests⁽⁵¹⁾ was to compare the strength obtained from five identical 8' x 8' walls tested by the standard ASTM E 72-68 racking procedure with that obtained from five identical 16" diameter circular discs tested by the method devised by Johnson and Thompson⁽⁴⁶⁾ (Figure 1-18). The result of the study was that the "apparent" shear strength of the walls tested by the standard ASTM Racking procedure (Figure 2.2) was 60% greater than the result obtained from the tests on the circular

TABLE 2-5

BEHAVIOR OF WALLS UNDER TEST

88

Wall	Type	Reinforcing			First crack**		Severe Cracking		Failure	
		Vertical bars Peripheral (in)	Vertical bars within Horizontal* (in)	Percentage† (%)	Load causing (lb)	Stiffness‡ (lb/in x 10 ⁻³)	Load causing (lb)	Stiffness‡ (lb/in x 10 ⁻³)	Load ^o ‡ (lb)	
E8	Partly-filled	2- $\frac{5}{8}$	1- $\frac{1}{2}$	1- $\frac{1}{2}$	0.173	48,000	2,400	60,000	1,900	72,000
E15	Fully-filled	2- $\frac{5}{8}$	1- $\frac{1}{2}$	1- $\frac{1}{2}$	0.173	84,000	3,800	88,000	3,100	92,000
E17	Reinforced concrete	2- $\frac{5}{8}$	1- $\frac{1}{2}$	1- $\frac{1}{2}$	0.173			----	----	160,000
E10	Partly-filled	2- $\frac{5}{8}$	3- $\frac{1}{2}$	2- $\frac{1}{2}$	0.272	40,000	2,400	68,000	1,900	76,000
E11	Fully-filled	2- $\frac{5}{8}$	3- $\frac{1}{2}$	2- $\frac{1}{2}$	0.272	100,000	2,800	100,000	2,000	116,000
E18	Reinforced concrete	2- $\frac{5}{8}$	3- $\frac{1}{2}$	2- $\frac{1}{2}$	0.272					176,000

* The horizontal reinforcing in the top bond beam for each wall consisted of two $\frac{1}{2}$ in diameter bars and is not included in the figures in the above table.

† The percentage of reinforcing is calculated on the area of steel divided by the gross cross-sectional area of the wall, i.e. 104 in x 5 $\frac{5}{8}$ in.

‡ The "stiffness" is calculated on the requisite load divided by the deflection of the load end at the tenth course.

** "First crack" is the first crack visible to the naked eye - usually some 0.001 in wide.

*+ "Severe cracking" is that stage where some part of the crack pattern has cracks of width 0.01 in.

*‡ "Failure load" is the maximum load that could just be sustained by the wall.

From Reference 50

discs. The authors concluded by stating that although the method of testing shown in Figure 1-18 was new to clay masonry testing and the extent to which the results represent the state of pure shear or diagonal tension are as yet unknown, the external hold-down force required in the ASTM racking test increases the apparent shear strength by 60%.

The purpose of the second series of tests⁽⁵²⁾ was to compare the shear strength of walls constructed from 4" structural clay facing tiles with those constructed from 4" clay brick units. The shear strengths were determined by the standard ASTM procedure (Figure 2-2). The results indicated that the apparent shear strength, based on net area, of walls constructed from facing tiles is significantly higher than the corresponding values for 4" brick specimens. The report concludes that the mode of failure in racking involves not only the rupture through the mortar joints but also in many cases through the tile units themselves, and that the high tensile strength of the fired clay body apparently influenced the results.

Haller⁽⁶¹⁾ in reporting on the various investigations performed at the Swiss Federal Laboratories included the work done on the shear strength of masonry walls. In these investigations two different test techniques were used. The first was similar to that shown in Figure 2-9. The second, shown in Figure 2-10, was unique to Haller's program. They used two different sizes of specimens, the larger 9'-6" x 8'-8" x 6" specimens were tested in the setup shown in Figure 2-10, while the smaller 4'-8" x 5'-3" x 6" specimens were tested in the setup shown in Figure 2-13. In addition to the two types of specimens, two different types of bricks were used; a normal quality brick laid with a lime-cement mortar and a special quality brick laid with a cement mortar. The

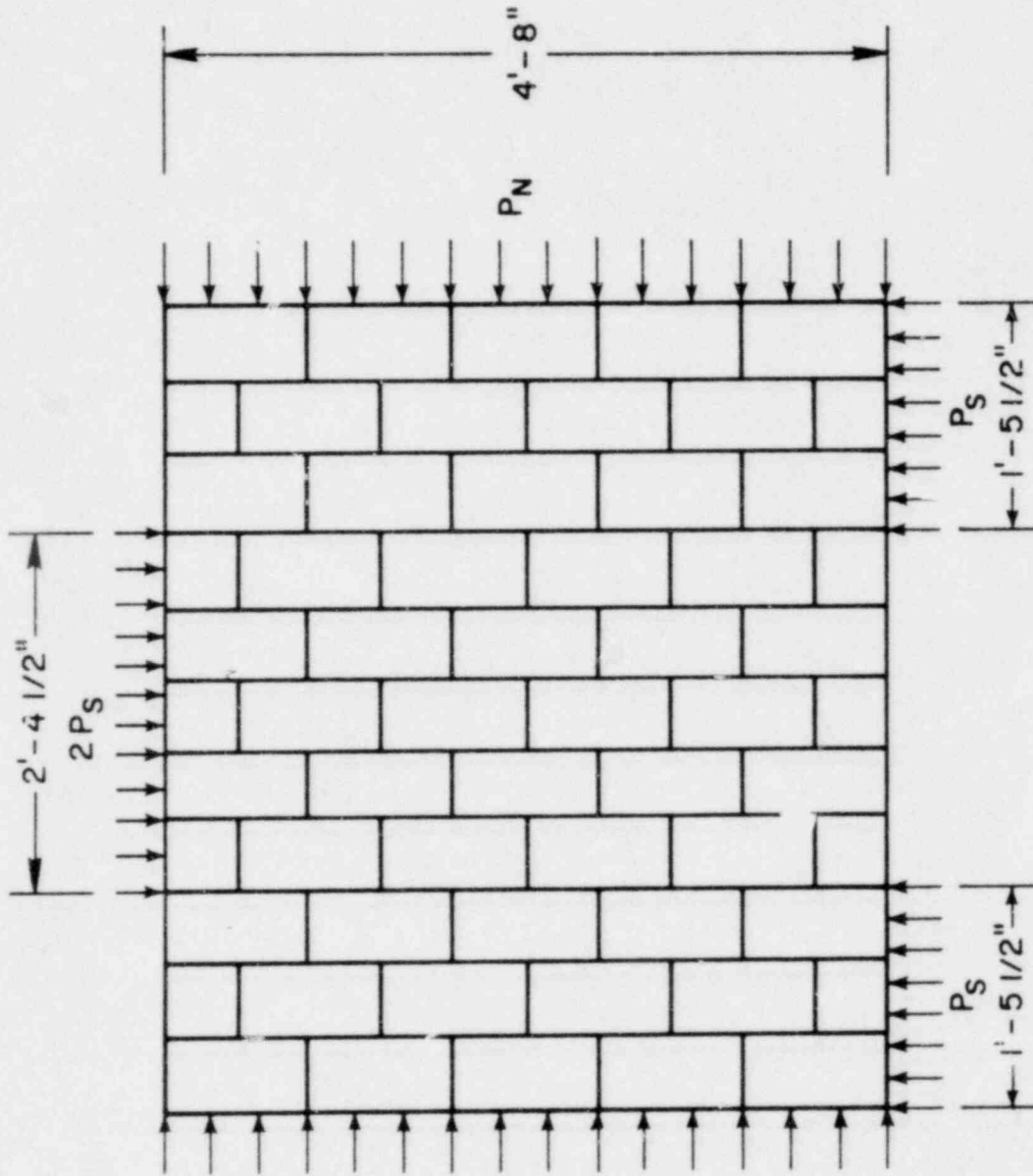


FIGURE 2-13

From Reference 61

results of the tests are presented in graphical form in Figure 2-14. An empirical relationship between the compressive stress (σ_c) and the shear strength (τ_{xy}) given in Figure 2-14 is

$$\tau_{xy} = (35 \sqrt{\sigma_c + 130} - 250) \text{ psi} \quad (2-2)$$

for the special quality bricks, and

$$\tau_{xy} = (35 \sqrt{\sigma_c + 280} - 540) \text{ psi} \quad (2-3)$$

for the normal quality bricks, where τ_{xy} is the shear stress and σ_c the compressive stress in psi.

From the results presented, Haller observed that the shear strength is composed of the adhesion of the mortar to the brick, the shear resistance of the mortar plugs (i.e. the mortar that penetrates into the perforations) and the friction forces which increase with compressive stress. In the absence of compressive stresses only the first two effects (i.e. adhesion and shear resistance) are active. Haller concluded by stating that with no compressive stress on the walls the shear strength is considerably affected by the absorptivity of the mortar, including the plugs.

As mentioned in Section 2-1, one of the most widely used techniques to determine the relative shear strength of masonry walls and wallettes is the diagonal test method shown in Figure 2-4. The largest study performed using this technique was that done by Blume⁽⁵⁵⁾ for the Western States Clay Products. The 84 walls used in Blume's tests were 4 feet square. The materials used were 8" hollow clay brick units and 4" wide clay brick units. Typical wall details are shown in Figure 2-15. The shear strength index of the walls was calculated from

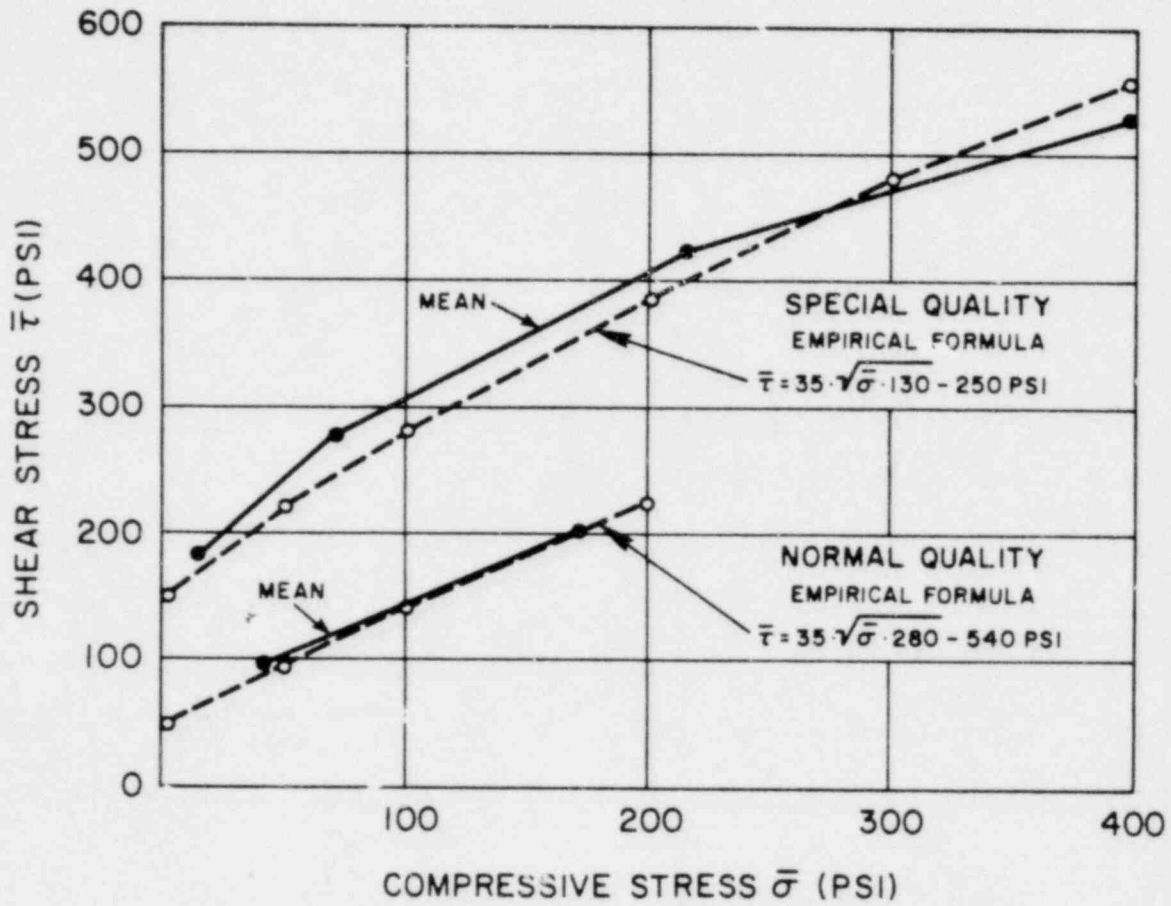


FIGURE 2-14 EMPIRICAL SHEAR STRENGTH VS. APPLIED COMPRESSIVE STRESS

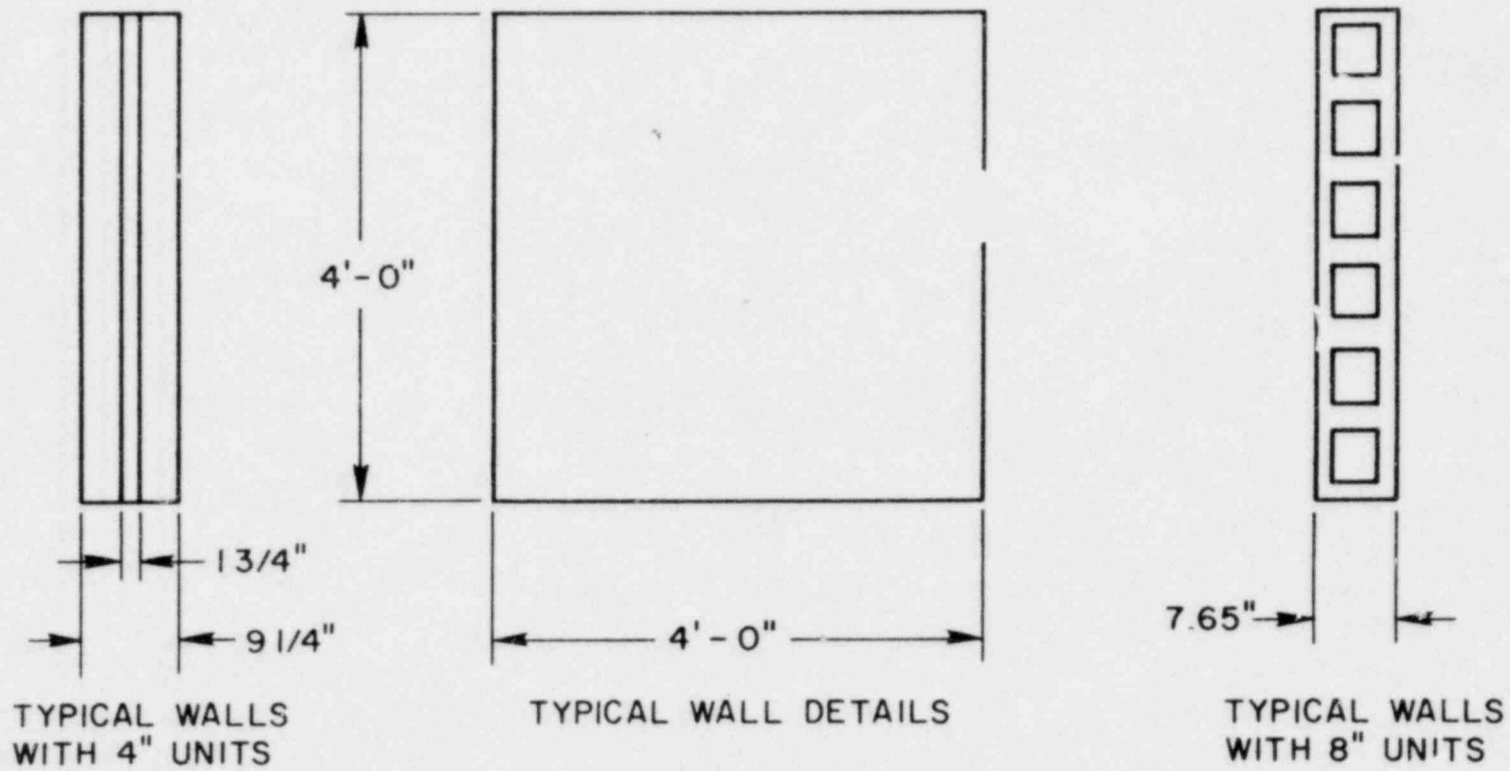


FIGURE 2-15 TYPICAL TEST SPECIMEN

$$V = \frac{0.707 P}{A} \quad (2-4)$$

where V is the average net or gross shear stress, P the diagonal load and A either the net or gross cross-sectional area. The more important conclusions presented in the study are as follows:

(1) The ultimate unit shear values obtained from the above index in nine unreinforced, 2 1/2 inch grout core, masonry wall specimens ranged from 324 psi to 413 psi, using the materials listed in conclusions 2 and 3.

(2) (a) The mortar must be workable and satisfactory to a good mason. It was recommended that the mortar be made of 1 part portland cement, 3/4 part hydrated lime and an average of 4 parts damp, loose mortar sand with an allowable range of 3 3/4 to 4 1/4. (b) The fine grout mix recommended was 1 part portland cement to not more than 3 parts of non-bulked dry sand or 4 parts of moist loose sand by volume. No lime is recommended. The grout must be fluid and suitable in all respects for proper placing, to entirely fill the core space. (c) There should be no arbitrary limits on the water content of the mortar or of the grout. Workability and placing characteristics are much more important than compression tests which may grossly exceed the code requirements. This conclusion implies that mortar with the given proportions satisfies strength and bond requirements provided the amount of water used is sufficient to satisfy workability requirements.

(3) Of the two brick properties, compression value and modulus of rupture, the latter is more significant for the shear value of the masonry. It was recommended for optimum shear capacity that the brick

compressive strength be 6,000 to 10,000 psi, and that the brick modulus of rupture be greater than 500 psi. It should be noted that in general there is a correlation between the compression value and the modulus of rupture (Section 1-3).

(4) Brick masonry panels with either minimal or no reinforcement have essentially no ductility. It was found that with more extensive reinforcement than that required by the building codes and especially with special disposition of the steel at the center of the panel, some ductility and increased energy absorption can be obtained. However, the cost of this special reinforcement is not justified by the extra values obtained, except for special situations. It should be noted that significant ductility has been obtained in cyclic load tests on masonry piers (3,58,76,77).

(5) The diagonal tension (shear) failures, whether the panels were reinforced or not, were not accompanied by heavy spalling, popping or the projection of fragments away from the wall (as occurs in compression failure). Instead, the tension crack opened up with a crunching sound. It was found that only a small amount of reinforcing, such as a single No. 4 bar in an entire wall was enough to hold the main pieces of the wall in place after failure.

(6) Unless reinforcement is required for a particular design stress function, its basic purpose must be (a) to help tie or anchor wall elements to a frame or other walls and (b) to hold the wall pieces together in the event of failure in an earthquake. These tests indicate that only nominal reinforcing is adequate for (b), and judgement indicates the same for (a). It therefore seems that the arbitrary use of

large percentages of steel area in grouted masonry walls serves no real purpose. Other investigators^(3,58,76) have shown that the amount and distribution of reinforcement in a panel affect both the strength and ductility.

(7) The average shear values of the hollow brick masonry panels varied from 123 psi to 391 psi depending upon the particular brick units. With all cells filled with grout the shear values using the entire gross wall area were 266, 266 and 387 psi for three different brick units. The corresponding values in the hollow state based on the net area were 123, 128 and 221 psi, respectively; i.e. a 75% to 112% increase in strength.

Two subsequent investigations were performed by Greenley and Cattaneo⁽⁶²⁾ and Borchelt⁽⁶³⁾ where a distributed compressive edge load was considered in addition to the point load applied on the corners of the panels. A diagrammatic illustration of the applied loads is shown in Figure 2-7. Greenely and Cattaneo⁽⁶²⁾ performed 32 tests on panels of 4' x 4' x 4" nominal dimensions. In the 32 different tests, they considered three different bricks and two mortars - one a high strength (with additive) and one a conventional mortar. The results of the study are presented in Table 2-6.

The authors concluded that a substantial improvement in the racking strength of the wall is obtained by the use of high strength mortar. Walls built with the conventional mortar all failed in a stepwise manner through the mortar/brick interface, while those with high bond mortar failed approximately straight along the diagonal. They further concluded that increasing the edge load will increase the racking strength of a masonry wall, and when more data are available from a wider variety of

TABLE 2
RACKING STRENGTHS

Brick A -- Conventional mortar				Brick A -- High-bond mortar			
Edge-load		Racking strength		Edge-load		Racking strength	
(Gross lbf x 10 ³)	(lbf/in ²)	(Gross lbf x 10 ³)	(lbf/in ²)	(Gross lbf x 10 ³)	(lbf/in ²)	(Gross lbf x 10 ³)	(lbf/in ²)
0	0	44	175	0	0	141	560
0	0	45.5	181	0	0	115	457
25	140	68	270	50	281	168.5	670
50	281	89.2	355	100	562	178	708
75	421	115	457	150	832	238	946
100	562	127	506	200	1120	209.5	833
125	702	133	530	250	1400	258	1020
150	843	141	560	450	2530	233	926
Compressive flexural tests on 8x8 ft wall panels							
Flexural strength (lbf/in ²)			80				360
Compressive strength (lbf/in ²)			3190				4830
Bed joint area (in ²)			178				178
Diagonal cross-sectional area (in ²)			252				252
Brick B -- High-bond mortar				Brick S -- High-bond mortar			
Edge-load		Racking strength		Edge-load		Racking strength	
(Gross lbf x 10 ³)	(Gross lbf/in ²)	(Gross lbf x 10 ³)	(lbf/in ²)	(Gross lbf x 10 ³)	(lbf/in ²)	(Gross lbf x 10 ³)	(lbf/in ²)
0	0	161	608	0	0	167	690
0	0	167.5	642	0	0	175	724
50	267	245	924	0	0	195	806
50	267	231	872	50	293	217	898
100	534	205	774	100	586	257	1060
150	800	246	928	125	732	274	1130
200	1066	261	984	150	879	297	1230
300	1595	280	1056	200	1172	306	1280
Compressive flexural tests on 8x8 ft wall panels							
Flexural strength (lbf/in ²)			452				220
Compressive strength (lbf/in ²)			5170				6100
Bed joint area (in ²)			187.5				171
Diagonal cross-sectional area (in ²)			265				242

From Reference 62

systems it will be possible to consider an analysis of stress interaction in such systems.

Borchelt⁽⁵⁶⁾ used Greenley and Cattaneo's⁽⁶²⁾ high strength mortar results and hypothesized that the failure of a high bond masonry system subjected to the joint action of an edge load and a racking load occurs when the principal tensile stress reaches a constant value. Borchelt assumed the stress distribution to be that shown in Figure 2-16. By assuming an equivalent homogeneous linear system in plane stress, Borchelt found the maximum principal tensile stress (σ_t) from equilibrium and Mohr's circle to be

$$\sigma_t = -\frac{\sigma_c}{2} + \sqrt{\left(\frac{\sigma_c}{2}\right)^2 + \tau_{xy}^2} \quad (2-5)$$

where $\sigma_c = \frac{P_e}{bt}$ and $\tau_{xy} = \frac{P_d}{\sqrt{2} bt}$; P_e and P_d are the compressive and edge loads, respectively; and b and t are the width and thickness of the panel, respectively. Borchelt divided Equation 2-5 by the compressive strength of the pier σ_{cp} and obtained the dimensionless equation

$$\frac{\tau_{xy}}{\sigma_{cp}} = \sqrt{\left(\frac{\sigma_t}{\sigma_{cp}}\right)^2 + \frac{\sigma_t \sigma_c}{\sigma_{cp}^2}} \quad (2-6)$$

The dimensionless data used by Borchelt from Greenley and Cattaneo's tests are presented in Table 2-7.

Borchelt assumed that failure results when the principal tensile stress reaches a constant maximum value. He determined this value by considering the average diagonal load at failure when there is no edge

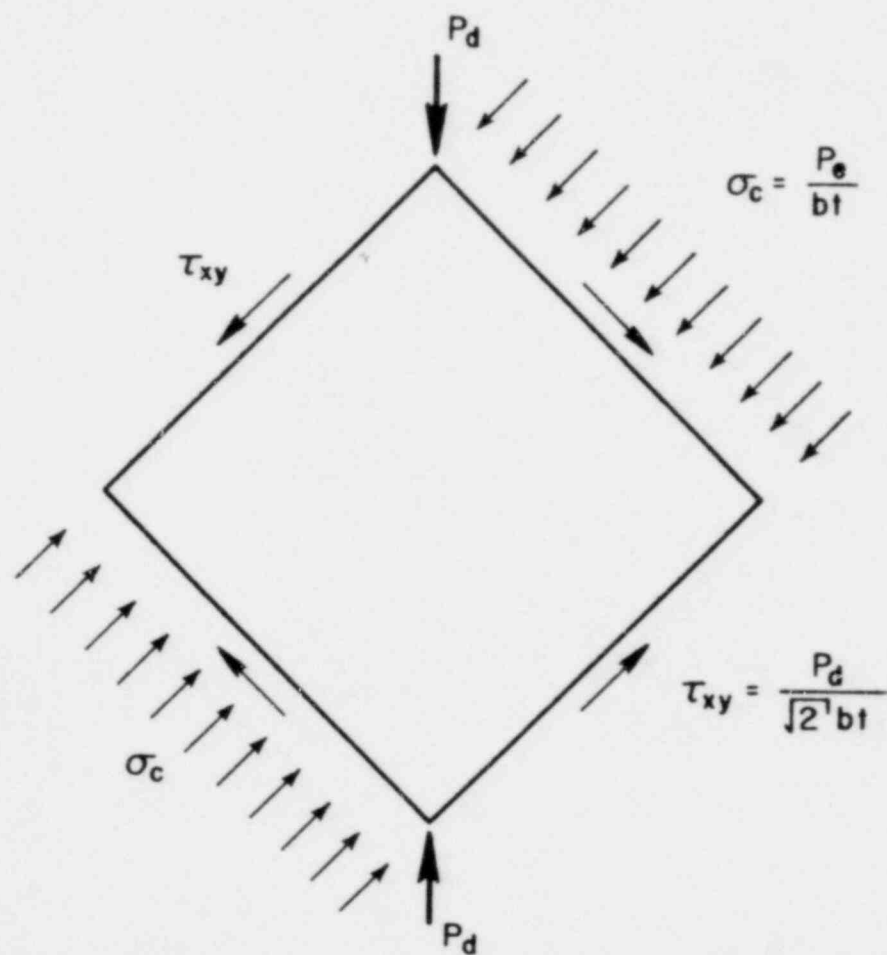


FIGURE 2-16 STRESS DISTRIBUTION FOR EDGE LOAD WITH RACKING

From Reference 56

TABLE 2-7

DIMENSIONLESS DATA FOR EDGE LOAD WITH RACKING

$\frac{\sigma_c}{\sigma_{cp}}$	$\frac{\sqrt{2} \tau_{xy}}{\sigma_{cp}}$	$\frac{\sigma_c}{\sigma_{cp}}$	$\frac{\sqrt{2} \tau_{xy}}{\sigma_{cp}}$	$\frac{\sigma_c}{\sigma_{cp}}$	$\frac{\sqrt{2} \tau_{xy}}{\sigma_{cp}}$
0	0.1642	0	0.1792	0	0.1862
0	0.1340	0	0.1661	0	0.1671
0.0582	0.1962	0.0516	0.253	0	0.1593
0.1166	0.2074	0.0516	0.2385	0.0478	0.207
0.1748	0.2772	0.1032	0.2118	0.0956	0.245
0.233	0.244	0.1548	0.254	0.1193	0.262
0.2912	0.3006	0.2065	0.269	0.1434	0.284
0.524	0.2715	0.3098	0.2886	0.1912	0.292

From Reference 63

load present. For the available data, the average value of the three different types of bricks combined is

$$\frac{\tau_{xy0}}{\sigma_{cp}} = 0.1161 = \frac{\sigma_t}{\sigma_{cp}}$$

where τ_{xy0} is the shear strength of the panel with no compressive load. Using these values it is merely a matter of substitution in Equation 2-6 to secure the final equation for the ultimate diagonal load in terms of the applied edge load.

$$\frac{\tau_{xy}}{\sigma_{cp}} = \sqrt{0.0135 + 0.1161 \frac{\sigma_c}{\sigma_{cp}}} \quad (2-7)$$

or in terms of the actual edge loads

$$\frac{P_d}{\sigma_{cp} bt} = \sqrt{0.0270 + 0.2322 \frac{P_e}{\sigma_{cp} bt}} \quad (2-8)$$

Borchelt plotted the results of Equation 2-8 with the experimental results in Figure 2-17, and concluded that Equation 2-8 seems to provide a good representation of the behaviour of the system. If the variable $\frac{\sigma_t}{\sigma_{cp}}$ had been calculated for each brick and mortar combination the dotted lines of Figure 2-17 would represent the theoretical results of each material. This is a more accurate and realistic approach as the maximum allowable tensile stress will always be a function of the materials used.

Borchelt stated in his paper that this method of analysis may not be valid for conventional systems. The basis of this conclusion was on the one set of results he used from Greenley and Cattaneo's tests with conventional mortar. The failure mechanism in this instance was reported

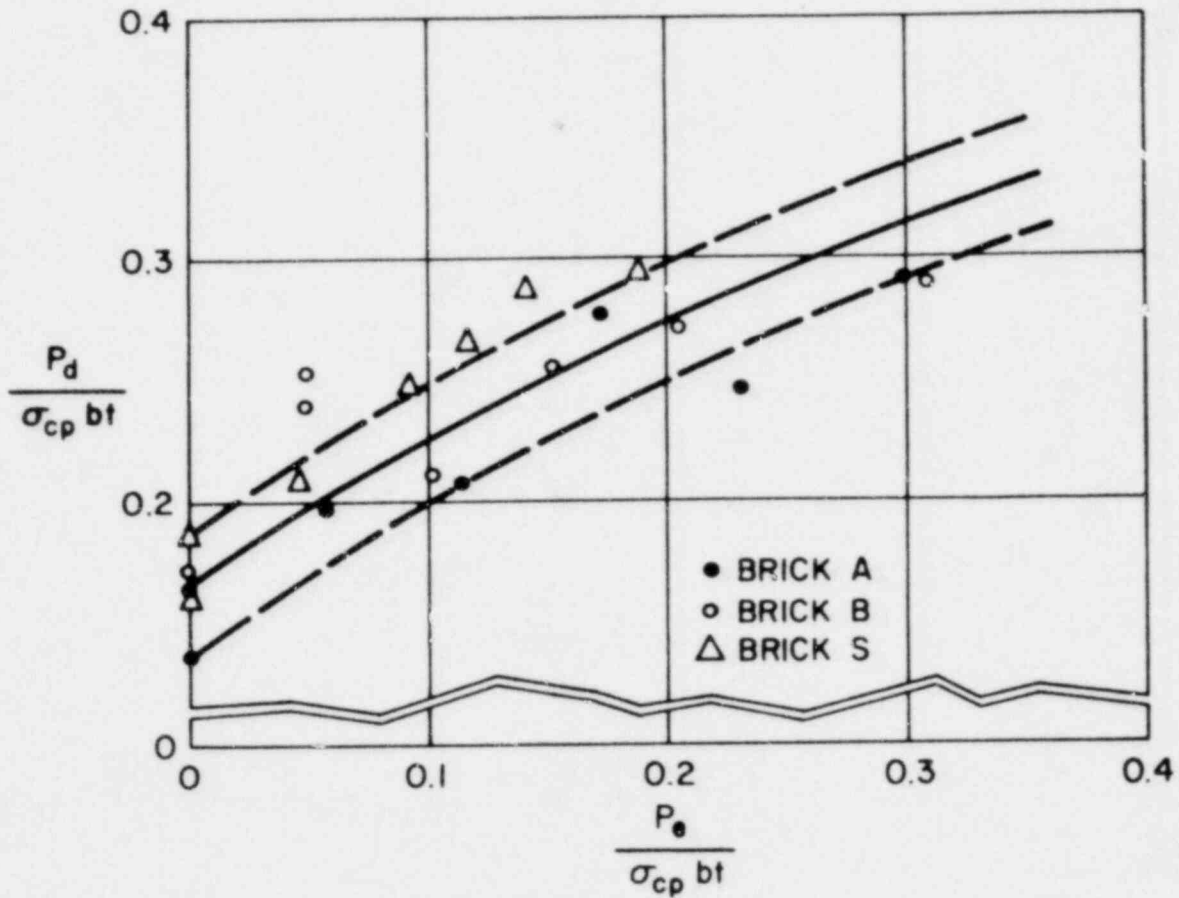


FIGURE 2-17 GRAPH OF DATA FOR EDGE LOAD VS. RACKING LOAD

to be stepwise through the mortar joints. For the purpose of this report the experimental and theoretical results are plotted in Figure 2-18. The equation for the ultimate diagonal load in terms of the actual edge loads is

$$\frac{P_d}{\sigma_{cp} bt} = \sqrt{.0062 + .1578 \frac{P_e}{\sigma_{cp} bt}} \quad (2-9)$$

and the theoretical results are consistently below the experimental results. This could be attributed to the fact that a bond and not a tensile failure is obtained.

In a paper that summarized much of the masonry research performed at the Research Institute in Ljubljana, Turnsek and Cacovic⁽⁶⁰⁾ included their work on masonry walls subjected to combined normal and shear stresses. They, like Borchelt, proposed a method for theoretically determining the failure load of the masonry elements they tested. They considered the element shown in Figure 2-19, subjected to a compressive stress and shear stress given by

$$\sigma_c = \frac{P_v}{A} \quad \text{and} \quad \tau_{xy} = \frac{P_H}{A}$$

where P_v and P_H are the compressive and shear forces, respectively, and A is the net or gross area of the wall. At the center point B on the wall the shear stress is $1.5 \tau_{xy}$ if the stress distribution across the width of the wall is assumed to be parabolic. From Mohr's circle the maximum principal tensile stress at B is

$$\sigma_t = \sqrt{\left(1.5 \tau_{xy}\right)^2 + \left(\frac{\sigma_c}{2}\right)^2} - \frac{\sigma_c}{2} \quad (2-10)$$

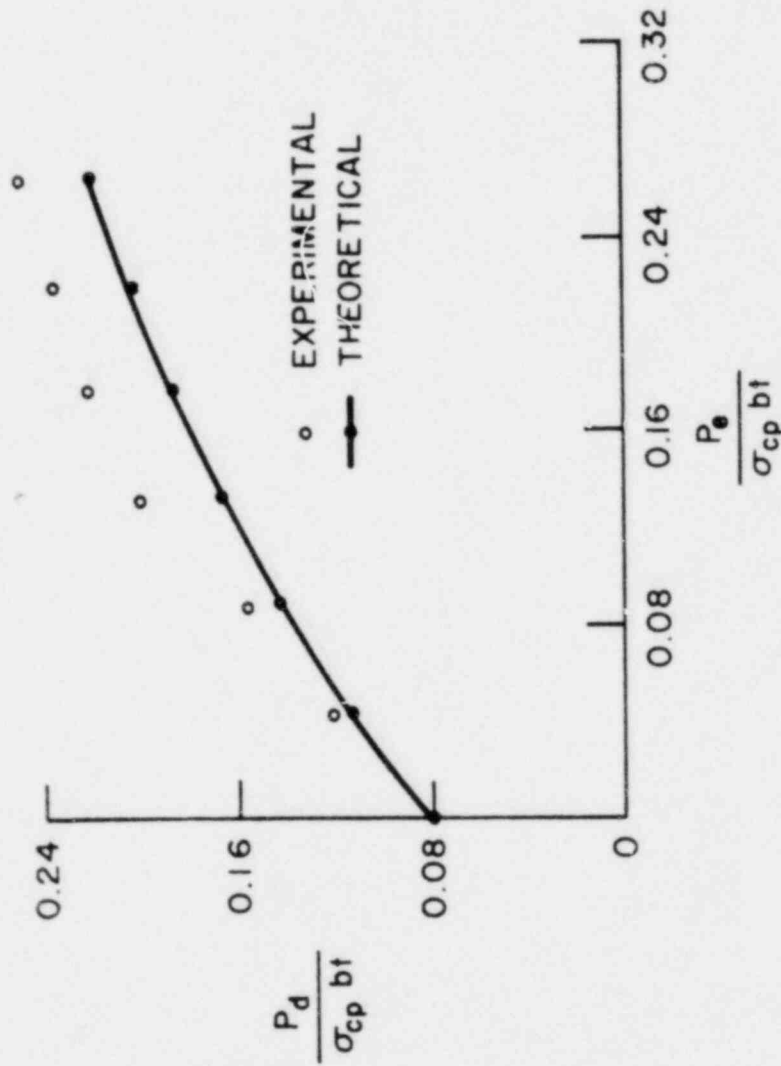


FIGURE 2-18 EDGE VS RACKING LOAD FOR LOW STRENGTH MORTAR

From Reference 56

NORMAL STRESS AT B

$$\sigma_B = \frac{P_V}{A}$$

SHEAR STRESS AT B

$$\begin{aligned} \tau_B &= 1.5 \frac{P_H}{A} \\ &= 1.5 \tau_{xy} \end{aligned}$$

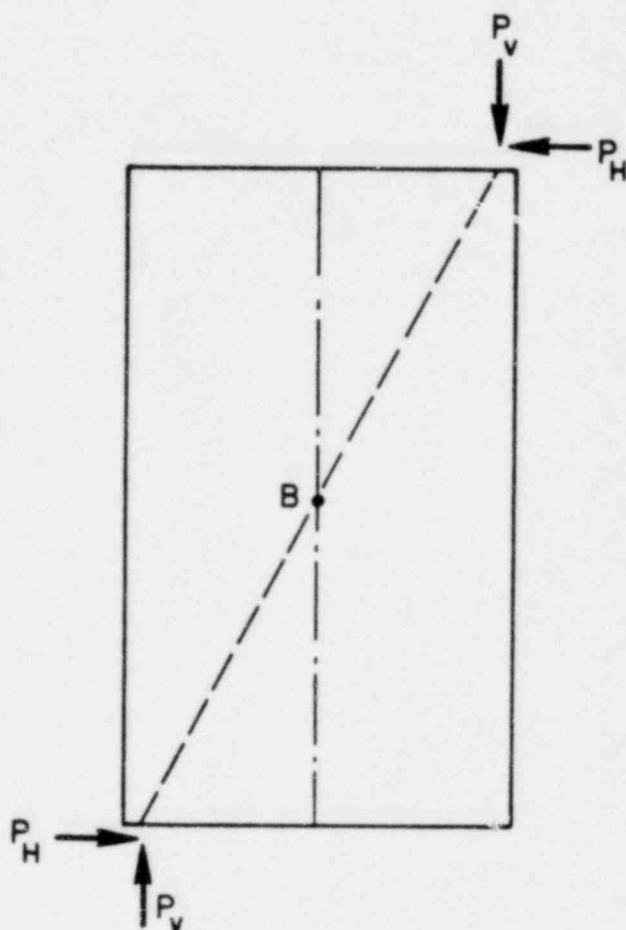


FIGURE 2-19 STRESSES AT THE CENTER OF THE ELEMENT

Turnsek and Cacovic stated that by photoelastic analysis it was found that σ_t calculated from the above formula is in good agreement with the actual stress when the height to width ratio of the wall is larger than 1.5. They also said that the expression is valid when the height to width ratio is greater than 0.67, but when it is smaller than 0.67 the calculated value is larger than the actual one.

Like Borchelt, Turnsek and Cacovic assumed that shear failure of the walls occurs when the maximum principal tensile stress reaches a critical value. They expressed the critical value in terms of the average shear stress (τ_{xy0}) that would cause failure without a compressive load

$$\text{i.e. } \sigma_{tcr.} = 1.5 \tau_{xy0} \quad (2-11)$$

Substituting Equation 2-11 into 2-10, the ultimate average shear stress τ_{xy} of a wall with a compressive stress σ_c is given by

$$\tau_{xy} = \tau_{xy0} \sqrt{1 + \frac{\sigma_c}{1.5 \tau_{xy0}}} \quad (2-12)$$

Turnsek and Cacovic attempted to verify their hypothesis experimentally. They tested six 4'-10" high x 3'-4" long x 9.8" thick brick walls. All walls were made of bricks with a compressive strength of 2845 lb/in² and the same cement-lime mortar. Each wall was tested with a different compressive stress and the value of τ_{xy0} was calculated from Equation 2-12. From the results presented in Table 2-8, Turnsek and Cacovic, concluded that τ_{xy0} was a constant for brickwork made from bricks and mortar of the same quality. They performed further experiments with bricks and mortars of different strengths, and plotted the dimensionless

TABLE 2-8

MEAN COMPRESSIVE STRESS, MEAN SHEAR STRESS AND
PRINCIPAL TENSILE STRESS FOR SIX WALLS

Wall No.	σ_c		τ_{xy}		τ_{xyo}	
	(kgf/cm ²)	(lbf/in ²)	(kgf/cm ²)	(lbf/in ²)	(kgf/cm ²)	(lbf/in ²)
1	2.00	28.45	1.55	22.04	1.03	14.65
2	3.00	42.67	1.96	27.88	1.21	17.21
3	5.00	71.12	2.19	31.15	1.07	15.22
4	5.00	71.12	2.26	32.15	1.13	16.07
5	10.00	142.23	2.94	41.82	1.10	15.65
6	10.00	142.23	3.12	44.38	1.20	17.07

From Reference 64

mean shear stress against the dimensionless compressive stress. The results, plotted in Figure 2-20, indicate the validity of their proposed method of calculating the ultimate shear strength for the materials used by them.

To determine the influence of the mortar strength on the shear strength of the walls the authors plotted their experimental results for τ_{xyo} against the mortar strength -- Figure 2-21. In addition, after two of the walls were initially cracked they were repaired and retested. The results of the two repaired walls are included in Figure 2-21.

Pieper and Trautsch⁽⁶³⁾ performed a parameter study on the relative shear strength of long walls, with the test setup shown in Figure 2-22. The variables included in the study were the applied compressive stress, the length and thickness of the wall, the age of the brickwork, the strength of the mortar and the effect of wetting bricks during construction. The results presented by the authors are shown in Figures

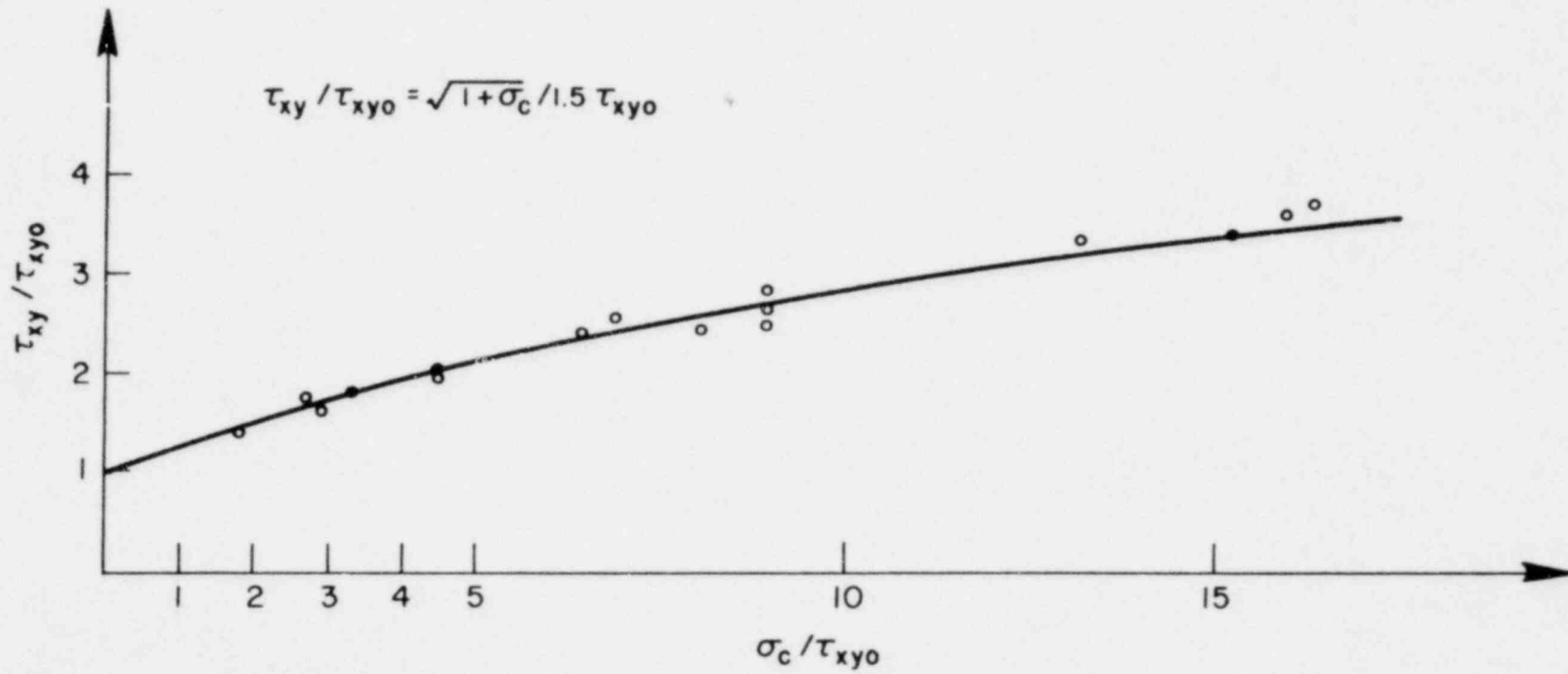


FIGURE 2-20 ULTIMATE STRENGTHS OF BRICKWORK WALLS SUBJECTED TO HORIZONTAL AND VERTICAL LOADS

From Reference 64



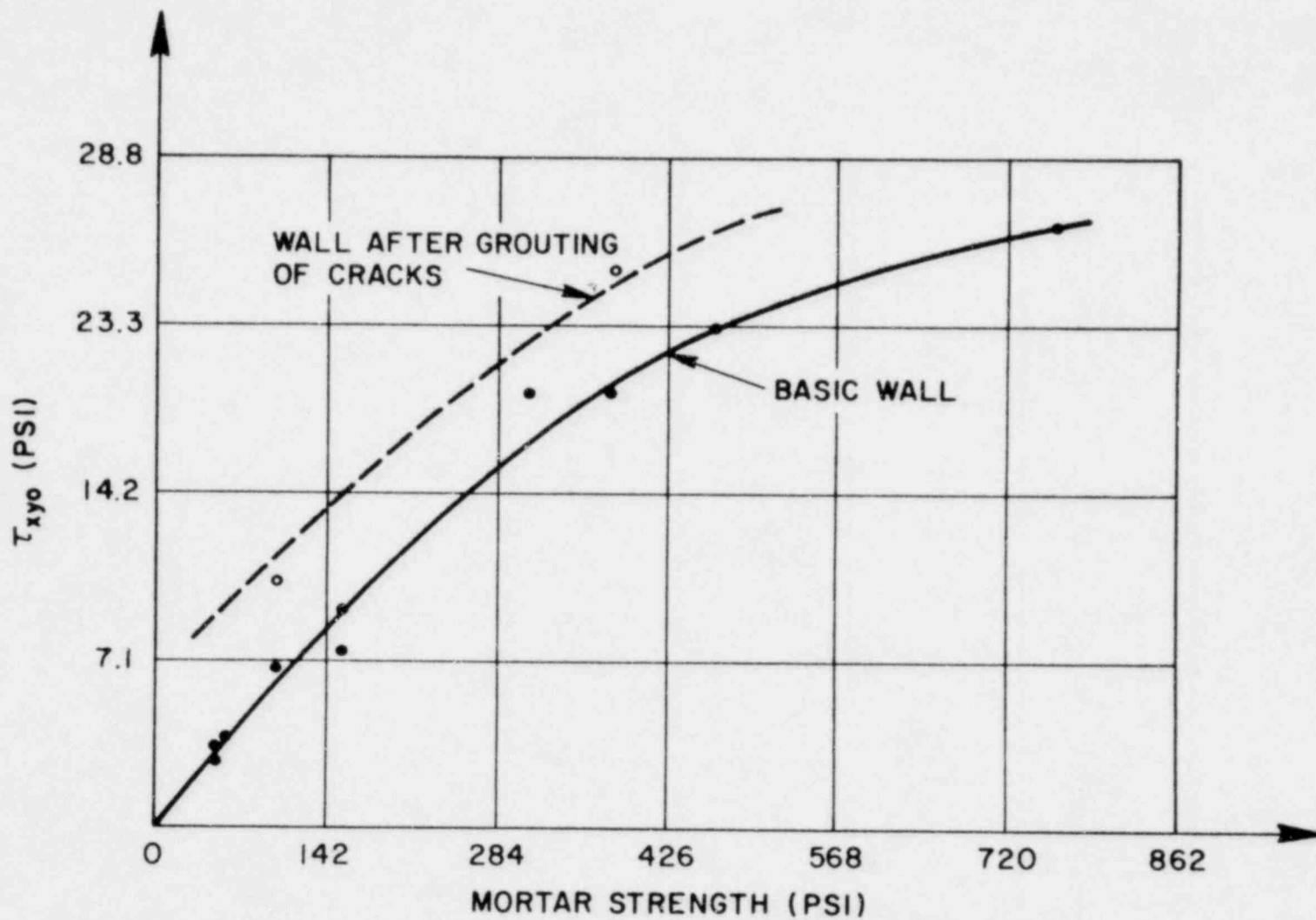


FIGURE 2-21 DEPENDENCE OF τ_{xyo} UPON THE QUALITY OF MORTAR

From Reference 64

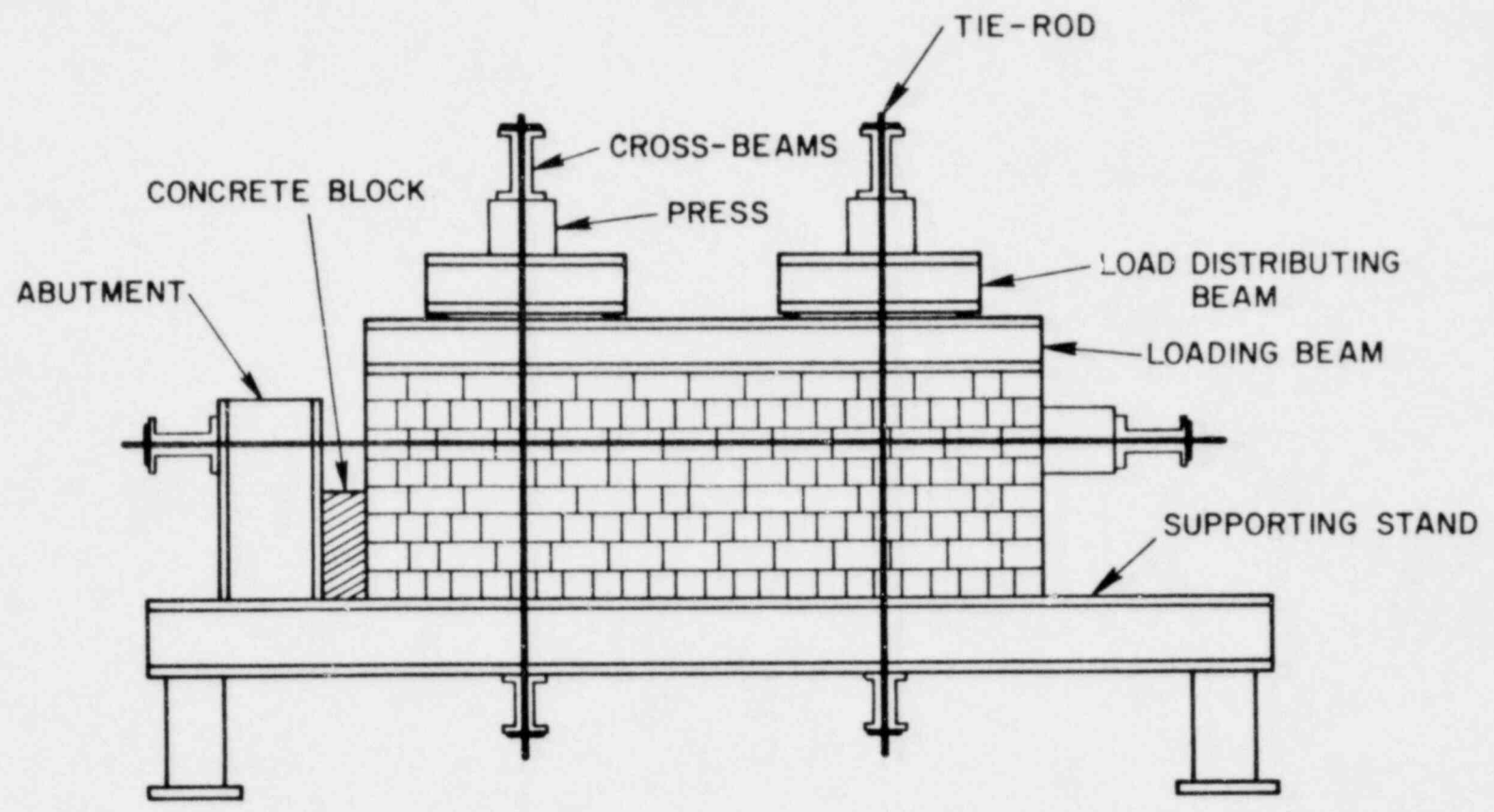


FIGURE 2-22 TEST SET-UP

From Reference 63

2-23 to 2-28. Because of the unusual method of applying the shear load, the results should only be regarded as indicative of the effects of the various parameters. The two dominating variables of the study were the strength of the mortar and the applied compressive stress. The shear strength of the assemblage increased with an increase in either parameter.

Meli^(58,72-75), and co-workers performed a comprehensive program on 56 6' x 6' cantilever walls. Each wall was built on a stiff concrete beam and tested monotonically with the test setup shown in Figure 2-29. Concrete blocks, hollow and solid clay bricks, were the main types of unit studied, while the reinforcement consisted of either interior reinforcement or tie columns and bond beams of the same thickness as the wall. A vertical load was also imposed on several of the walls.

Walls encased in concrete frames behaved as monolithic elements for small loads until separation occurred in the lower tensile corner and later also in the opposite corner. Major stiffness reduction was due to progressive flexural cracking in the frame or in the wall itself. Subsequent behaviour depended on the type of failure.

For walls with low vertical reinforcement and low vertical loads, failure was governed by flexure and behaviour was similar to that of an underreinforced concrete beam. Extensive flexural cracking occurred and strength was limited by yielding of the reinforcement followed by a rather long plateau (Figure 2-30). Failure was finally due to crushing of the compressive corner or to rupture of the extreme bars. Pre-compression on the wall caused an increase in strength but for high vertical stresses, behaviour tended to change to a brittle shear failure.

For high reinforcement ratios failure was governed by shear. A relatively high stiffness was maintained until a diagonal crack occurred at angular deformations between 0.001 and 0.002. The crack formed

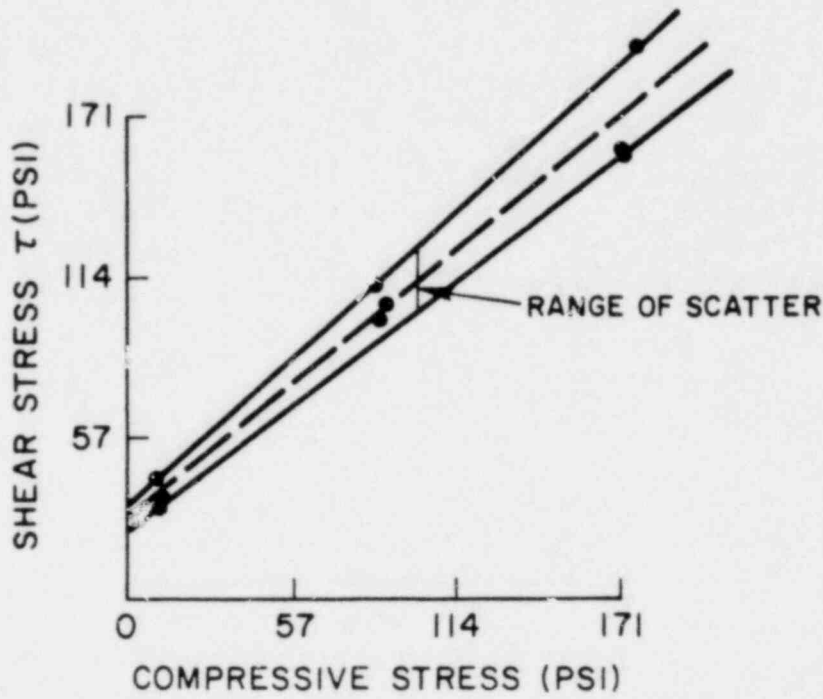


FIGURE 2-23 EFFECT OF COMPRESSIVE STRESS

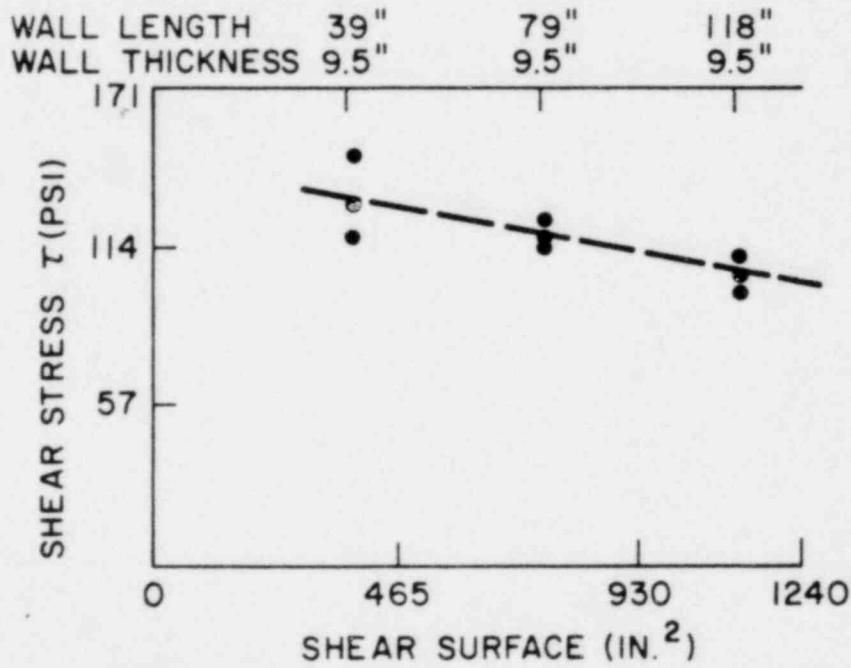


FIGURE 2-24 EFFECT OF THE LENGTH OF THE WALL. COMPRESSIVE STRESS = 85PSI

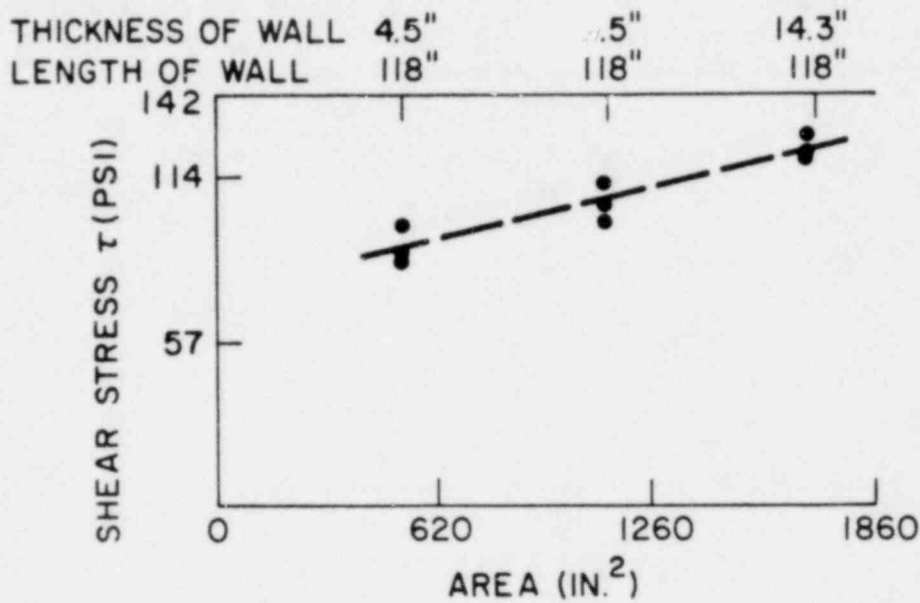


FIGURE 2-25 EFFECT OF THE THICKNESS OF THE WALL

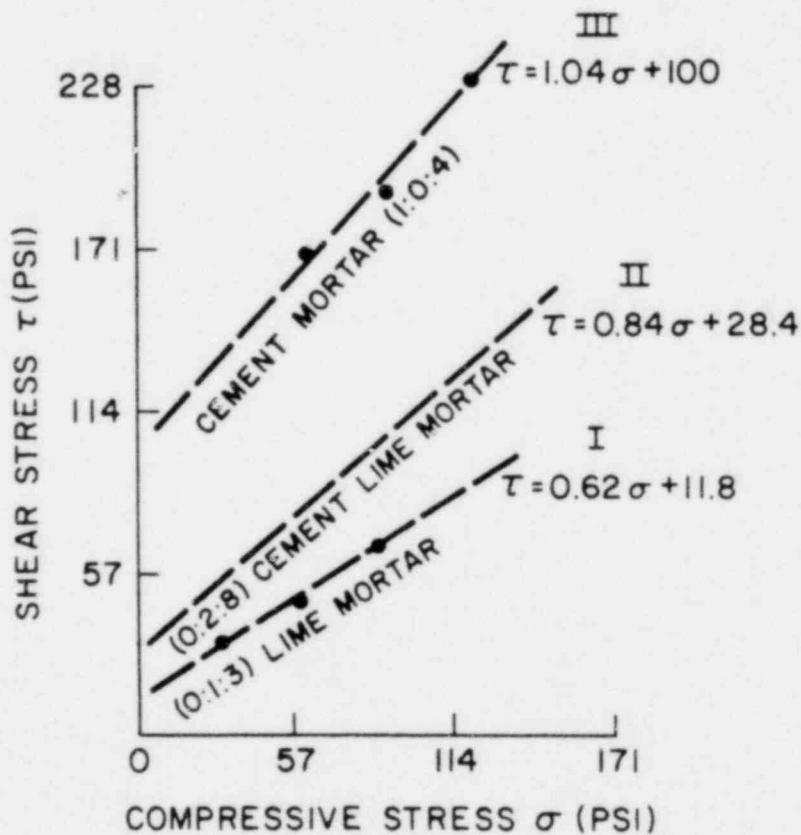


FIGURE 2-26 EFFECT OF MORTAR COMPOSITION. COMPRESSIVE STRESS = 35PSI

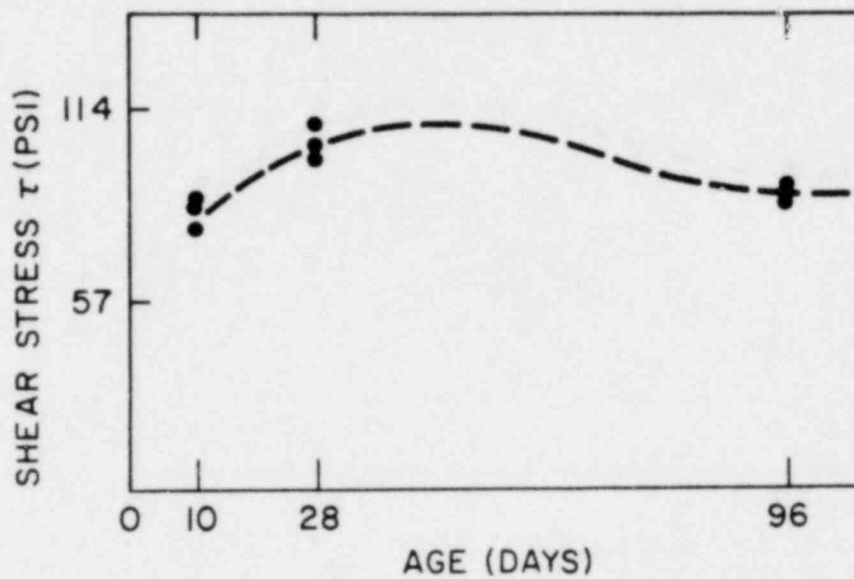


FIGURE 2-27 EFFECT OF BRICKWORK AGE

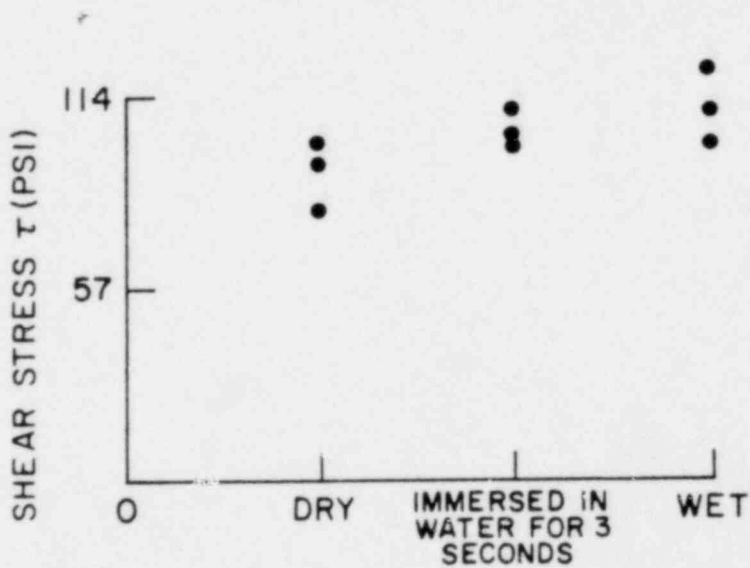


FIGURE 2-28 EFFECT OF WETTING BRICKS DURING CONSTRUCTION

generally through the joints. The diagonal crack crossed the units only for low strength units or for high precompression loads. For walls with interior reinforcement the load increase after cracking depended on the amount of reinforcement. If there was no precompression on the wall the maximum load could be maintained for high deformations due to the friction in the crack and to the dowel action in the reinforcement, and behaviour was rather ductile. On the contrary, for high vertical loads failure was extremely brittle (Figure 2-30).

Meli stated that the strength and general behaviour of walls with bending failure could be satisfactorily predicted with the usual hypotheses for reinforced concrete. For usual reinforcement ratios, simplified procedures give reasonable accuracy. Such procedures may consist in considering that the resultant of compressive interior forces is located in the center of the extreme reinforcement on the compressive side, and that all the remaining reinforcement yields at maximum load.

Shear strength was more difficult to predict. Cracking load was found to be less variable than maximum load for which the failure mechanism depends on more factors. Contribution of the exterior reinforcement to the cracking load was found to be negligible and prediction was based on the properties of masonry as determined in tests on small assemblages. The property that could best be related with wall strength was the average shear stress obtained in diagonal compression tests of small square panels (Figure 2-4). For walls tested in diagonal compression, average shear stress at diagonal cracking was found to be 85% of that obtained in small assemblages. The reduction can be attributed to the effect of confinement introduced by the loading plates in tests of small panels and to the greater number of possible cracking trajectories

in the walls. For walls tested as cantilevers, flexural stresses reduced shear strength and the ratio between mean shear stress in walls at diagonal cracking and that obtained in small tests was 0.5 on the average. Many attempts were made to relate wall strength with other mechanical properties of masonry. For low strength bricks, where the diagonal crack crossed the units, shear strength was found to be proportional to the square root of masonry compressive strength (the ratio was 0.8 for diagonal compression and 0.55 for cantilever tests). When cracking was through the joints, expressions in terms of bond and friction between mortar and units were found, but their accuracy is very poor.

Strength was increased by the addition of reinforcement in intermediate holes due to the effect of grout cast in holes and of the steel reinforcement. No general methods could be found for the prediction of those contributions; reinforcement seemed to be more effective for concrete blocks than for clay bricks due to the poor bond between clay and grout in the last case. The increase in cracking load due to precompression was found to be approximately 40% of the total vertical load applied. This result is limited to vertical load not exceeding one third of the wall capacity.

To describe the load deformation behaviour Meli chose the trilinear relationship shown in Figure 2-31. By changing the parameters of this curve a wide range of cases could be covered. The stiffness of the first branch is not supposed to represent the initial uncracked stiffness of the wall, but an average stiffness before diagonal cracking or severe flexural cracking. Such a stiffness can be calculated with reasonable accuracy by ordinary strength-of-materials methods considering cracked transformed sections for bending deformations and only the contribution of masonry for shear deformations. Remaining parameters

defining postcracking behaviour and ductility depend mainly on the type of failure, reinforcement and vertical load. Experimental values for typical cases are reported in Table 2-9.

As can be inferred from the table, for bending failure ductility ratios exceeding 4 were obtained even for relatively high precompression. For shear failure of interiorly reinforced walls, ductility ratios were between 2 and 3, while for walls with tie columns, ductility ratios were always higher than 4. In every case precompression increased the initial stiffness of the wall due to the reduction of flexural cracking.


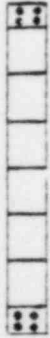
Meli went on to describe the results of cyclic load tests that were performed on walls similar to those tested monotonically. His conclusions and recommendations from the overall study are summarized in Section 2.5.

2.4 Shear Strength of Model Structures

The most comprehensive research performed on the shear strength of model structures was that carried out by Hendry and co-workers at the University of Edinburgh. They realized that performing tests on complete buildings or even large sections of such structures would be expensive and difficult to carry out, and in order to overcome this difficulty, they turned to reduced scale experiments. Most of their work was performed on unreinforced brick masonry using 1/3 and 1/6 scale models.

Before investigating the shear strength of complex, modelled structures Hendry and Murthy⁽⁶⁵⁾ compared the compressive strength of 1/3 and 1/6 scale piers and walls with that of full size specimens. The variables of the study were the mortar strength, joint thickness and the slenderness and eccentricity of the walls. Although the results are

TABLE 2-9
SUMMARY OF RESULTS OF WALLS TESTED WITH MONOTONIC LOAD

Reinforcement	Type of Unit	Other test characteristics	Precompression kg/cm ²	Strength, ton		Stiffness ton/rad	β	α_1	α_2
				racking	Maximum				
Interior Reinforcement 	Concrete Block	Bending	0	-	8.5	6,000	0.65	1.3	6
		Failure	3.5	-	14.4	12,000	0.45	2.2	7
			10	-	32.3	24,000	0.50	3.5	4
			0	8.7	13.5	5,200	0.65	1.5	2
		Shear Failure, Only	3.5	13.1	23	9,500	0.55	1.75	2
			10	18.4	32	17,000	0.45	2.5	3
	Intermediate Reinforcement Fully Grouted	0	11.3	20	10,000	0.6	1.75	3.2	
		0	15.1	35	12,500	0.5	2	2.7	
	Hollow Clay Brick	Shear Failure, Only	0	5.3	7.3	7,000	0.5	2	4.5
			6	10.9	13.3	14,000	0.6	2	4
12.5			11.9	19.6	10,000	0.6	1.75	1.75	
Intermediate Reinforcement	0	8.9	12.5	7,500	0.5	2	3		
	Hollow Clay Brick	0	6.3	7.5	8,000	0.6	4	>6	
Intermediate Reinforcement		0	9.2	12.7	6,000	0.65	3	4	
	Tie Columns and Bond Beams 	Solid Brick	Shear Failure	0	5.2	8.8	5,500	0.7	2
3				11.6	13.4	10,000	0.5	2	6
Perforated Brick		Shear Failure	0	6.9	9.3	5,200	0.4	3	6
			3	11.9	13.7	6,500	0.5	1.5	4
Hollow Clay Brick		Shear Failure	0	6.6	7.3	6,600	0.6	2.5	7
			3	12.3	12.3	13,500	0.6	2	5
Sand Lime Brick	Shear Failure	0	4.6	5.8	4,000	0.5	2.5	4	
		3	11.8	13.1	10,500	0.4	2	7	

$\beta, \alpha_1, \alpha_2$ are the parameters of idealized load deformation curve (see Figure 2.31)

From Reference 58

not presented here, the authors concluded that the strength of full-scale brickwork for given strengths of brick and mortar can be reproduced by means of model tests. The authors also stated that if the same mortar is used to construct the model and full-scale brickwork, the model brickwork would take higher stresses than the equivalent full-scale brickwork. In order to reproduce the strength of full-scale brickwork satisfactorily, it is necessary to use a mortar in the model structure, which has 1" cubes with the same strength as the 2.78" cubes of the mortar used in the full-scale structure. For a given mortar the strength index obtained from the 1" cube exceeds that of the 2.78" cube.

The first shear strength test reported⁽⁶⁶⁾ by the Edinburgh group was on a 1/6 scale model structure. The plan and elevation of the single-story, shear-wall, test structure is shown in Fig. 2-32. Sinha and Hendry⁽⁶⁶⁾ built five identical specimen and each was subjected to one of the following compressive loads: 55, 78, 109, 131 and 147.5 psi and tested to failure under a racking load. All five structures failed with cracks passing through the horizontal and vertical joints. Figure 2-33 shows the relationship between the racking load and the horizontal deflection measured at slab level; whilst Figure 2-34 shows the variation of the shearing modulus of the brickwork with applied, shear stress calculated from deflection measurements. The ultimate shearing strength in the brickwork is plotted against the compressive load in Figure 2-35. Also shown in this diagram are points relating to tests on model brick couplets and tests carried out on full-scale specimen by other investigators.

Like Borchelt⁽⁵⁶⁾ and Turnsek and Cacovic⁽⁶⁴⁾, Sinha and Hendry⁽⁶⁶⁾ presented a formulation to predict the shear strength of brickwork.

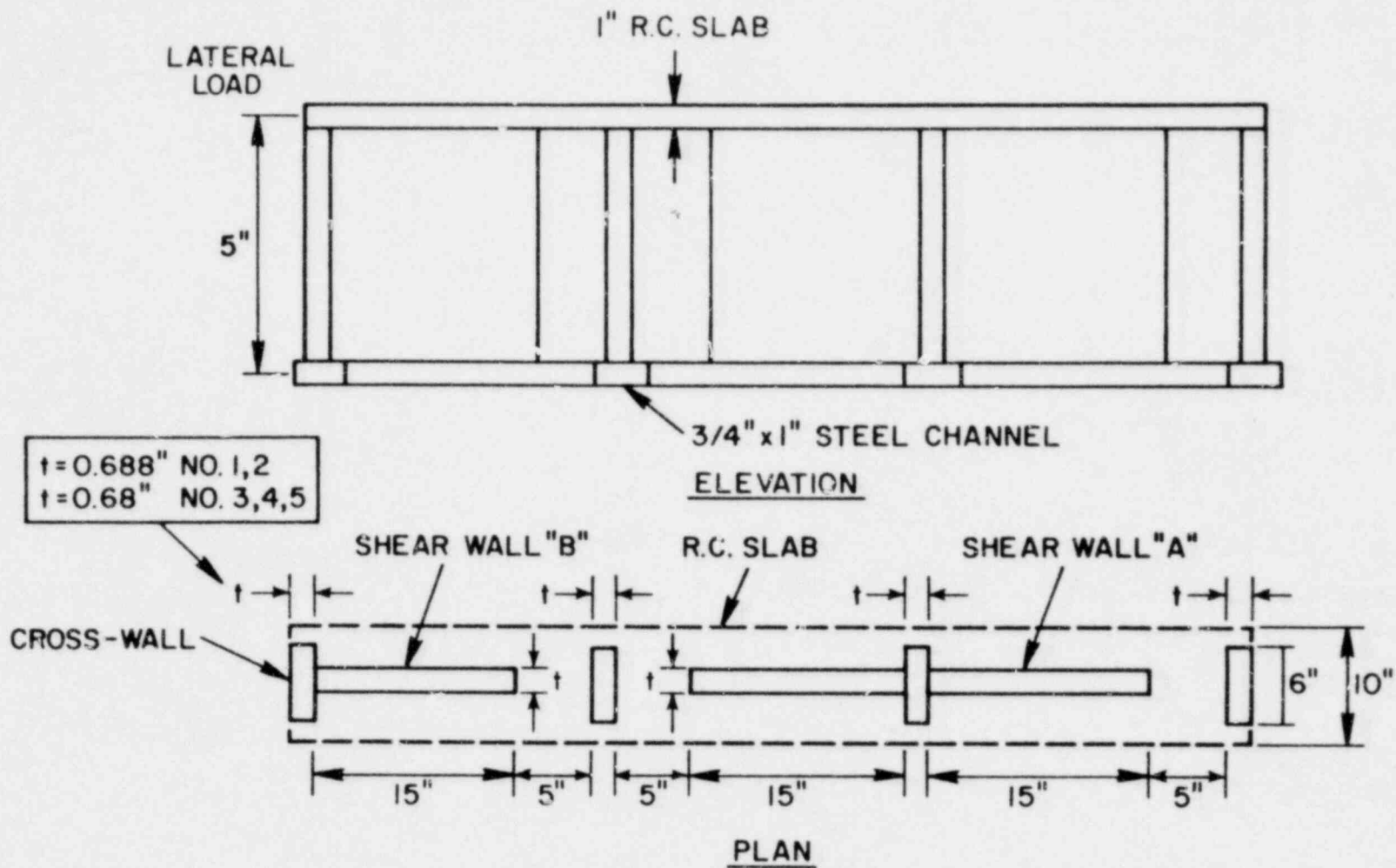


FIGURE 2-32 SHEAR WALL TEST STRUCTURE

From Reference 66

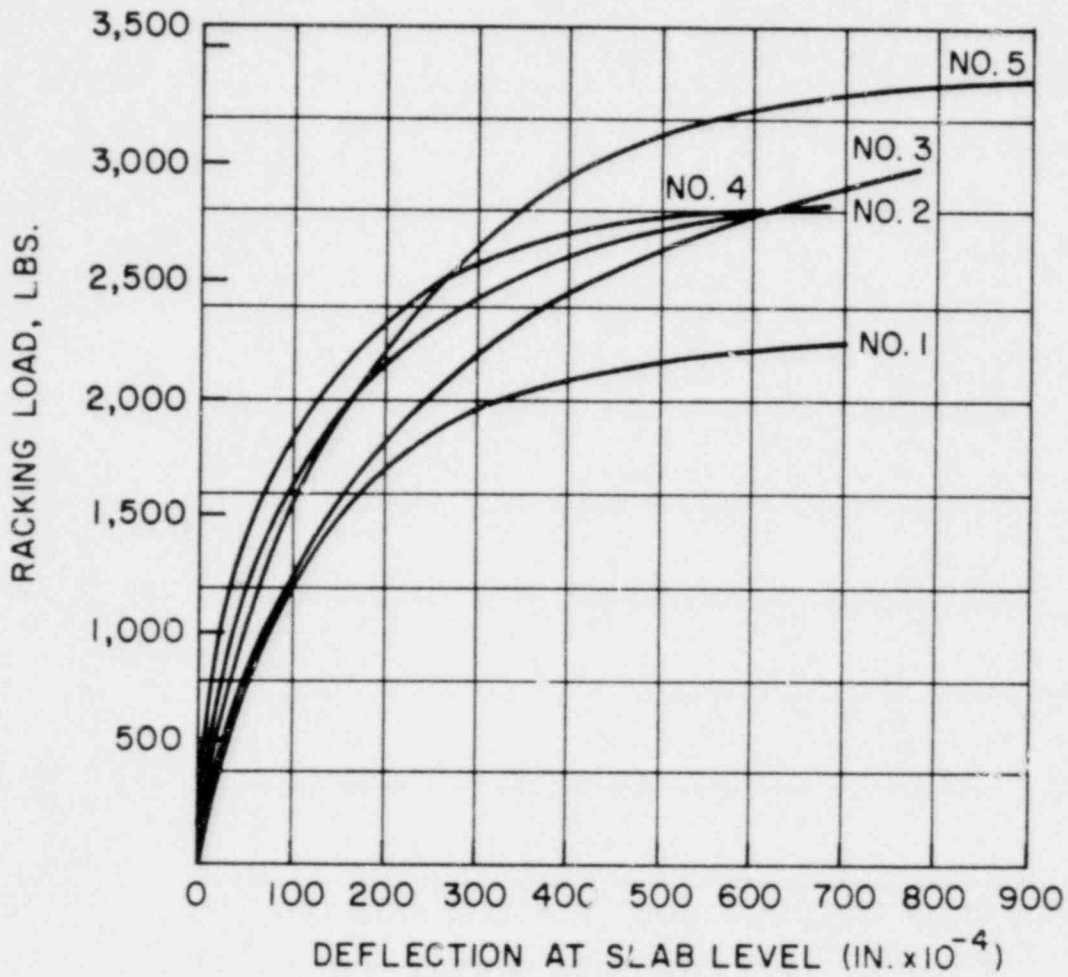


FIGURE 2-33 LOAD-DEFLECTION CURVES FOR SHEAR WALL STRUCTURES

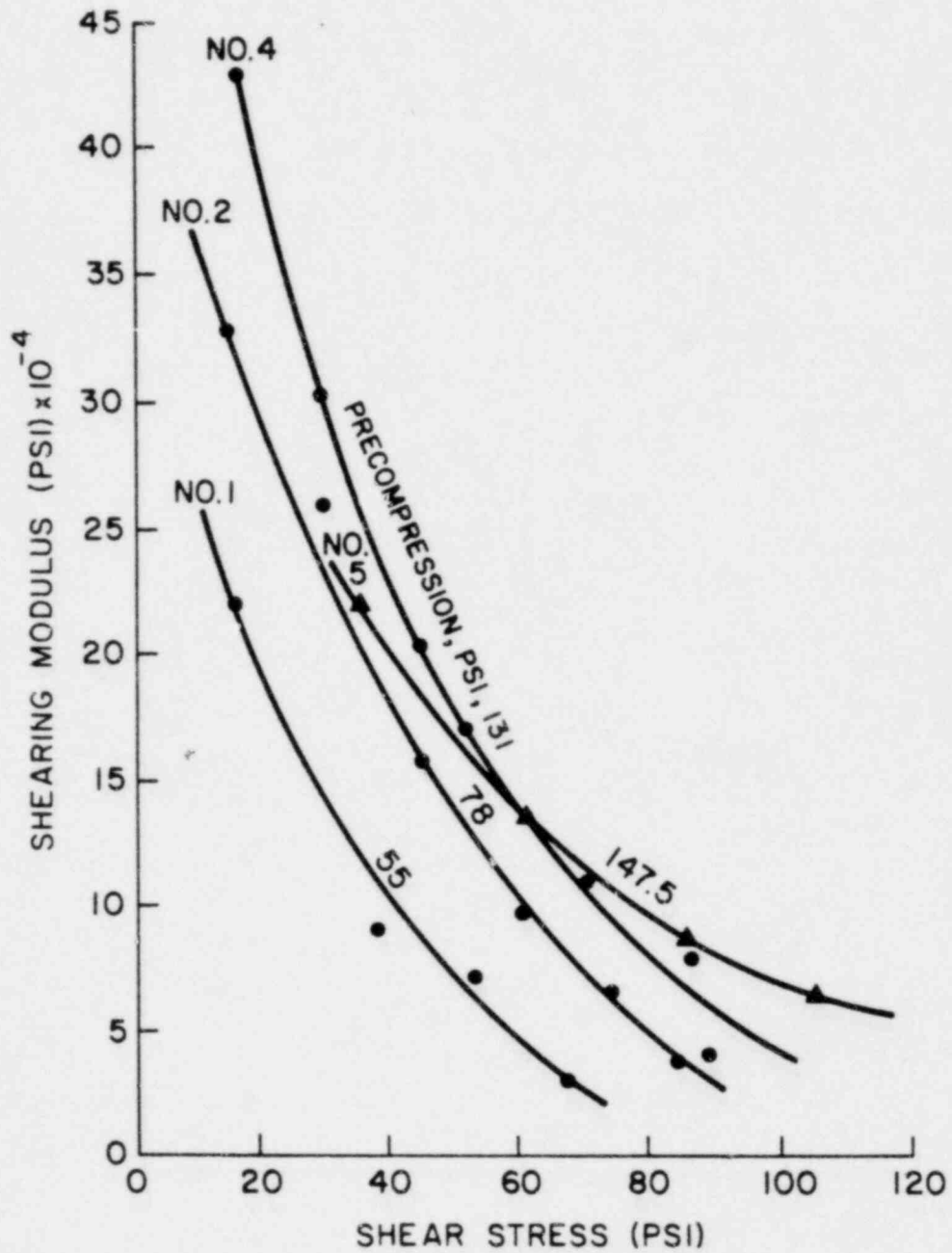


FIGURE 2-34 VARIATION OF SHEARING MODULUS OF BRICKWORK

From Reference 66

They stated that brickwork subjected to combined compression and shear exhibits two distinct types of failure:

1) Shear failure at the brick/mortar interface. The shear strength consists of initial bond shear and resistance proportional to the normal stress due to friction between brick and mortar. The authors considered two regions of shear failure. One a Coulomb-Mohr type of failure below a compressive stress σ_{c1} , where the shear strength τ_{xy} is given by

$$\tau_{xy} = V_{bo} + \mu \sigma_c \quad \sigma_c < \sigma_{c1}, \quad (2-13)$$

where V_{bo} is the bond strength and μ the coefficient of friction between the brick and mortar. The second region of shear failure considered by the authors was a Mohr type of failure above a compressive stress of σ_{c2} . The shear strength τ_{xy} is given by

$$\tau_{xy} = \mu \sigma_c \quad \sigma_c > \sigma_{c2} \quad (2-14)$$

2) Diagonal tensile cracking through bricks and mortar, governed by constant, maximum, tensile stress. The authors considered the diagonal tensile failure to occur between compressive stresses σ_{c1} and σ_{c2} . The maximum tensile stress was obtained from Mohr's circle and given by

$$\sigma_t = \sqrt{\frac{\sigma_c^2}{4} + \tau_{xy}^2} - \frac{\sigma_c}{2} \quad \sigma_{c1} < \sigma_c < \sigma_{c2} \quad (2-15)$$

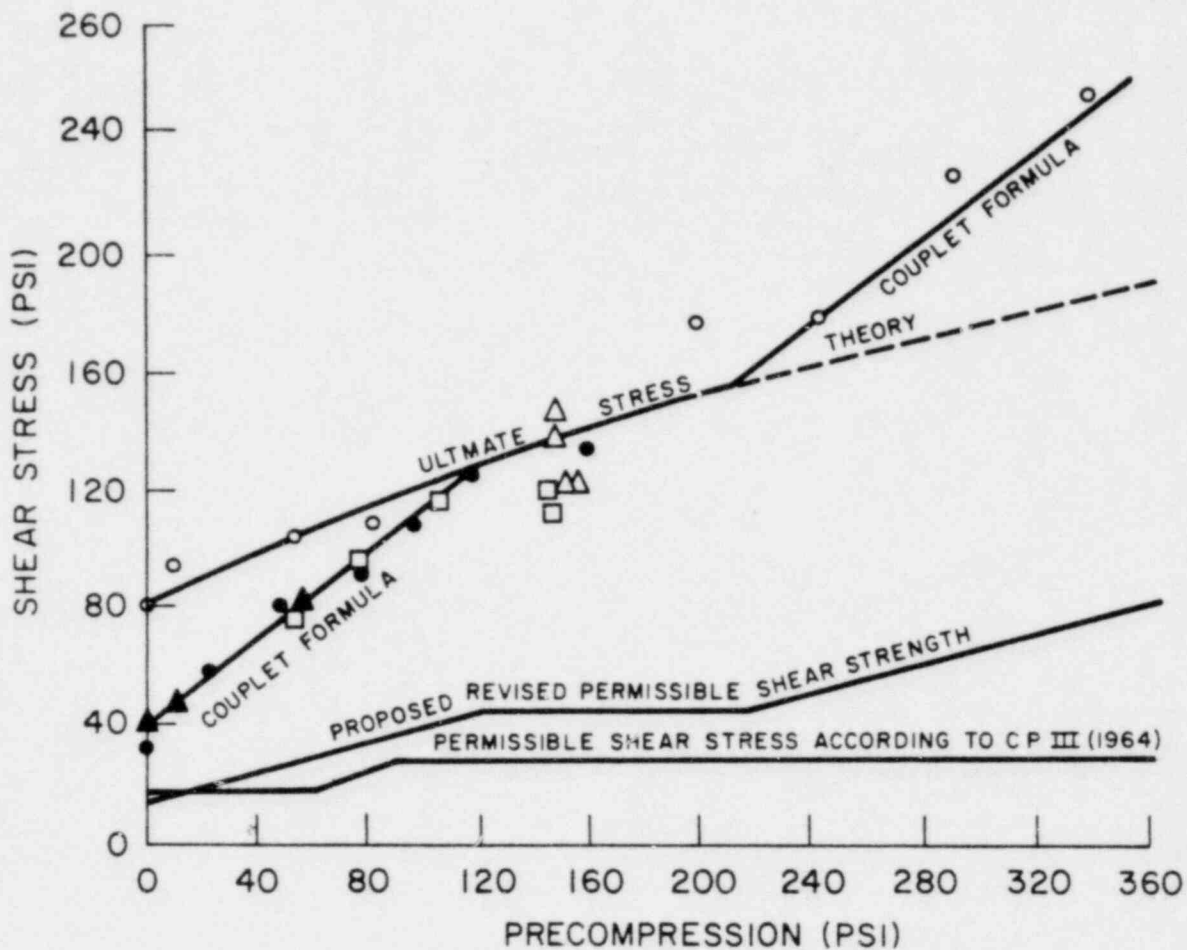
= const.

at failure.

Sinha and Hendry assumed that Equation 2-15 would be satisfied by σ_{c1} and σ_{c2} for the two conditions of τ_{xy} given by Equations 2-13 and 2-14. Having obtained σ_{c1} and σ_{c2} the authors stated that between these two values failure will occur by attaining the maximum tensile strength. Below and above this range failure will be governed by shear at the brick/mortar interface. (Equations 2-13 and 2-14). Compressive stresses above σ_{c2} will suppress the inherent failure due to diagonal tension and modify its value. Eventually at very high compressive values, failure of the brickwork will take place in compression, typically by vertical splitting. The authors did not consider the limiting shear stress at values of compression approaching the compressive strength of the brickwork.

The authors compared the experimental and theoretical results for the model structures they tested. A comparison of the results is shown in Figure 2-35. Included in the diagram are results of some couplet tests performed by them, as well as some test results obtained from other sources on full-size brickwork. They concluded that the ultimate shear stresses calculated from the suggested formulae agree well with the experimental results for the couplet tests and the model structures; and for such tests as are available, they are also applicable to full-scale brickwork. This tentative conclusion about full-scale brickwork is different from that presented by Borchelt and Turnsek and Cacovic. The latter indicate that the maximum tensile stress theory governs the complete compressive range.

From the results on the model structures Sinha and Hendry concluded that a compressive stress increases the shear strength of the brickwork up to a certain limit, dependent on the compressive strength of the



- MODEL BRICK COUPLLET (1:3) AVERAGE SHEAR STRENGTH
- MODEL BRICK STRUCTURES AVERAGE SHEAR STRENGTH
- △ FULL SIZE WALL SIMMS' TEST AVERAGE SHEAR STRENGTH
- ▲ FULL SIZE COUPLLET (1:0.3:5) POLYAKOV'S TEST AVERAGE TEST STRENGTH
- FULL SIZE COUPLLET (PERFORATED) (1:0.3:5) POLYAKOV'S TEST AVERAGE SHEAR STRENGTH

FIGURE 2-35 RELATIONSHIP BETWEEN ULTIMATE SHEAR STRESS AND PRE-COMPRESSION

brickwork. In addition they concluded that the rigidity and shearing modulus of brickwork decreases non-linearly with an increase in racking load and a decrease in compressive load (Figure 2-34).

In a later paper Murthy and Hendry⁽⁶⁸⁾ reported on a lateral load test that was performed on a 1/6 scale three story, three bay, cross wall structure with no openings. The purpose of the test was to examine the increase in the structural rigidity as shear panels were added and to determine the ultimate strength of the structure under lateral loading. A plan and elevation of the test structure are shown in Figure 2-36. Dead load stresses corresponding to those existing in a full-size structure were induced by lead weights placed on the floor and on roof slabs and suspended from the walls. These weights were equivalent to increasing the weight of the model brickwork six times and produced a maximum compressive stress in the cross walls of 49 psi.

The shear walls were infilled in stages, as follows:

- (1) No shear walls
- (2) Second bay, first story
- (3) Second bay, first and second storys
- (4) Second bay, all storys
- (5) Second and third bay, all storys
- (6) First, second and third bays, all storys

The load deflection curves for typical stages are shown in Figures 2-37 to 2-40. To give some indication of the stiffening effect of the shear panels the authors calculated the rigidity of the structure at the roof level at various stages of loading. The roof rigidity in test n was defined as

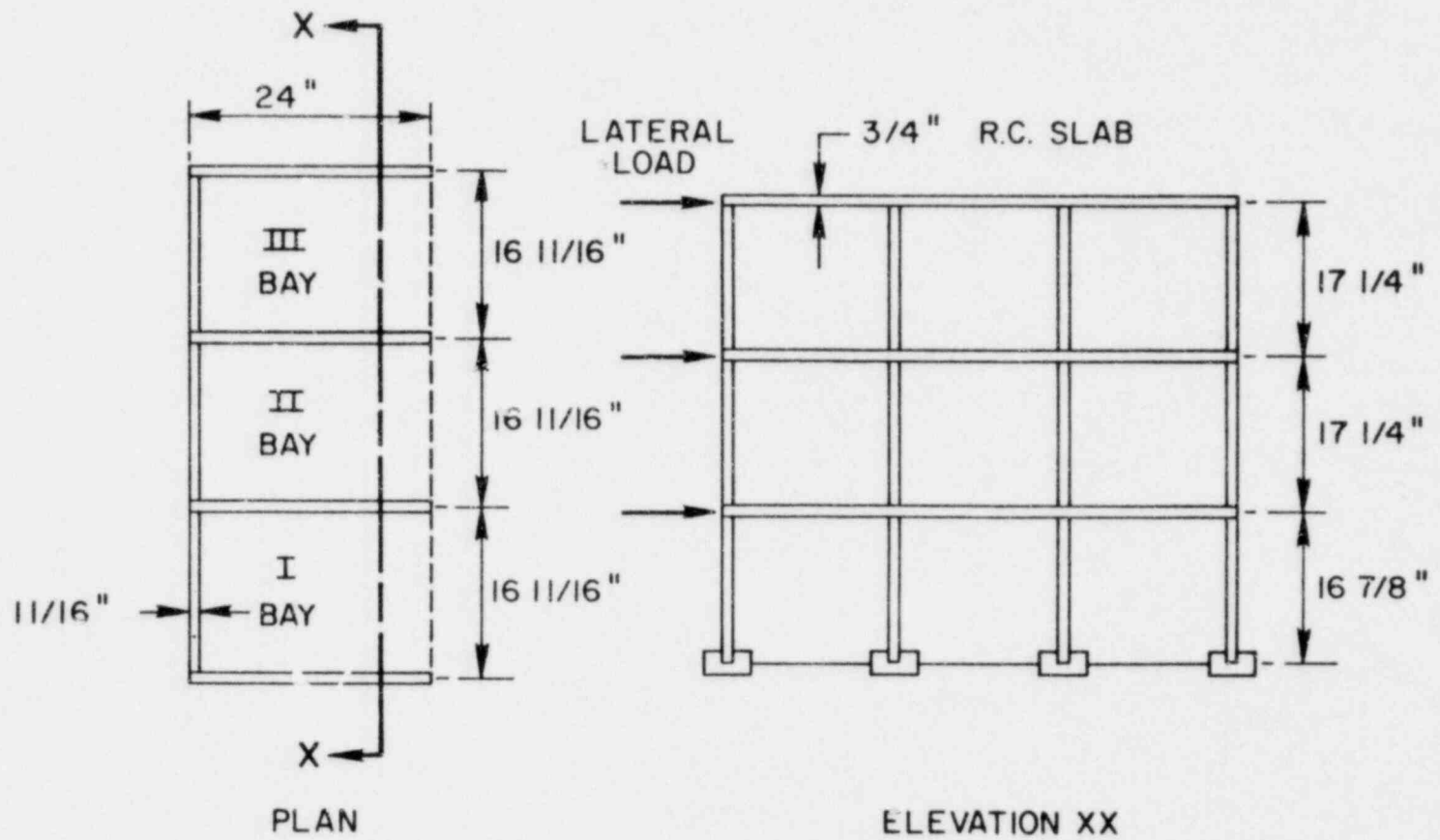


FIGURE 2-36 ONE-SIXTH SCALE MODEL TEST STRUCTURE

From Reference 68

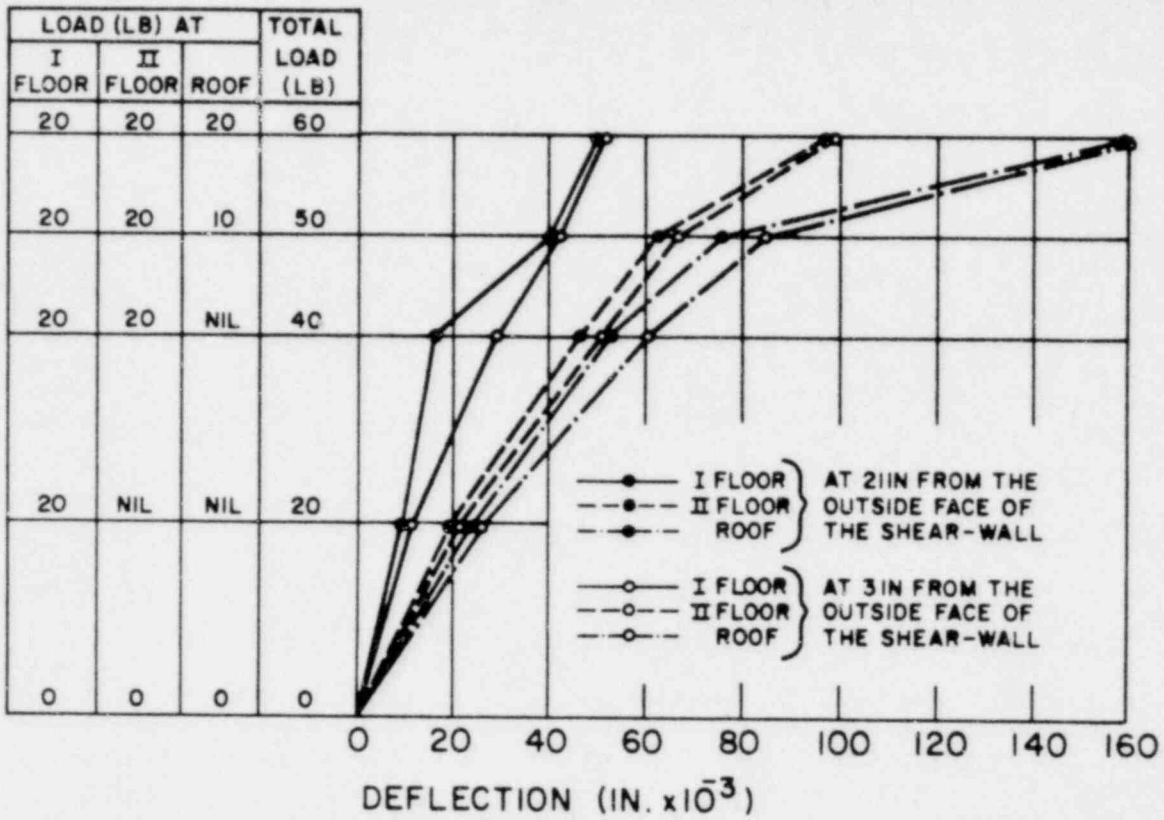


FIGURE 2-37 LOAD CASE 1

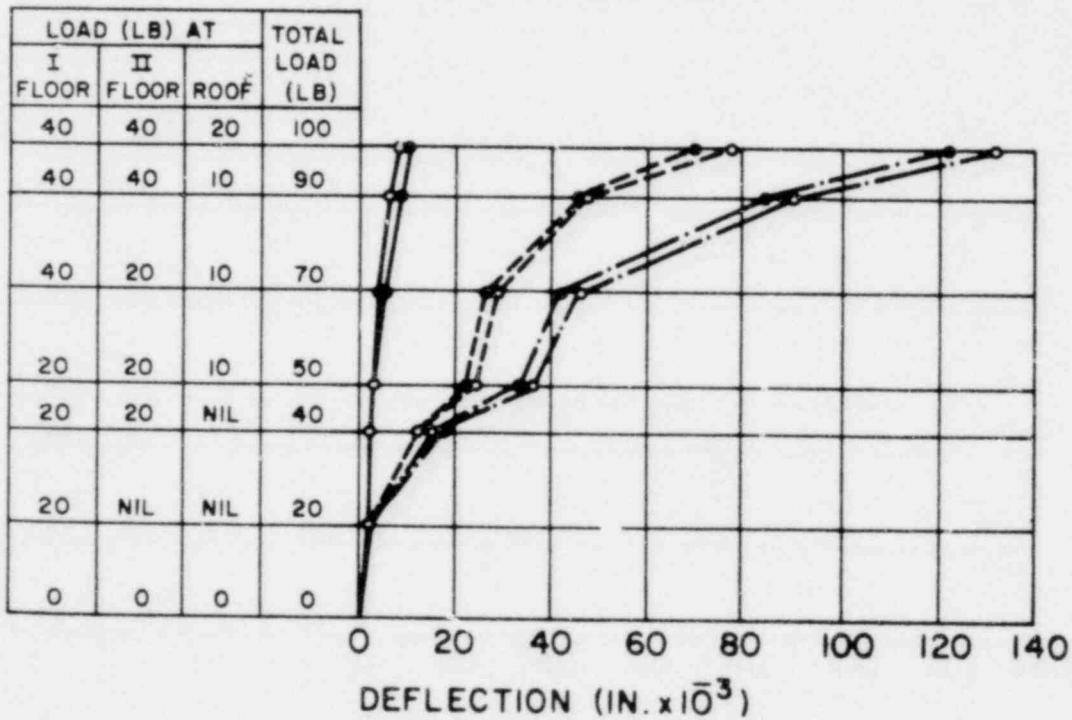


FIGURE 2-38 LOAD CASE 2

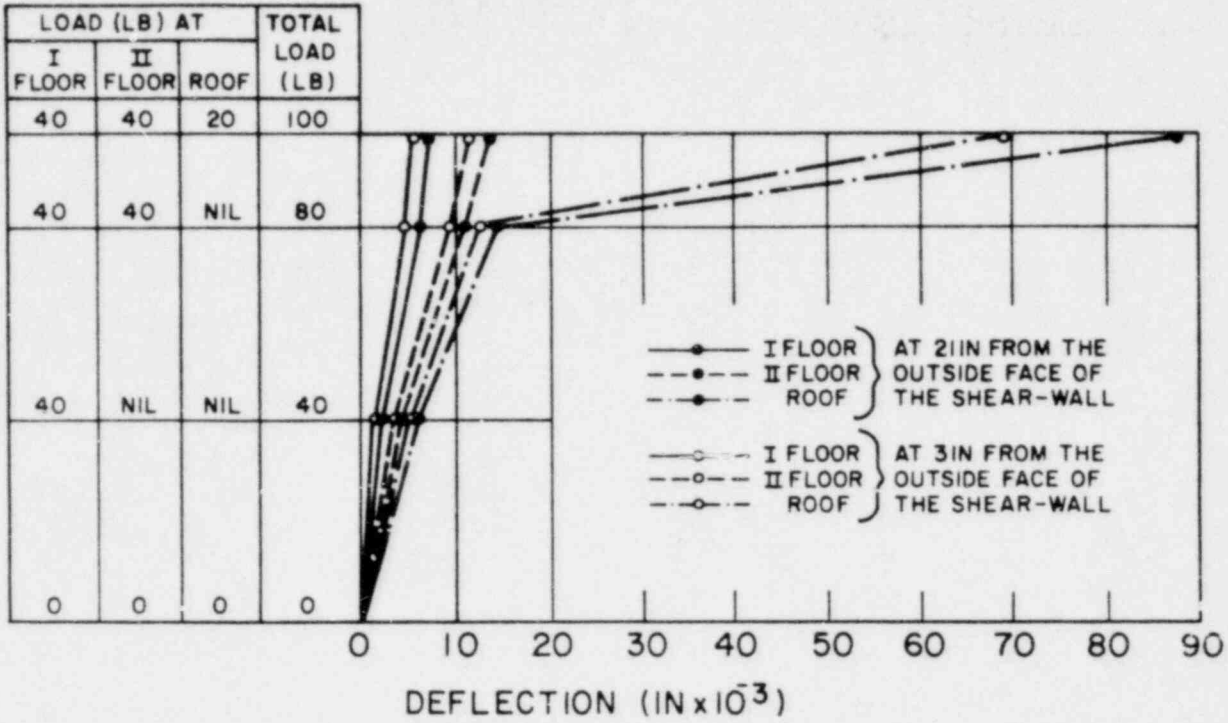


FIGURE 2-39 LOAD CASE 3

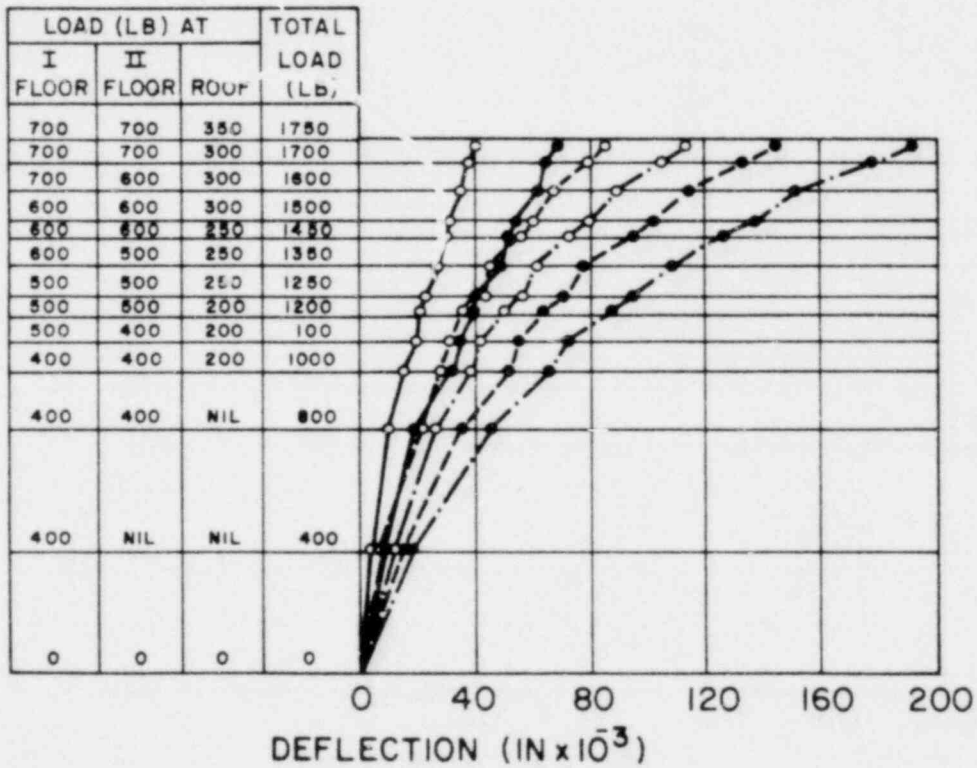


FIGURE 2-40 LOAD CASE 6

From Reference 68

$$R_n = \frac{\text{Total horizontal load}}{\text{Average deflection at roof level}}$$

The values of R_n at corresponding stages of loading were found to be in the following ratios.

$$\begin{aligned} R_1 : R_2 : R_3 : R_4 : R_5 : R_6 \\ = 1 : 2.14 : 3.43 : 15.7 : 52 : 104 \end{aligned}$$

This comparison is only valid for the maximum horizontal load that Case 1 can withstand. Infill panels in one bay only increased the rigidity by 15.7 times, in two bays by 52 times and in three bays by 104 times, as compared with the initial structure without any infill, which of course would not be considered stable. It should be noted that the stiffening effect is increased more than in direct proportion to the cross sectional area of the infill panels.

The structure was loaded to failure with all shear panels infilled. The primary failure took place when the horizontal load at each floor level reached 1400 lb, at which point the shear bond between bricks and mortar in the shear walls in the lowermost story broke down. The mode of failure was similar to that observed in the author's tests on single-story shear walls. As the resultant horizontal force did not pass through the shear center of the horizontal section of the structure, shear stresses were set up in the cross walls due to torsion and shear cracks developed in these walls at the ultimate load. The mean shear stress in the shear walls at failure was 123 psi. This is a comparatively high value indicating high bond strength between the bricks and mortar.

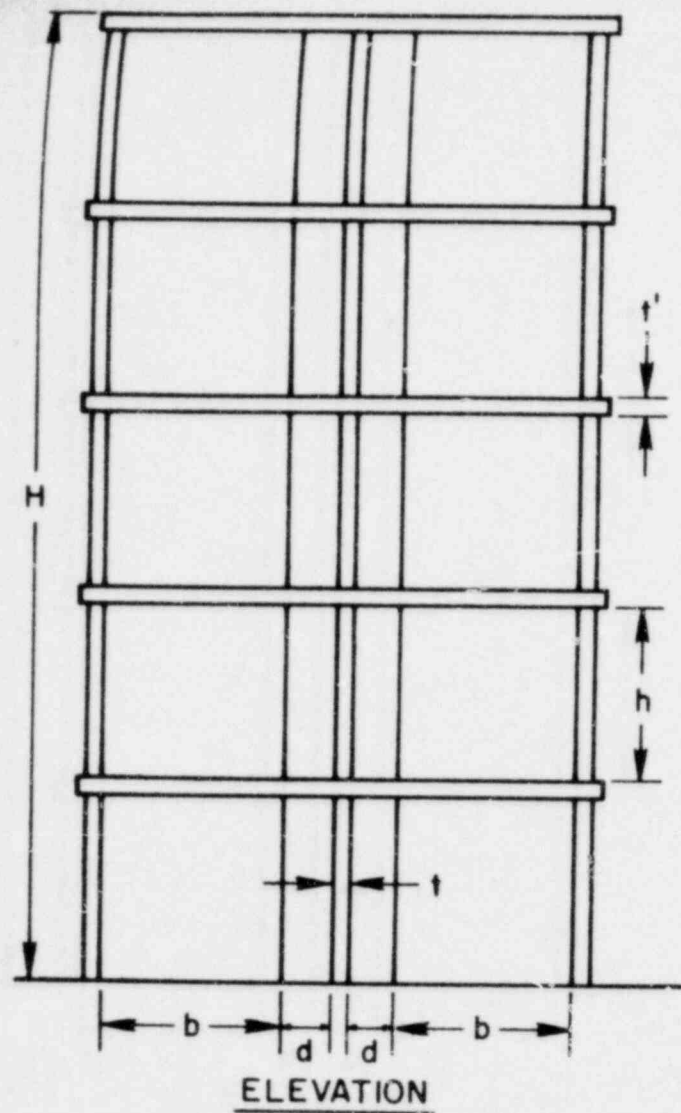
The authors concluded this study by stating that it is possible to obtain much valuable information on the behaviour of brick structures using model brickwork of 1/3 or 1/6 full scale; and that model experiments

can be used to extend our knowledge on a semi-quantitative basis and to serve as a guide to test programs to be undertaken at full scale.

In continuation of the model studies Sinha, Maurenbrecher and Hendry⁽⁶⁹⁾ compared the experimental results of lateral load tests on 1/6 and full-scale test structures. They also attempted to calculate the deflections in both structures by an approximate method, the continuum method and the finite element method. A plan and elevation of the test structures are shown in Figure 2-41. The lateral load was applied to both structures to investigate the overall deflections and in addition, for the full-scale structure, the distribution of vertical strains in the ground floor walls. The lateral load in terms of average shear stress in the bottom shear walls ranged from 5 to 28.4 psi. The deflection of both buildings at different stages of loading is given in Figures 2-42 and 2-43.

The model structure was analysed by the individual cantilever, the continuum and the wide column methods and the comparative results plotted in Figure 2-44. It appeared from consideration of Figure 2-44 that these methods could not be used for the design of brick cross-wall structures without some modification. From their earlier work the authors recognised that compressive stresses increase the rigidity of the structure, hence they corrected the modulus of rigidity values for compressive stress and then they recalculated the deflection of the model structure by an approximate method which takes each story as a separate unit so that the results of each floor are added cumulatively. The results plotted in Figure 2-44 are promising.

The full-scale structure was analysed by the same methods as the model and, in addition, by the finite element method. The results are plotted in Figure 2-45. Also shown in this figure is a comparison



	MODEL	FULL-SCALE
W	41.5 IN	20 FT 5 1/4 IN
L	44.5 IN	21 FT 9 3/8 IN
C	8 IN	4 FT
b	16 IN	7 FT 10.5 IN
d	5 IN	2 FT 6 IN
h	17 IN	8 FT
H	7 FT 6 1/4 IN	42 FT 1 IN
t'	1 IN	5 IN
t	0.688 IN	4.1 IN

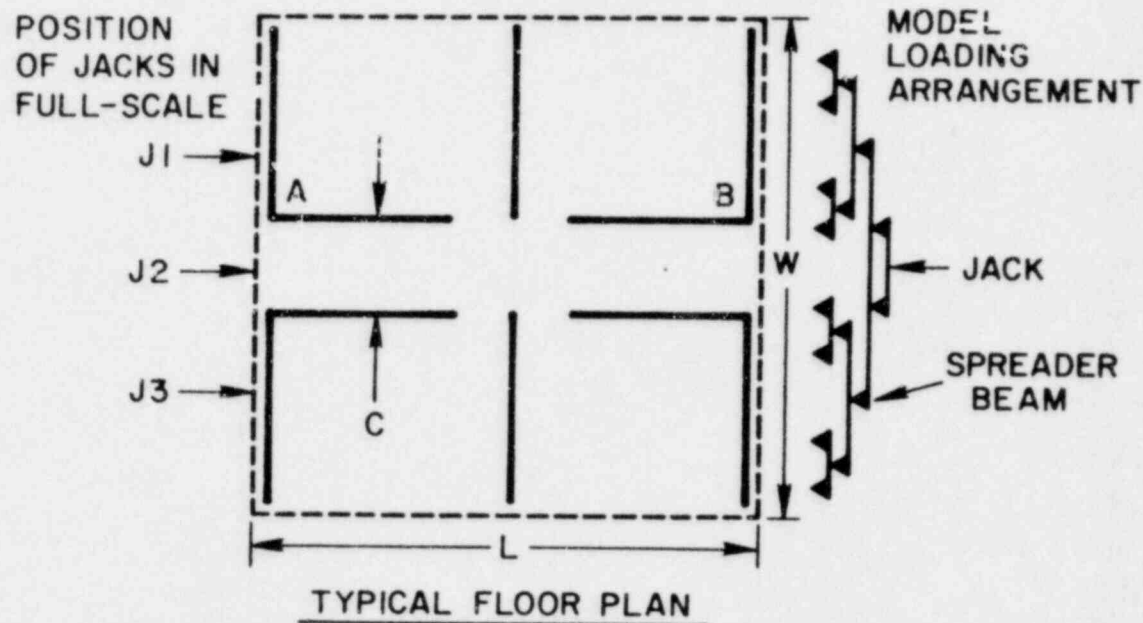


FIGURE 2-41 CROSS-WALL TEST STRUCTURE

From Reference 69

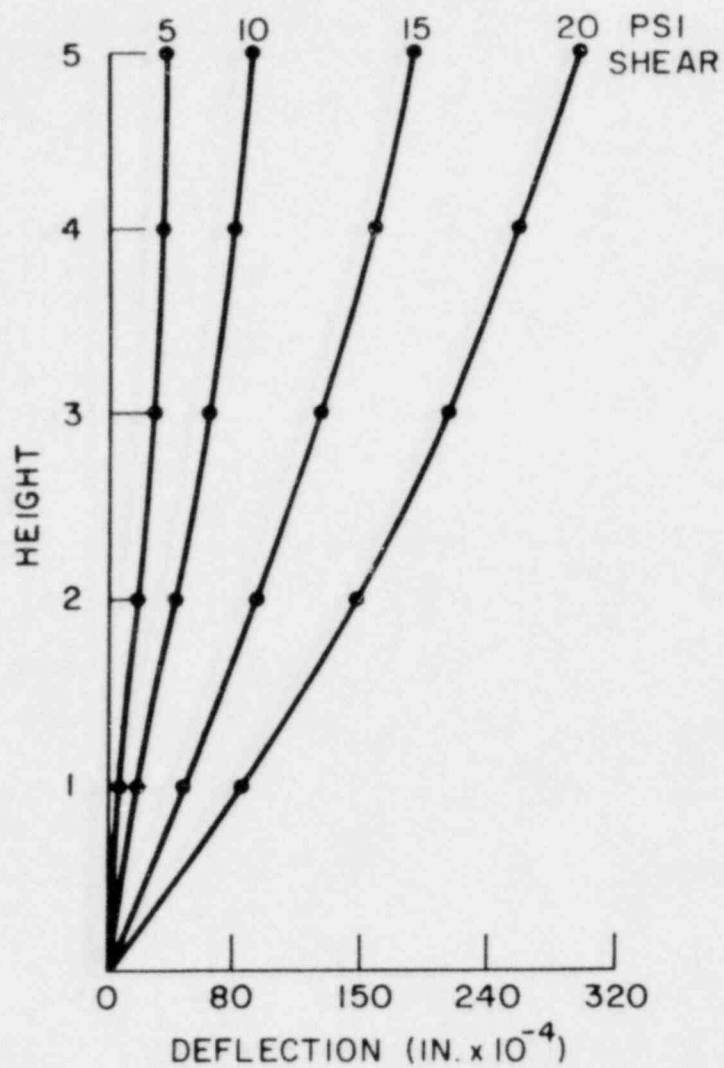


FIGURE 2-42 DEFLECTION OF MODEL STRUCTURE

From Reference 69

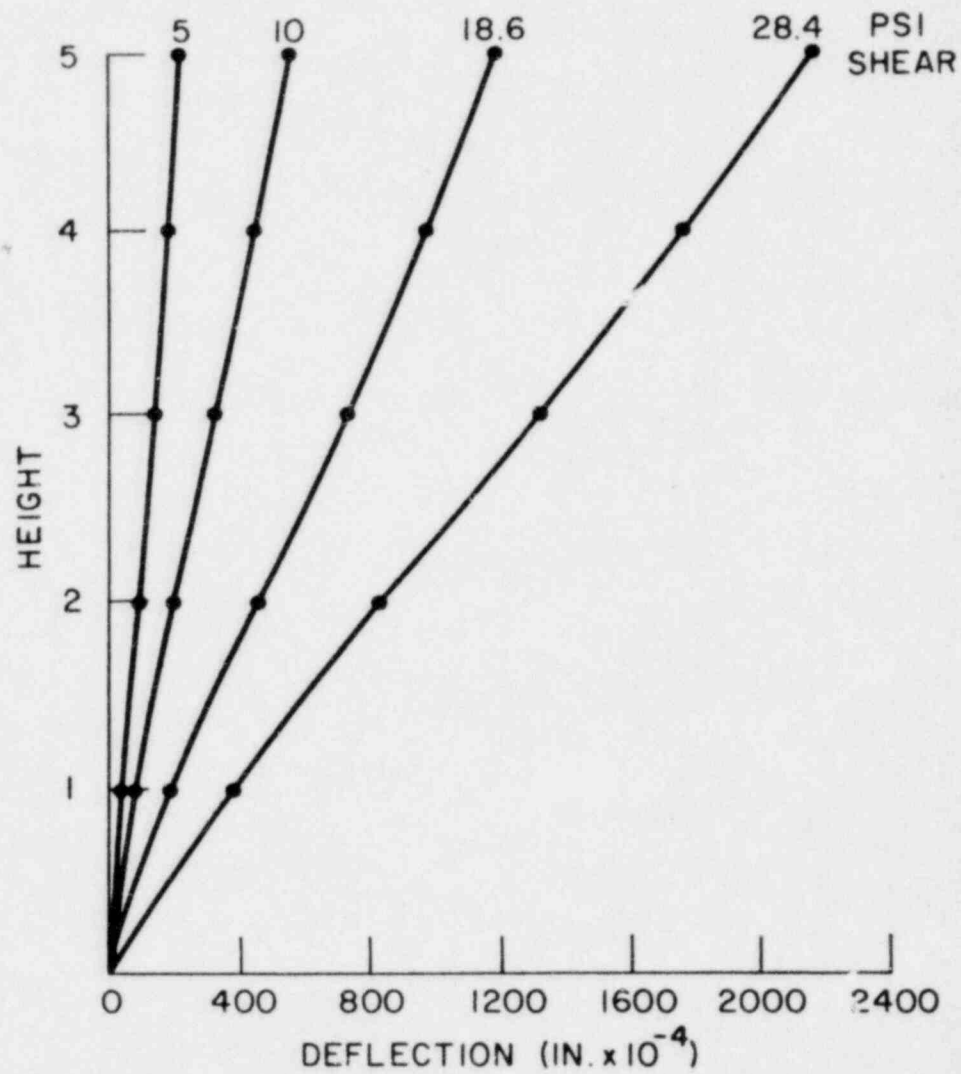


FIGURE 2-43 DEFLECTION OF MODEL OF FULL-SCALE STRUCTURE

From Reference 69

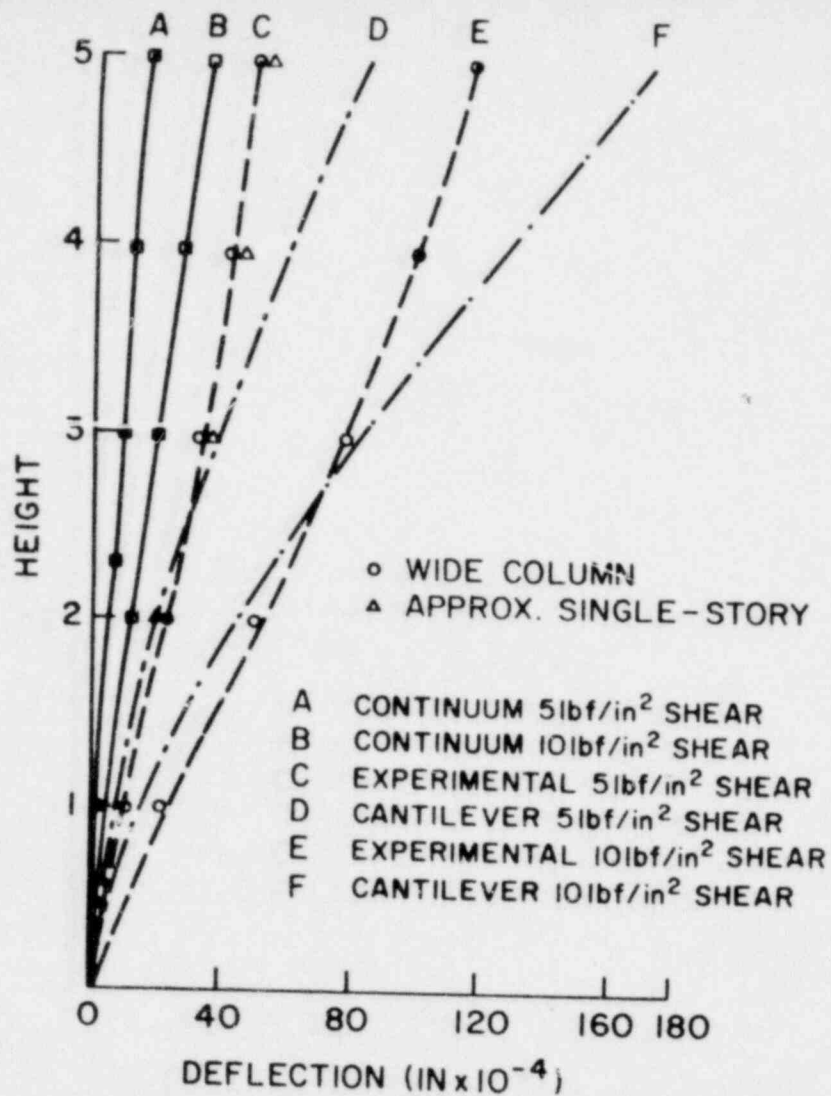


FIGURE 2-44 COMPARISON OF THE ANALYTICAL AND EXPERIMENTAL DEFLECTIONS

From Reference 69

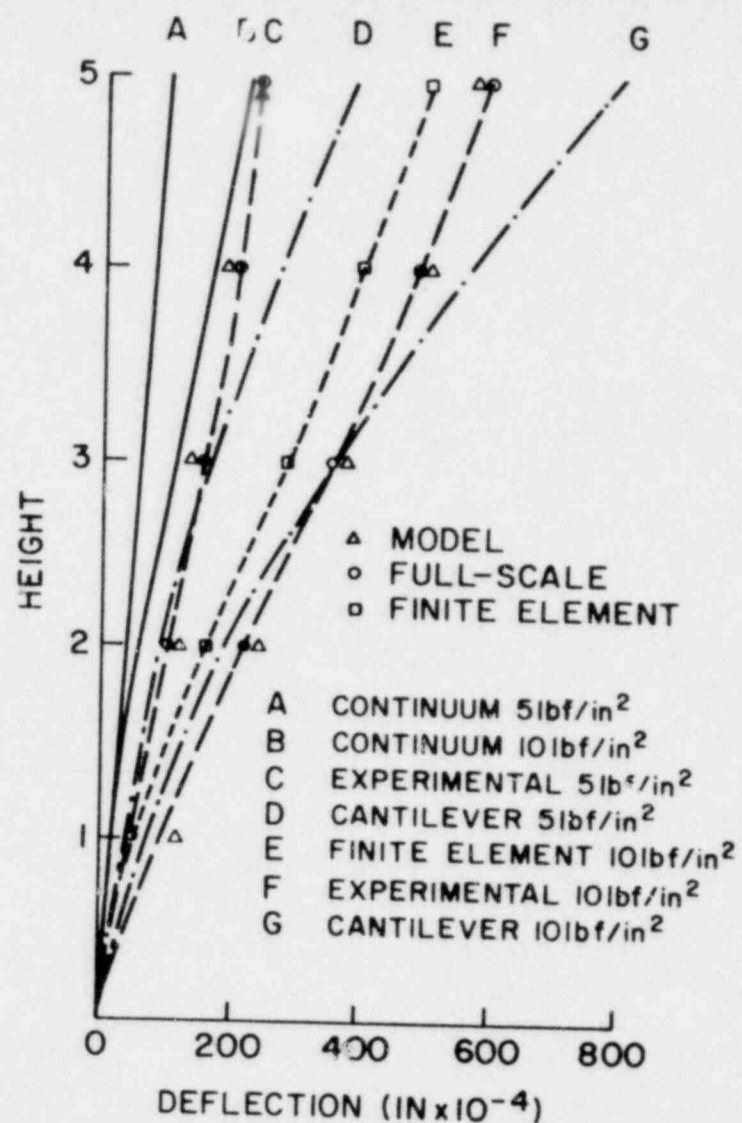


FIGURE 2-45 COMPARISON OF THE ANALYTICAL, EXPERIMENTAL FULL-SCALE AND ADJUSTED MODEL DEFLECTIONS

From Reference 69

between the full-scale and adjusted model deflections with the latter increased by a scale factor of 5. Both curves have similar shapes and agree well for low shear stresses up to 10 psi but with increasing stress the model deflections greatly exceed the full-scale deflections. The deflection versus shear stress for the two structures presented in Figure 2-46 shows that the load-deflection curve is non-linear and the effect is accentuated at higher stresses.

Sinha et al concluded by stating that existing analytical solutions do not give reliable results for stress or deflections in brick structures. The cantilever method overestimates the deflection and the extreme fibre stresses; the continuum method underestimates the deflection while it gives approximate values for maximum compressive stress but underestimates the maximum tensile stress. Finite element techniques appear promising but further work is necessary before a reliable solution can be suggested.

Kalita and Hendry⁽⁷⁰⁾ extended the work just described in order to clarify the applicability of the shear wall theory and to determine the contribution of return walls and floor slabs to the rigidity of shear walls. They worked on a simplified 1/6 scale, five story model, the plan and elevation of which are shown in Figure 2-47. After construction of the first story the authors determined the variation of the shear modulus with compressive stress for the material. The previous study had indicated that this was an important factor in correlating the analysis with the experimental results. The results are shown in Figure 2-48.

The authors used two analytical methods for calculating the inter-story deflection of the model. The first, the simplified approach used by Benjamin⁽⁷¹⁾, assumed the interstory deflection (n) to be

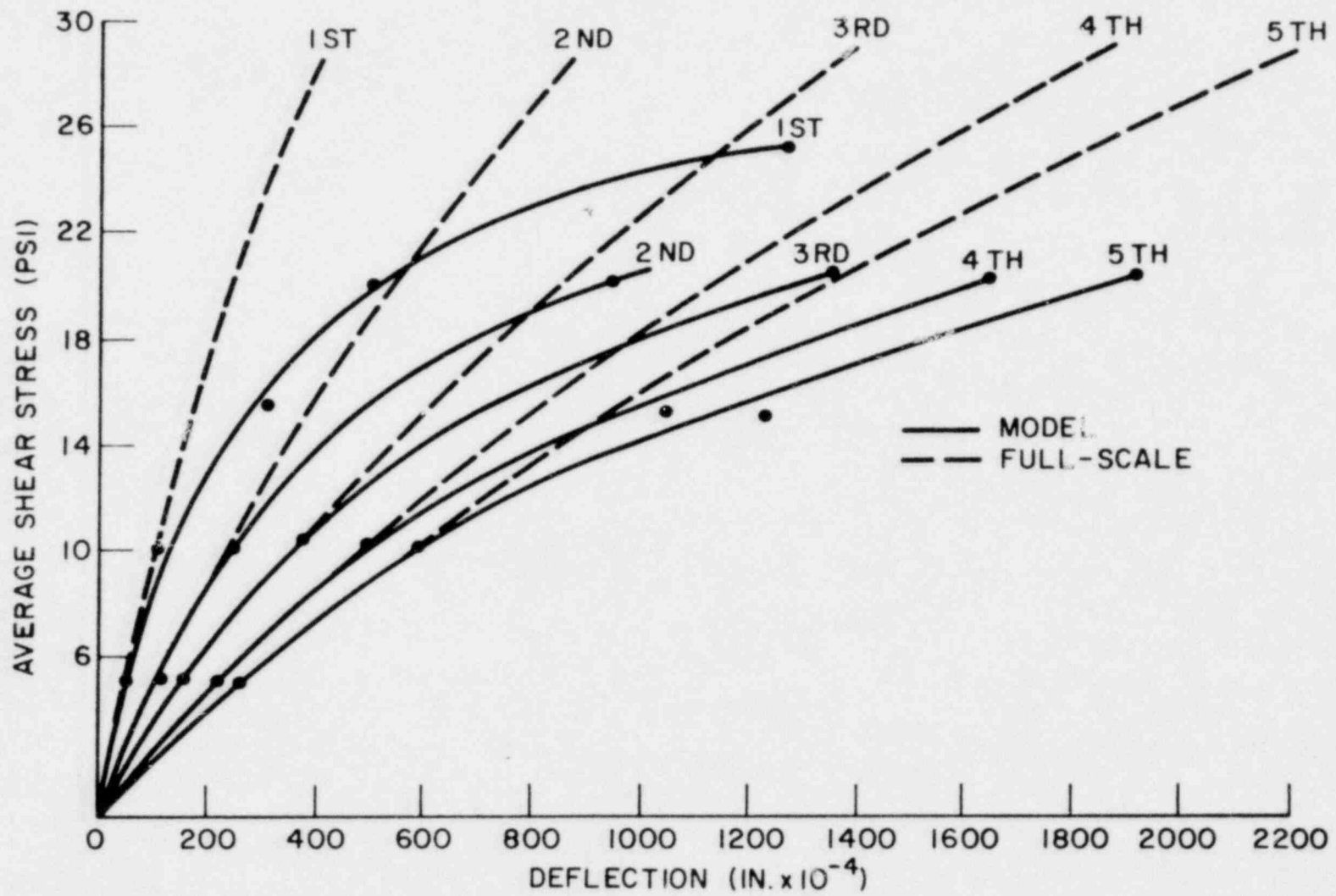


FIGURE 2-46 DEFLECTIONS OF THE STRUCTURES AT VARIOUS FLOOR LEVELS

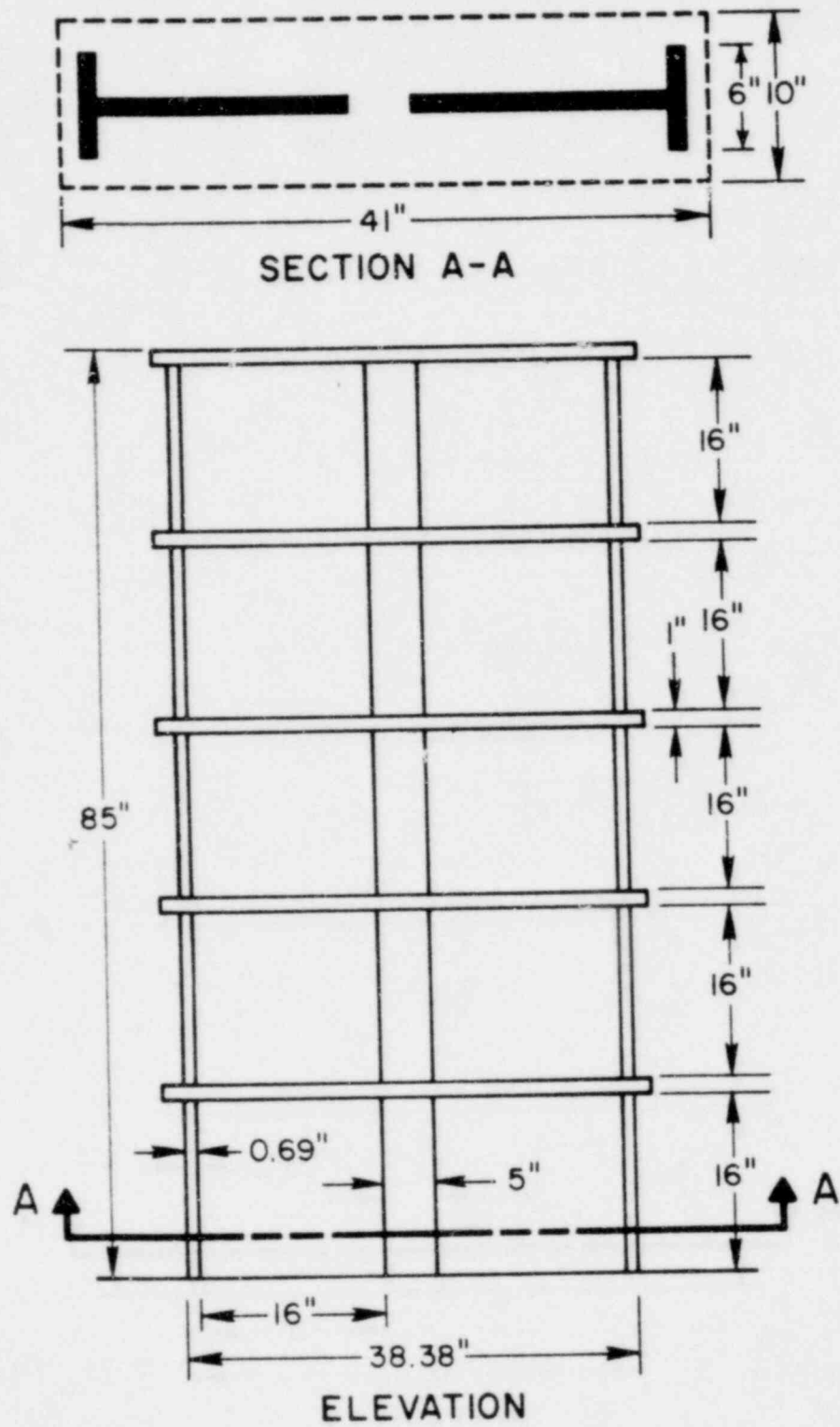


FIGURE 2-47 MODEL TEST STRUCTURE

From Reference 70

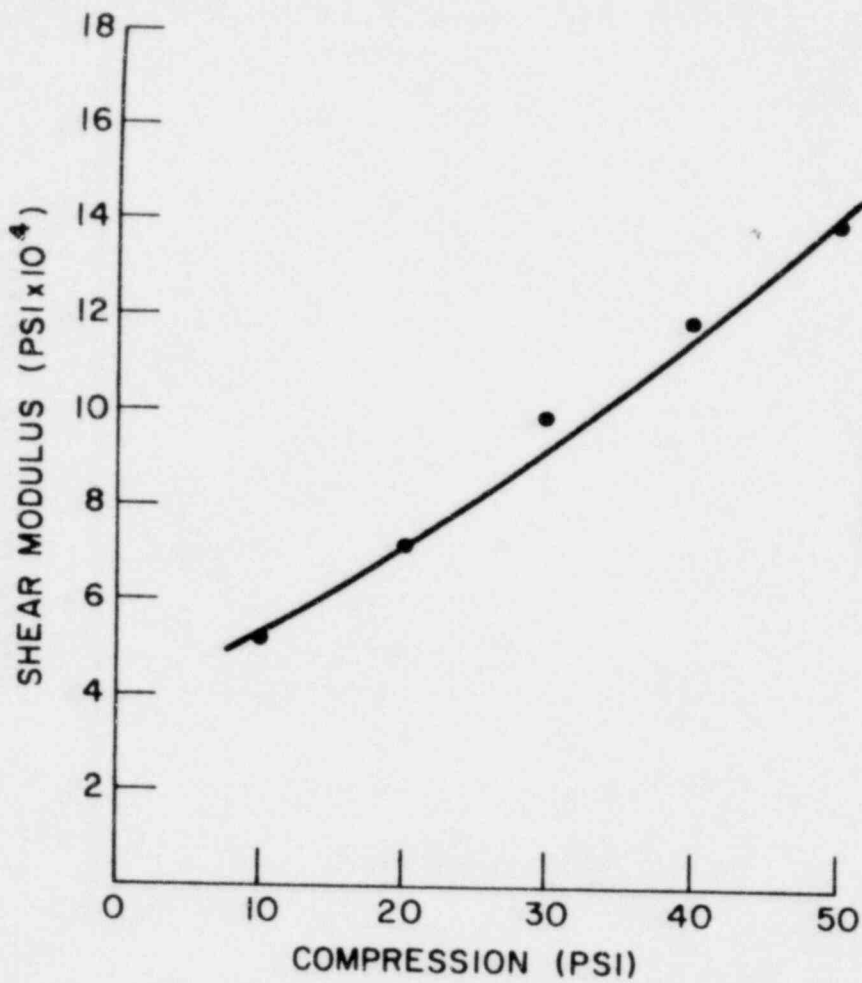


FIGURE 2-48 VARIATION OF SHEAR MODULUS WITH PRECOMPRESSION
From Reference 70

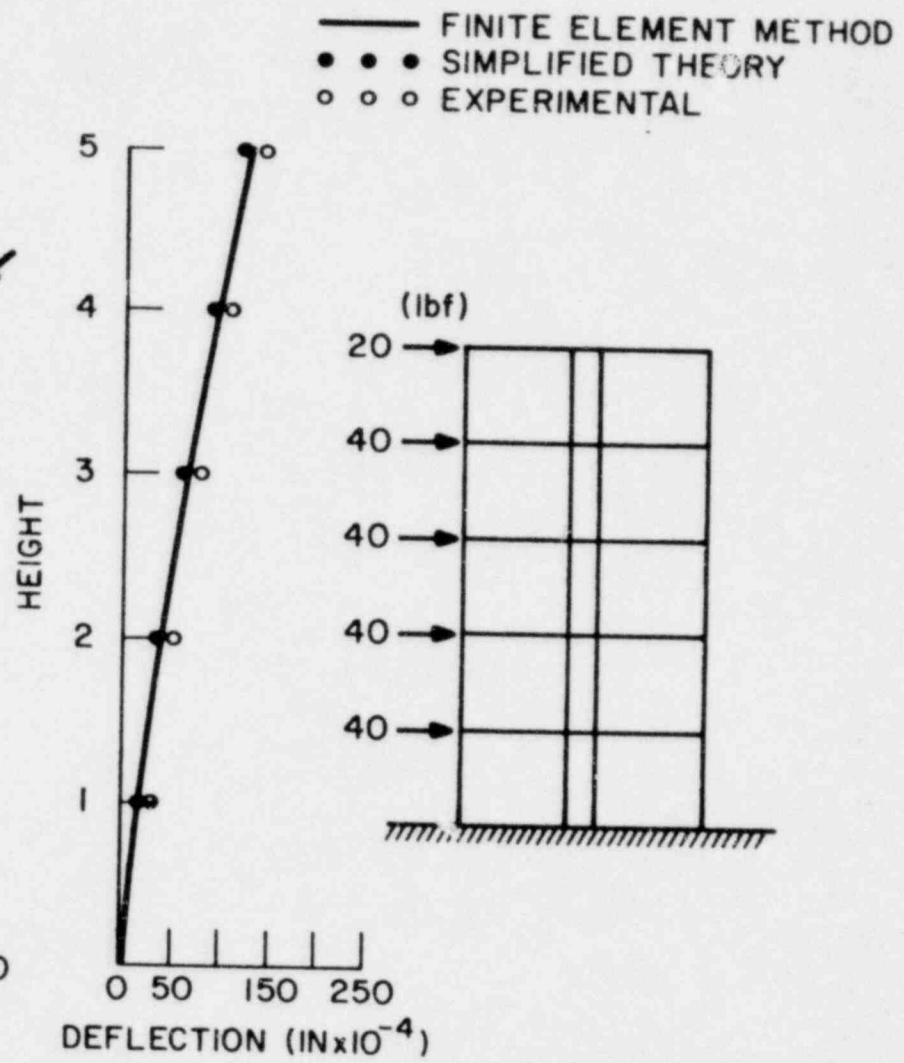


FIGURE 2-49 COMPARISON OF DEFLECTIONS OBTAINED FROM EXPERIMENTAL AND ANALYTICAL RESULTS

$$\Delta_n = \frac{P_n H_n^3}{12 E_n I_n} + \frac{1.2 P_n H_n}{A_n G_n} \quad (2-16)$$

where P_n is the story shear load, H_n the interstory height and G_n the shear modulus which is a function of the compressive load. E_n , the modulus of elasticity, was calculated from

$$E_n = 2 G_n (1 + \nu) \quad (2-17)$$

where ν , Poisson's Ratio, was assumed to be 0.1. The second method, the finite element method (constant strain element), was used and included the variation of G with compressive load. A comparison of the analytical and experimental results, shown in Figure 2-49, indicates that the finite element approach is slightly more accurate than the simplified approach and gives about 10% lower deflections than the experimental result for a racking load 1/3 of the ultimate load.

The finite element method was also used to determine the stresses in the lowermost story of the structure. A comparison of the analytical and experimental results, shown in Figure 2-50, indicates reasonable agreement.

In addition to determining the accuracy of analytical techniques in calculating interstory deflections and stresses, the authors investigated analytically (finite element method) and experimentally the effect of flange width, and analytically the effect of slab width on the rigidity of shear walls. The model structures investigated were single story. The plan views are shown in Figure 2-51, and the results in Figure 2-52. Although there was a uniform 20% discrepancy between the experimental and analytical results, the authors concluded that for the

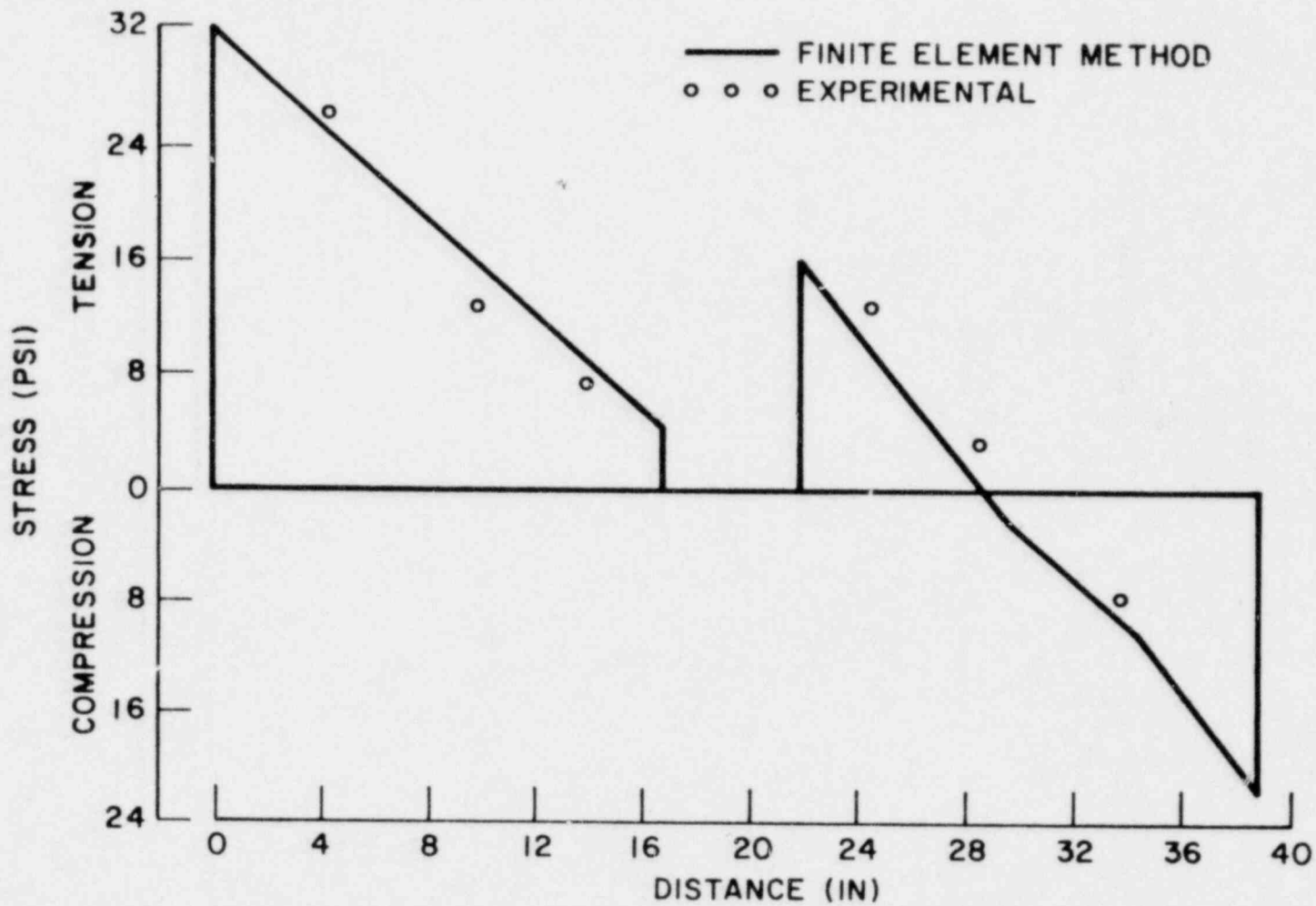


FIGURE 2-50 VERTICAL STRESS AT SECTION $X_1 - X_1$

From Reference 70

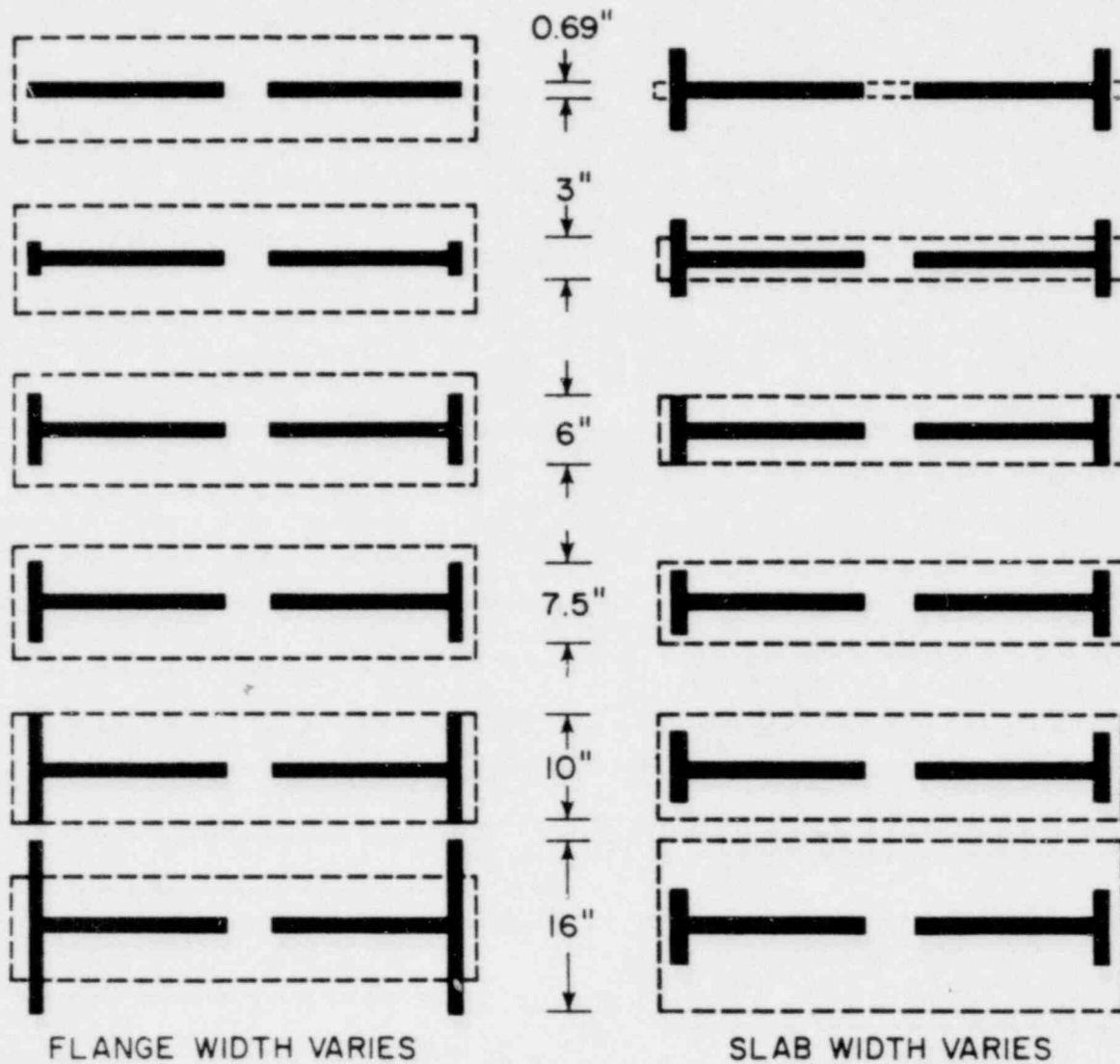


FIGURE 2-51 STRUCTURES ANALYSED TO INVESTIGATE INFLUENCE OF FLANGE AND SLAB WIDTH

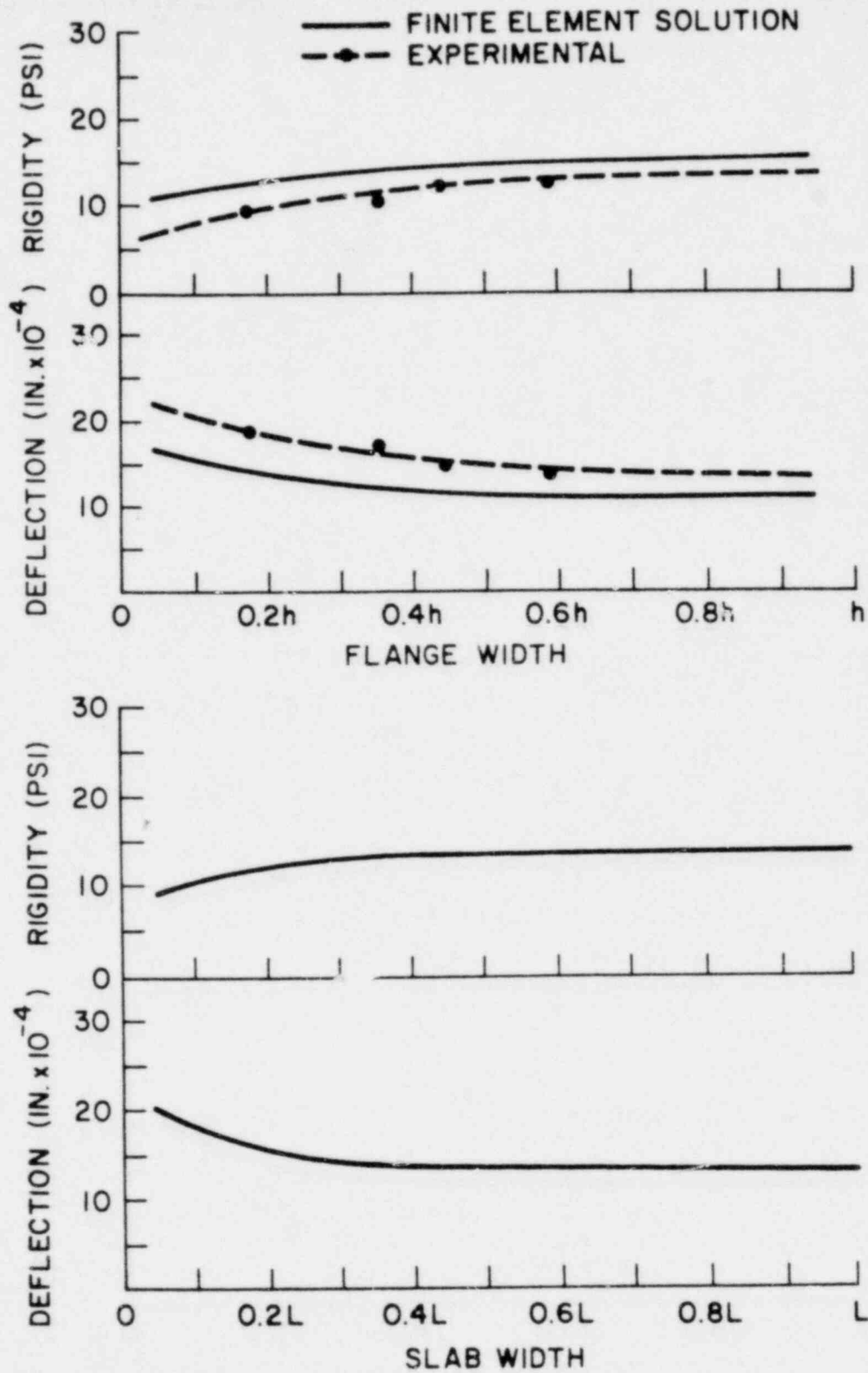


FIGURE 2-52 VARIATION OF DEFLECTION/RIGIDITY WITH FLANGE AND SLAB WIDTH

From Reference 70

simple structure investigated the "effective" flange width was 0.35 of the story height and the effective slab width was 0.5 of the bay width.

2.5 Cyclic Shear Behaviour of Masonry Assemblages

One of the most important properties of masonry structural components in seismic regions of the world is the ability of an assemblage to resist cyclic in plane shear loads. Because more sophisticated equipment is required for this type of experimental test, only a limited number of investigations has been performed in this area in the last five years. Four major investigations have been reported in the literature, one each by Williams⁽³⁾, Meli⁽⁵⁸⁾, Mayes and Clough^(60,76) and Priestly and Bridgeman⁽⁷⁷⁾.

In a paper presented at the 5th World Conference on Earthquake Engineering Meli⁽⁵⁸⁾ summarized a substantial amount of the research that was performed at the National University of Mexico by himself, Esteva and co-workers^(72,73,74,75). The cyclic load test program consisted of cantilever (Figure 2-29) and diagonal compression (Figure 2-4) load tests on 9' x 9' panels. There were twenty-six concrete block walls with interior reinforcement and four brick walls with the columns tested.

Meli summarized the experimental behaviour of the walls as follows. When subjected to cycles of alternating loads that cause cracking, walls suffered deterioration of stiffness and strength. The load-deformation curve changed significantly from the first to the second cycle; in most cases the curve tended to a stable pattern in subsequent cycles and the difference after the sixth cycle was negligible. The amount of deterioration depended mainly on the type of reinforcement and on the mode of failure. The type of unit and the vertical load applied also affected the behaviour.

Concrete block walls whose failure was governed by bending showed little deterioration before yielding of the reinforcement; after yielding important reduction of stiffness occurred in subsequent cycles but strength was not affected (Figure 2-53a). For high deformations progressive crushing of the unconfined compression corner gave rise to major deterioration.

When strength was governed by diagonal cracking the hysteretic loop was characterized by an initial branch of very low slope, corresponding to the closing of the cracks due to the load applied in the opposite direction, followed by a branch of higher stiffness similar to that of the first cycle in the cracked stage. For that reason the load was considerably lower than that of the first cycle for the same deformation, although the initial strength was usually reached for higher deformations. Behaviour was significantly influenced by the type of reinforcement.

Walls with interior reinforcement only, whose failure was governed by shear, showed very important deterioration after diagonal cracking (Figure 2-53b). Often stabilization of the curve did not take place and initial strength could not be attained again, because of the progressive shearing off of the interior reinforcement. Increasing the amount of interior reinforcement did not give rise to a clear improvement of the behaviour.

Walls with tie columns and bond beams deteriorated after diagonal cracking much less than interiorly reinforced walls on account of the confinement provided; nevertheless for high deformations, exceeding that of maximum load, shear failure of the tie column progressively reduced confinement and very important deterioration occurred (Figure 2-53c).

When a low level of precompression (40-60 psi) was applied to the walls deterioration decreased for all types of reinforcement and modes of failure.

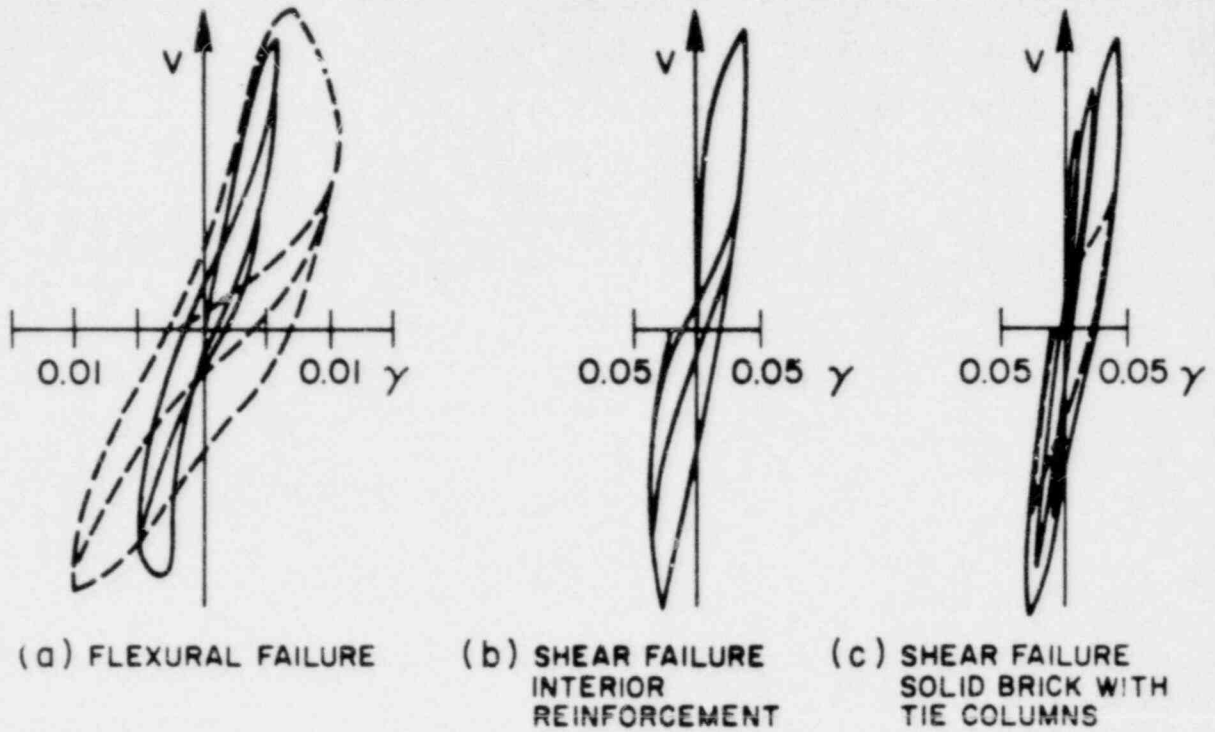


FIGURE 2-53 TYPICAL LOAD-DISTORTION CURVES UNDER ALTERNATING LOADS

From Reference 58

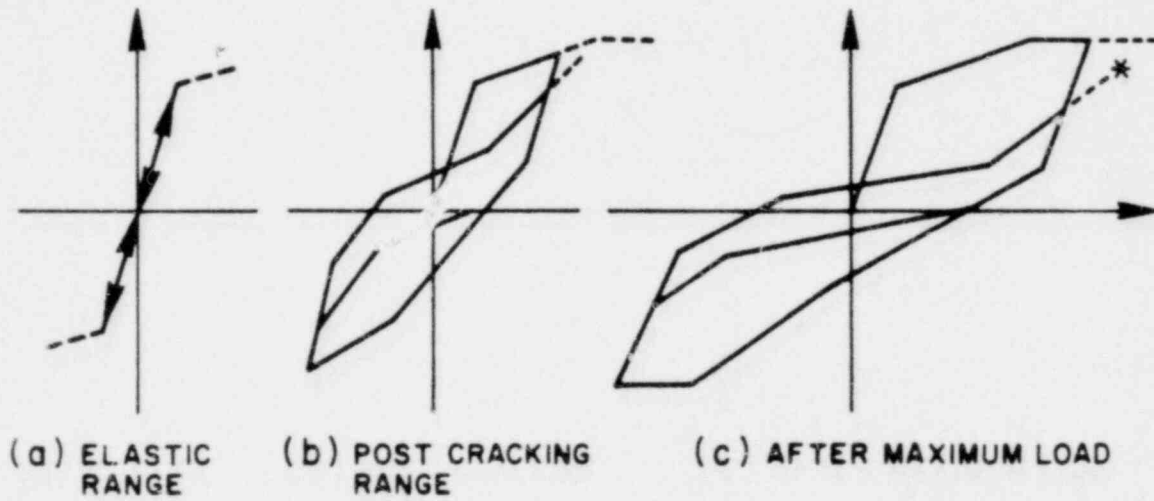


FIGURE 2-54 IDEALIZED HYSTERETIC BEHAVIOUR

From Reference 58

The author postulated that the load deformation behaviour under repeated loads can be represented by curves shown in Figure 2-54. Experimental results justify the adoption of a single hysteretic loop after the first cycle. The most important characteristics of the hysteretic loop are the ratio between the area contained in that loop and that contained in the first cycle and the ratio between the loads corresponding to the maximum deformation for the two cycles. The first parameter is a measure of the loss in energy absorption capacity and the second of the strength deterioration. A constant value of these parameters for each branch of the assumed trilinear load deformation curve can be considered. For the first branch, results justify the adoption of a non-deteriorating elastic behaviour; for each of the remaining two stages values of the parameters calculated from test results for different types of reinforcement, modes of failure and units are shown in Table 2-10.

Meli concluded the paper by stating that the behaviour of walls with interior reinforcement, where failure is governed by bending, is nearly elastoplastic with remarkable ductility and small deterioration under alternating load except for very high deformations where important deterioration is caused by progressive crushing and shearing off of the compressive corner. If failure is governed by diagonal cracking, ductility is smaller and, when high vertical loads are applied, behaviour is frankly brittle. Furthermore, walls with this type of reinforcement showed important deterioration after diagonal cracking. Possibly, behaviour could be improved by using much higher ratios of vertical and horizontal closely-spaced reinforcement, or more effectively by confining grout and vertical reinforcement in the corners by means of closely-spaced ties. In conclusion, for adequate behaviour under alternating

TABLE 2-10

EXPERIMENTAL PARAMETERS OF HYSTERETIC LOOPS

Reinforcement	Type of Unit	Type of Failure	Precompression	Maximum Deformation	V/V_0 %	A/A_0 %
INTERIOR	Concrete Block	Flexure	NO	0.0015 0.0030	85 85	80 70
			YES	0.002 0.005	95 95	80 70
		Shear	NO	0.0015 0.004	75 40	35 20
			YES	0.0015 0.0035	75 50	60 30
	Hollow Brick	Shear	NO	0.002	35	20
			YES	0.002	30	35
TIE COLUMNS	Solid Brick	Shear	NO	0.001 0.003	90 70	80 40
			YES	0.001 0.0025	100 100	80 60
FRAME (25 x 40 cm)	Solid Brick		YES	0.015	70	40

V/V_0 : Ratio between the load at maximum deformation in the hysteretic loop and the load corresponding to the same deformation in the first cycle.

A/A_0 : Ratio between the area contained in the hysteretic loop and the area contained in the first cycle.

loads, the layout, aspect ratio and reinforcement of walls have to be chosen, when possible, in such a way as to give rise to a bending failure.

For walls of solid units strengthened by tie columns and bond beams, large ductilities are reached in spite of important damage in the wall itself and in the column. Deterioration is still important for high deformations due to the loss of confinement caused by the progressive destruction of the column in the corner. Nevertheless behaviour is definitely better than that of unreinforced or interiorly reinforced walls; this has also been made evident by their better seismic behaviour.

Williams⁽³⁾ performed a series of cyclic load tests on twenty one cantilever walls made of varying materials and aspect ratios. Seventeen of the tests were performed with a quasi-static, displacement-controlled, cyclic load while the other four were tested with a sinusoidally-varying, displacement-controlled load. The frequencies of the sinusoids were 1 cps and below. The test setup used in the investigation is shown in Figure 2-9. Tables 2-11 and 2-12 summarise the results presented by Williams. The theoretical values tabulated are calculated from the formulae presented in Equation 2-1. Typical force-deflection curves are presented in Figures 2-55 and 2-56 and others can be found in Reference 3. Figure 2-55 is typical of the flexural or yield failure while Figure 2-56 is typical of the shear failure.

Williams discussed the results of the tests under the following headings.

(a) Stiffness Degradation - In all tests stiffness degradation with load repetition was apparent. For walls behaving flexurally the major loss was between the first and second cycle of several cycles at the same amplitude. Additional cycles at the same amplitude were relatively

TABLE 2.11
STATIC TEST WALL DETAILS

Material	Designation	Height	Length	Nominal Aspect Ratio	Vertical Reinforcing (1)	Reinforcing (2) (%)	Bearing Stress (2) (psi)
Brick	1	3'-9"	3'-8"	1	4/8" bars uniformly distributed	0.24	0
"	2	"	"	1			
"	3	"	"	1			
"	4 (3)	"	"	1			
"	5	"	"	1			
Concrete block	CB 1	4'-0"	4'-0"	1	4/8" bars uniformly distributed	0.26	0
"	CB 2	"	"	1			
"	CB 3	"	"	1			
"	CB 4	"	"	1			
Brick	A1	3'-9"	3'-8"	1	2/8" bars on periphery	0.67	250
"	A2	"	"	1			
"	B1	3'-11"	2'-2"	2	2/8" bars on periphery & 2/8" bars horizontally	0.33	250
"	B2	"	"	2	2/8" bars on periphery	0.20	
"	B3	"	"	2	"	"	
"	B4	"	"	2	"	"	
"	D1	3'-2"	6'-1"	0.5	4/8" bars on periphery	1.63	250
"	D2	"	"	0.5	6/8" bars uniformly distributed	0.22	0
					"	"	250

(1) All reinforcing bars deformed mild steel butt welded to base - 3/8" bars anchored into top beam with standard 180° hook (1" radius, 3" turndown); other vertical bars and horizontal bars anchored with 90° bend and 8" extension.

(2) Based on gross horizontal section.

(3) Only reinforced cores grouted.

From Reference 3

D2 D1 B1 B2 B3 B4

TABLE 2-12
STATIC TEST RESULTS

Wall	Area (in ²)	Theoretical Yield Load (kip)	Experimental Maximum Load (kip)	Shear Strength (psi)	Predicted Behavior
CB1	172	10	11.2	65	flexural
CB2	"	20	20.5	119	"
CB3	"	30	29.5	174	transitional
CB4	"	40	44.7	260	shear
1	186	10	12.5	67	flexural
2	"	20.6	20.5	110	"
3	"	31.3	30.6	165	transitional
4 ⁽¹⁾	"	52.6	32.8	176	shear
5	"	52.6	39.5	212	"
A1	178	48	37.5	210	shear
A2	"	48	40.0	225	"
B1	108	9.7(10.8)*	10.6	98	flexural
B2	"	16.7	16.6	154	transitional
B3	"	6.2(7.3)*	7.4	68	flexural
B4	"	25.2	16.0	148	shear
D1	300	30	30.0	100	flexural
D2	"	98	70.5	235	shear

*Theoretical Ultimate Load

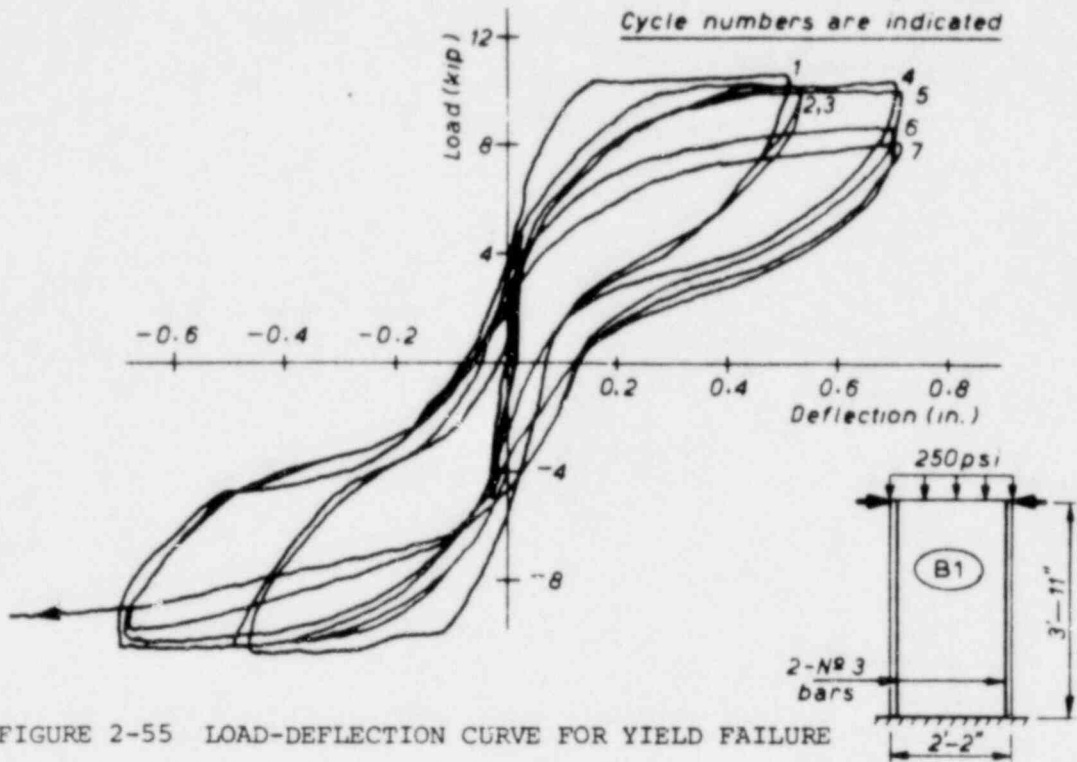


FIGURE 2-55 LOAD-DEFLECTION CURVE FOR YIELD FAILURE

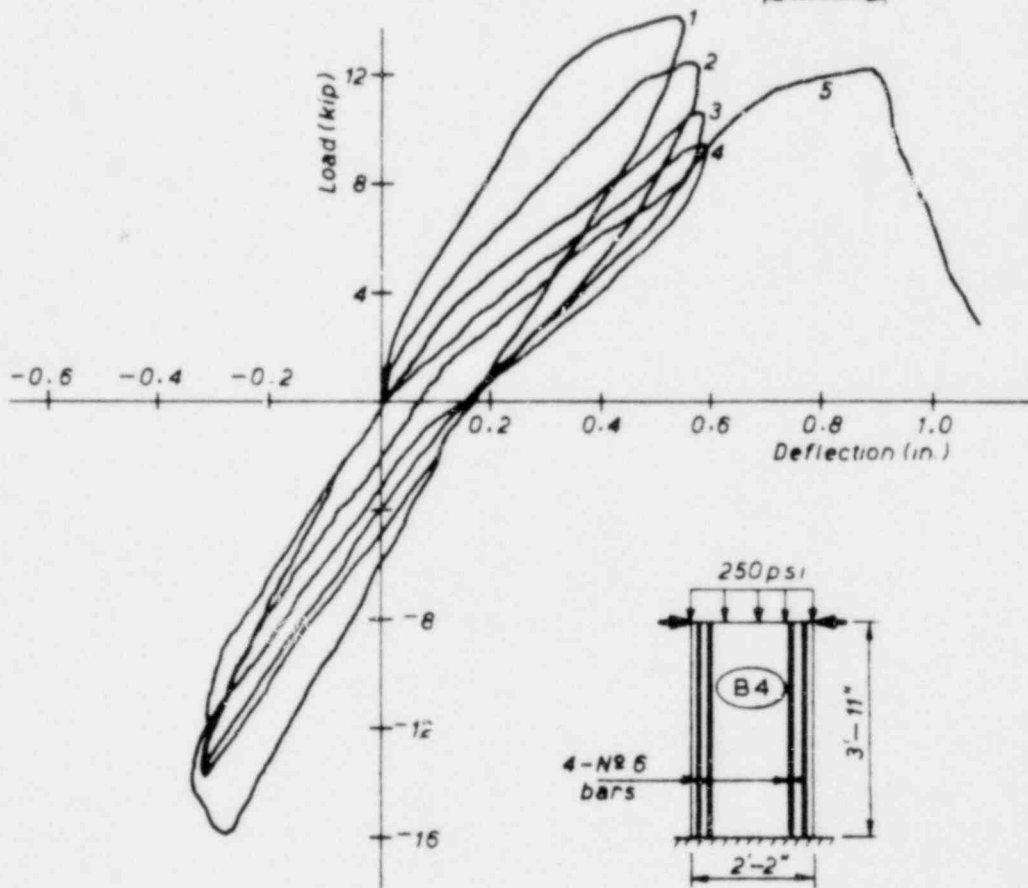


FIGURE 2-56 LOAD-DEFLECTION CURVE FOR SHEAR FAILURE

From Reference 3

stable. The more flexural the situation the less pronounced the stiffness degradation. On the other hand for walls which failed predominantly in shear the initial stiffness degradation was large with severe load reduction, and further stiffness degradation occurred on each subsequent cycle. Deterioration of the reaction corner causes the reduction in shear resistance, whereas in flexural behaviour the post-elastic deformations are due to steel yielding, and load capacity of the reaction corner is not impaired until large displacements are reached.

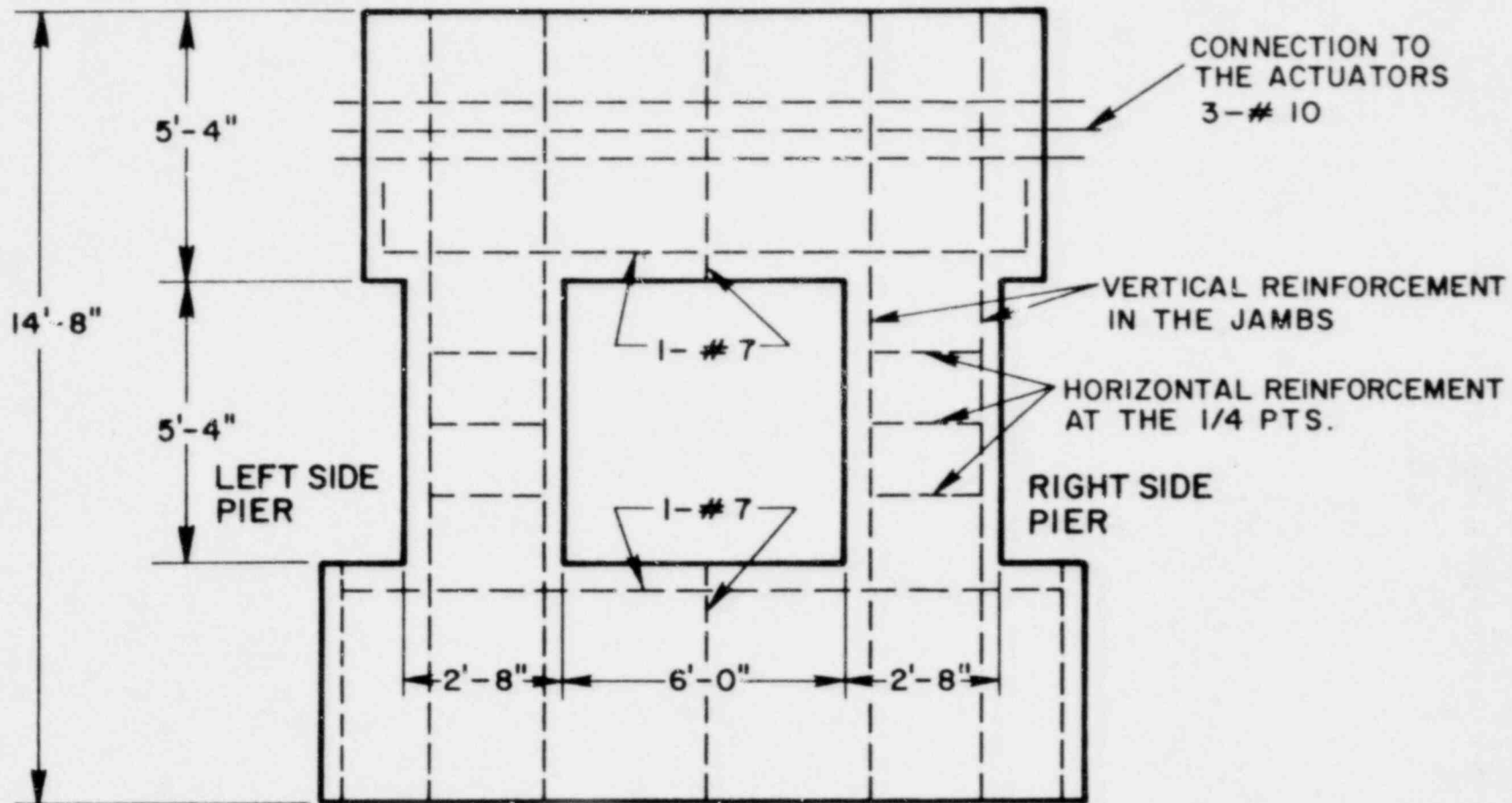
(b) Effect of Bearing Load - Every wall was capable of supporting its bearing load until severe damage had drastically reduced its lateral strength. The tests indicated that the elastic lateral strength of the wall increases with increasing bearing stress. However of greater concern in many instances is the post-elastic cyclic behaviour, and increasing bearing loads are associated with a trend towards more shear-like behaviour. The ultimate strength increases and the ductility decreases with an increase in bearing load. This implies a beneficial effect in an elastic consideration but conversely a detrimental effect in a post-elastic consideration.

(c) Effect of Wall Geometry - It was considered that walls within the geometric range tested (height (H) to width (W) of 0.5 to 2) have the most complex and unpredictable behaviour. As the H/W ratio increases a more flexural wall results. Walls of very high aspect ratio can be regarded as long shallow beams with a characteristic flexural behaviour. Low aspect ratio walls essentially have a shear type of deformation and so, may be considered as pure, shear-resisting elements with non-ductile behaviour. The walls whose aspect ratios fall between these distinct types, form a transition zone where behaviour is not

clearly defined. Of course the transition zone has no distinct boundaries and its range is affected by bearing loads and reinforcing percentages

(d) Effect of Reinforcing - The tests of Schneider⁽⁵⁷⁾ and Scrivener⁽⁴⁹⁾ established that for any one masonry material, a reasonably constant, shear strength was obtained provided a nominal amount of reinforcing (horizontal or vertical) was incorporated. Hence an increase of vertical reinforcing increases the horizontal load to cause yielding of the steel without altering the shear strength appreciably; and while other factors remain the same it has the effect of increasing the tendency to shear failure.

(e) Effect of Dynamic Loading - The tests performed were limited and confined to frequencies below 1 cps, however the results were very interesting and indicated the need for further research in the dynamic aspects of masonry shear walls. Williams found that there was no indication of an increase in the steel yield strength with dynamic loading. Of the four walls he tested three, that showed a high degree of structural deterioration in the static tests, behaved similarly under dynamic conditions. However for the "flexural" brick wall dynamic testing revealed that, in contrast to the satisfactory ductile behaviour of the comparable wall tested statically, a severe but unexpected loss of structural capability occurred with load repetition. This lead Williams to conclude that contrary to normally accepted opinion, cyclic static test results may be inappropriate for use as a conservative basis for seismic design with reinforced masonry. Mayes and Clough⁽⁷⁶⁾ presented the results of tests on eight dimensionally similar specimens constructed from 6" wide x 8" high x 16" long hollow concrete block units, see Figure 2-57. The eight specimens consisted of four pairs of identical



MATERIAL : HOLLOW CONCRETE BLOCKS 6" WIDE x 8" HIGH x 16" LONG.

FIGURE 2-57 TYPICAL DOUBLE PIER TEST SPECIMEN

panel. One of each pair was tested at an input displacement frequency of 0.02 cps and the other at 3 cps. The other variables of the four sets are listed in Table 2-13. The results of the study were presented in the form of hysteresis loops, graphs of the energy dissipation characteristics and stiffness degradation properties and tabulated data on the ultimate strength and ductility indicators.

In presenting their results the authors defined several "indicators" that were associated with the force-deflection characteristics of the piers, Figures 2-58 and 2-59.

(a) Peak Ultimate Loads - P_{u1} and P_{u2} .

These are the maximum loads, one in either direction, that were attained during a test.

(b) Average Ultimate Loads - P_1 and P_2 .

The loads P_1 and P_2 , one in either direction, are approximately 90% of the mean of the peak ultimate loads and were maintained for more than one cycle of input displacement.

(c) Working Ultimate Load - P_3 .

P_3 was chosen as the load at which the first visible cracks form in the piers. P_3 varied between 70 and 80% of the mean of the peak ultimate loads.

(d) Ductility Indicators - δ_1 to δ_4 .

Ductility indicators associated with P_1 , P_2 and P_3 were defined to give an indication of the displacement range over which loads P_1 , P_2 and P_3 were maintained. δ_1 and δ_2 are associated with the average ultimate strengths P_1 and P_2 , and are defined as the ratio of the displacement at

TABLE 2-13

MATERIAL AND PIER PROPERTIES

Test No.	Frequency (1) cps	Bearing Stress (2) (psi)	Vertical Reinforcement (3)	Horizontal Reinforcement (4)	Prism Strength (psi)	Mortar Strength (psi)	Grout Strength (psi)	Reinforcement Stresses (5) Horizontal (ksi) Vertical (ksi)	Average Ultimate Shear Strength (6) (psi)
1	0.02	250	2 - #6	—	2280	4955	4510	— 43.1 (64.9)	125
2	3	250	2 - #6	—	2280	4955	4510	— 43.1 (64.9)	161
3	0.02	125	2 - #4	—	2115	3985	3420	— 54.1 (83.4)	135
4	3	125	2 - #4	—	2115	3985	3420	— 54.1 (83.4)	119
5	0.02	0	2 - #6	—	2430	5260	6150	— 78.1 (108.8)	99
6	3	0	2 - #6	—	2430	5260	6150	— 78.1 (108.8)	113
7	0.02	250	2 - #6	1 - #5	2630	5610	4330	67.8 (94.6) 78.1 (108.8)	203
8	3	250	2 - #6	1 - #5	2630	5610	4330	67.8 (94.6) 78.1 (108.8)	229

Notes 1. Frequency of the sinusoidally applied actuator displacement.

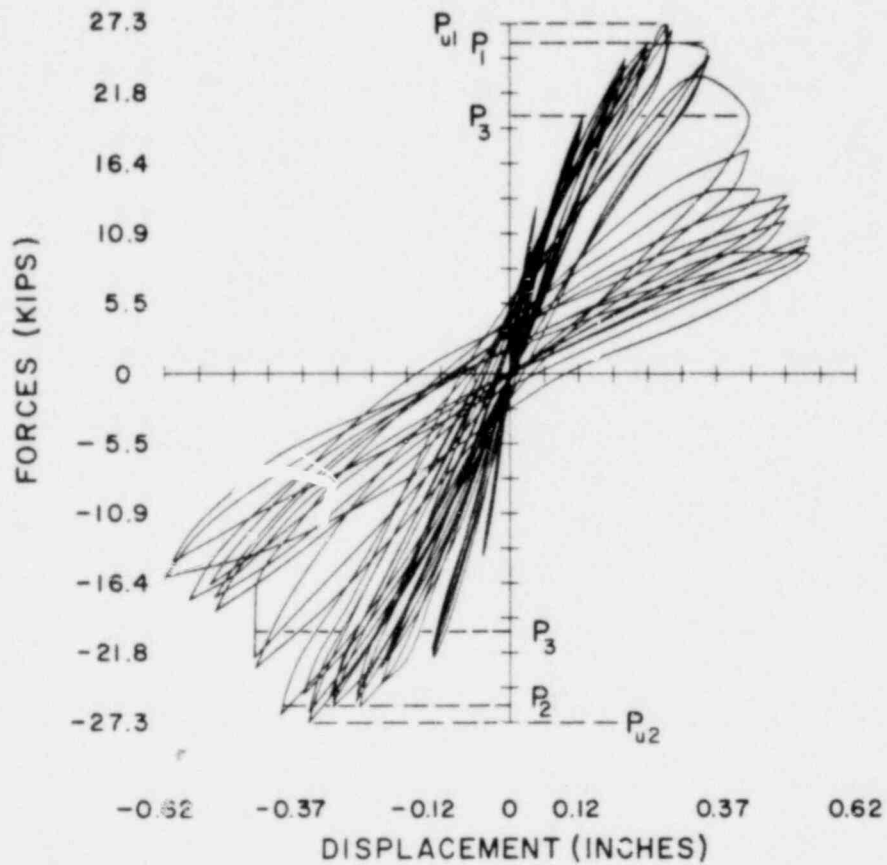
2. Bearing stress based on the gross area (192 sq. in.).

3. Vertical Reinforcement in each jamb of the piers.

4. Horizontal Reinforcement at the 1/4 points of each pier.

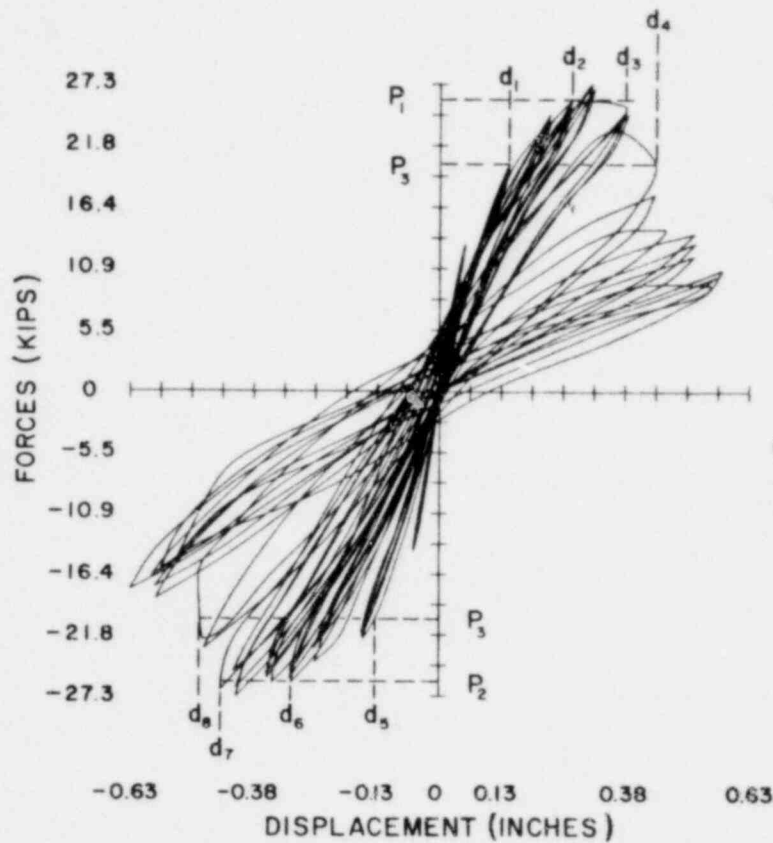
5. The top value is the yield stress, the value in brackets is the ultimate strength.

6. Average ultimate shear strength - $(P_1 + P_2)/(2 \times \text{gross area})$ where P_1 and P_2 are defined in Figure 2-58.



- P_{u1}, P_{u2} - PEAK ULTIMATE STRENGTHS
 P_1, P_2 - AVERAGE ULTIMATE STRENGTHS
 APPROXIMATELY 90% OF P_{u1}, P_{u2}
 P_3 - WORKING ULTIMATE STRENGTH
 APPROXIMATELY 70-80% OF P_{u1}, P_{u2}

FIGURE 2-58 DEFINITION OF ULTIMATE LOADS



DUCTILITY INDICATORS

(1) AT AVERAGE ULTIMATE STRENGTH - P_1, P_2

$$\delta_1 = \frac{d_3}{d_2} \quad \delta_2 = \frac{d_7}{d_6}$$

VARIED BETWEEN
1.45 — 1.85

(2) AT WORKING ULTIMATE STRENGTH - P_3

$$\delta_3 = \frac{d_4}{d_1} \quad \delta_4 = \frac{d_8}{d_5}$$

VARIED BETWEEN
2.4 — 5.6

FIGURE 2-59 DEFINITION OF DUCTILITY INDICATORS

From Reference 76

which the pier can no longer withstand the lateral load P_1 or P_2 to the displacement at which P_1 or P_2 is first attained. δ_3 and δ_4 are similar ratios, one in either direction, associated with the load P_3 .

The mean of the loads P_{u1} and P_{u2} , the mean of the loads P_1 and P_2 , P_3 and their respective shear strengths based on the gross area of 192 sq in. are listed in Table 2-14. δ_1 to δ_4 are defined as $\delta_1 = \frac{d_3}{d_2}$; $\delta_2 = \frac{d_7}{d_6}$; $\delta_3 = \frac{d_4}{d_1}$ and $\delta_4 = \frac{d_8}{d_5}$ where d_1 to d_8 are shown in Figure 2-59. The mean of δ_1 and δ_2 , and the mean of δ_3 and δ_4 are listed in Table 2-14.

To give an indication of the stiffness degradation occurring between different sequences of loading a stiffness coefficient (K_I) defined as

$$K_I = \frac{\text{Maximum +ve force} - \text{Maximum -ve force}}{\text{Corresponding +ve displ} - \text{Corresponding -ve displ.}}$$

was calculated for each cycle of loading. K_I for the right side pier was plotted against the average lateral displacement and shear force for each cycle of loading - typical plots are shown in Figures 2-60 to 2-63. On each of these graphs a line indicating the first cracks visible to the eye and a line indicating the formation of the first major crack are also plotted.

The energy dissipated per cycle of loading was expressed in terms of a dimensionless ratio EDT. EDT is defined as the ratio of the energy dissipated to the total stored energy per cycle and is diagrammatically shown in Figure 2-64.

$$\begin{aligned} \text{EDT} &= \frac{\text{Energy Dissipated/cycle}}{\text{Total Stored Energy/cycle}} \\ &= \frac{A}{A + B} \quad (\text{Figure 2-64}) \end{aligned}$$

TABLE 2-14
ULTIMATE STRENGTHS AND DUCTILITY INDICATORS

TEST NO.	Frequency ⁽¹⁾ (cps)	Bearing Stress ⁽²⁾ (psi)	Vertical Reinforcement ⁽³⁾	Horizontal Reinforcement ⁽⁴⁾	$\frac{P_{u1} + P_{u2}}{2}, \frac{\tau_{u1} + \tau_{u2}}{2}$ ⁽⁵⁾		$\frac{P_1 + P_2}{2}, \frac{\tau_1 + \tau_2}{2}$ ⁽⁶⁾		P_3, τ_3 ⁽⁷⁾		$\frac{\delta_1 + \delta_2}{2}$ ⁽⁸⁾	$\frac{\delta_3 + \delta_4}{2}$ ⁽⁹⁾
					(kips)	(psi)	(kips)	(psi)	(kips)	(psi)		
1	0.02	250	2 - #6	—	26.0;	135	24;	125	20;	104	1.55	3.5
2	3	250	2 - #6	—	34.3;	179	31;	161	28;	146	1.55	2.4
3	0.02	125	2 - #4	—	27.3;	142	26;	135	21;	106	1.5	4.1
4	3	125	2 - #4	—	24.0;	125	22.8;	119	18;	94	1.8	5.6
5	0.02	0	2 - #6	—	20.5;	107	18.5;	96	15;	78	1.55	5.6
6	3	0	2 - #6	—	25.0;	130	21.7;	113	19;	99	1.85	5.3
7	0.02	250	2 - #6	1 - #5	40.7;	212	39;	203	33;	172	1.5	4.4
8	3	250	2 - #6	1 - #5	46.8;	244	44;	229	33;	172	1.45	3.0

- Notes:
1. Frequency of the sinusoidally applied actuator displacement
 2. Bearing stress based on the gross area (192 sq. in.)
 3. Vertical Reinforcement in each jamb of the piers
 4. Horizontal Reinforcement at the 1/4 points of each pier
 5. P_{u1} and P_{u2} are the peak shear loads in either direction, and defined in Figure 2-58. τ_{u1} and τ_{u2} are the corresponding shear stresses based on the gross area.
 6. P_1 and P_2 are the average ultimate shear strengths as defined in Figure 2-58. τ_1 and τ_2 are the corresponding shear stresses based on the gross area.
 7. P_3 is a working ultimate shear strength defined in Figure 2-58. τ_3 is the corresponding shear strength based on the gross area.
 8. δ_1 and δ_2 are approximate ductility ratios associated with P_1 and P_2 and defined in Figure 2-59.
 9. δ_3 and δ_4 are ductility indicators associated with P_3 and defined in Figure 2-59.

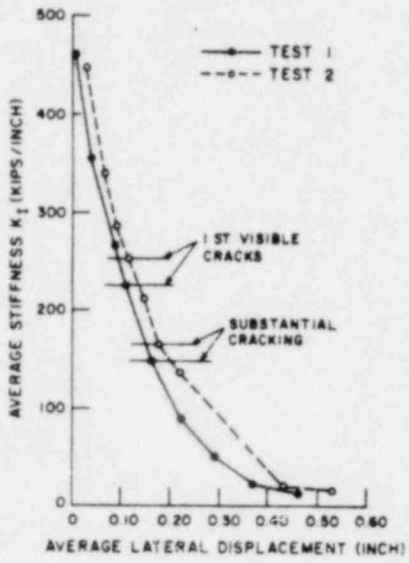


FIGURE 2-60

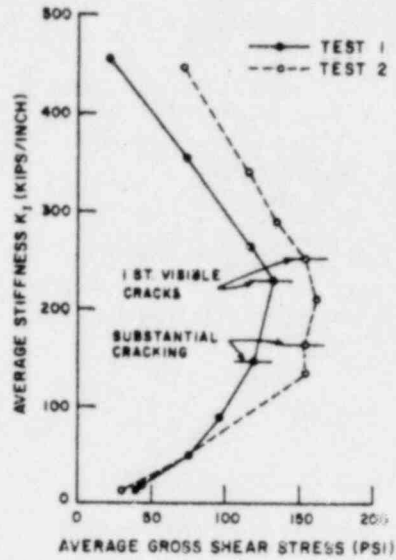


FIGURE 2-61

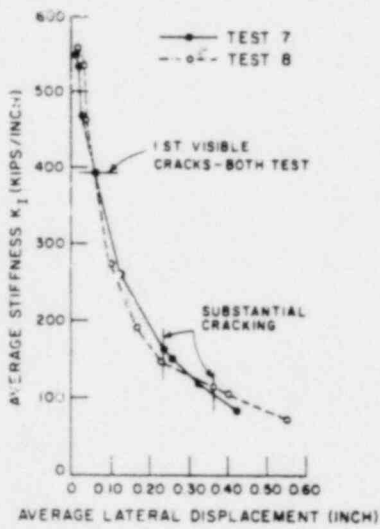


FIGURE 2-62

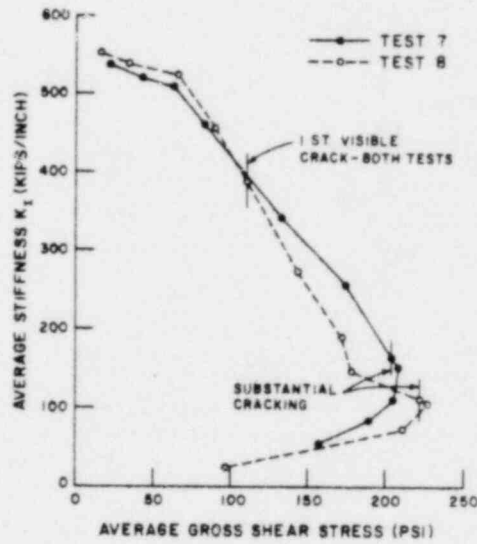


FIGURE 2-63

TYPICAL K_I PLOTS

From Reference 76

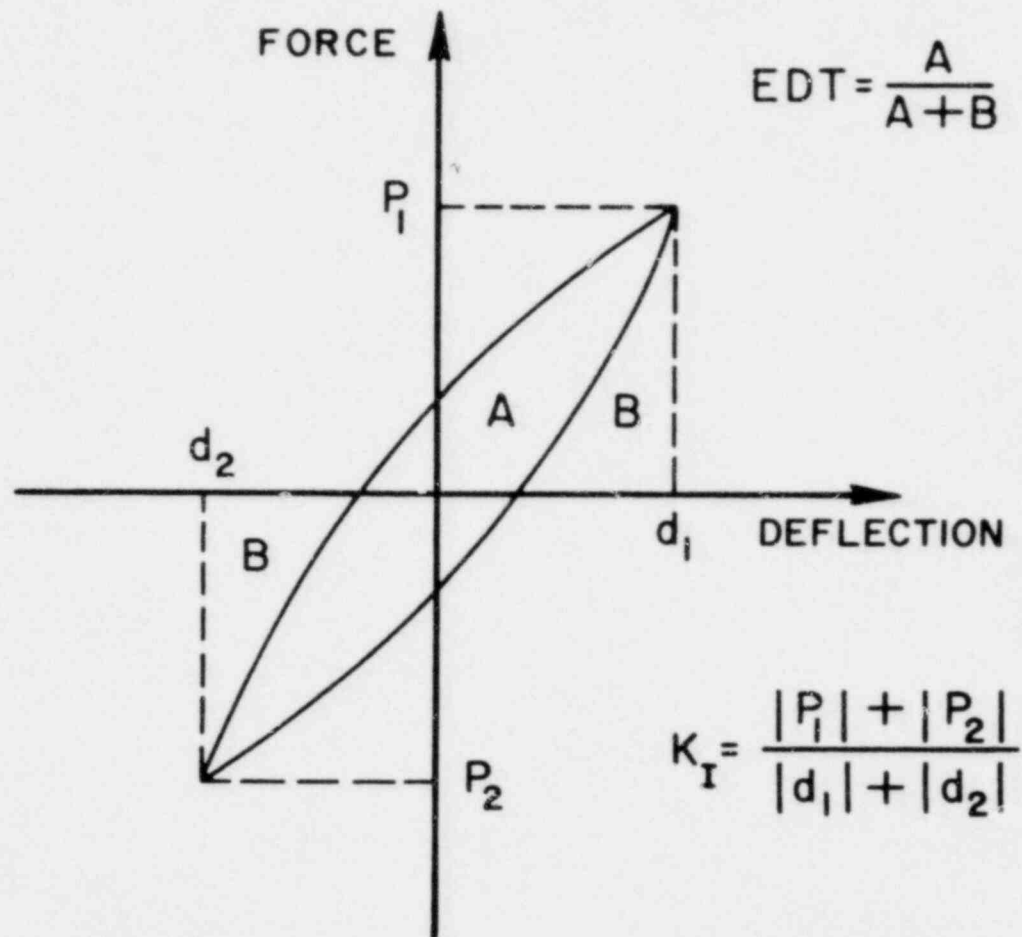


FIGURE 2-64 DIAGRAMMATIC REPRESENTATION OF ENERGY DISSIPATION

From Reference 76

From the results presented the authors made the following observations.

(1) The ultimate strength of the piers tested was affected by the rate of loading, the bearing stress and the amounts of vertical and horizontal reinforcement.

(2) Piers that failed in the shear mode of failure had a peak ultimate strength 13-23% less in the pseudo-static test than in the corresponding 3 cps test, whereas piers that failed in a combination of the shear and flexure modes of failure had a pseudo-static peak ultimate strength 16% greater than the corresponding 3 cps test. Consequently pseudo-static tests do not always produce conservative ultimate strengths.

(3) At a shear stress of 20-25 psi the piers tested with horizontal reinforcement were 16% stiffer (K_I) than piers with no horizontal reinforcement.

(4) As the shear stress increased from 25 to 50 psi the piers with no horizontal reinforcement suffered a 14-20% decrease in their stiffness, whereas piers with horizontal reinforcement had a corresponding decrease of 4%.

(5) The piers tested do exhibit a ductile type of behaviour under gradually increasing lateral displacements. They are able to resist 90% of the peak ultimate load over a displacement (ductility indicator) range of 1.45 to 1.85 and 70-80% of the peak ultimate strength over a displacement range of 2.4 to 5.6.

Priestly and Bridgeman⁽⁷⁷⁾ conducted a very thorough investigation on the effect of horizontal and vertical reinforcement on the shear strength of cantilever piers. In addition they investigated the effect

of a confining plate in the mortar joints at the compression toes of the piers and found that this considerably improved the inelastic behaviour of the piers.

Priestly and Bridgeman tested 14 reinforced, brick masonry walls (RBM - two skins of solid bricks separated by a reinforced grout gap and four hollow cell brick panels all of unit aspect ratio and between 3.41 ft (1.04 m) and 5.90 ft (1.80 m) square. Table 2-15 summarizes the wall dimensions, amounts and distribution of deformed reinforcing bars and material properties. For walls F2 to F15 RBM construction was used and CBU-1 to CBU-4, hollow cell construction was used. All RBM walls were constructed from 9" x 3" x 2.75" high bricks separated by a 2.5" grout gap. The hollow cell walls were constructed from block units of 5.5" nominal width. All cells were filled with grout. The main variable in the tests was the amount of reinforcing. Vertical and horizontal reinforcing steel was evenly distributed along the length and height of the walls except where designated 'P' in Table 2-15, 'P' indicates that all vertical steel was concentrated at the ends of the panels. Except in the cases of walls F9 and F10 all were tested without an applied bearing load. The walls were tested cyclically by the cantilever method shown in Figure 2-9, at very low rates of loading (less than $0.1 H_z$).

The authors discussed the results of their tests in the following categories:

(a) Ultimate Flexural Capacity - Table 2-16 compares failure loads with the theoretical capacities in flexure and shear of the walls constructed without confining plates in the critical mortar joints. The yield load P_y is defined as the theoretical load at which the extreme

TABLE 2-15
WALL PANEL DIMENSIONS AND PROPERTIES

Wall	Size LXHX (in)	Confining Plates	Vertical Prestress (psi)	Reinforcing* Steel				Material Strengths (psi)						
				Vertical (in)	$\frac{w}{h}$	Horizontal (in)	$\frac{w}{h}$	Brick f_b	Grout f_g	Mortar f_m	Vert. f_y	Steel f_u	Horiz. f_y	Steel f_u
F2	70.5x70.9x8.7	NO	0	P2-0.626	0.10	----	----	9361	3628	3251	46,444	68,505	----	----
F3	"	NO	0	4-0.626	0.20	----	----	9361	4209	1654	43,396	64,441	----	----
F4	"	NO	0	6-0.500HY	0.19	----	----	9361	2206	1364	67,199	101,016	----	----
F5	"	NO	0	4-0.626	0.20	3-0.500HY	0.10	9361	3483	1509	43,396	64,441	58,200	77,068
F6	"	NO	0	6-0.500HY	0.19	3-0.500HY	0.10	9361	3425	1625	67,199	101,016	67,199	101,016
F7	"	NO	0	8-0.750	0.57	----	----	9361	3483	1509	45,138	67,634	----	----
F8	"	NO	0	8-0.750	0.57	3-0.500HY	0.10	9361	3062	1553	43,541	65,892	58,200	77,068
F9	"	NO	130	8-0.750	0.57	----	----	9361	3236	1741	45,138	67,634	----	----
F10	"	NO	260	8-0.750	0.57	----	----	9361	3236	1741	45,138	67,634	----	----
F11	"	NO	0	8-0.750	0.57	6-0.750	0.43	9361	3425	1407	42,235	66,763	42,235	66,763
F12	"	NO	0	8-0.750HY	0.57	8-0.750	0.57	9361	3425	1407	63,425	107,112	42,235	66,763
F13	64.2x59.4x8.7	YES	0	8-0.750HY	0.63	7-0.626	0.41	9361	5645	2162	64,441	105,080	45,573	66,038
F14	"	YES	0	8-0.750HY	0.63	7-0.626HY	0.41	9361	5645	2162	64,441	105,080	63,861	95,791
F15	"	YES	0	4-0.626	0.22	4-0.500	0.15	9361	4121	2525	43,831	66,038	39,913	57,184
CBU1	40.9x41.5x5.5	NO	0	P6-0.750HY	1.17	5-0.750HY	0.96	7677	3410	1407	63,425	107,112	63,425	107,112
CBU2	"	NO	0	6-0.750HY	1.17	5-0.750HY	0.96	7677	3410	1407	63,425	107,112	63,425	107,112
CBU3	59.8x61.4x5.5	YES	0	8-0.750HY	1.07	6-0.750HY	0.77	7677	3744	2002	61,693	102,612	61,684	102,612
CBU4	59.8x61.4x5.5	YES	0	4-0.750	0.54	5-0.500HY	0.29	7677	4513	1959	42,380	66,763	44,993	70,972

* Deformed Bar throughout.

P-Indicates all the vertical steel is concentrated at the peripheries of the panel.

TABLE 2-16

FAILURE LOADS FOR WALLS WITHOUT CONFINING PLATES

Wall	Theoretical Loads (kips)			Failure Mode	Experimental Loads (kips)			P1/Pu	P2/Pu	P3/Pu	Shear Stress at Max. Load (psi)
	Yield P _Y	Ult. Flexural	Shear Capacity P _Y *		First Loading P1	First Load Reversal P2	Second Load Reversal P3				
F2	29.0	29.0	----	Flexure	30.6	28.1	19.1	1.05	0.97	0.66	49
F3	20.7	27.2	----	Flexure	32.1	15.7	22.0	1.18	0.58	0.81	52
F4	31.0	40.0	----	Flexure	47.2	----	----	1.18	----	----	77
F5	20.7	27.2	34.1	Flexure	31.9	15.1	7.9	1.17	0.55	0.29	52
F6	31.0	40.0	39.6	Flexure	44.3	----	----	1.11	----	----	73
F7	49.0	74.2	----	Shear	62.1	40.0	9.9	0.84	0.54	0.13	100
F8	47.7	71.7	34.2	Shear	65.0	22.0	11.7	0.91	0.31	0.16	106
F9	69.0	103.9	----	Shear	100.0	100.0	28.1	0.96	0.96	0.27	163
F10	92.9	132.0	----	Shear	119.8**	119.8**	100.0	0.91	0.91	0.76	196
F11	40.9	65.2	111.7	Flexure	67.4	46.5	----	1.03	0.71	----	115
F12	60.7	94.6	148.8	Flexure	96.0	78.9	----	1.01	0.83	----	163
CBU-1	51.3	65.6	139.4	Bond	55.3	39.3	----	0.84	0.60	----	247
CBU-2	38.4	65.6	139.4	Bond	56.2	----	----	0.86	----	----	255

* Based on horizontal steel only.

** Max. capacity of load system.

tension bar first attains its yield strain, and the ultimate flexural capacity P_u is based on normal reinforced concrete design methods using an assumed brickwork crushing strength of $f'_m = 3000$ psi, a crushing strain of 0.003, and an undercapacity factor of unity. Table 2-16 also includes the shear capacity of the horizontal reinforcing.

The first five walls listed (F2 - F6) contained only moderate percentages of flexural reinforcing ($\leq 0.25\%$) and were expected to exhibit flexural failures. On initial loading these walls sustained loads averaging 14% higher than the theoretical ultimate flexural capacities. This can be explained on the basis of the high steel strains existing at the stage when crushing of the brickwork occurs. As shown in Figure 2-65 the low steel percentages typically result in steel strains in the vicinity of 3 - 5% in the extreme tensile bar. The end of the yield plateau for N.Z. deformed bars is in the range 1.3% - 2.0%, after which steel stress begins to rise rapidly with increasing strain. At strains of 3 - 5% , steel stresses are 10 - 25% above yield stress, resulting in the over-strength observed in walls F2 to F6.

(b) Ultimate Shear Strength - Walls F7 to F10 exhibited diagonal shear failures. In the first two, which were tested without bearing load, failure occurred soon after the formation of the diagonal crack, at a rather low average shear stress of 103 psi. The failures were sudden, involving large horizontal displacements across the diagonal crack (see Figure 2-66) associated with severe load degradation. Walls F9 and F10 sustained much higher shear stresses due to the precompression applied by the bearing load.

Examination of Table 2-16 shows that of walls F7 - F10, one wall F8 which contained horizontal steel had a shear capacity roughly half the ultimate flexural capacity, while the others contained no horizontal

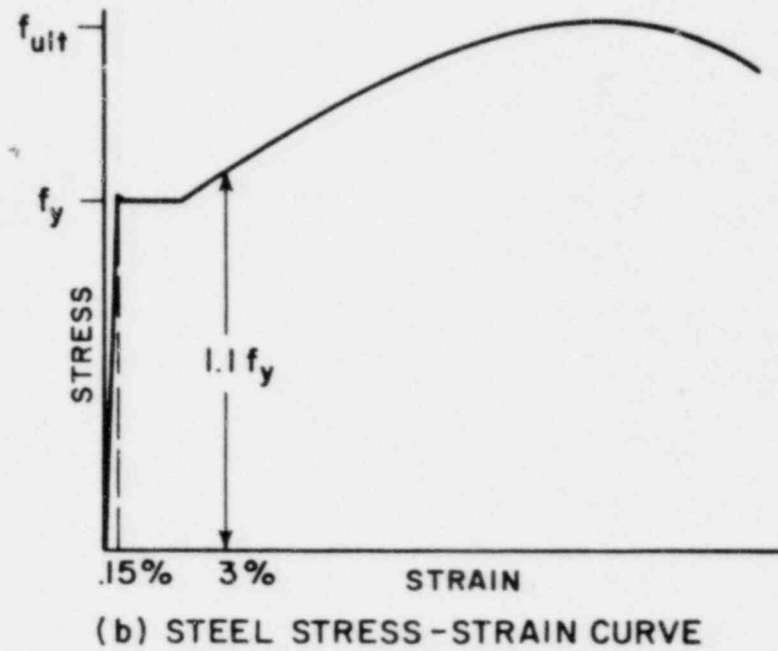
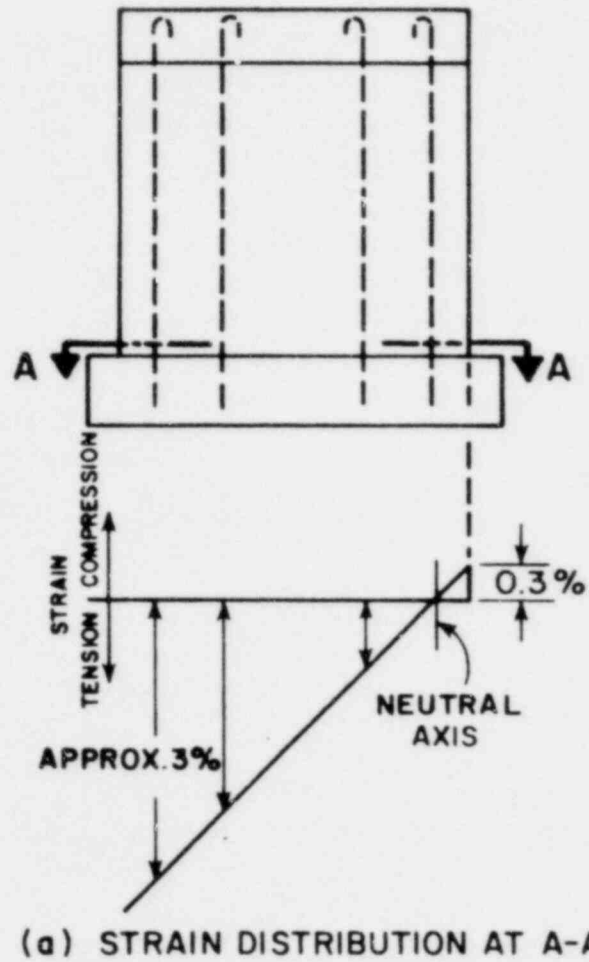


FIGURE 2-65 STRAIN HARDENING ENHANCEMENT OF ULTIMATE LOAD

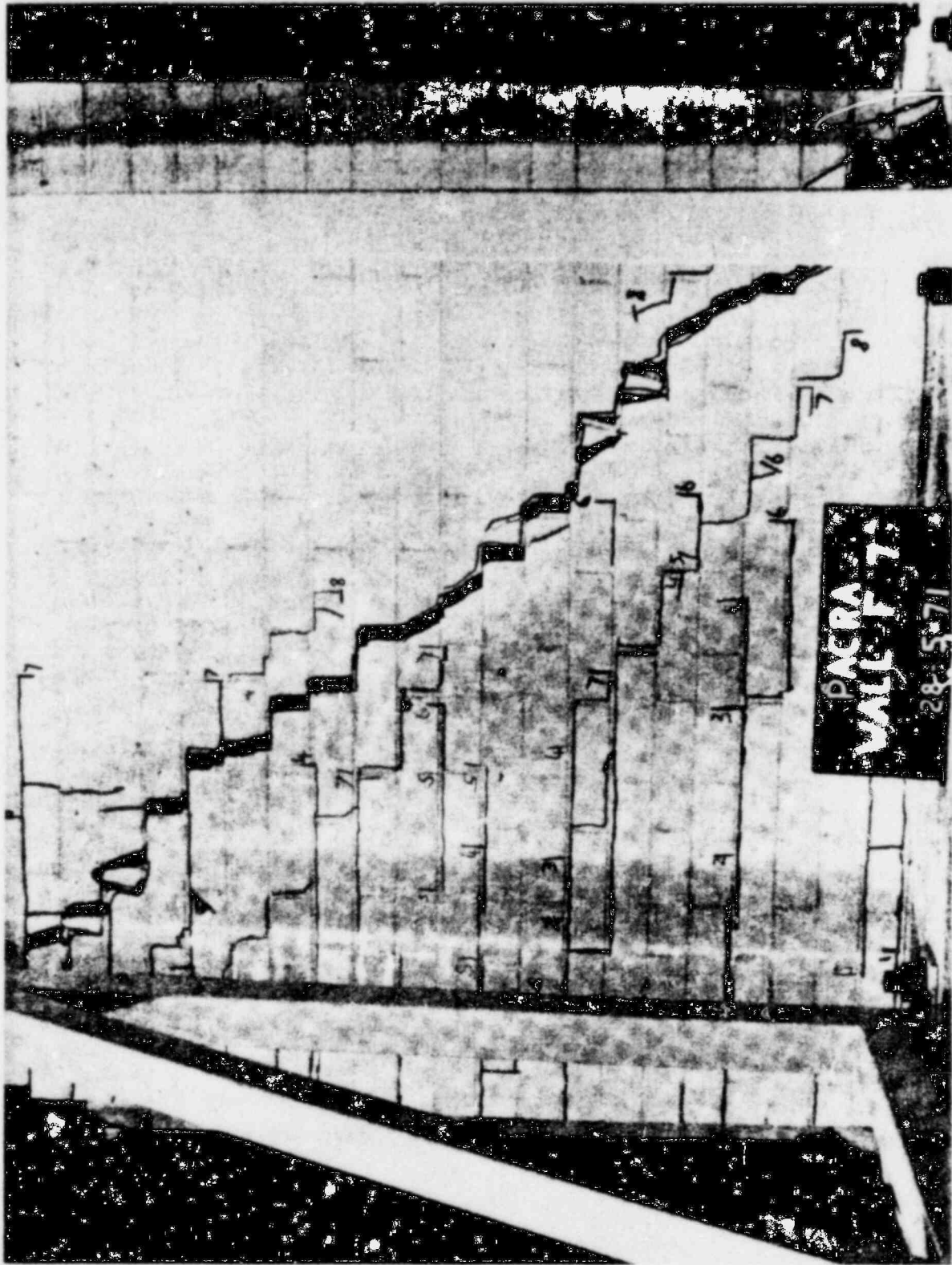


FIGURE 2-66 TYPICAL SHEAR FAILURE UNDER MONOTONIC LOADING

From Reference 77

steel. However, in each wall vertical steel with comparatively low flexural tensions passed through the diagonal crack at 45°, and might thus be supposed to have close to the same shear capacity as an equivalent number of horizontal bars. This is based on a common misconception. Prior to cracking, the principal tensile stresses near the middle of the panel are close to 45° to the vertical resulting in the formation of the diagonal crack. After formation of this crack the situation can no longer be represented by stress analyses of an elastic medium. The imposed load is not a true shear loading, and tends to move the top half of the wall horizontally past the bottom, widening the crack horizontally, rather than perpendicular to the crack. As illustrated by Figure 2-67, this results in any properly anchored horizontal steel crossing the crack resisting the shear in direct tension, while vertical steel must carry the load by dowel action.

Thus the shear capacity of n horizontal bars of diameter d crossing the shear crack will be

$$V_H = 0.785nd^2f_y \quad (2-16)$$

where f_y is the yield stress.

The dowel strength of vertical bars crossing the crack can be estimated by assuming a triangular pressure distribution exerted by the bars on the grout, with a maximum value equal to f'_g , the crushing strength of the grout, as illustrated by Figure 2-68(a) and (b). This will result in moments of the form shown in Figure 2-68(c).

For equilibrium

$$V = \frac{f'_g d l}{2}$$

$$l = \frac{2V}{f'_g d} \quad .$$

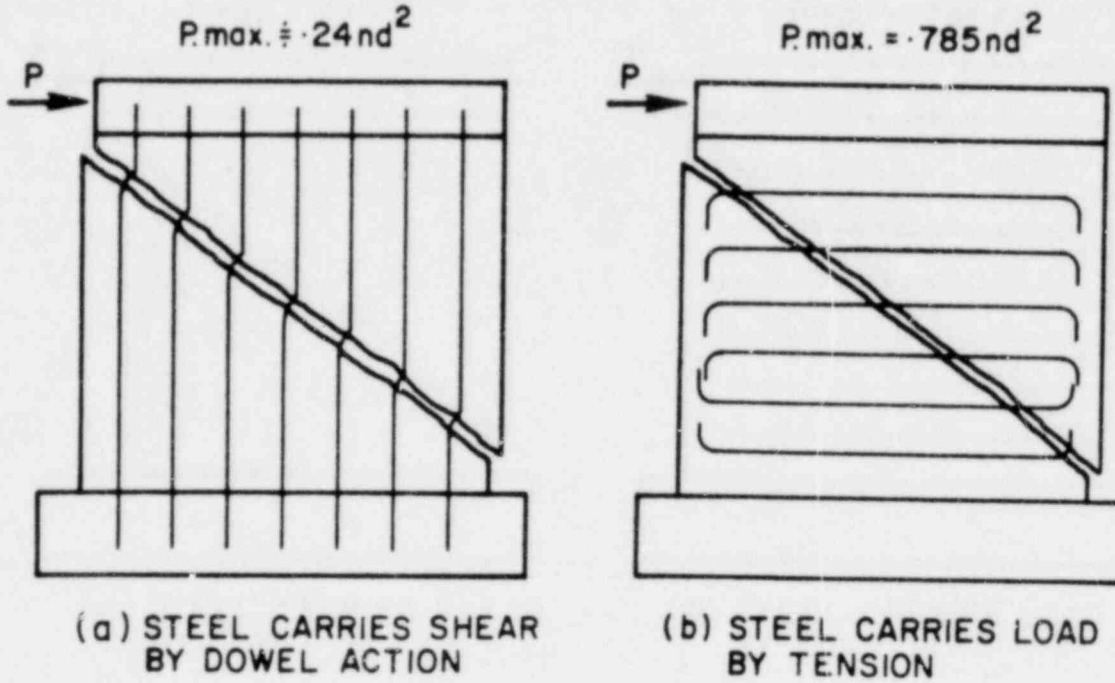


FIGURE 2-67 RELATIVE EFFECTIVENESS OF VERTICAL AND HORIZONTAL SHEAR STEEL

From Reference 77

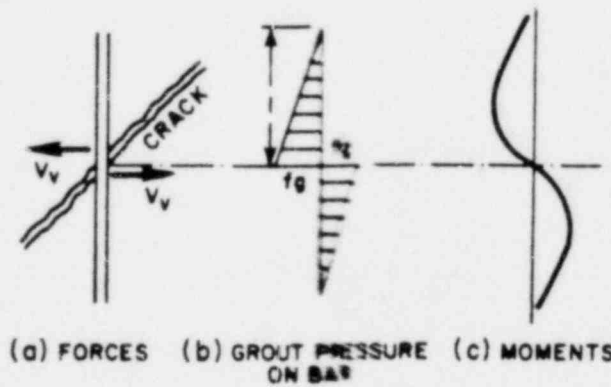


FIGURE 2-68 SHEAR TRANSFER BY DOWEL ACTION

From Reference 77

This will result in a maximum moment in the bar of

$$\begin{aligned} M_{\max} &= 0.064 f'_g d l^2 \\ &= \frac{0.256V^2}{f'_g d} \end{aligned}$$

Thus, since $M = Z f_y$

$$\frac{0.256V^2}{f'_g d} = \frac{\pi d^3}{32} f_y$$

$$\text{giving } V = 0.619d^2 \sqrt{f_y f'_g} \quad (2-19)$$

To compare this with equation 2-19 it is assumed that

$$\frac{f'_g}{f_y} = 0.15 \quad (2-20)$$

This rather high value is adopted to take some account of biaxial stress conditions that may occur in the crushing. Substituting from Equation 2-20 into Equation 2-19 gives, for n bars,

$$V_v = 0.240nd^2 f_y \quad (2-21)$$

Thus

$$\frac{V_H}{V_v} = 3.27,$$

indicating that the horizontal steel will be roughly 3 times as efficient as the same amount of vertical steel in carrying the shear load. In fact, this comparison flatters the vertical steel. As the crack opens, the flexural resistance of the steel in dowel action will rapidly reduce, whereas direct tension action of the horizontal bars results in the added protection of strain hardening at large crack widths.

Both Schneider⁽⁵⁷⁾ and Scrivener⁽⁴⁹⁾ had previously reported that shear reinforcing was effective only up to maximum percentages of 0.2%

and 0.3%, respectively, regardless of the orientation or distribution of the steel. However, examination of their data indicates that in all of these test walls insufficient shear steel was provided to carry the full shear load.

To investigate this further, walls F11 and F12 duplicated F7 and F8 except that in both walls sufficient horizontal steel was provided to carry the full shear load associated with a flexural failure, and that in F12, the Grade 40 vertical bars were replaced by HY60 bars to increase further the flexural failure load, and thus the required shear strength. Both walls sustained loads exceeding their theoretical flexural capacity, and though diagonal shear cracks developed well before the failure load, crack widths were small, and closed up on unloading, indicating the shear steel was remaining elastic. Two further walls, both of hollow cell construction (CBU-1 and CBU-2) with extremely high percentages of both vertical and shear steel (see Table 2-16) failed in bond along the extreme tension bars. The shear stress at failure at 247 and 255 psi, respectively, was very high, and again shear cracks were adequately controlled by the horizontal steel.

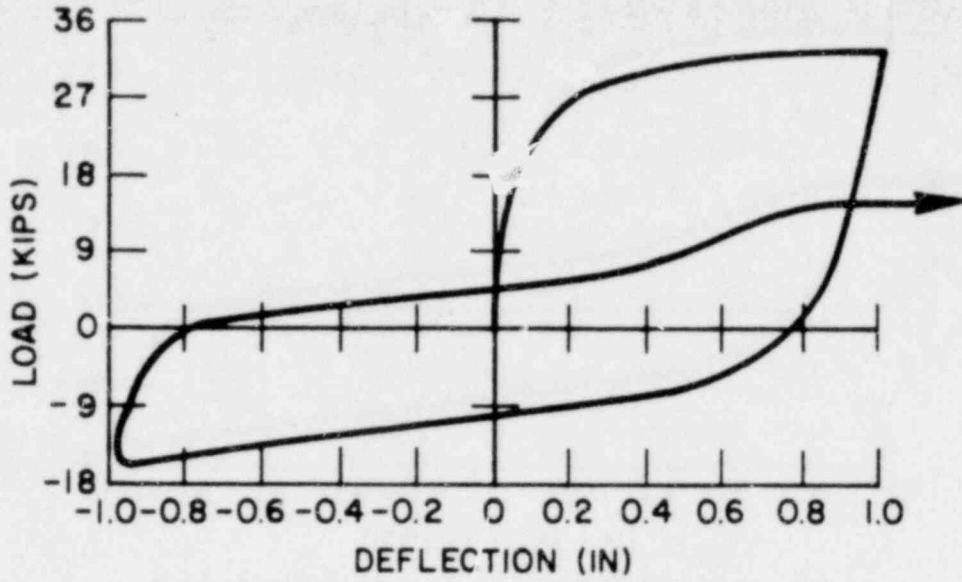
It is thus apparent, that contrary to the conclusions of earlier researchers, shear steel is effective provided it is designed to carry the full shear load, and that very high average shear stresses, based on the gross cross-sectional area can be sustained by brick cantilever walls.

(c) Load Degradation - Table 2-16 lists maximum loads sustained on the first and second load reversals, as well as the initial maxima. As might be expected, walls F7 to F10, which suffered shear failure, exhibited rapid load degradation on successive reversals of load. Perhaps less expected was the load degradation displayed by walls with

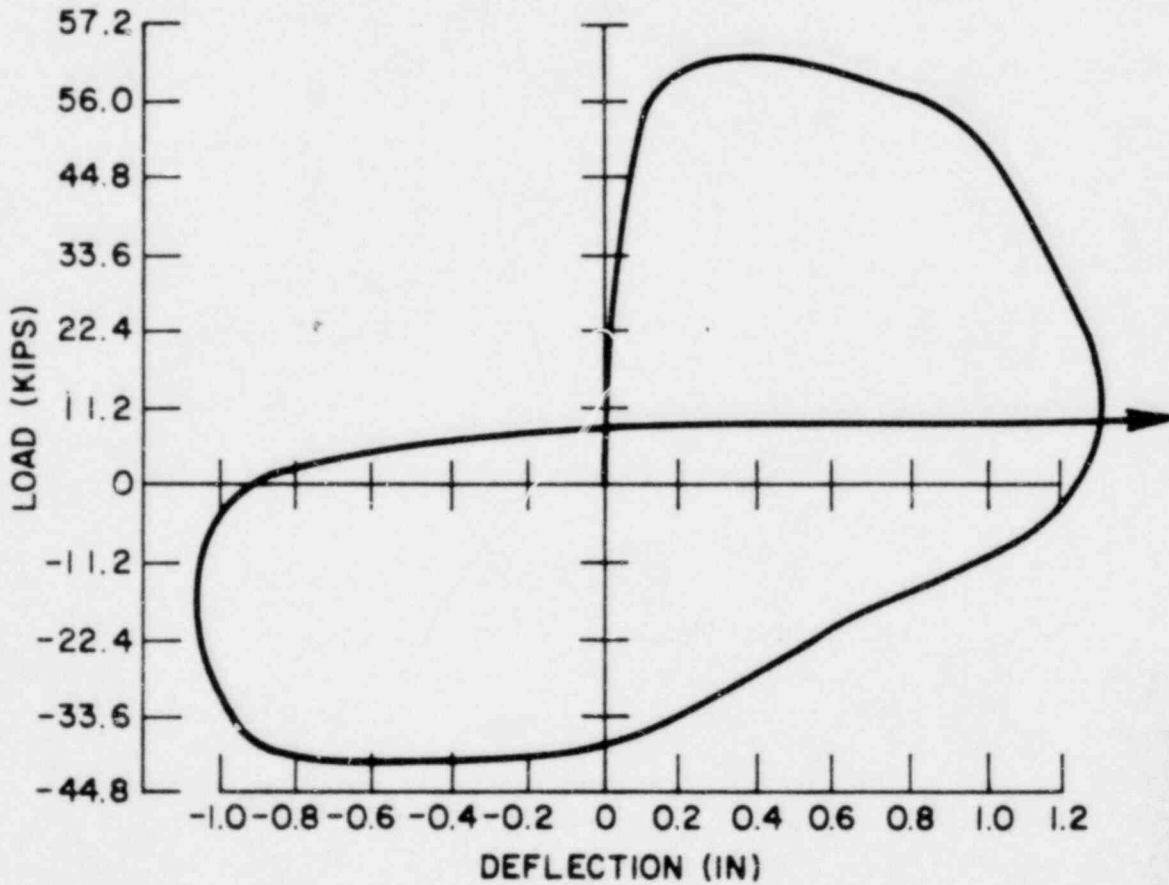
initial flexural failure modes. In all walls this occurred after initial loading to displacement ductilities of the order of 5. Figure 2-69 shows load deflection curves for typical walls exhibiting flexural failures (F2) and shear failures (F7). The extent of load degradation was such that testing of these early walls was abandoned after two load reversals.

Load degradation was largely the result of instability of the brick work at the toe and heel of the walls, as noted by previous researchers⁽³⁾. On the initial load application, vertical cracks would develop close to the toe in the crushing zone of the wall, and the resulting isolated columns of brickwork were 'blown out' under the combined action of shear and compression. A typical example is shown in Figure 2-70(a). This resulted in loss of bond for the extreme tension bars on reversal of the load direction, which compounded the effect. Further, after initial load reversals, any steel close to such a crushing zone became inadequately supported laterally and buckled, as shown in Figure 2-70(b). As this process continued with each load reversal, degradation rapidly increased.

(d) Reinforcing Against Load Degradation - Walls F13 to F15, CBU-3 and CBU-4 were constructed with confining plates in the bottom four courses at each end of the wall. The 1/8" thick x 16" long stainless steel plates, shown in Figures 2-71 and 2-72 were placed in the mortar courses during normal construction. Width of the plates was such as to give 1/2" cover to the wall faces and ends, to allow normal pointing of the courses. Holes were precut in the plates to allow reinforcing bars and grout to pass through unimpeded, and to improve bonding with the mortar. As well as restricting lateral expansions of the mortar, and thus eliminating vertical cracking of the bricks, the plates were



(a) FLEXURAL FAILURE - WALL F2



(b) SHEAR FAILURE - WALL F7

FIGURE 2-69 WALLS WITHOUT CONFINING PLATES. CYCLE LOAD DEGRADATION

From Reference 77



FIGURE 2-70 (a) UNCONFINED COMPRESSION
ZONE FAILURE

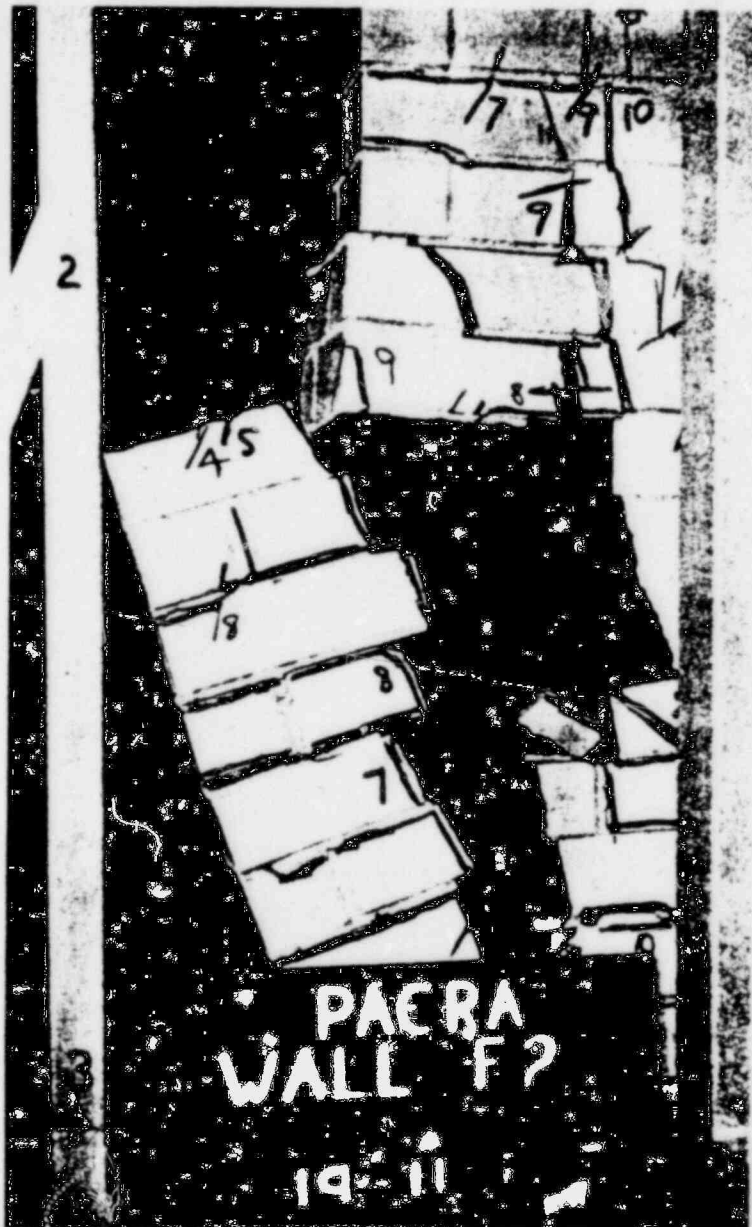
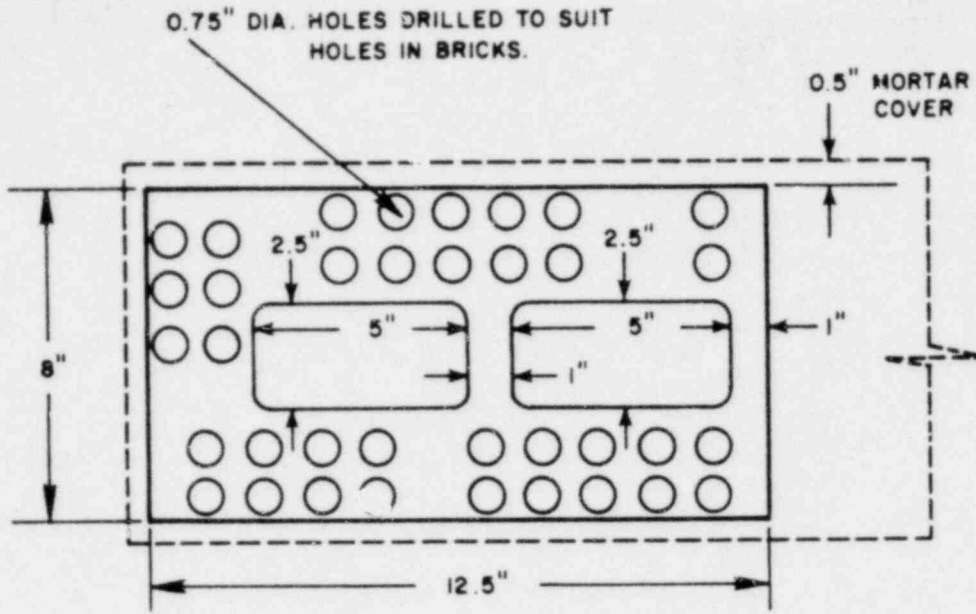
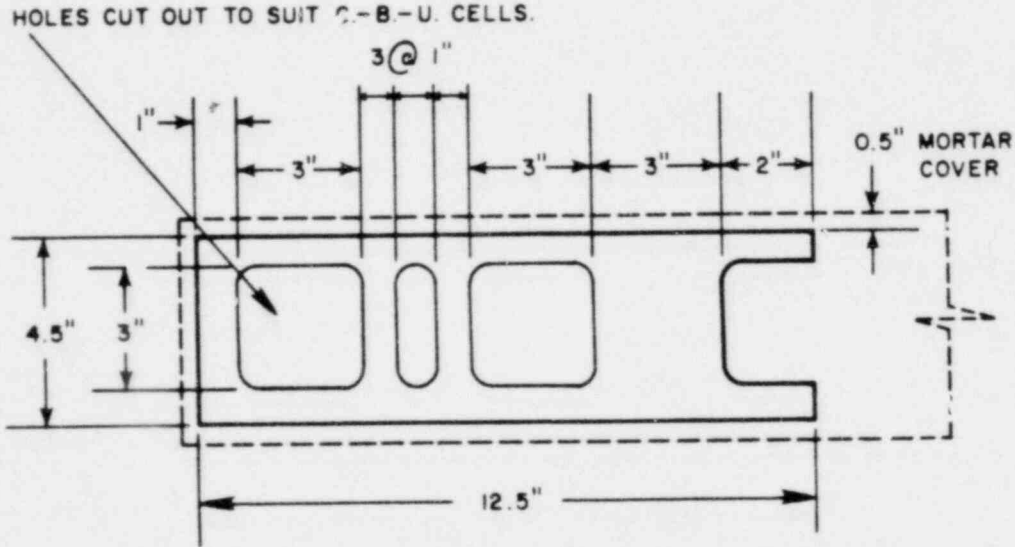


FIGURE 2-70 (b) BUCKLING OF PREVIOUSLY YIELDED
REINFORCING



0.12" THICK STAINLESS STEEL CONFINING PLATE FOR REINFORCED BRICK MASONRY WALLS.



0.12" THICK STAINLESS STEEL CONFINING PLATE FOR CERAMIC-BUILDING-UNIT WALLS.

FIGURE 2-71 DIMENSIONS OF CONFINING PLATES



FIGURE 2-72 (a) CONFINING PLATE IN RBM CONSTRUCTION



FIGURE 2-72 (b) CONFINING PLATE IN HOLLOW CELL CONSTRUCTION

expected to provide strong support against buckling of compression steel after a previous tensile yield excursion. No particular problems were experienced by the bricklayer in placing the plates during normal brick-laying operations.

(e) Results of Walls Containing Confining Plates - Two of the five walls tested with confining plates (F15 and CBU-4) contained typical percentages of flexural reinforcing, but sufficient shear steel to carry the full flexural failure load. The other three walls contained higher percentages of steel to investigate the capabilities of the confining plates under conditions which could be considered to be the most severe conceivable in design practice. Of these, two walls F13 and F14 were virtual duplicates; the sole differences being the provision of HY60, rather than Grade 40 steel as shear reinforcing for F14.

All five of the walls displayed greatly improved behaviour in comparison with the earlier walls. Effective confinement of the crushing zones was obtained throughout the cyclic loading sequences for the RBM walls, despite displacement ductility factors (based on the deflection on first attaining yield load) as high as 16 for wall F15. The crushing zones of hollow cell walls were also adequately confined for ductility factors up to 5, but at higher levels face shells tended to separate from webs under the action of shear and, in some cases, fell from the walls. It appears that bond between the grout and the smooth moulded surface of the ceramic block units was poor. Figure 2-73 shows the condition of the confined zones of F13 and CBU-3 after 3 cycles at 2.1 displacement (D.F. \approx 5). Compare these with Figure 2-70. Figure 2-74 shows the general condition of walls at this stage of loading.

Priestly and Bridgeman presented the following conclusions from the results of their study:



FIGURE 2-73 (a) F13 - CONFINED CRUSHING ZONE AFTER CYCLING AT ± 1 IN.
(D. F. = 6.3)



FIGURE 2-73 (b) CB-3 CONFINED CRUSHING ZONE AFTER CYCLING AT ± 1 IN.
(D. F. = 5.0)

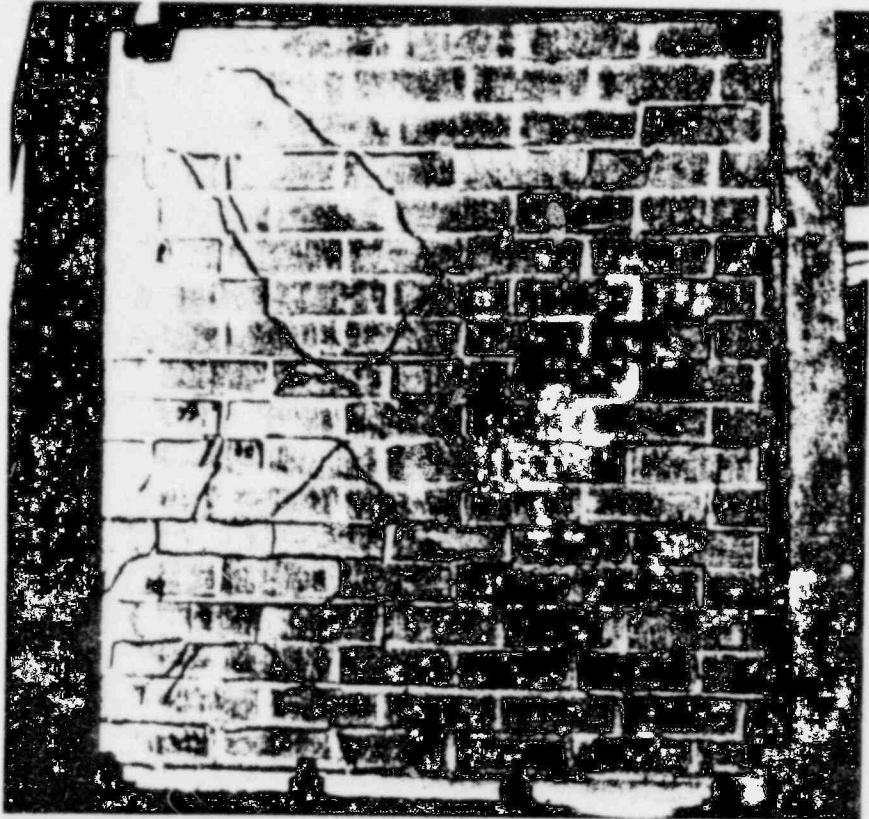


FIGURE 2-74 (a) F13 AFTER CYCLING AT \pm 1 IN.

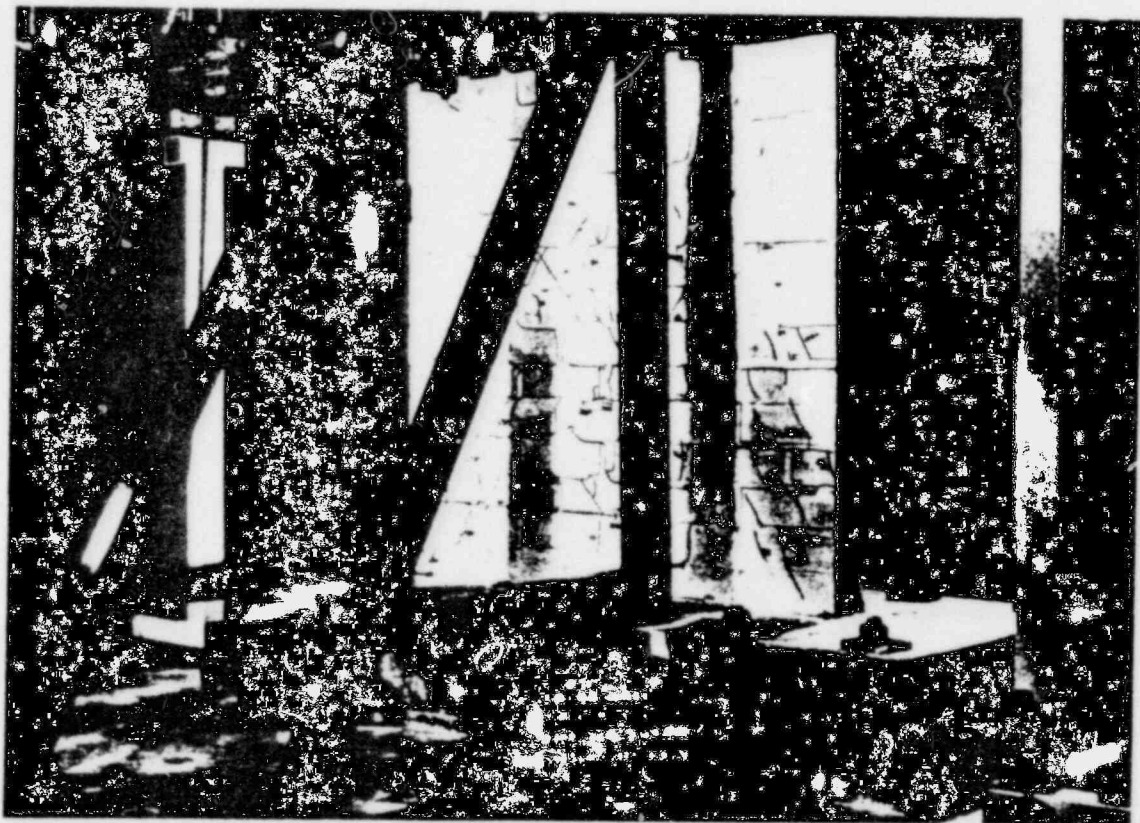


FIGURE 2-74 (b) CBU-3 AFTER CYCLING AT \pm 1 IN.

1. Under monotonic loading, the strength of walls failing in flexure exceeded the theoretical ultimate flexural capacity by an average of 14% due to the effect of strain-hardening of the tension steel.

2. Contrary to the conclusion of earlier researchers, shear steel is effective in improving the ultimate shear capacity of masonry, provided sufficient shear steel is provided to carry the full ultimate flexural load. It is felt that the normal under-capacity factor for shear is low enough to ensure adequate shear strength despite possible flexural overstrength resulting from strain-hardening. This is confirmed by one wall, F13, which contained marginally less horizontal steel than theoretically required to carry the full shear force, but still gave satisfactory behaviour.

3. Horizontal steel is approximately three times as efficient as vertical steel in carrying the shear force across a diagonal crack.

4. Load degradation was effectively eliminated at ductility factors up to 5 by the inclusion of stainless steel confining plates in the bottom few mortar courses at each end of the wall. These confined the crushing zone, thus eliminating vertical tension cracks in the bricks, and provided restraint against buckling of the compression steel. The cost of these plates is small in comparison with the benefits that accrue from their use. Further research is needed into the optimum design of confining steel.

It should be emphasized that confining plates are only required in regions where crushing is expected. In general, protection for the bottom 400 to 500mm should be adequate for practical cantilever wall design. The length of the plate should adequately protect the full length of the compression block, and the authors favour a detail that

extends just past the second vertical bar from the wall end, to provide additional support against compression buckling of the extreme bar. It is expected that mass production techniques would result in a unit price of \$3 - \$4 for the confining plates.

5. For walls with adequately confined crushing zones, it is suggested that a conservative seismic design approach would involve use of the first-yield load rather than the ultimate flexural capacity, associated with a ductility factor of 4. However, it should be pointed out that satisfactory behaviour would result from use of the full flexural capacity in design, if standard material and undercapacity factors⁽¹³⁾ are used.

6. RBM walls appeared to give slightly better behaviour than the hollow cell units, possibly due to poor adhesion between the face shells and grout in the latter case, and a greater area of confinement in the former.

REFERENCES

1. Monk, C. B., "A Historical Survey and Analysis of the Compressive Strength of Brick Masonry," Structural Clay Products Research Foundation, Geneva, Illinois, Research Report 12, 1967.
2. Foster, P. K., "Prism Tests for the Design and Control of Brick Masonry," New Zealand Pottery and Ceramics Research Association Technical Report, No. 22.
3. Williams, D., "Seismic Behaviour of Reinforced Masonry Shear Walls," Ph.D. Thesis, University of Canterbury, New Zealand, 1971.
4. Hilsdorf, H. K., "Investigation into the Failure Mechanism of Brick Masonry Loaded in Axial Compression," Proceedings of International Conference on Masonry Structural Systems, Texas, Nov., 1967.
5. Richart, F. E., Brandtzaeg, A. and Brown, R. L., "A Study of the Failure of Concrete under Combined Compressive Stresses," Bulletin 185, University of Illinois Engineering Experiment Station, 1928.
6. Francis, A. J., Horman, C. B. and Jerrems, L. E., "The Effect of Joint Thickness and Other Factors on the Compressive Strength of Brickwork," Proceedings of the 2nd International Brick Masonry Conference, Stoke-on-Trent, April, 1970.
7. West, H. W. H., Hodgkinson, H. R. and Davenport, S. T. E., "The Performance of Walls Built of Wirecut Bricks With and Without Perforations," Transactions of British Ceramic Society, 67, (10), 434, 1968.
8. Bradshaw, R. E., "The Brick in Slender Cross Wall Construction," Clay Products Technical Bureau, Technical Note 1, 1965.
9. Stedham, M. E. C., "Quality Control for Load-Bearing Brickwork I: 9 inch Cube Test - Preliminary Results," Transactions of British Ceramic Society of Testing and Materials, 64, (1), 1, 1965.
10. Sinha, B. P. and Hendry, A. W., "Further Tests on Model Brick Walls and Piers," Proceedings of British Ceramic Society, No. 17, Feb., 1970.
11. Bradshaw, R. E. and Hendry, A. W., "Further Crushing Tests on Story Height Walls 4 1/2 inch Thick," Proceedings of British Ceramic Society, No. 11, 1968.
12. Francis, A. J., "The SAA Brickwork Code: The Research Background," Institute of Engineers, Australia Civil Engineering Transactions, Cell, Oct., 1969.

13. Krefeld, W. J., "The Effect of Shape of Specimen on the Apparent Compressive Strength of Brick Masonry," Proceedings of American Society for Testing Materials, 38(1), 1938.
14. de Grave, A. and Molten, H., "Testing and Calculation of Masonry Recommendations Based on Research in Belgium," Proceedings of Second International Conference on Brick Masonry, Stoke-on-Trent, April, 1970.
15. West, H. W. H., Everill, J. B. and Beech, D. G., "The Testing of Bricks and Blocks for Load Bearing Brickwork," Xth International Ceramic Congress, The Congress, Stockholm, 1966.
16. West, H. W. H., Everill, J. B. and Beech, D. G., "Development of a Standard 9 inch Cube Test for Brickwork," Transactions of British Ceramic Society, 65, 1966.
17. Lenczner, D., "Strength and Elastic Properties of the 9 inch Brickwork Cube," Transactions of British Ceramic Society, 65(6), 1966.
18. Yokel, F. Y., Mathey, R. G. and Dikkers, R. D., "Strength of Masonry Walls under Compressive and Transverse Loads," U. S. National Bureau of Standards of Building Science, Series 34, 1971.
19. Structural Clay Products Research Foundation, "Compressive and Transverse Tests of 5 inch Brick Walls," S.C.P.R.F., Research Report, No. 8, 1965.
20. Structural Clay Products Research Foundation, "Compressive Transverse and Racking Tests of 4 inch Brick Walls," S.C.P.R.F., Research Report, No. 9, 1965.
21. Stafford-Smith, B. and Carter, C., "Distribution of Stresses in Masonry Walls Subjected to Vertical Loading," Proceedings of Second International Brick Masonry Conference, Stoke-on-Trent, April, 1970.
22. Prasan, S., Hendry, A. W. and Bradshaw, R. E., "Crushing Tests on Story Height Walls 4 1/2 inch Thick," Proceedings of British Ceramic Society, No. 4, July, 1965.
23. Monk, C. B., "Old and New Research on Clay Masonry Bearing Walls, Proceedings of First National Brick and Tile Bearing Wall Conference, 17-24, Structural Clay Products Institute, Washington, 1965.
24. Structural Clay Products Research Foundation, "Small Scale Specimen Testing - National Testing Program," S.C.P.R.F., Research Report, No. 1, 1964.
25. Monk, C. B., "Testing High-Bond Clay Masonry Assemblages," Symposium on Masonry Testing, ASTM, Special Publication, No. 320, 1962.

26. U. S. Department of Commerce, "Compression Tests on Brick Masonry," Building Code Committee, U. S. Department of Commerce, March, 1926.
27. Stang, A. H., Parsons, D. E. and McBurney, J. W., "Compressive Strength of Clay Brick Walls," Journal of Research Bureau of Standards, (Department of Commerce) V. 3, No. 4, Research Paper 108, Oct., 1929.
28. Bragg, J. C., "Compressive Strength of Large Brick Piers," Bureau of Standards, Technological Paper, No. 111, 1918.
29. West, N. W. H., Hodgkinson, H. R., Beech, D. G. and Davenport, S. T. E., "The Performance of Walls Built of Wirecut Bricks With and Without Perforations," Proceedings of British Ceramic Society, No. 17, Feb., 1970.
30. Armour Research Foundation, "Evaluation of Bond Strength of Standard Mortar," Report No. 32, Project No. G 516, Armour Research Foundation, June 6, 1956.
31. Greenley, D. G., "Study of the Effect of Certain Modified Mortars on Compressive and Flexural Strength of Masonry," Proceedings of First International Conference on Masonry Structural Systems, Texas, 1967.
32. Watstein, D. and Allen, M. H., "Structural Performance of Clay Masonry Assemblages Built with High-Bond Organic Modified Mortars," Proceedings of Second International Brick Masonry Conference, Stoke-on-Trent, April, 1970.
33. Structural Clay Products Research Foundation, "Compressive and Transverse Strength Tests on 8 inch Brick Walls," S.C.P.R.F., Research Report, No. 10, 1966.
34. Thomas, K. and O'Leary, D. C., "Tensile Strength Tests on Two Types of Brick," Proceedings of Second International Brick Masonry Conference, Stoke-on-Trent, April, 1970.
35. Rosenhaupt, S., Van Riel, A. C. and Wyler, L. A., "A New Indirect Tensile Test for Concrete Theoretical Analysis and Preliminary Experiments," Bulletin of Research Council of Israel, 6C, (1), 13, 1957.
36. Polyakov, S. V., "Masonry in Framed Buildings," Gosudatst Vennoe Izdatel' stvo Literature po Straitel' stvu' i Arkhitekture," Moscow, 1956. (Translated by Building Research Station and Published by National Lending Library for Science and Technology, Boston Spa, England).
37. Pearson, J. C., "Measurement of Bond Between Bricks and Mortar," Proceedings American Society for Testing Materials, 43, 1963.
38. Kampf, L., "Factors Affecting Bond Between Bricks and Mortar," Symposium on Masonry Testing, ASTM, S.T.P. 320, Feb., 1963.

39. Murthy, C. K. and Hendry, A. W., "Preliminary Investigation of the Shear Strength of one-sixth scale Model Brickwork," Technical Note No. 65, British Ceramic Research Association, Feb., 1965.
40. Thomas, F. G. and Simms, L. G., "The Strength of Some Reinforced Brick Masonry Beams in Bending and Shear," *Structural Engineer*, July, 1939.
41. Benjamin, J. R. and Williams, H. A., "The Behaviour of One Story Brick Shear Walls," *Proceedings of ASCE, Journal of Structural Division*, V. 84, No. ST4, 1958.
42. Youl, V. A. and Foster, P. K., "Miniature Tensile and Panel Flexure Properties of Brickwork," *Designing, Engineering and Constructing with Masonry Products*, Houston, Texas, 1967.
43. Sinha, B. P. and Hendry, A. W., "Further Investigations of Bond Tension, Bond Shear and the Effect of Precompression on the Shear Strength of Model Brick Masonry Couplets," *British Ceramic Research Association, Technical Note No. 80*, 1966.
44. Sahlin, S., Structural Masonry, Prentice-Hall, 1971.
45. Davison, J. I., "Loss of Moisture from Fresh Mortars to Bricks," *ASTM Materials Research and Standards*, ASTM 1, (5), 1961.
46. Johnson, F. B. and Thompson, J. N., "The Development of Diametral Testing Procedures to Provide a Measure of Strength Characteristics of Masonry Assemblages," *First International Conference on Masonry Structural Systems*, Texas, Nov., 1967.
47. Stafford-Smith, B., Carter, C and Choudhury, J. R., "The Diagonal Tensile Strength of Brickwork," *The Structural Engineer*, No. 4, V. 48, June, 1970.
48. Schneider, R. R., "Tests on Reinforced Grouted Brick Masonry Shear Panels," Report issued by California State Division of Architecture, Los Angeles, 1956.
49. Scrivener, J. C., "Static Racking Tests on Masonry Walls," *Designing, Engineering and Constructing with Masonry Products*, Edited by F. B. Johnson, Gulf Publishing Company, Houston, Texas, May, 1969.
50. Moss, P. J. and Scrivener, J. C., "Concrete Masonry Wall Panel Tests the Effect of Cavity Filling on Shear Behaviour," *New Zealand Concrete Construction*, Apr. 1968.
51. Structural Clay Products Research Foundation, "Compressive Tensile and Racking Tests of 4" Brick Walls," *SCPRF, Research Report No. 9*, 1965.

52. Structural Clay Products Research Foundation, "Compressive, Transverse and Racking Strength Tests of Four Inch Structural Clay Facing Tile Walls," SCPRF, Research Report No. 11, 1967.
53. Schneider, R. R., "Lateral Load Tests on Reinforced Grouted Masonry Shear Walls," University of Southern California Engineering Center, Report No. 70-101, 1959.
54. Scrivener, J. C., "Concrete Masonry Wall Panel Tests - Static Racking Tests with Predominant Flexural Effect," New Zealand Concrete Construction, July, 1966.
55. Blume, J. A. and Associates, "Available and Needed Data for More Effective Structural Utilization of Brick Masonry," - Report to Western States Clay Products, Feb., 1964.
56. Borchelt, J. G., "Analysis of Brick Walls Subject to Axial Compression and In-Plane Shear," Proceedings of Second International Brick Masonry Conference, Stoke-on-Trent, Apr., 1970.
57. Schneider, R. R., "Shear Tests in Concrete Masonry Piers," Report of California State Polytechnic College, Pomona, California.
58. Meli, R., "Behaviour of Masonry Walls Under Lateral Loads," Proceedings of Fifth World Conference on Earthquake Engineering, Rome, 1972.
59. New Zealand Pottery and Ceramics Division, Private Communication.
60. Mayes, R. L., Mostaghel, N. M., Clough, R. W. and Dickey, W. L., "Cyclic Tests on Masonry Piers," 3rd Congress of the Association for Earthquake Engineering, Budva, Yugoslavia, October, 1974 and Bulletin of the New Zealand National Society for Earthquake Engineering, Vol. 7, No. 3, Sept. 1974.
61. Haller, P., "Load Capacity of Brick Masonry," Designing, Engineering and Constructing with Masonry Products, Edited by F. B. Johnson, Gulf Publishing Co., Houston, Texas, May, 1969.
62. Greenley, D. G. and Cattaneo, D. G., "The Effect of Edge Load on the Racking Strength of Clay Masonry," Proceedings of Second International Brick Masonry Conference, Stoke-on-Trent, Apr. 1970.
63. Pieper, K. and Trautsch, W., "Shear Tests on Walls," Proceedings of Second International Brick Masonry Conference, Stoke-on-Trent, Apr., 1970.
64. Turnsek, V. and Cacovic, F., "Some Experimental Results on the Strength of Brick Masonry Walls," Proceedings of Second International Brick Masonry Conference, Stoke-on-Trent, Apr. 1970.
65. Murthy, C. K. and Hendry, A. W., "Comparative Tests on Third and Sixth Scale Model Brickwork Piers and Walls," Proceedings British Ceramic Society, No. 4, July, 1965.

66. Sinha, B. P. and Hendry, A. W., "Racking Tests on Story Height Shear-Wall Structures with Openings, Subjected to Precompression," *Designing, Engineering and Constructing with Masonry Products*, Edited by F. B. Johnson, Gulf Publishing Co., Houston, Texas, May, 1969.
67. Simms, L. G., "The Shear Strength of Some Story Height Brickwork and Blockwork Walls," Clay Products Technical Bureau (London), Technical Note No. 1, 1964.
68. Murthy, C. K. and Hendry, A. W., "Model Experiments in Load Bearing Brickwork," *Building Science*, Vol. 1, 1966.
69. Sinha, B. P., Maurenbrecher, A. H. P. and Hendry, A. W., "Model and Full Scale Tests on a Five-Story Cross-Wall Structure Under Lateral Loading," *Proceedings of Second International Brick Masonry Conference, Stoke-on-Trent, Apr., 1970.*
70. Kalita, U. C. and Hendry, A. W., "An Experimental and Theoretical Investigation of the Stresses and Deflections in Model Cross-Wall Structures," *Proceedings of Second International Brick Masonry Conference, Stoke-on-Trent, Apr., 1970.*
71. Benjamin, J. R., Statically Indeterminate Structures, New York, McGraw Hill, 1959.
72. Meli, R. and Reyes, A., "Propiedades mecanicas de la mamposteria," (Mechanical Properties of Masonry), Instituto de Ingenieria, UNAM, Informe No. 288, July, 1971.
73. Meli, R. and Salgado, G., "Comportamiento de muros de mamposteria sujetos a cargas laterales," (Behavior of Masonry Walls under Lateral Loads. Second Report.) Instituto de Ingenieria, UNAM, Informe No. 237, Sept., 1969.
74. Meli, R., Zeevart, W. and Esteva, L., "Comportamiento de muros de mamposteria hueca ante cargas alternadas," (Behavior of Reinforced Masonry under Alternating Loads), Instituto de Ingenieria, UNAM, Informe No. 156, July, 1968.
75. Esteva, L., "Behavior under Alternating Loads of Masonry Diaphragms Framed by Reinforced Concrete Members," *Symposium on the Effects of Repeated Loading on Materials and Structural Elements, RILEM, Mexico, 1966.*
76. Mayes, R. L. and Clough, R. W., "Cyclic Shear Tests on Fixed Ended Masonry Piers," *ASCE National Conference, New Orleans, April, 1975.*
77. Priestly, M. J. N. and Bridgeman, D. O., "Seismic Resistance of Brick Masonry Walls," *Bulletin of the New Zealand National Society for Earthquake Engineering, Vol. 7, No. 4, Dec. 1974.*

EARTHQUAKE ENGINEERING RESEARCH CENTER REPORTS

- EERC 67-1 "Feasibility Study Large-Scale Earthquake Simulator Facility," by J. Penzien, J. G. Bouwkamp, R. W. Clough and D. Rea - 1967 (PB 187 905)
- EERC 68-1 Unassigned
- EERC 68-2 "Inelastic Behavior of Beam-to-Column Subassemblages under Repeated Loading," by V. V. Bertero - 1968 (PB 184 888)
- EERC 68-3 "A Graphical Method for Solving the Wave Reflection-Refracton Problem," by H. D. McNiven and Y. Mengi - 1968 (PB 187 943)
- EERC 68-4 "Dynamic Properties of McKinley School Buildings," by D. Rea, J. G. Bouwkamp and R. W. Clough - 1968 (PB 187 902)
- EERC 68-5 "Characteristics of Rock Motions during Earthquakes," by H. B. Seed, I. M. Idriss and F. W. Kiefer - 1968 (PB 188 338)
- EERC 69-1 "Earthquake Engineering Research at Berkeley" - 1969 (PB 187 906)
- EERC 69-2 "Nonlinear Seismic Response of Earth Structures," by M. Dibaj and J. Penzien - 1969 (PB 187 904)
- EERC 69-3 "Probabilistic Study of the Behavior of Structures during Earthquakes," by P. Ruiz and J. Penzien - 1969 (PB 187 886)
- EERC 69-4 "Numerical Solution of Boundary Value Problems in Structural Mechanics by Reduction to an Initial Value Formulation," by N. Distefano and J. Schujman - 1969 (PB 187 942)
- EERC 69-5 "Dynamic Programming and the Solution of the Biharmonic Equation," by N. Distefano - 1969 (PB 187 941)

Note: Numbers in parentheses are Accession Numbers assigned by the National Technical Information Service. Copies of these reports may be ordered from the National Technical Information Service, Springfield, Virginia, 22151. Accession Numbers should be quoted on orders for the reports.

- EERC 69-6 "Stochastic Analysis of Offshore Tower Structures," by A. K. Malhotra and J. Penzien - 1969 (PB 187 903)
- EERC 69-7 "Rock Motion Accelerograms for High Magnitude Earthquakes," by H. B. Seed and I. M. Idriss - 1969 (PB 187 940)
- EERC 69-8 "Structural Dynamics Testing Facilities at the University of California, Berkeley," by R. M. Stephen, J. G. Bouwkamp, R. W. Clough and J. Penzien - 1969 (PB 189 111)
- EERC 69-9 "Seismic Response of Soil Deposits Underlain by Sloping Rock Boundaries," by H. Dezfulian and H. B. Seed - 1969 (PB 189 114)
- EERC 69-10 "Dynamic Stress Analysis of Axisymmetric Structures under Arbitrary Loading," by S. Ghosh and E. L. Wilson - 1969 (PB 189 026)
- EERC 69-11 "Seismic Behavior of Multistory Frames Designed by Different Philosophies," by J. C. Anderson and V. V. Bertero - 1969 (PB 190 662)
- EERC 69-12 "Stiffness Degradation of Reinforcing Concrete Structures Subjected to Reversed Actions," by V. V. Bertero, B. Bresler and H. Ming Liao - 1969 (PB 202 942)
- EERC 69-13 "Response of Non-Uniform Soil Deposits to Travel Seismic Waves," by H. Dezfulian and H. B. Seed - 1969 (PB 191 023)
- EERC 69-14 "Damping Capacity of a Model Steel Structure," by D. Rea, R. W. Clough and J. G. Bouwkamp - 1969 (PB 190 663)
- EERC 69-15 "Influence of Local Soil Conditions on Building Damage Potential during Earthquakes," by H. B. Seed and I. M. Idriss - 1969 (PB 191 036)
- EERC 69-16 "The Behavior of Sands under Seismic Loading Conditions," by M. L. Silver and H. B. Seed - 1969 (AD 714 982)
- EERC 70-1 "Earthquake Response of Concrete Gravity Dams," by A. K. Chopra - 1970 (AD 709 640)
- EERC 70-2 "Relationships between Soil Conditions and Building Damage in the Caracas Earthquake of July 29, 1967," by H. B. Seed, I. M. Idriss and H. Dezfulian - 1970 (PB 195 762)

- EERC 70-3 "Cyclic Loading of Full Size Steel Connections," by E. P. Popov and R. M. Stephen - 1970 (PB 213 545)
- EERC 70-4 "Seismic Analysis of the Charaima Building, Caraballeda, Venezuela," by Subcommittee of the SEAONC Research Committee: V. V. Bertero, P. F. Fratessa, S. A. Mahin, J. H. Sexton, A. C. Scordelis, E. L. Wilson, L. A. Wyllie, H. B. Seed and J. Penzien, Chairman - 1970 (PB 201 455)
- EERC 70-5 "A Computer Program for Earthquake Analysis of Dams," by A. K. Chopra and P. Chakrabarti - 1970 (AD 723 994)
- EERC 70-6 "The Propagation of Love Waves across Non-Horizontally Layered Structures," by J. Lysmer and L. A. Drake - 1970 (PB 197 896)
- EERC 70-7 "Influence of Base Rock Characteristics on Ground Response," by J. Lysmer, H. B. Seed and P. B. Schnabel - 1970 (PB 197 897)
- EERC 70-8 "Applicability of Laboratory Test Procedures for Measuring Soil Liquefaction Characteristics under Cyclic Loading," by H. B. Seed and W. H. Peacock - 1970 (PB 198 016)
- EERC 70-9 "A Simplified Procedure for Evaluating Soil Liquefaction Potential," by H. B. Seed and I. M. Idriss - 1970 (PB 198 009)
- EERC 70-10 "Soil Moduli and Damping Factors for Dynamic Response Analysis," by H. B. Seed and I. M. Idriss - 1970 (PB 197 869)
- EERC 71-1 "Koyna Earthquake and the Performance of Koyna Dam," by A. K. Chopra and P. Chakrabarti - 1971 (AD 731 496)
- EERC 71-2 "Preliminary In-Situ Measurements of Anelastic Absorption in Soils Using a Prototype Earthquake Simulator," by R. D. Borcherdt and P. W. Rodgers - 1971 (PB 201 454)
- EERC 71-3 "Static and Dynamic Analysis of Inelastic Frame Structures," by F. L. Porter and G. H. Powell - 1971 (PB 210 135)
- EERC 71-4 "Research Needs in Limit Design of Reinforced Concrete Structures," by V. V. Bertero - 1971 (PB 202 943)
- EERC 71-5 "Dynamic Behavior of a High-Rise Diagonally Braced Steel Building," by D. Rea, A. A. Shah and J. G. Bouwkamp - 1971 (PB 203 584)

- EERC 71-6 "Dynamic Stress Analysis of Porous Elastic Solids Saturated with Compressible Fluids," by J. Ghaboussi and E. L. Wilson - 1971 (PB 211 396)
- EERC 71-7 "Inelastic Behavior of Steel Beam-to-Column Subassemblages," by H. Krawinkler, V. V. Bertero and E. P. Popov - 1971 (PB 211 335)
- EERC 71-8 "Modification of Seismograph Records for Effects of Local Soil Conditions," by P. Schnabel, H. B. Seed and J. Lysmer - 1971 (PB 214 450)
- EERC 72-1 "Static and Earthquake Analysis of Three Dimensional Frame and Shear Wall Buildings," by E. L. Wilson and H. H. Dovey - 1972 (PB 212 904)
- EERC 72-2 "Accelerations in Rock for Earthquakes in the Western United States," by P. B. Schnabel and H. B. Seed - 1972 (PB 213 100)
- EERC 72-3 "Elastic-Plastic Earthquake Response of Soil-Building Systems," by T. Minami and J. Penzien - 1972 (PB 214 868)
- EERC 72-4 "Stochastic Inelastic Response of Offshore Towers to Strong Motion Earthquakes," by M. K. Kaul and J. Penzien - 1972 (PB 215 713)
- EERC 72-5 "Cyclic Behavior of Three Reinforced Concrete Flexural Members with High Shear," by E. P. Popov, V. V. Bertero and H. Krawinkler - 1972 (PB 214 555)
- EERC 72-6 "Earthquake Response of Gravity Dams Including Reservoir Interaction Effects," by P. Chakrabarti and A. K. Chopra - 1972 (AD 762 330)
- EERC 72-7 "Dynamic Properties of Pine Flat Dam," by D. Rea, C. Y. Liaw and A. K. Chopra - 1972 (AD 763 928)
- EERC 72-8 "Three Dimensional Analysis of Building Systems," by E. L. Wilson and H. H. Dovey - 1972 (PB 222 438)
- EERC 72-9 "Rate of Loading Effects on Uncracked and Repaired Reinforced Concrete Members," by S. Mahin, V. V. Bertero, D. Rea and M. Atalay - 1972 (PB 224 520)
- EERC 72-10 "Computer Program for Static and Dynamic Analysis of Linear Structural Systems," by E. L. Wilson, K.-J. Bathe, J. E. Peterson and H. H. Dovey - 1972 (PB 220 437)

- EERC 72-11 "Literature Survey - Seismic Effects on Highway Bridges," by T. Iwasaki, J. Penzien and R. W. Clough - 1972 (PB 215 613)
- EERC 72-12 "SHAKE-A Computer Program for Earthquake Response Analysis of Horizontally Layered Sites," by P. B. Schnabel and J. Lysmer - 1972 (PB 220 207)
- EERC 73-1 "Optimal Seismic Design of Multistory Frames," by V. V. Bertero and H. Kamil - 1973
- EERC 73-2 "Analysis of the Slides in the San Fernando Dams during the Earthquake of February 9, 1971," by H. B. Seed, K. L. Lee, I. M. Idriss and F. Makdisi - 1973 (PB 223 402)
- EERC 73-3 "Computer Aided Ultimate Load Design of Unbraced Multistory Steel Frames," by M. B. El-Hafez and G. H. Powell - 1973
- EERC 73-4 "Experimental Investigation into the Seismic Behavior of Critical Regions of Reinforced Concrete Components as Influenced by Moment and Shear," by M. Celebi and J. Penzien - 1973 (PB 215 884)
- EERC 73-5 "Hysteretic Behavior of Epoxy-Repaired Reinforced Concrete Beams," by M. Celebi and J. Penzien - 1973
- EERC 73-6 "General Purpose Computer Program for Inelastic Dynamic Response of Plane Structures," by A. Kanaan and G. H. Powell - 1973 (PB 221 260)
- EERC 73-7 "A Computer Program for Earthquake Analysis of Gravity Dams Including Reservoir Interaction," by P. Chakrabarti and A. K. Chopra - 1973 (AD 766 271)
- EERC 73-8 "Behavior of Reinforced Concrete Deep Beam-Column Subassemblages under Cyclic Loads," by O. Kustu and J. G. Bouwkamp - 1973
- EERC 73-9 "Earthquake Analysis of Structure-Foundation Systems," by A. K. Vaish and A. K. Chopra - 1973 (AD 766 272)
- EERC 73-10 "Deconvolution of Seismic Response for Linear Systems," by R. B. Reimer - 1973 (PB 227 179)
- EERC 73-11 "SAP IV: A Structural Analysis Program for Static and Dynamic Response of Linear Systems," by K.-J. Bathe, E. L. Wilson and F. E. Peterson - 1973 (PB 221 967)
- EERC 73-12 "Analytical Investigations of the Seismic Response of Long, Multiple Span Highway Bridges," by W. S. Tseng and J. Penzien - 1973 (PB 227 816)

- EERC 73-13 "Earthquake Analysis of Multi-Story Buildings Including Foundation Interaction," by A. K. Chopra and J. A. Gutierrez - 1973 (PB 222 970)
- EERC 73-14 "ADAP: A Computer Program for Static and Dynamic Analysis of Arch Dams," by R. W. Clough, J. M. Raphael and S. Majtahedi - 1973 (PB 223 763)
- EERC 73-15 "Cyclic Plastic Analysis of Structural Steel Joints," by R. B. Pinkney and R. W. Clough - 1973 (PB 226 843)
- EERC 73-16 "QUAD-4: A Computer Program for Evaluating the Seismic Response of Soil Structures by Variable Damping Finite Element Procedures," by I. M. Idriss, J. Lysmer, R. Hwang and H. B. Seed - 1973 (PB 229 424)
- EERC 73-17 "Dynamic Behavior of a Multi-Story Pyramid Shaped Building," by R. M. Stephen and J. G. Bouwkamp - 1973
- EERC 73-18 "Effect of Different Types of Reinforcing on Seismic Behavior of Short Concrete Columns," by V. V. Bertero, J. Hollings, O. Kustu, R. M. Stephen and J. G. Bouwkamp - 1973
- EERC 73-19 "Olive View Medical Center Material Studies, Phase I," by B. Bresler and V. V. Bertero - 1973 (PB 235 986)
- EERC 73-20 "Linear and Nonlinear Seismic Analysis Computer Programs for Long Multiple-Span Highway Bridges," by W. S. Tseng and J. Penzien - 1973
- EERC 73-21 "Constitutive Models for Cyclic Plastic Deformation of Engineering Materials," by J. M. Kelly and P. P. Gillis - 1973 (PB 226 024)
- EERC 73-22 "DRAIN - 2D User's Guide," by G. H. Powell - 1973 (PB 227 016)
- EERC 73-23 "Earthquake Engineering at Berkeley - 1973" - 1973 (PB 226 033)
- EERC 73-24 "Seismic Input and Structural Response during the 1971 San Fernando Earthquake," by R. B. Reimer, R. W. Clough and J. M. Raphael - 1973
- EERC 73-25 "Earthquake Response of Axisymmetric Tower Structures Surrounded by Water," by C. Y. Liaw and A. K. Chopra - 1973 (AD 773 052)
- EERC 73-26 "Investigation of the Failures of the Olive View Stairtowers during the San Fernando Earthquake and Their Implications in Seismic Design," by V. V. Bertero and R. G. Collins - 1973 (PB 235 106)

- EERC 73-27 "Further Studies on Seismic Behavior of Steel Beam-Column Subassemblages," by V. V. Bertero, H. Krawinkler and E. P. Popov - 1973 (PB 234 172)
- EERC 74-1 "Seismic Risk Analysis," by C. S. Oliveira - 1974 (PB 235 920)
- EERC 74-2 "Settlement and Liquefaction of Sands under Multi-Directional Shaking," by R. Pyke, C. K. Chan and H. B. Seed - 1974
- EERC 74-3 "Optimum Design of Earthquake Resistant Shear Buildings," by D. Ray, K. S. Pister and A. K. Chopra - 1974 (PB 231 172)
- EERC 74-4 "LUSH - A Computer Program for Complex Response Analysis of Soil-Structure Systems," by J. Lysmer, T. Udaka, H. B. Seed and R. Hwang - 1974 (PB 236 796)
- EERC 74-5 "Sensitivity Analysis for Hysteretic Dynamic Systems: Applications to Earthquake Engineering," by D. Ray - 1974 (PB 233 213)
- EERC 74-6 "Soil-Structure Interaction Analyses for Evaluating Seismic Response," by H. B. Seed, J. Lysmer and R. Hwang - 1974 (PB 236 519)
- EERC 74-7 "Response of Radiation-Shielding Blocks to Earthquake Motions," by M. Aslam, W. G. Godden and D. T. Scalise - 1974
- EERC 74-8 "Shaking Table Tests of a Steel Frame - A Progress Report," by R. W. Clough and D. Tang - 1974
- EERC 74-9 "Hysteretic Behavior of Reinforced Concrete Flexural Members with Special Web Reinforcement," by V. V. Bertero, E. P. Popov and T. Y. Wang - 1974 (PB 236 797)
- EERC 74-10 "Applications of Reliability-Based, Global Cost Optimization to Design of Earthquake Resistant Structures," by E. Vitiello and K. S. Pister - 1974 (PB 237 231)
- EERC 74-11 "Liquefaction of Gravelly Soils under Cyclic Loading Conditions," by R. T. Wong, H. B. Seed and C. K. Chan - 1974
- EERC 74-12 "Site-Dependent Spectra for Earthquake-Resistant Design," by H. B. Seed, C. Ugas and J. Lysmer - 1974

- EERC 74-13 "Earthquake Simulator Study of a Reinforced Concrete Frame," by P. Hidalgo and R. W. Clough - 1974
- EERC 74-14 "Nonlinear Earthquake Response of Concrete Gravity Dams," by N. Pal - 1974
- EERC 74-15 "Modeling and Identification in Nonlinear Structural Dynamics, I- One Degree of Freedom Models," by N. Distefano and A. Rath - 1974
- EERC 75-1 "Determination of Seismic Design Criteria for the Dumbarton Bridge Replacement Structure, Vol. 1: Description, Theory and Analytical Modeling of Bridge and Parameter," by F. Baron and S.-H. Tang - 1975
- EERC 75-2 "Determination of Seismic Design Criteria for the Dumbarton Bridge Replacement Structure, Vol. 2: Numerical Studies and Establishment of Seismic Design Criteria," by F. Baron and S.-H. Tang - 1975
- EERC 75-3 "Seismic Risk Analysis for a Site and a Metropolitan Area," by C. S. Oliveira - 1975
- EERC 75-4 "Analytical Investigations of Seismic Response of Short, Single or Multiple-Span Highway Bridges," by M. Chen and J. Penzien - 1975
- EERC 75-5 "An Evaluation of Some Methods for Predicting Seismic Behavior of Reinforced Concrete Buildings," by Stephen A. Mahin and V. V. Bertero - 1975
- EERC 75-6 "Earthquake Simulator Study of a Steel Frame Structure, Vol. I: Experimental Results," by R. W. Clough and Daniel T. Tang - 1975
- EERC 75-7 "Dynamic Properties of San Bernardino Intake Tower," by Dixon Rea, C.-Y. Liaw and Anil K. Chopra - 1975
- EERC 75-8 "Seismic Studies of the Articulation for the Dumbarton Bridge Replacement Structure, Vol. I: Description, Theory and Analytical Modeling of Bridge Components," by F. Baron and R. E. Hamati - 1975
- EERC 75-9 "Seismic Studies of the Articulation for the Dumbarton Bridge Replacement Structure, Vol. 2: Numerical Studies of Steel and Concrete Girder Alternates," by F. Baron and R. E. Hamati - 1975
- EERC 75-10 "Static and Dynamic Analysis of Nonlinear Structures," by Digambar P. Mondkar and Graham H. Powell - 1975

- EERC 75-11 "Behavior of Reinforced Concrete Deep Beam-Column Subassemblages Under Cyclic Loads," by O. Kustu and J. G. Bouwkamp - 1975
- EERC 75-12 "Earthquake Engineering Research Center Library Printed Catalog" - 1975
- EERC 75-13 "Three Dimensional Analysis of Building Systems," Extended Version, by E. L. Wilson, J. P. Hollings, and H. H. Dovey - 1975
- EERC 75-14 "Determination of Soil Liquefaction Characteristics by Large-Scale Laboratory Tests," by Pedro De Alba, Clarence K. Chan and H. Bolton Seed - 1975
- EERC 75-15 "A Literature Survey - Compressive, Tensile, Bond and Shear Strength of Masonry," by Ronald L. Mayes and Ray W. Clough - 1975